

OPPORTUNITIES AND CHALLENGES IN USING SOIL MOISTURE FROM
COSMIC RAY NEUTRON SENSING FOR RAINFALL-RUNOFF MODELLING

A THESIS SUBMITTED TO
THE GRADUATE SCHOOL OF NATURAL AND APPLIED SCIENCES
OF
MIDDLE EAST TECHNICAL UNIVERSITY

BY

MUSTAFA BERK DUYGU

IN PARTIAL FULFILLMENT OF THE REQUIREMENTS
FOR
THE DEGREE OF DOCTOR OF PHILOSOPHY
IN
CIVIL ENGINEERING

SEPTEMBER 2021

Approval of the thesis:

**OPPORTUNITIES AND CHALLENGES IN USING SOIL MOISTURE
FROM COSMIC RAY NEUTRON SENSING FOR RAINFALL-RUNOFF
MODELLING**

submitted by **MUSTAFA BERK DUYGU** in partial fulfillment of the requirements
for the degree of **Doctor of Philosophy in Civil Engineering Department, Middle
East Technical University** by,

Prof. Dr. Halil Kalıpçılar
Dean, Graduate School of **Natural and Applied Sciences**

Prof. Dr. Ahmet Türer
Head of Department, **Civil Engineering**

Prof. Dr. Zuhal Akyürek
Supervisor, **Civil Engineering, METU**

Examining Committee Members:

Prof. Dr. İsmail Yücel
Civil Engineering Dept., METU

Prof. Dr. Zuhal Akyürek
Civil Engineering Dept., METU

Prof. Dr. Mehmet Akif Sarıkaya
Eurasia Institute of Earth Sciences, ITU

Assoc. Prof. Dr. Koray K. Yılmaz
Geological Engineering Dept., METU

Dr. Arda Şorman
Civil Engineering Dept., ESTÜ

Date:

I hereby declare that all information in this document has been obtained and presented in accordance with academic rules and ethical conduct. I also declare that, as required by these rules and conduct, I have fully cited and referenced all material and results that are not original to this work.

Name, Surname: Mustafa Berk Duygu

Signature :

ABSTRACT

OPPORTUNITIES AND CHALLENGES IN USING SOIL MOISTURE FROM COSMIC RAY NEUTRON SENSING FOR RAINFALL-RUNOFF MODELLING

Duygu, Mustafa Berk

Ph.D., Department of Civil Engineering

Supervisor: Prof. Dr. Zuhar Akyürek

September 2021, 174 pages

Retrieving or estimating soil moisture is one of the most important elements of hydrology, since most of the hydrological studies consider the absence (drought) or excessiveness (flood) of water stored in the soil. Water stored in a basin has a very strong relation with the amount of soil moisture thus knowing the soil moisture significantly facilitates the estimation of other parameters of the hydrological cycle. For agricultural decision making systems, it is also vital to know whether the plants receive the amount of water necessary for their growth, which can be indicated by the amount of soil moisture. There are various ways of measuring soil moisture, where each technique has its own advantages and disadvantages. Some of these methods can provide very accurate measurements with very high costs or they may have very high temporal resolutions with limited spatial coverages. Among different methods, soil moisture measurement from recently invented Cosmic Ray Neutron Probes (CRNPs) has a good potential to be used in hydrological studies due to its larger spatial coverage, low cost and high temporal resolution. It is also possible to use this product together with satellite soil moisture products to obtain reliable soil moisture informa-

tion with even more spatial coverage. The aim of this study is to assess the effectiveness of CRNPs in determination of soil moisture at basin scale, to validate satellite soil moisture products and to use the soil moisture information derived from CRNP and satellite products for improving hydrological modeling. For this study, the first CRNP of Turkey has been installed in Çakıt Basin, south of Turkey, and the neutron counts obtained from the CRNP have been converted into soil moisture values after a series of correction and conversion processes. The CRNP based soil moisture data have been used in the validation of different soil moisture satellite products to test the effectiveness of CRNPs in satellite product validation and assess the potential of using CRNPs in conjunction with satellite soil moisture products for studies covering relatively larger areas. The relation between soil moisture and evaporation is also investigated through CRNP soil moisture values. Finally, CRNP based soil moisture data have been introduced into the calibration of a conceptual hydrological model and it has been found that introducing CRNP soil moisture data into NAM conceptual model improves the model statistics of Çakıt Basin (421 km²) and one of its sub basins, Darboğaz sub-basin (121 km²). Using CRNP based soil moisture data to calibrate the NAM model increased the Kling-Gupta Efficiency score for the discharge data of Çakıt Basin from 0.56 (Calibration) and 0.42 (Validation) to 0.81 (Calibration) and 0.64 (Validation). Similar improvements were noted for most of the statistical measures for both Çakıt Basin and Darboğaz sub-basin.

Keywords: Cosmic Ray Neutron Sensing, Soil Moisture, NAM Conceptual Model, Satellite Soil Moisture Products

ÖZ

YAĞIŞ-AKIŞ MODELLEMESİ İÇİN KOZMİK IŞIN NÖTRON ALGILAMASI İLE ELDE EDİLEN TOPRAK NEMİNİNİN KULLANILMASINDAKİ FIRSATLAR VE ZORLUKLAR

Duygu, Mustafa Berk

Doktora, İnşaat Mühendisliği Bölümü

Tez Yöneticisi: Prof. Dr. Zuhâl Akyürek

Eylül 2021 , 174 sayfa

Toprak nemini ölçmek veya tahmin etmek, hidrolojinin en önemli unsurlarından olup hidrolojik çalışmaların çoğu toprakta depolanan suyun yokluğunu (kuraklık) veya fazlalığını (taşkın) dikkate alır. Bir havzada depolanan suyun toprak nemi miktarı ile çok güçlü bir ilişkisi vardır, bu nedenle toprak nemini bilmek hidrolojik döngünün diğer parametrelerinin tahminini önemli ölçüde kolaylaştırır. Tarımsal karar verme sistemlerinde, bitkilerin büyümeleri için gerekli olan miktarda su alıp almadıklarını bilmek de hayati önem taşımakla birlikte bu bilgi toprak nem miktarı ile oldukça ilişkilidir. Her teknik kendi avantaj ve dezavantajlarına sahip olmakla birlikte, toprak nemini ölçmenin çeşitli yolları vardır. Bu yöntemlerden bazıları çok yüksek maliyetlerle çok doğru ölçümler sağlayabilir veya sınırlı mekansal kapsama alanıyla çok yüksek zamansal çözünürlüklere sahip olabilir. Farklı yöntemler arasında, yakın zamanda icat edilen Kozmik Işın Nötron Sayaçlarından (CRNP'ler) toprak nemi ölçümleri, daha geniş mekansal kapsamı, düşük maliyeti ve yüksek zamansal çözünürlüğü nedeniyle hidrolojik çalışmalarda kullanılmak için iyi bir potansiyele sahip-

tir. Bu ürünü uydu toprak nemi ürünleri ile birlikte kullanarak daha fazla mekansal kapsama ile güvenilir toprak nemi bilgisi elde etmek de mümkündür. Bu çalışmanın amacı, havza ölçeğinde toprak nemi tayininde CRNP'lerin etkinliğini değerlendirmek, uydu toprak nemi ürünlerini doğrulamak ve CRNP ile uydu ürünlerinden elde edilen toprak nemi bilgilerini hidrolojik modellemeyi geliştirmek için kullanmaktır. Bu çalışma için Türkiye'nin ilk CRNP'si Türkiye'nin güneyindeki Çakıt Havzası'na kurulmuş ve CRNP'den elde edilen nötron sayıları bir dizi düzeltme ve dönüştürme işleminden sonra toprak nem değerlerine dönüştürülmüştür. CRNP'ye dayalı toprak nemi verileri, uydu doğrulamasında CRNP'lerin etkinliğini test etmek ve nispeten daha geniş alanları kapsayan çalışmalar için uydu toprak nemi ürünleri ile birlikte CRNP'leri kullanma potansiyelini değerlendirmek için farklı toprak nemi uydu ürünlerinin doğrulamasında kullanılmıştır. Toprak nemi ile buharlaşma arasındaki ilişki de CRNP toprak nemi değerleri üzerinden araştırılmıştır. Son olarak, kavramsal bir hidrolojik modelin kalibrasyonuna CRNP bazlı toprak nemi verileri dahil edilmiş ve CRNP toprak nemi verilerinin NAM kavramsal modeline dahil edilmesinin Çakıt Havzası'nda (421 km²) ve alt havzalarından biri olan Darboğaz alt havzası'nda (121 km²) model istatistiklerini geliştirdiği sonucuna ulaşılmıştır. NAM modelini kalibre etmek için CRNP bazlı toprak nemi verilerinin kullanılması, Çakıt Havzası debi verileri için Kling-Gupta Verimlilik skorunu 0,56 (Kalibrasyon) ve 0,42 (Doğrulama)'dan 0,81 (Kalibrasyon) ve 0,64 (Doğrulama)'ya yükseltmiştir. Hem Çakıt Havzası hem de Darboğaz Alt Havzası için istatistiksel ölçütlerin çoğunda benzer gelişmeler kaydedilmiştir.

Anahtar Kelimeler: Kozmik Işın Nötron Algılama, Toprak Nemi, NAM Kavramsal Modeli, Uydu Toprak Nemi Ürünleri

To My Daughter Defne

ACKNOWLEDGMENTS

I would like to express my sincere gratitude to my supervisor Prof. Dr. Zuhâl Akyürek for her support and guidance throughout the research.

I would also like to thank to the jury members, Prof. Dr. İsmail Yücel, Prof. Dr. Mehmet Akif Sarıkaya, Assoc. Prof. Dr. Koray K. YILMAZ and Dr. Arda Şorman for their time and valuable comments that helped a lot to improve the thesis.

I am grateful to TUBITAK, the Scientific and Technological Research Council of Turkey, BİDEB 2211-A General National Doctorate Scholarship Program for the financial support that has been received during the PhD education.

I would also like to express my appreciation to all of the directors of the General Directorate of Water Management; General Director Bilal Dikmen, Deputy General Director Maruf Aras, Head of Department Satuk Buğra Fındık and Head of Working Group Ahmet Murat Özeltin for encouraging me to conduct this study and providing me great convenience and ease. I would also like thank all of my co-workers for their support and motivation.

I owe many thanks to Çağrı Karaman and Kenan Bolat for their invaluable technical supports. I would also like to thank my friend M.Kemal Ardoğa for his endless support throughout my graduate education.

I also express my sincere appreciation to my parents and my brother for supporting me in the most difficult times and motivating me to keep going no matter what. Without their support and encouragement this thesis would not have been completed. Saving the best for the last, my final gratitude goes to my beloved daughter. It is always a great honor to be her father.

TABLE OF CONTENTS

ABSTRACT	v
ÖZ	vii
ACKNOWLEDGMENTS	x
TABLE OF CONTENTS	xi
LIST OF TABLES	xvi
LIST OF FIGURES	xvii
LIST OF ABBREVIATIONS	xxvi
CHAPTERS	
1 INTRODUCTION	1
1.1 General	1
1.2 Problem Statement	3
1.3 Objectives	4
1.3.1 Thesis Outline	5
2 METHODS OF SOIL MOISTURE DETERMINATION AND COSMIC RAY NEUTRON SENSING	7
2.1 General	7
2.2 Methods of Obtaining Soil Moisture Data	7
2.2.1 Determination of Soil Moisture by Laboratory Testing (Direct Method)	8

2.2.2	Determination of Soil Moisture by Using the Capillary Tension in Soil	8
2.2.3	Determination of Soil Moisture Using the Dielectric Properties of Soil (TDR, FDR and GPR)	9
2.2.4	Determination of Soil Moisture by Using the Heat Capacity of Soil	9
2.2.5	Determination of Soil Moisture by Using Micro Electro Mechanical System (MEMS)	10
2.2.6	Determination of Soil Moisture by Using Neutron Scattering Techniques	10
2.2.6.1	Cosmic Ray Neutron Sensing (CRNS)	10
2.2.7	Determination of Soil Moisture by Using Gamma Rays	11
2.2.8	Remote Sensing of Soil Moisture	11
3	STUDY AREA, DATASETS AND METHODOLOGY	13
3.1	Description of the Study Area	13
3.2	Data	17
3.2.1	Cosmic Ray Neutron Probe (CRNP) Data	17
3.2.1.1	Correction of Neutron Counts	18
3.2.1.2	Obtaining Soil Moisture Data from Çakıt Basin CRNP	21
3.2.2	CRNP Networks	24
3.2.3	Satellite Soil Moisture Data	24
3.2.3.1	METOP-A/B Advanced Scatterometer (ASCAT)	24
3.2.3.2	Soil Moisture and Ocean Salinity (SMOS)	26
3.2.3.3	Soil Moisture Active and Passive (SMAP)	26
3.2.3.4	Advanced Microwave Scanning Radiometer (AMSR)	27

3.2.3.5	Climate Change Initiative (CCI)	27
3.2.3.6	Global Land Data Assimilation System (GLDAS) and Noah LSM	28
3.2.4	Discharge Data	30
3.3	Methodology	30
3.4	Statistical Measures Used In this Study	31
3.4.1	Nash Sutcliffe Efficiency (NSE) and Logarithmic Nash Sut- cliffe Efficiency (logNSE)	31
3.4.2	Root Mean Square Error (RMSE) and Unbiased Root Mean Square Error (ubRMSE)	33
3.4.3	Percent Bias (PBIAS)	34
3.4.4	Coefficient of Determination (r^2)	34
3.4.5	Relative Volume Error (VE)	34
3.4.6	Kling-Gupta Efficiency (KGE)	34
4	VALIDATION OF SATELLITE BASED SOIL MOISTURE PRODUCTS	37
4.1	General	37
4.2	Satellite Based Soil Moisture Products	38
4.3	Methodology of Validation	40
4.3.1	Triple Collocation	40
4.4	Comparison of Soil Moisture Products	41
4.4.1	Comparison of Soil Moisture Products for Çakıt Basin	41
4.4.2	Comparison of Soil Moisture Products for COSMOS Database	44
4.5	Summary and Discussion of the Results	49
5	ASSESSMENT OF THE RELATION BETWEEN EVAPORATION AND SOIL MOISTURE	53

5.1	General	53
5.2	Evaporation Data of the Study Area	54
5.3	Methodology of Comparing Soil Moisture and Evaporation	55
5.4	Results	58
5.4.1	The Relation Between Evapotranspiration and Soil Moisture Products of GLDAS	58
5.4.2	The Relation Between Evapotranspiration and CRNP Based Soil Moisture	58
5.5	Summary and Discussion of the Results	67
6	INTEGRATION OF SOIL MOISTURE DATA INTO HYDROLOGICAL MODELLING	69
6.1	General	69
6.2	Hydrological Models	70
6.2.1	NAM Model	71
6.2.2	Noah Land Surface Model	74
6.3	The Use of Soil Moisture Data in NAM Conceptual Hydrological Model	74
6.3.1	Obtaining Soil Moisture Time Series for NAM	75
6.3.1.1	SMAP Based Soil Moisture Data for the Root Zone	75
6.3.1.2	CRNP Based Continuous Soil Moisture Data for the Root Zone	76
6.3.2	Calculation of Root Zone Soil Moisture	76
6.3.3	Calibration of the Parameters in NAM model	78
6.3.4	Setup of the NAM Model	81
6.4	Results of the Hydrological Modelling	83

6.5	Comparison of Basin Water Balance with Observed and Simulated Soil Moisture Data	95
6.6	Summary and Discussion of the Results	97
7	CONCLUSIONS AND RECOMMENDATIONS	101
7.1	Conclusions	101
7.2	Recommendations	104
	REFERENCES	107
APPENDICES		
A	THE DIRECT RELATIONS BETWEEN SOIL MOISTURE PRODUCTS EXAMINED IN THIS STUDY WITH IN-SITU SOIL MOISTURE OBSERVATIONS	127
B	MAPS OF STATISTICAL MEASURES FOR SATELLITE PRODUCTS VS. COSMOS DATABASE	133
C	EVAPORATION AND SOIL MOISTURE CORRELATION MAPS FOR GLDAS	157
D	GRAPHS OF SENSITIVITY ANALYSIS FOR THE WEIGHT FACTOR	165
	CURRICULUM VITAE	173

LIST OF TABLES

TABLES

Table 4.1	Satellite soil moisture products that are compared with Çakıt Station CRNP soil moisture content data.	39
Table 4.2	Mean Values of r^2 , RMSE, ubRMSE and bias values of soil moisture products with CRNPs	47
Table 4.3	Median Values of r^2 , RMSE, ubRMSE and bias values of soil moisture products with CRNPs	47
Table 6.1	Statistical Measures of NAM simulations with Respect to the Calibration Methods - Çakıt Basin	90
Table 6.2	Statistical Measures of NAM simulations with Respect to the Calibration Methods - Darboğaz sub-basin	91

LIST OF FIGURES

FIGURES

Figure 3.1	Study Area: Çakıt Basin and Darboğaz Sub-Basin, CRNP, Stream-flow Gauging Stations and SMAP pixels whose centers are within the basin	14
Figure 3.2	Hypsometric curves of Çakıt Basin and Darboğaz sub-basin . . .	15
Figure 3.3	CRNP Located at the Çakıt Basin	15
Figure 3.4	a) The cumulative fraction of neutron counts and the distance from the device for both dry (straight line) and wet (dashed line) soil indicating the horizontal footprint of a CRNP, b) The cumulative fraction of neutron counts and depth beneath the soil for both dry and wet soil indicating the vertical footprint of a CRNP [1]	16
Figure 3.5	a) Sampling locations for initial calibration of CRNP b) One of the soil samples obtained during the initial calibration study [61]	18
Figure 3.6	Iso-rigidity contours for vertical geomagnetic cutoff rigidities [69]	20
Figure 3.7	Precipitation, mean temperature, soil moisture measurements (TDR), soil temperature and snow height data observed at the site. . . .	22
Figure 3.8	a) Correction factors for pressure, humidity and cosmic ray intensity, b) Combination of environmental correction factors	23
Figure 3.9	Corrected neutron counts of CRNP (red) and corresponding soil moisture time series (blue).	25
Figure 3.10	Input Parameters of NOAH LSM that are used in the analyses . .	29

Figure 3.11	Discharge Data of Çakıt Basin and Darboğaz Sub-Basin	30
Figure 3.12	Schematic Representation of the Methodology	32
Figure 4.1	Comparisons of time series for different soil moisture products with CRNP. CRNP soil moisture values are shown in black, excluded days due to snow are shown in grey, other soil moisture products are shown in different colors.	42
Figure 4.2	Comparisons of the anomalies (with respect to fifteen days averages) for different soil moisture products with the anomalies of CRNP. CRNP soil moisture values are shown in black, excluded days due to snow are shown in grey, other soil moisture products are shown in different colors.	43
Figure 4.3	a) r^2 and b)RMSE values between Satellite and CRNP Based Soil Moisture Data. Points in red indicate Çakıt Basin CRNP, gray points indicate the other CRNP stations and pink lines indicate the average values.	45
Figure 4.4	a) Bias and b)ubRMSE values between Satellite and CRNP Based Soil Moisture Data. Points in red indicate Çakıt Basin CRNP, gray points indicate the other CRNP stations and pink lines indicate the average values.	46
Figure 4.5	Triple collocation errors of soil moisture products of data triplets including SMAP (a) rootzone and (b) surface products, average values are indicated with pink lines.	48
Figure 5.1	Time series of actual daily evapotranspiration values of GLDAS, Noah LSM and Eddy covariance sensor for Çakıt Basin.	56
Figure 5.2	Time series of scaled soil moisture and evapotranspiration products.	57

Figure 5.3	r^2 values of the comparison between GLDAS Noah LSM soil moisture and evapotranspiration outputs	59
Figure 5.4	The relation between CRNP based daily volumetric soil moisture and evaporation values based on a) GLDAS b) Local Noah LSM c) Eddy Covariance Sensor.	60
Figure 5.5	a) r^2 and b) RMSE c) r^2 of the quantiles of CRNP based standardized soil moisture and GLDAS based standardized actual evapotranspiration data.	61
Figure 5.6	a) RMSE values between standardized GLDAS evapotranspiration outputs and soil moisture data of COSMOS stations shown on the world map b) Histogram of RMSE values.	62
Figure 5.7	a) r^2 values between standardized GLDAS evapotranspiration outputs and soil moisture data of COSMOS stations shown on the world map b) Histogram of r^2 values.	63
Figure 5.8	Cumulative Distribution Functions of Soil Moisture (CRNP) and Evapotranspiration (Noah LSM or Eddy). (Blue:Soil Moisture, Red:Evapotranspiration)	64
Figure 5.9	Cumulative Distribution Functions of daily changing values for Soil Moisture (CRNP) and Evapotranspiration (Noah LSM or Eddy). (Blue:Soil Moisture, Red:Evapotranspiration)	65
Figure 5.10	Q-Q Plots of Soil Moisture (CRNP) and Evapotranspiration (Noah LSM or Eddy). (Blue:Soil Moisture, Red:Evapotranspiration)	66
Figure 6.1	Schematic Representation of Modeling with NAM [155]	71
Figure 6.2	Estimated Soil Moisture Profiles of Çakıt Basin by Richards Equation	78
Figure 6.3	Estimated root zone soil moisture values of CRNP and SMAP based soil moisture	79

Figure 6.4	Effective depth of CRNP soil moisture observations, water balance, root zone soil moisture along with the meteorological data for Çakıt and Darboğaz Basins	82
Figure 6.5	Hydrological model parameters obtained from different calibration methods for Çakıt Basin	83
Figure 6.6	Hydrological model parameters obtained from different calibration methods for Darboğaz sub-basin	84
Figure 6.7	Simulated and Observed Discharge Values for Çakıt basin, vertical dashed line indicates the calibration and validation periods	86
Figure 6.8	Simulated and Observed Discharge Values for Çakıt basin (Logarithmic Scale), vertical dashed line indicates the calibration and validation periods	87
Figure 6.9	Simulated and Observed Discharge Values for Darboğaz sub-basin, vertical dashed line indicates the calibration and validation periods	88
Figure 6.10	Simulated and Observed Discharge Values for Darboğaz sub-basin (Logarithmic Scale), vertical dashed line indicates the calibration and validation periods	89
Figure 6.11	Statistical measures for Calibration period - Çakıt Basin.	92
Figure 6.12	Statistical measures for Validation period - Çakıt Basin.	93
Figure 6.13	Statistical measures for Calibration period - Darboğaz sub-basin.	94
Figure 6.14	Statistical measures for Validation period - Darboğaz sub-basin.	95
Figure 6.15	Variables of Water Balance Calculations for Çakıt Basin and Darboğaz sub-basin, vertical dashed line indicates the calibration and validation periods	96
Figure 6.16	Comparison of Water Balance and Model Soil Moisture Outputs of Çakıt Basin and Darboğaz sub-basin	97

Figure A.1	AMSR (ascending) soil moisture vs. a) CRNP and b) TDR . . .	127
Figure A.2	AMSR (descending) soil moisture vs. a) CRNP and b) TDR . . .	127
Figure A.3	SMOS (ascending) soil moisture vs. a) CRNP and b) TDR . . .	128
Figure A.4	SMOS (descending) soil moisture vs. a) CRNP and b) TDR . . .	128
Figure A.5	ASCAT soil moisture vs. a) CRNP and b) TDR	129
Figure A.6	SMAP surface soil moisture vs. a) CRNP and b) TDR	129
Figure A.7	SMAP rootzone soil moisture vs. a) CRNP and b) TDR	130
Figure A.8	CCI soil moisture vs. a) CRNP and b) TDR	130
Figure A.9	GLDAS soil moisture vs. a) CRNP and b) TDR	131
Figure A.10	NOAH LSM soil moisture vs. a) CRNP and b) TDR	131
Figure B.1	a) r^2 values between SMAP surface product and COSMOS stations shown on the world map b) Histogram of r^2 values between SMAP surface product and COSMOS stations	133
Figure B.2	a) r^2 values between SMAP rootzone product and COSMOS stations shown on the world map b) Histogram of r^2 values between SMAP rootzone product and COSMOS stations	134
Figure B.3	a) r^2 values between ASCAT and COSMOS stations shown on the world map b) Histogram of r^2 values between ASCAT and COSMOS stations	135
Figure B.4	a) r^2 values between SMOS descending node product and COSMOS stations shown on the world map b) Histogram of r^2 values between SMOS descending node product and COSMOS stations	136
Figure B.5	a) r^2 values between SMOS ascending node product and COSMOS stations shown on the world map b) Histogram of r^2 values between SMOS ascending node product and COSMOS stations	137

Figure B.6	a) r^2 values between AMSR descending node product and COSMOS stations shown on the world map b) Histogram of r^2 values between AMSR descending node product and COSMOS stations	138
Figure B.7	a) r^2 values between AMSR ascending node product and COSMOS stations shown on the world map b) Histogram of r^2 values between AMSR ascending node product and COSMOS stations	139
Figure B.8	a) r^2 values between GLDAS and COSMOS stations shown on the world map b) Histogram of r^2 values between GLDAS and COSMOS stations	140
Figure B.9	a) RMSE values between SMAP surface product and COSMOS stations shown on the world map b) Histogram of RMSE values between SMAP surface product and COSMOS stations	141
Figure B.10	a) RMSE values between SMAP rootzone product and COSMOS stations shown on the world map b) Histogram of RMSE values between SMAP rootzone product and COSMOS stations	142
Figure B.11	a) RMSE values between ASCAT and COSMOS stations shown on the world map b) Histogram of RMSE values between ASCAT and COSMOS stations	143
Figure B.12	a) RMSE values between SMOS descending node product and COSMOS stations shown on the world map b) Histogram of RMSE values between SMOS descending node product and COSMOS stations	144
Figure B.13	a) RMSE values between SMOS ascending node product and COSMOS stations shown on the world map b) Histogram of RMSE values between SMOS ascending node product and COSMOS stations .	145
Figure B.14	a) RMSE values between AMSR descending node product and COSMOS stations shown on the world map b) Histogram of RMSE values between AMSR descending node product and COSMOS stations	146

Figure B.15	a) RMSE values between AMSR ascending node product and COSMOS stations shown on the world map b) Histogram of RMSE values between AMSR ascending node product and COSMOS stations .	147
Figure B.16	a) RMSE values between GLDAS and COSMOS stations shown on the world map b) Histogram of r^2 values between GLDAS and COSMOS stations	148
Figure B.17	a) ubRMSE values between SMAP surface product and COSMOS stations shown on the world map b) Histogram of ubRMSE values between SMAP surface product and COSMOS stations	149
Figure B.18	a) ubRMSE values between SMAP rootzone product and COSMOS stations shown on the world map b) Histogram of ubRMSE values between SMAP rootzone product and COSMOS stations	150
Figure B.19	a) ubRMSE values between ASCAT and COSMOS stations shown on the world map b) Histogram of ubRMSE values between ASCAT and COSMOS stations	151
Figure B.20	a) ubRMSE values between SMOS descending node product and COSMOS stations shown on the world map b) Histogram of ubRMSE values between SMOS descending node product and COSMOS stations	152
Figure B.21	a) ubRMSE values between SMOS ascending node product and COSMOS stations shown on the world map b) Histogram of ubRMSE values between SMOS ascending node product and COSMOS stations .	153
Figure B.22	a) ubRMSE values between AMSR descending node product and COSMOS stations shown on the world map b) Histogram of ubRMSE values between AMSR descending node product and COSMOS stations	154
Figure B.23	a) ubRMSE values between AMSR ascending node product and COSMOS stations shown on the world map b) Histogram of ubRMSE values between AMSR ascending node product and COSMOS stations .	155

Figure B.24	a) ubRMSE values between GLDAS and COSMOS stations shown on the world map b) Histogram of ubRMSE values between GLDAS and COSMOS stations	156
Figure C.1	r^2 values of the comparison between monthly averages of GLDAS Noah LSM soil moisture and evapotranspiration outputs	157
Figure C.2	r^2 values of the comparison between weekly averages of GLDAS Noah LSM soil moisture and evapotranspiration outputs	158
Figure C.3	r^2 values of the comparison between GLDAS Noah LSM soil moisture and evapotranspiration outputs for January	158
Figure C.4	r^2 values of the comparison between GLDAS Noah LSM soil moisture and evapotranspiration outputs for February	159
Figure C.5	r^2 values of the comparison between GLDAS Noah LSM soil moisture and evapotranspiration outputs for March	159
Figure C.6	r^2 values of the comparison between GLDAS Noah LSM soil moisture and evapotranspiration outputs for April	160
Figure C.7	r^2 values of the comparison between GLDAS Noah LSM soil moisture and evapotranspiration outputs for May	160
Figure C.8	r^2 values of the comparison between GLDAS Noah LSM soil moisture and evapotranspiration outputs for June	161
Figure C.9	r^2 values of the comparison between GLDAS Noah LSM soil moisture and evapotranspiration outputs for July	161
Figure C.10	r^2 values of the comparison between GLDAS Noah LSM soil moisture and evapotranspiration outputs for August	162
Figure C.11	r^2 values of the comparison between GLDAS Noah LSM soil moisture and evapotranspiration outputs for September	162

Figure C.12	r^2 values of the comparison between GLDAS Noah LSM soil moisture and evapotranspiration outputs for October	163
Figure C.13	r^2 values of the comparison between GLDAS Noah LSM soil moisture and evapotranspiration outputs for November	163
Figure C.14	r^2 values of the comparison between GLDAS Noah LSM soil moisture and evapotranspiration outputs December	164
Figure D.1	KGE Values for different weight factors used for joint calibration of NAM model a) Çakıt Basin b) Darboğaz Sub-Basin	166
Figure D.2	logNSE Values for different weight factors used for joint calibration of NAM model a) Çakıt Basin b) Darboğaz Sub-Basin	167
Figure D.3	NSE Values for different weight factors used for joint calibration of NAM model a) Çakıt Basin b) Darboğaz Sub-Basin	168
Figure D.4	PBIAS Values for different weight factors used for joint calibration of NAM model a) Çakıt Basin b) Darboğaz Sub-Basin	169
Figure D.5	r^2 Values for different weight factors used for joint calibration of NAM model a) Çakıt Basin b) Darboğaz Sub-Basin	170
Figure D.6	RMSE Values for different weight factors used for joint calibration of NAM model a) Çakıt Basin b) Darboğaz Sub-Basin	171
Figure D.7	VE Values for different weight factors used for joint calibration of NAM model a) Çakıt Basin b) Darboğaz Sub-Basin	172

LIST OF ABBREVIATIONS

AMSR	Advanced Microwave Scanning Radiometer
ASCAT	METOP-A/B Advanced Scatterometer
BEC	Barcelona Experts Center
CCI	Climate Change Initiative
COSMOS	The COsmic-ray Soil Moisture Observing System
CRNP	Cosmic Ray Neutron Probe
CRNS	Cosmic Ray Neutron Sensing
EOSDIS	NASA's Earth Observing System Data and Information System
ESA	European Space Agency
EUMETSAT	European Organisation for the Exploitation of Meteorological Satellites
GLDAS	Global Land Data Assimilation System
H-SAF	EUMETSAT Satellite Application Facility on Support to Operational Hydrology and Water Management
HWSDDB	Harmonized World Soil Database
JAXA	Japan Aerospace Exploration Agency
KGE	Kling-Gupta Efficiency
LIS	Land Information System
logNSE	Logarithmic Nash Sutcliffe Efficiency
NASA	The National Aeronautics and Space Administration
NDVI	Normalized Difference Vegetation Index
NMDB	Neutron Monitor Database
NOAH LSM	NOAH Land Surface Model
NSE	Nash Sutcliffe Efficiency

PBIAS	Percent Bias
RMSE	Root Mean Square Error
SMAP	Soil Moisture Active and Passive
SMOS	Soil Moisture and Ocean Salinity
TERENO	Terrestrial Observation Network
ubRMSE	Unbiased Root Mean Square Error
VE	Relative Volume Error

CHAPTER 1

INTRODUCTION

1.1 General

Soil moisture measurement is the key element of hydrological cycle, since knowing the soil moisture helps calculation of the other unknowns of the hydrological cycle such as evaporation and infiltration. From an agricultural point of view, soil moisture is the most important element for decision making processes of irrigation systems. Soil moisture measurements are also vital for prediction and assessment of water related disasters such as floods and droughts. Measurement of soil moisture is possible via several methods, which differ by certain factors such as spatio-temporal accuracy, ease of application and environmental friendliness. Among many other methods, as one of the most recently invented method, Cosmic Ray Neutron Probes (CRNPs) [1] proposes a promising alternative for providing the valuable soil moisture information required for the basin scale hydrological studies. Measurement of soil moisture amount using CRNPs solely depends on the inverse relation between the amount of water available within the measurement range of CRNP and the decelerated neutron counts. The dynamics of the inverse relation depends on environmental and atmospheric factors as well as the intensity of the incoming cosmic rays. Although CRNP is not the first device exploiting the above mentioned relation between neutron counts and water availability, it is the first device of this type that does not include any radioactive content, which makes it possible to measure soil moisture continuously by leaving the device unattended at study area.

The first neutron counting device is known to be developed after the World War II [2] and the first appearance of the relation between neutron counts and soil moisture in

literature was in 1952 ([3]). The main principle of determination of soil moisture by using neutron probes is as follows; fast neutrons which are generated by a neutron source are decelerated by soil moisture and then counted by a neutron probe. In a previously prepared calibration curve, the amount of soil moisture corresponding to the number of decelerated neutrons can be obtained directly. For conventional neutron probes, radioactive materials are used as a fast neutron source. Radioactive material, usually a mixture of americium beryllium, must be buried to the depth at which moisture is measured. The difficulty and risk of controlling the radioactive substances by means of environmental aspects limit the use of these devices.

Cosmic rays, which include high energy atomic particles and originate from the outer space, were first discovered in 1912 [4]. The secondary particles that emerge as a result of the contact between atmospheric cosmic rays and earth were discovered in 1952 [5]. The effect of soil moisture on low-energy (1 keV) neutron intensity at the lower layer of atmosphere was presented theoretically by Bethe and coworkers [6] and practically using cosmic ray neutrons by Hendrick and Edge [7]. The inverse relation between cosmic ray neutron intensity and soil moisture was shown by Kodama and coworkers [8]. The required methodology of measuring low energy cosmogenic neutrons via proportional counters was presented by Knoll [9].

In order to overcome the limitation for neutron probes, a non-radioactive and clean source of neutron had to be found. As an environmentally friendly alternative, a recently invented CRNP uses cosmic rays as the neutron source [1]. With this approach, soil moisture content can be inferred from the measurements of low-energy cosmic ray neutrons that are generated within soil, moderated mainly by hydrogen atoms, and diffused back to the atmosphere. Neutron intensity above the surface is inversely correlated with the hydrogen content of the soil and hydrogen content is a good indicator of water (H_2O) availability [1]. Since this method does not have environmental limitations such as the conventional one, the probes can be carried easily and left in the field unattended. This feature enables continuous monitoring of soil moisture and computerized automatizing of measurements. Furthermore, relatively large footprint of CRNP (approximately a circle having a diameter of 670m) enables soil moisture monitoring on a hectometer scale [10]. This method is also capable of detecting all of the parameters of hydrological cycle (such as precipitation, infiltration, snow, runoff

and biomass) except evaporation and transpiration [11].

1.2 Problem Statement

As one of the key elements of the hydrological cycle, soil moisture data are vital for all kinds of applications which involve hydrology. Most of the applications in hydrology, such as flood or drought early warning and agricultural management systems rely on the soil moisture data. Despite its crucial importance, in most of the cases, it is still challenging to obtain reliable soil moisture information for such studies, since measuring soil moisture within the desired time and spatial scales of an hydrological application, either requires a great workload and financial support or is inaccurate/insufficient to be used for decision making. For example, it is vital to accurately estimate the discharge for flood forecasting which often requires a hydrological model involving reliable precipitation, evaporation and, in some cases, the soil moisture data. The above mentioned variables are all related to each other, hence the efficiency of an hydrological model is expected to be increased by involving as many variables as possible. However, the performance of such models depend on the quality of the input data. Hydrological studies are often conducted in a basin scale where the spatial representation of point scale data is not sufficient. Remote sensing data can be also widely used in hydrological studies however, the spatial resolution of these products is usually too coarse for hydrological studies and temporal resolution is too sparse.

Soil moisture data that should be used in an hydrological application have to be temporally continuous and spatially representative. In 2008, in order to meet the specified need, a group of researchers have invented a new technique of soil moisture determination, which is called the Cosmic Ray Neutron Sensing (CRNS) [1]. This technique is based on the inverse relation between low-energy cosmic ray neutrons and the presence of Hydrogen atoms. In the soil structure, hydrogen is primarily in the form of H_2O and most of the times the amount of hydrogen is negligible in forms other than water. Consequently, inferring soil moisture is possible by measuring decelerated cosmic ray neutrons and making use of the above-mentioned inverse relation. There are two main advantages of using CRNPs in hydrological modelling, firstly the rel-

atively large footprint of CRNP (approximately a circle having a diameter of 670m) enables soil moisture monitoring on a hectometer scale [10] which helps preventing the irregularities in the field properties from creating misleading results as in the case of point scale measurement techniques; secondly the probes contain solar panels and remote communication devices, in other words they are self sufficient and can be carried easily and left in the field unattended which allows it to produce data with high temporal resolution in real time.

Advances in satellite technology in recent years have enabled satellite soil moisture products to be used in many hydrological studies [12, 13, 14]. However, validation of satellite soil moisture products is a necessity due to low spatial and temporal resolution of satellite soil moisture data especially to produce reliable hydrological data for ungauged locations, thus there are numerous studies involving validation of satellite products by using in-situ soil moisture observations [15, 16, 17]. The relatively larger horizontal footprint of CRNPs and their ability to provide continuous data creates an important opportunity to use their promising spatial and temporal resolution in the validation of soil moisture satellite products [18]. The above mentioned ability of CRNPs are also discussed in our previously published paper [19].

In addition to the direct measurement of hydrological cycle parameters such as stream flow and soil moisture, estimation of these parameters with a modeling approach based on their interrelationship is also a very important tool for the science of hydrology. Among various types of hydrological models, conceptual models are one of the most common tools to mimic the rainfall runoff relation of a specific basin. While these type of models are calibrated through observed discharge values, including other parameters of the hydrological cycle has also been discussed in many studies [20, 21, 22, 23]. Basin or sub-basin scale coverage of CRNP uniquely suits to the task of improving conceptual hydrological models [24].

1.3 Objectives

The aim of this study is to assess the effectiveness of Cosmic Ray Neutron Probes (CRNPs) in determination of soil moisture from neutron counts at intermediate scale

and making use of them in hydrological models. The effectiveness of CRNPs in validation of soil moisture satellite products has also been tested against different satellite products to further assess the potential of using CRNPs in satellite product validation. The main objectives of this study are listed below:

- To retrieve soil moisture data by making use of the neutron counts with CRNP and evaluate the obtained soil moisture values by other sources of information on soil moisture.
- To validate remote sensing based soil moisture data and land surface models by using several CRNPs installed all around the world.
- To investigate the relation between evaporation and CRNP based soil moisture.
- To make use of soil moisture data obtained from CRNPs in hydrological modeling.

1.3.1 Thesis Outline

In this study, an application with Cosmic Ray Neutron Sensing (CRNS), which is one of the most promising soil moisture sensing techniques, is presented. The detailed descriptions of various soil moisture retrieval methods including CRNS are given in Chapter 2. In this thesis, studies are conducted by making use of the datasets obtained for Çakıt Basin, which is located at the southern part of Turkey. Detailed information for the basin and the datasets used in this study are provided in Chapter 3. CRNS has a promising potential to be used for satellite validation due its intermediate scale footprint. Validation of satellite soil moisture products with CRNP's of the COSMOS database and Çakıt Basin CRNP are provided in Chapter 4. The relation between CRNP soil moisture and evaporation has also been thoroughly investigated in Chapter 5. In Chapter 6, the use of CRNP in rainfall-runoff modeling is presented. The related literature reviews and discussions are provided in each chapter, namely Chapter 4, Chapter 5 and Chapter 6. Conclusions and recommendations are provided in Chapter 7.

CHAPTER 2

METHODS OF SOIL MOISTURE DETERMINATION AND COSMIC RAY NEUTRON SENSING

2.1 General

Soil moisture is the amount of water that is kept by the soil medium. Understanding the soil moisture and its relation with other elements of water cycle is an essential part of hydrology. In practical applications such as flood or drought management, knowing the amount of water inside the soil is vital for the decision making systems. Correspondingly, the importance of knowing the soil moisture lead researchers develop several techniques to measure or infer soil moisture. A few of the most well known techniques are explained in Section 2.2. Models are often used in hydrology to estimate unknown or future conditions (e.g. run-off) based on other elements of the cycle. Various types of models used in hydrology and the intrusion of CRNP soil moisture data into these models are discussed in Section 6.3.

2.2 Methods of Obtaining Soil Moisture Data

Measurement of soil moisture is possible via several methods including: laboratory tests and time domain reflectometers (having high accuracies but smaller measurement footprints), ground penetrating radar and remote sensing methods (having large measurement footprints but lower accuracies and resolutions). More recently invented Cosmic Ray Neutron Probes (CRNPs) propose an intermediate alternative to the above mentioned methods with a footprint of a circle having a diameter of approximately 670m. There are numerous methods to obtain information on soil moisture

including but not limited to the ones mentioned in this thesis.

2.2.1 Determination of Soil Moisture by Laboratory Testing (Direct Method)

The properties of different states of soil moisture and measurement of soil moisture via laboratory testing were presented more than a century ago [25]. Within the long process after the first presentation of the calculation of soil moisture by gravimetric methods, numerous different soil moisture detection methods have been developed. However, measurement of soil moisture via the direct method is still the most reliable method of measurement by means of its accuracy. On the other hand, the high accuracy of this technique comes with a great cost, it requires enormous amount of workforce and resources to obtain soil moisture compared to the other methods. Spatial scale of the measurements are very limited, thus obtaining soil moisture at basin scale requires measurements in several different locations of the basin. The measurements with laboratory testing provide information for a single point in time, thus continuous monitoring with acceptable temporal resolution is not possible with this method.

2.2.2 Determination of Soil Moisture by Using the Capillary Tension in Soil

Measurement of soil moisture is also possible via measuring the changes in hydrostatic pressure inside the soil by using tensiometers [26, 27]. Although hydrostatic pressure is a direct indicator of soil moisture availability, tensiometers can only measure low hydrostatic pressures properly, thus measurements with this technique can not be made for higher soil moisture values and they are only available for a limited range of low values [28]. Besides the disadvantage on data availability, workforce and resources required for this technique are much lower than the direct method, and if regularly maintained, the same probe can be used repeatedly.

2.2.3 Determination of Soil Moisture Using the Dielectric Properties of Soil (TDR, FDR and GPR)

Methods of using the dielectric properties of soil depends on the predefined relation between the dielectric constant and wetness of the soil. In other words, soil moisture can be inferred through measuring the dielectric constant [29]. Time Domain Reflectometry (TDR) and Frequency Domain Reflectometry (FDR) are the two main methods exploiting the relation between dielectric constant and soil moisture. There is a temporal delay between the emitted and reflected electromagnetic pulses produced by TDR within the soil. The dielectric permeability of the soil can be determined by measuring the amount of this delay [30]. TDR provides great ease for studies require high temporal resolution since measurements with the same probe can be made repeatedly and it is possible to automate the measurement process [31]. FDR, on the other hand, is a capacitive technique which depends on the charging time of a capacitor which is formed by the electrodes embedded in the soil [32, 33]. The capacitor is connected to an oscillator to form an electric circuit. The operating frequency of the circuit indicates the dielectric constant, thus the soil moisture content. Unlike TDR, FDR depends on the soil properties and requires calibration before usage [34]. After the invention of earth observation radars which transmit pulses underground and measure the travel speeds of the waves, the Ground Penetrating Radar (GPR) technology was adopted to infer soil moisture data. GPR provide information about the permeability and dielectric constant of the soil by measuring the reflection speeds of high frequency electromagnetic waves beneath the soil [35]. This non-invasive technique is capable of measuring soil moisture content at high spatial and temporal resolution. The downside of this technique is, it may not work properly for conductive soil types, and interpretation of the data obtained requires expertise of end-users thus automation of the process is rather difficult with respect to the other methods [36].

2.2.4 Determination of Soil Moisture by Using the Heat Capacity of Soil

Another method to detect soil moisture, albeit indirectly, is to measure the heat dissipation or heat capacity of the soil. Devices using this technique depend on the predefined relation between heat capacity and the soil moisture[37]. There are vari-

ous devices, which function on the above-mentioned relation including heat pulse and heat flux sensors and thermal dissipation blocks [38, 39].

2.2.5 Determination of Soil Moisture by Using Micro Electro Mechanical System (MEMS)

A recently invented MEMS uses high technology nano-sensors to measure temperature and soil moisture at point scale indirectly via measuring the shear resistance occurs on the sensor [40]. Recent studies using MEMS technique suggest that in-situ soil moisture measurements by using sensors fabricated using MEMS technique produce highly reliable results by means of soil moisture and temperature [41].

2.2.6 Determination of Soil Moisture by Using Neutron Scattering Techniques

Soil moisture measurements via neutron meters depend on the ability of Hydrogen atoms to decelerate scattered fast neutrons more than any other element of the periodic table since hydrogen atoms and neutrons have similar weights and collision of fast neutrons and hydrogen atoms greatly reduces the energy of the neutron [42]. In other words, there exist an inverse relation between the amount of water and decelerated neutrons, thus, soil moisture can be inferred indirectly through counting the slow neutrons by using neutron moisture meters [3]. Conventional techniques of neutron scattering requires radioactive neutron sources, which raises serious safety concerns and it is very costly to make continuous measurements with conventional neutron meters due to their radioactive natures [43].

2.2.6.1 Cosmic Ray Neutron Sensing (CRNS)

CRNS uses a similar approach with conventional neutron meters without using any radioactive neutron source. The neutron source in this case is the cosmic ray neutrons, which hit the surface of the earth [1]. In this method, before converting decelerated neutron counts to soil moisture, several corrections must be applied to neutron counts due to changes in environmental conditions such as atmospheric pressure, water vapor

and intensity of incoming cosmic rays. More calculation details on determining soil moisture with CRNS are provided in Section 3.2.1 of this thesis. Unlike most of the other soil moisture determination techniques, neutron scattering methods including CRNP is capable of measuring soil moisture in hectare scale [44]. Soil moisture retrieval by using CRNPs in large areas are also possible via attaching the device to a rover [45]. The same technique can also be used to estimate the snowpack via attaching the device to an uncrewed aerial vehicle (UAV) [46].

2.2.7 Determination of Soil Moisture by Using Gamma Rays

Similar to the pre-definable inverse relation between decelerated neutrons and water availability, the inverse relation between gamma rays and soil moisture can also be used in determination of the soil moisture content [47]. This method is known as the Proximal Gamma Ray Spectroscopy Sensing (PGR), which has been used in many studies involving measurement of continuous soil moisture data [48, 49]. However, techniques including working with gamma rays is even more unsafe than using conventional neutron meters [36].

2.2.8 Remote Sensing of Soil Moisture

As a result of the developments in satellite technologies and optics, studies of determining soil moisture using satellite images have gained importance in recent years. Remote sensing of soil moisture mainly depends on measuring the difference between incoming rays to the Earth surface and the reflected ones. [50]. Polarized light technique and near infrared techniques are the most common approaches in remote sensing [51]. There are two main approaches in remote sensing of soil moisture: active and passive microwave sensing. In active microwave sensing, radiation is emitted from satellite to Earth surface and the reflection from the Earth surface is measured, whereas in passive microwave sensing, natural radiation coming from the earth surface is measured. METOP-A/B Advanced Scatterometer (ASCAT) [52] and Soil Moisture Active and Passive (SMAP) [53] are the examples of active remote sensing based soil moisture products, on the other hand, Soil Moisture and

Ocean Salinity (SMOS) [54], Advanced Microwave Scanning Radiometer (AMSR) [55] are the examples of passive remote sensing based soil moisture products. These products are used alone or in combination in various studies. Climate Change Initiative (CCI) dataset of European Space Agency (ESA) combines available satellite based soil moisture products to be used in studies involving satellite soil moisture [56, 57, 58].

CHAPTER 3

STUDY AREA, DATASETS AND METHODOLOGY

3.1 Description of the Study Area

The research study carried out within the scope of this thesis was conducted for Çakıt basin, which is located in the south of Turkey. Darboğaz sub-basin, which is one of the sub-basins of Çakıt Basin was also investigated for the hydrological studies. Çakıt Basin has 526 km² area and it is located in elevations between 963 m and 3450 m. Location of the basin is shown in Figure 3.1. Proportion of land at various elevations for both basins are shown with the hypsometric curves provided in Figure 3.2.

A CRS200B type Cosmic Ray Neutron Probe (Hydroinnova, USA) has been installed in the Çakıt Basin (Figure 3.3) within the scope of TUBITAK project (115Y041) at 37.5155E°-34.4979N°. The CRNP can count decelerated neutrons up to 335 meters away, in other words the horizontal footprint is within a 670m diameter [1] circle which corresponds to an area of approximately 35 hectares. Horizontal footprint has been determined by comparing the cumulative fraction of neutron counts and the distance from the device for both dry and wet soil [1] and as shown in Figure 3.4a, the horizontal footprint does not depend on the soil moisture. On the other hand, vertical footprint of the device is sensitive to soil moisture changes (Figure 3.4b, [1]) and this issue will be further discussed in Chapter 6. Inside the area of the theoretical horizontal footprint of Çakıt Basin CRNP, the natural vegetation mainly consists of short bushes, there are also young cherry trees planted in 2016.

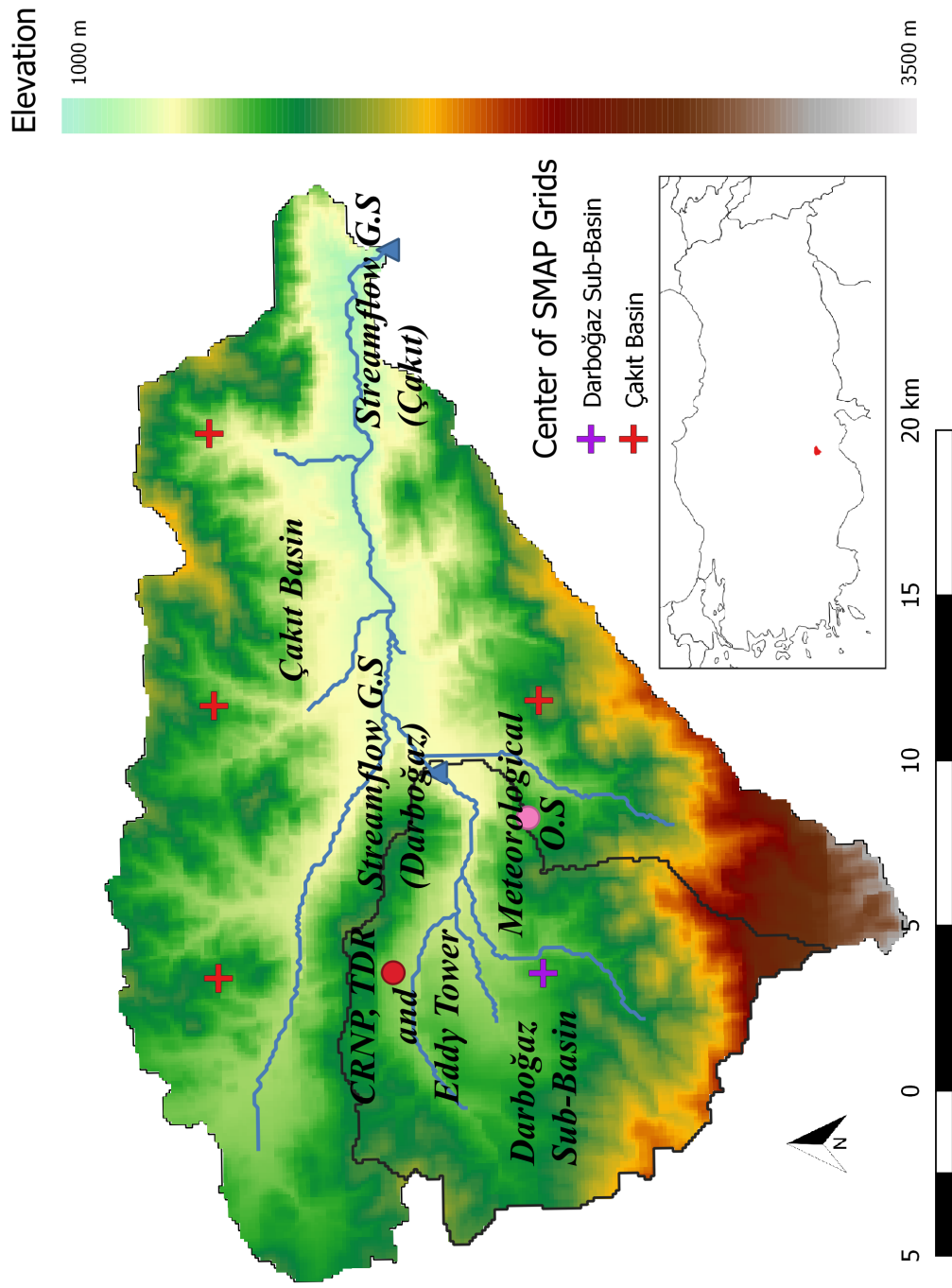


Figure 3.1: Study Area: Çakıt Basin and Darboğaz Sub-Basin, CRNP, Streamflow Gauging Stations and SMAP pixels whose centers are within the basin

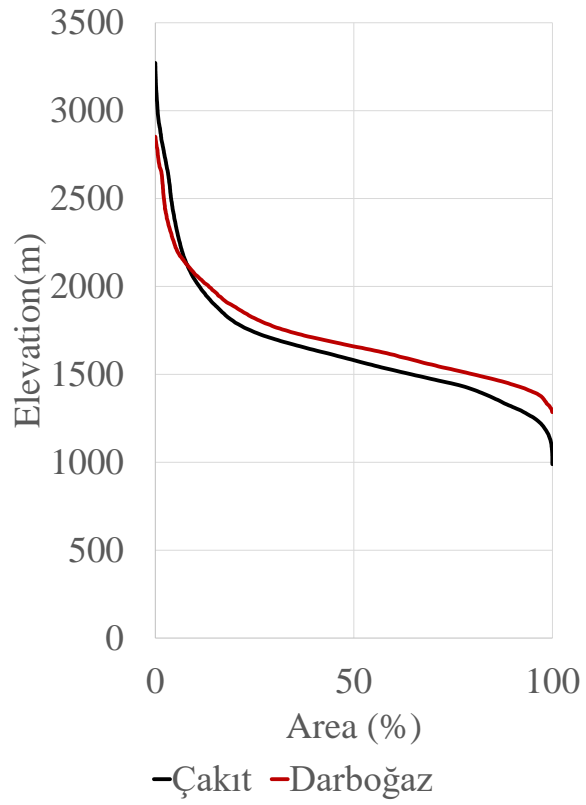
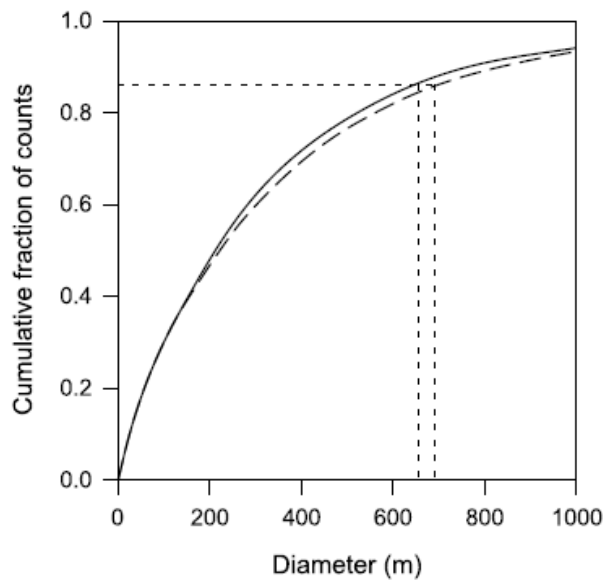


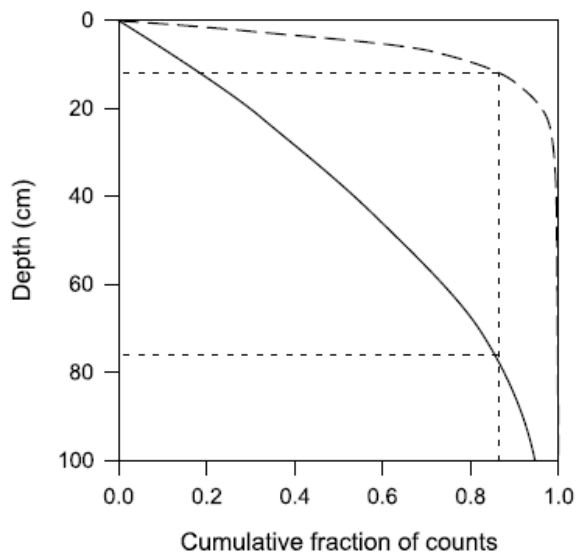
Figure 3.2: Hypsometric curves of Çakıt Basin and Darboğaz sub-basin



Figure 3.3: CRNP Located at the Çakıt Basin



(a)



(b)

Figure 3.4: a) The cumulative fraction of neutron counts and the distance from the device for both dry (straight line) and wet (dashed line) soil indicating the horizontal footprint of a CRNP, b) The cumulative fraction of neutron counts and depth beneath the soil for both dry and wet soil indicating the vertical footprint of a CRNP [1]

3.2 Data

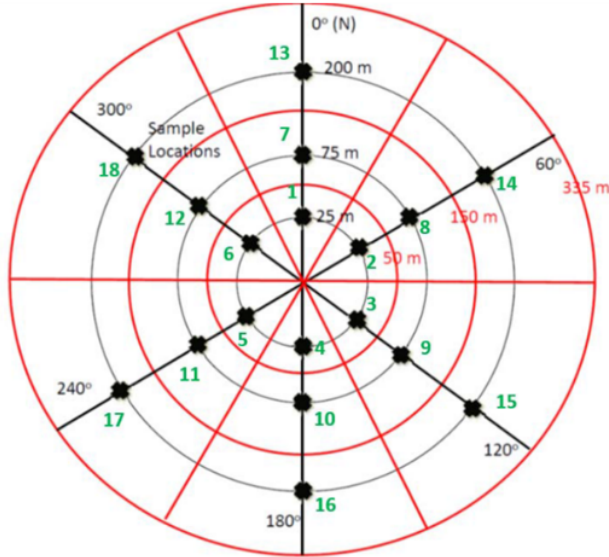
3.2.1 Cosmic Ray Neutron Probe (CRNP) Data

Although CRNP is considered as a soil moisture measurement device, what it actually measures is the decelerated neutrons which should be converted into soil moisture estimates through a series of correction conversion process. Volumetric soil moisture from CRNP can be estimated by using Eq.3.1, where N is the neutron counting rate corrected by environmental factors, θ is the volumetric water content, N_0 is the dry soil neutron counting rate under the same reference conditions. a_0 , a_1 and a_2 are the calibration constants which are taken as 0.0808, 0.372 and 0.115 in accordance with [59]. Eq.3.1 has been further developed to take into account the lattice water [45] and the amount of organic matter in the soil [60]. The formulation established by considering these additional considerations is shown in Eq.3.2, where ρ_{bd} is the bulk density of soil (g/cm^3), w_{lat} is lattice water and w_{som} is the water available in organic matter. In this study, w_{lat} and w_{som} values are assumed to be negligible due to arid characteristics of the study area and Eq.3.1 is used in soil moisture calculations.

$$\theta(N) = \left(\frac{a_0}{\left(\frac{N}{N_0}\right) - a_1} - a_2 \right) \rho_{bd} \quad (3.1)$$

$$\theta(N) = \left(\frac{a_0}{\left(\frac{N}{N_0}\right) - a_1} - a_2 - w_{lat} - w_{som} \right) \rho_{bd} \quad (3.2)$$

N_0 value is obtained from the initial calibration and sampling study. For Çakıt Basin, this study has been done on 3-5 December 2016. Soil samples were obtained for the horizontal footprint of CRNP as shown in Figure 3.5 [61]. As it is suggested in [62], soil sampling has been made for six soil depths (5cm, 10cm, 15cm, 20cm, 25cm and 30cm) at 18 locations within the footprint. In total, there are 108 different soil samples that has been obtained during the initial calibration study.



(a)

(b)

Figure 3.5: a) Sampling locations for initial calibration of CRNP b) One of the soil samples obtained during the initial calibration study [61]

As a result of the initial calibration study, mean bulk density of soil ρ_{bd} is found as 1.495g/cm^3 , mean volumetric soil moisture has been found as 0.148, porosity is found as $\rho_{avg}=0.51$ and the reference neutron counting rate N_0 has been found as 1933.4cph.

In [63] codes for calculation of soil moisture values from neutron counts and the raw data have been provided.

3.2.1.1 Correction of Neutron Counts

Relationship between soil moisture and decelerated neutron counts are examined with Eq.3.1. However, in order to apply this formulation, it is necessary to eliminate the effects of environmental factors from neutron count rates obtained from CRNPs. In other words, the neutrons counted with CRNP may vary in accordance with the field characteristics in terms of air pressure, absolute humidity and intensity of incoming cosmic rays. f_{bar} , f_{hum} and f_{int} are the correction factors for air pressure, humidity and incoming cosmic neutron intensity respectively. Corrected neutron counts that

can be used in equations 3.1 and 3.2 are calculated by using Eq. 3.3 where, N is the corrected neutron flux and N_{raw} is the raw neutron count data obtained from the CRNP.

The water stored in the vegetation may also vary in time and affect the response of CRNPs and should also be corrected accordingly [64]. However in the Çakıt Basin study area, the vegetation is sparse enough to neglect the effects of vegetation.

$$N = (f_{bar} \cdot f_{hum} \cdot f_{int}) \cdot N_{raw} \quad (3.3)$$

Correction factor for atmospheric pressure variation f_{bar} is calculated by using Eq.3.4 [65], correction factor for absolute humidity f_{hum} is calculated by using Eq.3.5 [66] and correction factor for the intensity of the cosmic rays by using Eq.3.6 [62],

$$f_{bar} = e^{\beta*(P-P_{ref})} \quad (3.4)$$

$$f_{hum} = 1 + 0.0054(p_{v0} - p_{v0}^{ref}) \quad (3.5)$$

$$f_{int} = \frac{I_{ref}}{I_m} \quad (3.6)$$

where; P : Atmospheric pressure (mb), P_{ref} : Reference atmospheric pressure at sea level ($1013.25 hPa$), β : Atmospheric attenuation coefficient ($cm^2 g^{-1}$ or mb^{-1}), p_{v0}^{ref} : Reference absolute humidity (gm^{-3}), p_{v0} : Near-surface absolute humidity (gm^{-3}), I_{ref} : Reference counting rate for the same neutron monitor from an arbitrary fixed point in time, I_m : Selected neutron monitor counting rate at any desired point in time.

Calculation of f_{int} is based on the fact that the cosmic-ray based high-energy secondary neutron flux is not affected by soil moisture unlike decelerated neutrons. High energy neutron flux is measured with various stations by Neutron Monitor Database (NMDB) [67] which is founded under the European Union's FP7 programme (contact no. 213007) [60]. Neutron intensity values measured via NMDB stations can be used to determine I_m value for the calculation of f_{int} . It is important to choose the

NMDB station, which has similar geomagnetic cutoff rigidity with the location where the CRNP has been installed since the magnetic field of the Earth affects the neutron intensity [62]. Selecting a neutron monitor station with a different geomagnetic cutoff rigidity than CRNP is also possible and this approach is also applied to the CRNPs in the COSMOS database [68] (Section 3.2.2) for intensity correction of neutron counts [62]. In this approach, correction for all probes are made by one neutron monitor at Jungfraujoch, Switzerland and to account for the difference in geomagnetic cut-off rigidities, a further correction has been made as it is provided in [60]. However, for this study conducted at the Çakıt Basin, Athens NMDB station has been selected for the neutron monitor station, which has geomagnetic cutoff rigidity (8 GV). As it can be seen in Figure 3.6 [69], which shows the distribution of vertical cutoff rigidities among the globe, Athens and Çakıt Basin have approximately the same cutoff rigidity value.

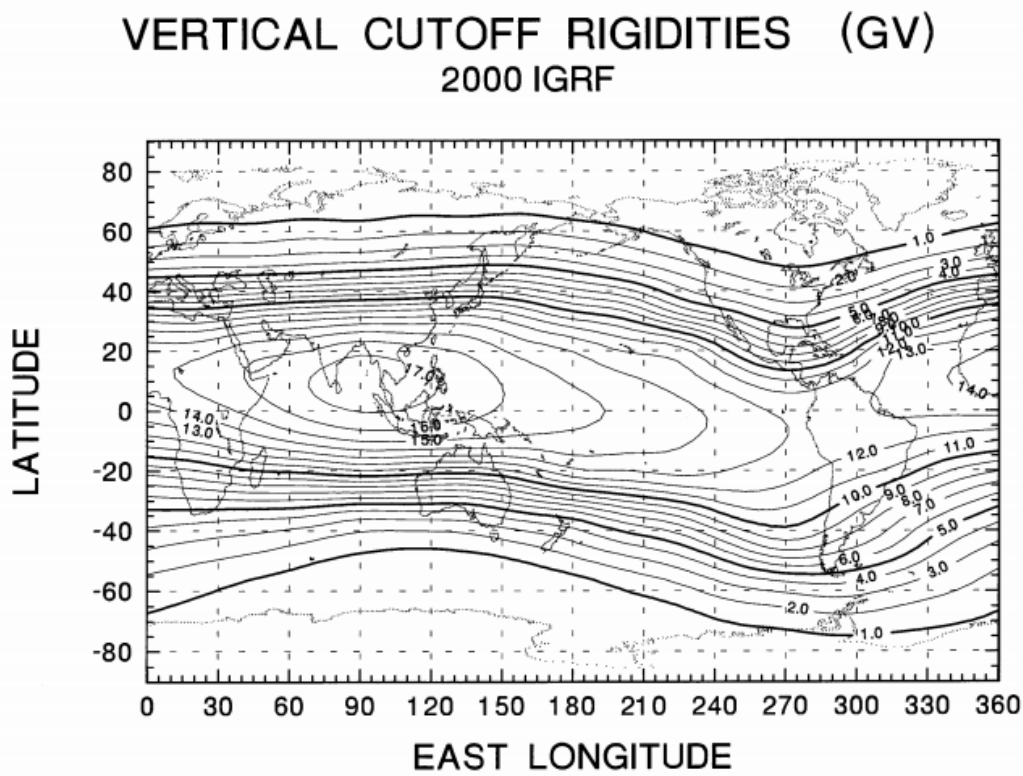


Figure 3.6: Iso-rigidity contours for vertical geomagnetic cutoff rigidities [69]

3.2.1.2 Obtaining Soil Moisture Data from Çakıt Basin CRNP

The CRNP located in the Çakıt basin had been providing real time neutron count data since November 11, 2016. Alongside the CRNP, there is also a TDR sensor which is installed 100m away from CRNP and at 5cm depth to monitor soil moisture. Meteorological parameters needed for the neutron correction operation mentioned in Section 3.2.1.1 has been obtained from the nearest meteorological observation station (Figure 3.1) located in the Çakıt Basin. Neutron counts obtained from CRNP, soil moisture obtained from TDR and precipitation, mean temperature, soil temperature, snow depth data obtained from the meteorological observation station are shown in Figure 3.7, neutron counts and calculated soil moisture values are shown in Figure 3.9 [19]. Due to excessive snow cover, a part of the neutron data can not be obtained for a short and snowy period between 2016-12-30 and 2017-01-03, which is explicitly shown in the previous study [19]. Correction factors have been calculated by following the procedure described in Section 3.2.1.1 and are presented in Figure 3.8.

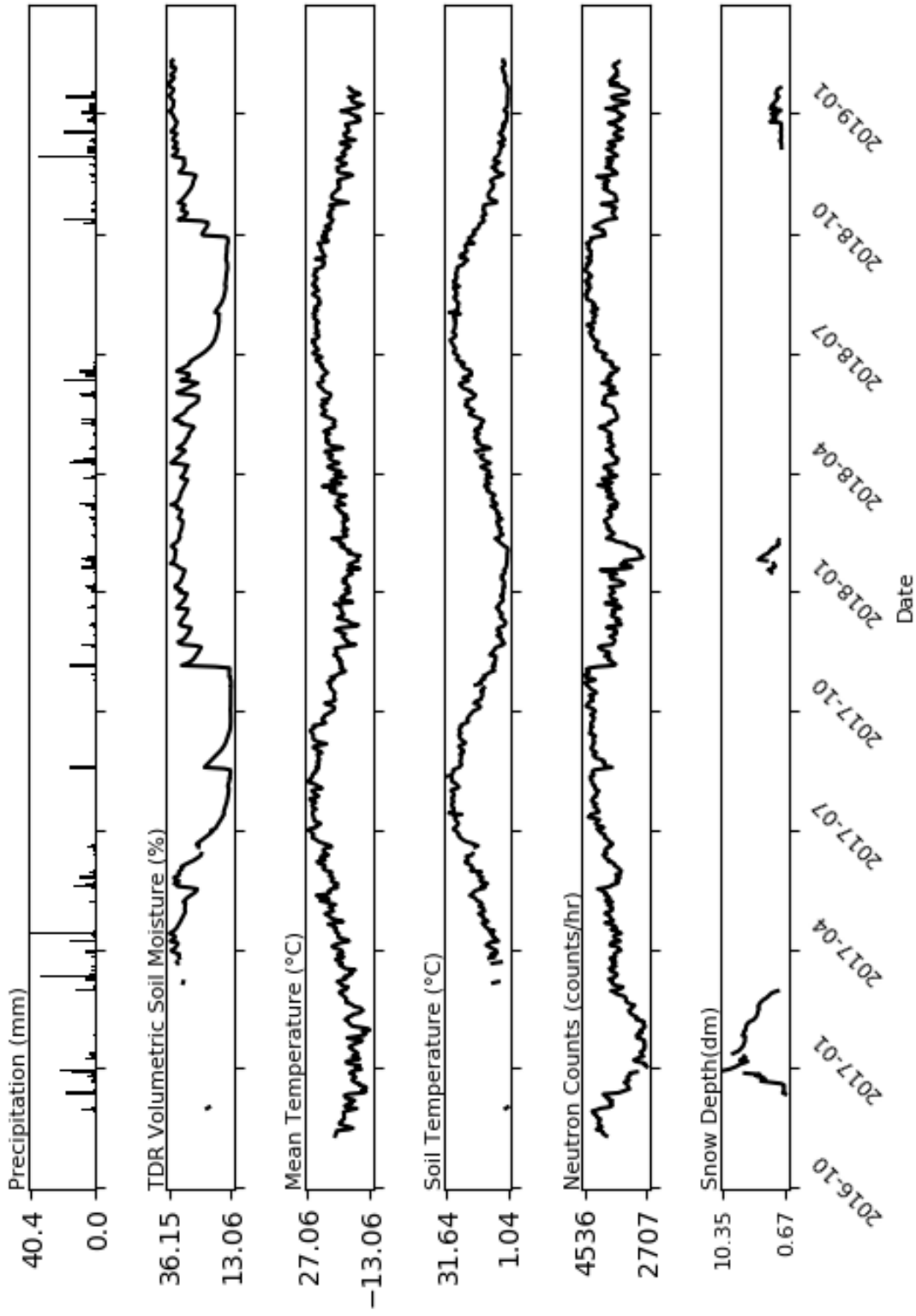
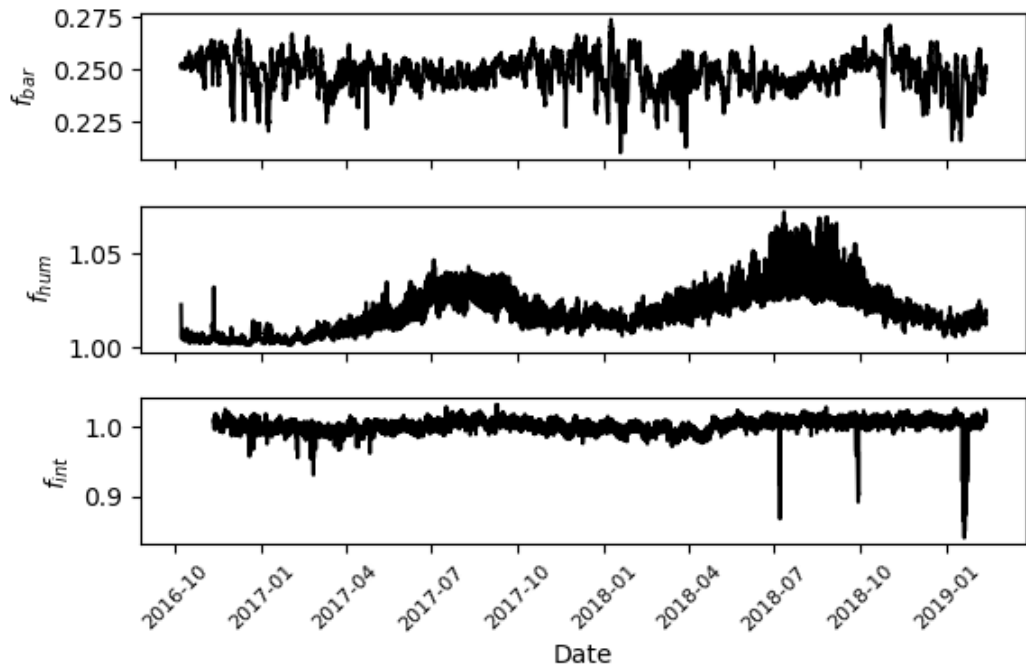
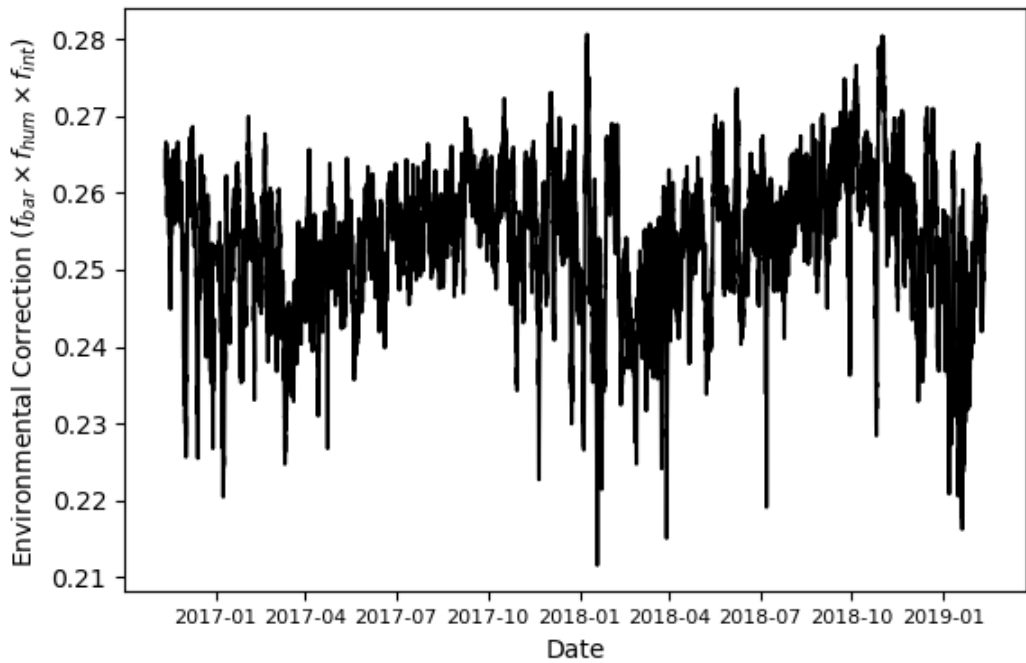


Figure 3.7: Precipitation, mean temperature, soil moisture measurements (TDR), soil temperature and snow height data observed at the site.



(a)



(b)

Figure 3.8: a) Correction factors for pressure, humidity and cosmic ray intensity, b) Combination of environmental correction factors

3.2.2 CRNP Networks

Besides individual efforts on inferring soil moisture through neutron monitoring via CRNPs, there are several global networks of CRNP stations. The COsmic-ray Soil Moisture Observing System (COSMOS) [62, 68] is a CRNP network, which provides real time soil moisture data. COSMOS has more than hundred stations, most of which are located in the USA. Similarly, COSMOS-UK [70, 71] is a CRNP network for stations located in the United Kingdom. TERENO is a terrestrial observation network including CRNPs in Germany [72, 73]. CosmOz is a network of CRNP stations located in Australia [60, 74]. Besides these data networks, a new initiative has been recently started for the European CRNPs, where long term soil moisture measurements recorded by 65 CRNPs (including the the CRNP that has been installed in the Çakıt basin) operated by 23 institutions and distributed across major climate zones in Europe [75].

In this study, data of COSMOS network has been utilized to validate satellite products and compare the findings with the Çakıt Basin CRNP data. Data of all 104 stations of COSMOS [68, 62] have been obtained and used for satellite product validation.

3.2.3 Satellite Soil Moisture Data

In this study, five different sources of remote sensing soil moisture products have been used for validation and comparison purposes. These products are namely, ASCAT, SMOS, SMAP, AMSR and CCI. Besides these soil moisture products, GLDAS data have also been used since it also constitutes a global soil moisture database and partially makes use of satellite based information for the land surface modelling.

3.2.3.1 METOP-A/B Advanced Scatterometer (ASCAT)

ASCAT is an active microwave remote sensing instrument and the name of it is the abbreviation for advanced scatterometer. Main purpose of ASCAT is to provide satellite based data for weather prediction [52]. Soil moisture processing and dissemination service for ASCAT has been developed by joint efforts of European Organisation for

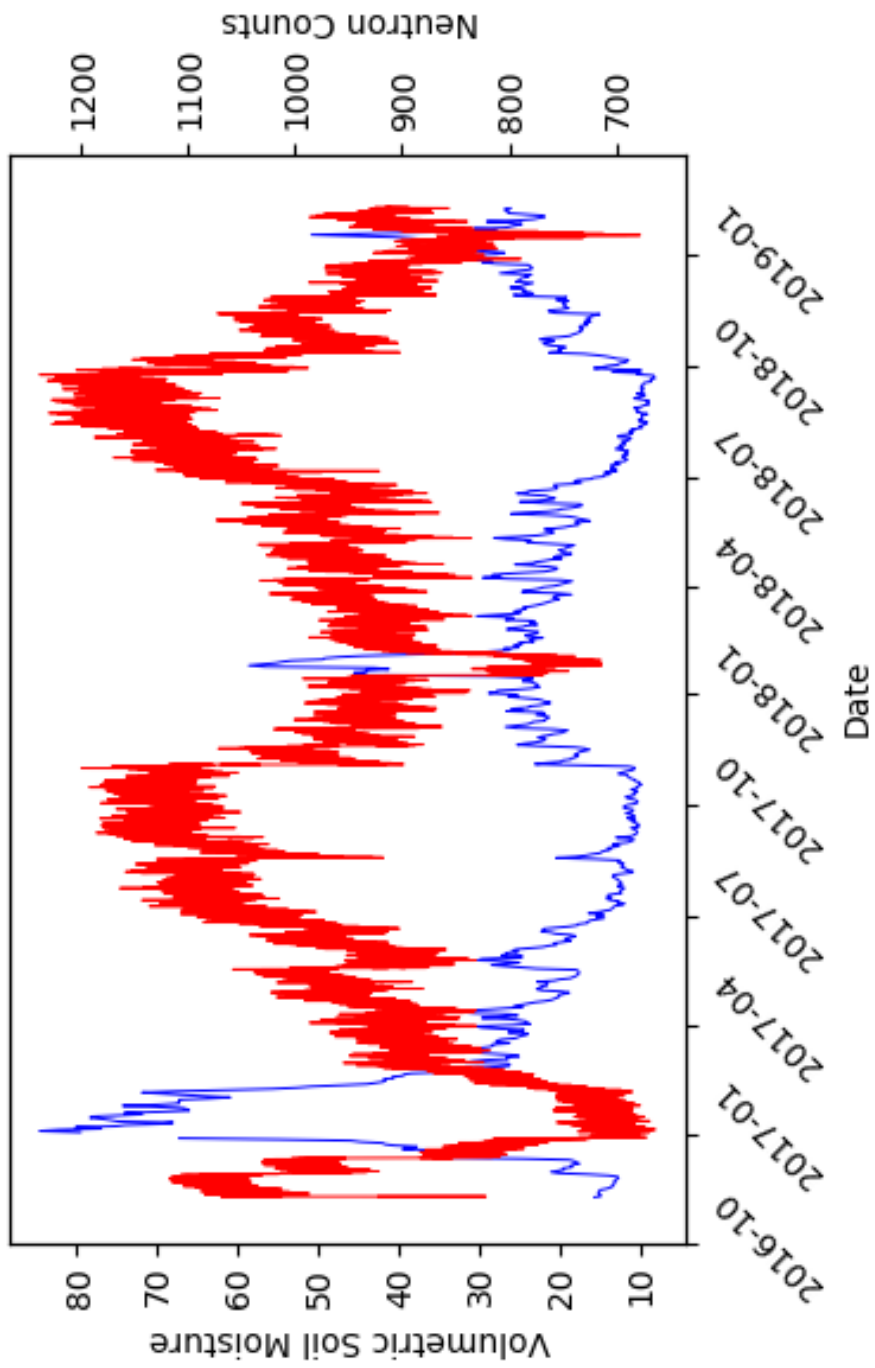


Figure 3.9: Corrected neutron counts of CRNP (red) and corresponding soil moisture time series (blue).

the Exploitation of Meteorological Satellites (EUMETSAT) and Vienna University of Technology. Soil moisture data of ASCAT have been obtained from the website of EUMETSAT Satellite Application Facility on Support to Operational Hydrology and Water Management (H-SAF) [76]. H113 and H114 soil moisture products were used in comparison and validation studies. These data have been provided as saturation index values unlike other products, which have been provided as volumetric soil moisture. In order to have comparable values, saturation index values obtained from ASCAT have been converted to volumetric soil moisture values by multiplying these values with the porosity of the samples (ρ_{avg}). Soil moisture data of ASCAT product for the location of the CRNPs of the COSMOS database have been obtained by multiplying the ASCAT soil moisture value with the average values of the porosity data obtained from GLDAS [77] and HWSDB [78].

3.2.3.2 Soil Moisture and Ocean Salinity (SMOS)

SMOS is a passive microwave remote sensing instrument, which is one of the satellite missions of European Space Agency (ESA) and it was launched in November 2009 [54]. SMOS stands for the Soil Moisture and Ocean Salinity and as its name implies, the main purpose of this mission is to provide spaceborne soil moisture and ocean salinity data [79]. Microwave Imaging Radiometer using Aperture Synthesis (MIRAS) has been used to pick up faint microwave emissions from Earth's surface. Level 3 SMOS data have been retrieved from Barcelona Experts Center (BEC) as daily volumetric soil moisture values. As SMOS is a passive sensor, it has ascending and descending nodes, which were retrieved separately. SMOS Level 3 soil moisture data have been produced and disseminated by BEC [80].

3.2.3.3 Soil Moisture Active and Passive (SMAP)

SMAP is a mission of NASA for providing various types of spaceborne data including soil moisture. SMAP stands for Soil Moisture Active Passive and as its name implies that it observes soil moisture via active and passive microwave sensing techniques. It mainly infers soil moisture at the top few centimeters of the soil, however, level

4 product of SMAP, where level 3 data have been highly enriched by utilizing land surface modeling [81], provides soil moisture estimates for the root zone. SMAP L4 9 km EASE-Grid Surface and Root Zone Soil Moisture Analysis products, which have been obtained from NASA's Earth Observing System Data and Information System (EOSDIS) [82], has been providing 3 hourly continuous soil moisture data which means it can also provide data for the days with snow cover [83, 53]. Although this product has higher temporal resolution (3 hourly), in order to have comparable data with other satellite datasets, daily average products have been obtained for descending and ascending orbits. According to the recent studies on satellite soil moisture product validation with CRNPs, especially for arid and semi-arid areas, SMAP soil moisture products have the best accuracy and least uncertainty among all of the other satellite products [19, 18].

3.2.3.4 Advanced Microwave Scanning Radiometer (AMSR)

AMSR is a passive microwave sensor which is one of the satellite missions of Japan Aerospace Exploration Agency (JAXA). AMSR has various versions and in this study AMSR 2 data have been used, which are mainly based on AMSR-E product. AMSR stands for Advanced Microwave Scanning Radiometer which can infer soil moisture through observed brightness and temperature values. For this purpose, it utilizes the Land Parameter Retrieval Model (LPRM) [55]. For this study C-band (6.93 GHz) soil moisture products of AMSR2 were used for both descending and ascending nodes. Soil moisture data of AMSR2 have also been retrieved from EOSDIS [82].

3.2.3.5 Climate Change Initiative (CCI)

CCI is not a satellite soil moisture product, it is rather a combination of different spaceborne soil moisture products, which are disseminated through ESA's Climate Change Initiative [84, 58, 56, 57]. In this study, CCI soil moisture datasets were retrieved from ESA's Climate Change Initiative [84] as active, passive and combined products separately.

3.2.3.6 Global Land Data Assimilation System (GLDAS) and Noah LSM

GLDAS provides a global dataset of calculated soil moisture values from land surface with different land surface models [85]. In this study, Çakıt Basin CRNP and CRNPs of COSMOS database have been used for the validation of GLDAS Noah LSM Level 4 product which is obtained from EOSDIS [82]. GLDAS Noah LSM Level 4 product has a temporal resolution of 3 hours and daily average values have been used in the studies. Unlike the satellite products which mainly provides soil moisture data for a thin top layer of the soil, GLDAS Noah LSM product provides soil moisture information for 10cm, 40cm, 100cm and 200cm depth of soil layers. In this study, only the first 10cm soil layer data have been used. Noah LSM is also used in this study as a stand alone physical model as it is described in Section 6.2.2 and a standalone version of Noah LSM has also been run within the scope of this study using in-situ meteorological data obtained from Ulukışla meteorological station. Noah LSM requires forcing variables as input, which are shown in Figure 3.10. The required atmospheric forcing variables are precipitation, wind speed, air temperature, relative humidity, surface pressure. Meteorological observation data obtained from the nearby meteorological station have been re-scaled temporally to match 30min temporal resolution of the Noah LSM. The radiative forcing variables are solar radiation and longwave radiation. Downward solar radiation has been obtained from an Eddy-Covariance sensor located at the close vicinity of the CRNP (Figure 3.1) and longwave radiation has been estimated by utilizing the Stefan Boltzmann law with the formulation provided by [86]. The analyses start at the first day of the water year of 2016 (October 1, 2016) and ends at the last day of the water year of 2017 (September 30, 2018) Four different soil layers have been defined which have 10cm, 30cm, 60cm and 100cm depths. For comparison studies, top soil layer with 10cm depth has been used.

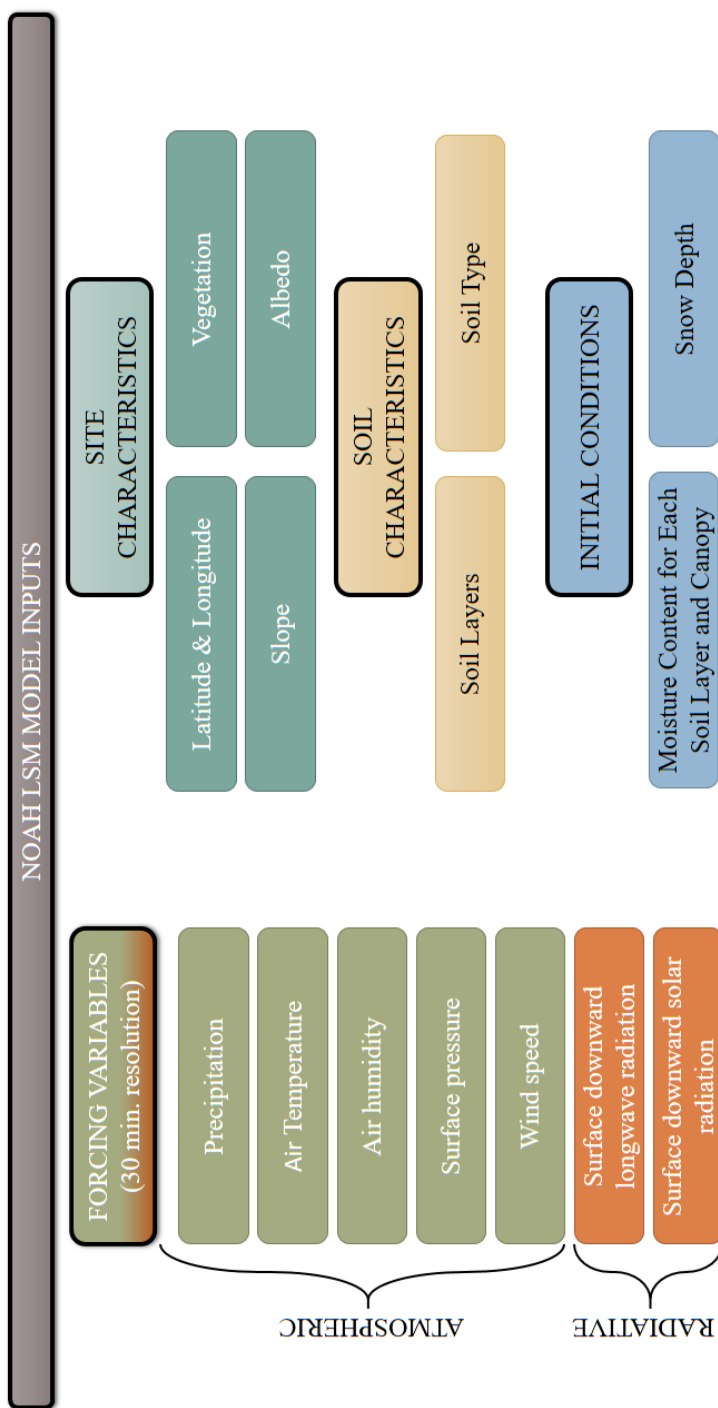


Figure 3.10: Input Parameters of NOAH LSM that are used in the analyses

3.2.4 Discharge Data

In this study, hydrological studies have been performed for Çakıt Basin and one of its sub-basins; Darboğaz sub-basin as shown in Figure 3.1. Discharge is the most obvious and the most important output of a hydrological process, thus the basis of the hydrological modeling approach is to simulate the flow as closely as it is observed. For this purpose, two streamflow gauging stations have been installed at the exit locations of Çakıt Basin and Darboğaz sub-basin. The correlation between these two datasets is very high since they are affected from the same conditions and represent similar basins (Figure 3.11). Total precipitation measured for 2016-2017 water year is 350mm and the maximum snow depth is 1.03m, total precipitation measured for 2017-2018 water year is 454mm and the maximum snow depth is 0.49m, total precipitation measured for 2019-2020 water year is 409mm and the maximum snow depth is 0.31m. Due to the effects of snow melting, 2016-2017 water year is wetter than the other years as it is shown in Figure 3.11.

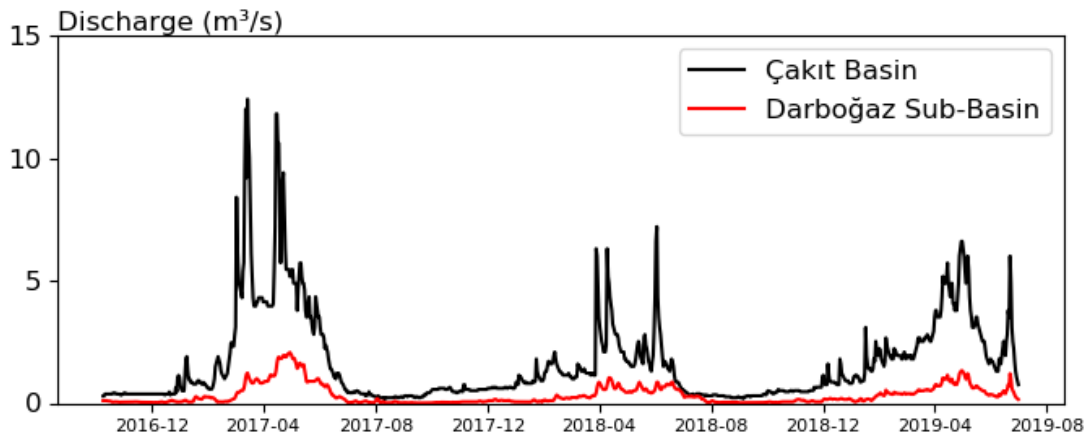


Figure 3.11: Discharge Data of Çakıt Basin and Darboğaz Sub-Basin

3.3 Methodology

In this study, the methodology to fulfill the objectives defined in Chapter 1 are summarized with the flowchart provided in Figure 3.12. The neutron data obtained from CRNP have been converted into soil moisture values and compared with TDR and

Noah LSM soil moisture outputs. CRNP soil moisture values have been used for the validation of satellite soil moisture products. Evaporation data have also been compared with CRNP soil moisture data to assess the relation between evaporation and soil moisture. Finally, soil moisture data have been used in a conceptual model, namely NAM, to improve the model statistics.

3.4 Statistical Measures Used In this Study

In this study, statistical measures are used for the comparison between different soil moisture products, comparisons between soil moisture and evaporation data and evaluation of the discharge simulations of the conceptual model. Coefficient of determination (r^2), root mean square error (RMSE) and unbiased root mean square error (ubRMSE) are used for statistical measures of validation of satellite products.

The calibration of the parameters defined in conceptual models rely on simulating the hydrological variables (discharge, soil moisture) as similar as possible with the observed ones. The similarity between two datasets can be measured via several statistical methods and few of the most commonly used ones are presented in this thesis. Nash Sutcliffe Efficiency (NSE), Logarithmic Nash Sutcliffe Efficiency (logNSE), Root Mean Square Error (RMSE), Percent Bias (PBIAS), Coefficient of Determination (r^2), Relative Volume Error (VE) and Kling-Gupta Efficiency (KGE) are the statistical measures that are used in this study for calibration of the model.

3.4.1 Nash Sutcliffe Efficiency (NSE) and Logarithmic Nash Sutcliffe Efficiency (logNSE)

Nash Sutcliffe Efficiency (NSE) is commonly used in hydrological modelling to indicate the error of estimation [87]. A perfect estimation would yield $NSE=1$, which means the estimation of the model is improving if NSE value is getting closer to 1. Logarithmic NSE (logNSE) is generally used to estimate low flow conditions and hydrological modelling in drought conditions. NSE is calculated by using Eq. 3.7 and

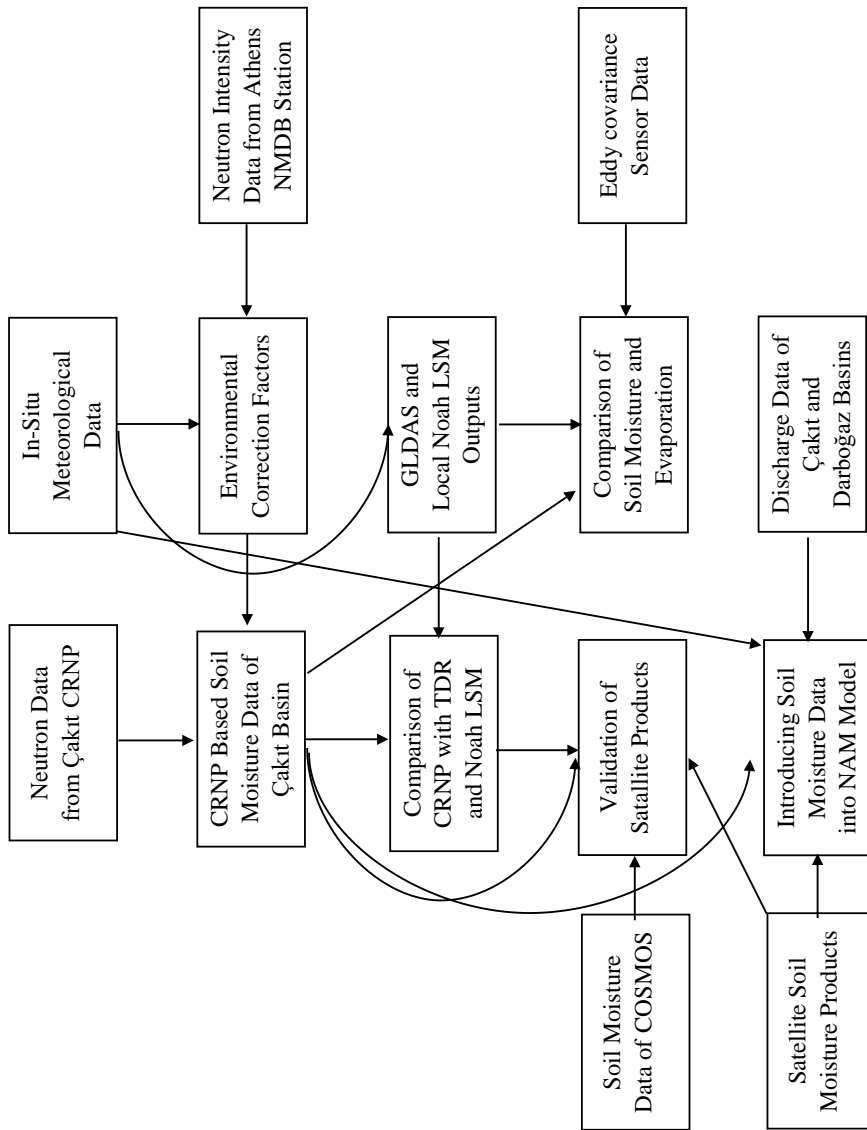


Figure 3.12: Schematic Representation of the Methodology

logNSE is calculated by using Eq. 3.8.

$$NSE_X = 1 - \frac{\sum_{t=1}^T (X_{sim}(t) - X_{obs}(t))^2}{\sum_{t=1}^T (X_{obs}(t) - \bar{X}_{obs})^2} \quad (3.7)$$

$$\logNSE_X = 1 - \frac{\sum_{t=1}^T (\ln(X_{sim}(t)) - \ln(X_{obs}(t)))^2}{\sum_{t=1}^T (\ln(X_{obs}(t)) - \ln(\bar{X}_{obs}))^2} \quad (3.8)$$

where; X_{obs} : Time series of observed variable, X_{sim} : Time series of model simulated variable, \bar{X}_{obs} : Mean of the observed variable, \bar{X}_{sim} : Mean of the simulated variable, $X_{obs}(t)$: Observed value of the variable at time t, $X_{sim}(t)$: Model simulated value of the variable at time t.

3.4.2 Root Mean Square Error (RMSE) and Unbiased Root Mean Square Error (ubRMSE)

Root Mean Square Error (RMSE) indicates the mean error of simulations [88]. A perfect estimation would yield RMSE=0, which means the estimation of the model is improving if RMSE value is getting closer to 0. RMSE is calculated by using Eq. 3.9. In this study in order to eliminate the bias effects and have more meaningful results, unbiased version of root mean square error (ubRMSE) has also been used for the validation of satellite products. ubRMSE is calculated by using Eq.3.10.

$$RMSE = \sqrt{\frac{1}{N} \sum_{t=1}^N (x_i - y_i)^2} \quad (3.9)$$

$$ubRMSE = \sqrt{\frac{\sum_{i=1}^N [(x_i - \bar{x}) - (y_i - \bar{y})]^2}{N}} \quad (3.10)$$

where: x and y: The datasets, N: Number of data points, \bar{x} and \bar{y} : The mean value of x and y.

3.4.3 Percent Bias (PBIAS)

Percent Bias (PBIAS) indicates the general tendency of simulations to differ from observations [89]. A perfect estimation would yield PBIAS=0, which means the estimation of the model is improving if PBIAS value is getting closer to 0. PBIAS is calculated by using Eq.3.11.

$$PBIAS_X = \frac{\sum_{t=1}^T X_{obs}(t) - \sum_{t=1}^T X_{sim}(t)}{\sum_{t=1}^T X_{sim}(t)} \cdot 100 \quad (3.11)$$

3.4.4 Coefficient of Determination (r^2)

Coefficient of Determination (r^2) indicates the linear relation between two datasets [90]. r^2 value of 1 indicates a perfect linear correlation, 0 indicates no linear correlation, and -1 indicates a perfect inverse linear correlation. r^2 is calculated by using Eq. 3.12.

$$r^2 = \frac{N \sum xy - \sum x \sum y}{\sqrt{[N \sum x^2 - (\sum x)^2] [N \sum y^2 - (\sum y)^2]}} \quad (3.12)$$

3.4.5 Relative Volume Error (VE)

Relative Volume Error (VE) indicates the cumulative error in the estimation [91]. A perfect estimation would yield VE=0, which means the estimation of the model is improving if VE value is getting closer to 0. VE is calculated by using Eq.3.13.

$$VE_X = \frac{\sum X_{sim} - \sum X_{obs}}{\sum X_{obs}} \quad (3.13)$$

3.4.6 Kling-Gupta Efficiency (KGE)

Kling-Gupta Efficiency (KGE) [92] is used in various hydrological studies and it is basically the combination of three different indicators namely linear relation (r),

bias ratio (α) and ratio of standard deviations (β). A perfect estimation would yield $KGE=1$, which means the estimation of the model is improving if KGE value is getting closer to 1. r is calculated by using Eq. 3.14, (α) is calculated by using Eq. 3.15 and β is calculated by using Eq. 3.16. KGE is calculated by using Eq. 3.17.

$$r_{X,m} = \frac{cov(X_{m,sim}, X_{m,obs})}{\sigma_{X_{m,sim}} \sigma_{X_{m,obs}}} \quad (3.14)$$

$$\alpha_{X,m} = \frac{\sigma_{X_{m,obs}}}{\sigma_{X_{m,sim}}} \quad (3.15)$$

$$\beta_{X,m} = \frac{\bar{X}_{m,obs}}{\bar{X}_{m,sim}} \quad (3.16)$$

$$KGE_X = 1 - \sqrt{(r_{X,m} - 1)^2 + (\alpha_{X,m} - 1)^2 + (\beta_{X,m} - 1)^2} \quad (3.17)$$

where: $X_{m,obs}$: Monthly average of observed values, $X_{m,sim}$: Monthly average of simulated values, $r_{X,m}$: Monthly pearson correlation coefficient.

CHAPTER 4

VALIDATION OF SATELLITE BASED SOIL MOISTURE PRODUCTS

4.1 General

Soil moisture data provide significant information for most of the hydrological studies such as estimating floods and droughts or agricultural decision support systems. CRNS is one of the most promising techniques for providing continuous data for such studies at an applicable scale. Horizontal footprint of a CRNP constitutes a 670m diameter circle according to [1] and a 360-420m diameter circle according to [93]. In a similar manner, satellite based soil moisture data can provide information for much larger areas with relatively lower spatial and temporal resolution. Although CRNP is able to infer soil moisture with a reliable accuracy, its spatial scale may not be sufficient for greater study areas and a few hundred CRNPs may be required to fully cover the site. Since having large numbers of CRNPs is not practical for such studies, soil moisture information obtained from satellites can be used in conjunction with lesser number of CRNPs to obtain the soil moisture information required for hydrological studies. It is important to analyze the errors of the satellite products since it makes the potential users of these products aware of the strong and weak sides of a product and if they are known, these errors can be eliminated to some extent by improving the soil moisture retrieval algorithms of satellite products [13]. There has been significant number of studies which focus on validation of soil moisture products with CRNP based ground observations [70, 94, 95, 96, 97]. The main approach of these studies is determination of the correlation between ground and satellite observations for a certain CRNP or a group of CRNPs located in the same hydrological basin. In this study, in order to evaluate the possible support of space-borne satellite products for filling the scale gap between the horizontal footprint of CRNPs and the area of

hydrological study sites, various types of satellite based soil moisture products have been validated with several CRNPs of COSMOS database [68] and the CRNP station located in the study area which is mentioned in Chapter 3. CRNP based soil moisture values were also compared with TDR measurements and Noah Land Surface Model outputs. Although previous studies on passive microwave sensors suggest that ascending products are more accurate than the descending ones [98], both products have been investigated in this study. Combination of different products is also possible and it is suggested that combination of SMAP and ASCAT soil moisture products more accurately matches with the ground observations [95]. Satellite products' success also depends on the seasons that they operate and the vegetation on the ground, for example it has been suggested that ASCAT performs better in colder and wet seasons [99], whereas SMAP performs better in arid and semi arid locations [19]. Recent studies [19, 18] suggest that the SMAP product is more reliable than the other satellite products when validated with the CRNPs.

4.2 Satellite Based Soil Moisture Products

In this study, Soil Moisture and Ocean Salinity (SMOS), the METOP-A/B Advanced Scatterometer (ASCAT), Soil Moisture Active Passive (SMAP), Advanced Microwave Scanning Radiometer 2 (AMSR2), Climate Change Initiative (CCI) soil moisture products have been used. Besides these products, Global Land Data Assimilation System (GLDAS) Noah LSM products have also been used for the validation of soil moisture products. In addition, a stand alone Noah LSM has been run for the study area by using the measured atmospheric and radiative forcing data. The details of these data have been provided in Section 3.2.3. For the Çakıt Basin study site, the grid cells of each product and their pixel sizes are provided in Table 4.1. The sensing depths of all products are not more than a few centimeters of the soil surface apart from the rootzone product of SMAP. The revisit time of each product differs mostly due to the operational schedules of the satellites. In general, active products have better temporal resolution.

Table 4.1: Satellite soil moisture products that are compared with Çakıt Station CRNP soil moisture content data.

Soil Moisture Product	Pixel Size (km)	Coordinate of the Pixel Center (Closest to Çakıt CRNP)	Sensor Type
METOP-A/B Advanced Scatterometer (ASCAT) EUMETSAT H113-H114 SSM	12.5x12.5	37.597 °N 34.625 °E	Active
Soil Moisture and Ocean Salinity (SMOS) L3 1-day Binned Product	25x25	37.482 °N 34.484 °E	Passive
Soil Moisture Active and Passive (SMAP) L4 3-hourly EASE-Grid SSM	9x9	37.4746 °N 34.4969 °E	Active and Passive
Advanced Microwave Scanning Radiometer (AMSR2) L3 1 day c band 6.9 Ghz	9x9	37.55 °N 34.45 °E	Passive
ESA Climate Change Initiative (CCI) v04.4 (Active, Passive and Combined)	25x25	37.5155 °N 34.4979 °E	Active and Passive
Global Land Data Assimilation System (GLDAS) Noah LSM L4 3 hourly V2.1	25x25	37.625 °N 34.375 °E	-

Besides Çakıt basin, stations in the COSMOS database have also been analyzed with the products shown in Table 4.1. For this purpose, closest satellite grids to the CRNP locations have been selected as it has been done for the Çakıt Basin CRNP. Since the data of CRNPs and the satellite products are compared directly, the soil moisture is assumed to be homogeneously distributed in the grid cell no matter where the CRNP is located. The comparisons were made with the existing data without filling the missing data of satellite products or re-scaling them.

SMAP is the most recent satellite mission which can provide data starting from March, 2015. In order to have compatible comparisons, the time between March, 2015 and December 2018 is taken as the time period of the studies. In the COSMOS database, there exist 82 stations, which have data in this period. For these stations, days with snow cover has been excluded from the analyses since the CRNP is not able to measure soil moisture in snow conditions [1]. For this purpose, snow height data, which have been obtained from SMAP [82, 81] and snow probabilities, which have been obtained from ASCAT [76] have been used. It is assumed that if the snow probability is greater than 10% and snow height data is greater than 8mm, the snow storage affects CRNP measurements adversely and the data of these periods are excluded.

4.3 Methodology of Validation

Validation of satellite products have been evaluated through one-to-one comparisons with statistical measures defined in Section 3.4. In order to account for the uncertainties in different types of products (measured, model based and satellite based) triple collocation analyses have been performed as it is explained in section 4.3.1. In order to directly compare the satellite based products and CRNP based soil moisture data, the horizontal and vertical measurement scales of the satellite products are assumed to be constant and compatible with those of CRNPs.

4.3.1 Triple Collocation

Triple collocation is a tool which is utilized to understand uncertainties of three datasets indicating the same variable with different sources of information [100].

For the triple collocation analyses, soil moisture information has been classified into three groups: In-situ soil moisture measurements, soil moisture outputs of a land surface model and satellite based soil moisture measurements. CRNP is used for in-situ measurements and GLDAS is used for the land surface model outputs. SMAP is selected to represent the satellite based soil moisture products due to its continuity. Both SMAP rootzone and surface products have been utilized separately in the triple collocation study, in other words, two different triplets of datasets have been investigated

for each station in the COSMOS database [19]. The scaling factor (β) is taken as 1 for CRNP product in order to calculate the β values for SMAP and GLDAS without changing the CRNP data. Comparison of the results for two triplets with each other is not valid since the errors produced depend on the datasets in the triplets [101] and the results are examined for each triplet separately.

4.4 Comparison of Soil Moisture Products

4.4.1 Comparison of Soil Moisture Products for Çakıt Basin

All soil moisture products have been re-sampled to obtain daily soil moisture time series and shown in Figure 4.1.

Anomalies of soil moisture time series with respect to their fifteen days averages are provided in Figure 4.2. Figure 4.1 and Figure 4.2 indicate that SMAP, CCI and ASCAT products can provide more continuous and more accurate soil moisture data for Çakıt Basin when compared to the other products. The direct relations between soil moisture products examined in this study with in-situ soil moisture observations are provided in Appendices A (Figures A.1-A.10).

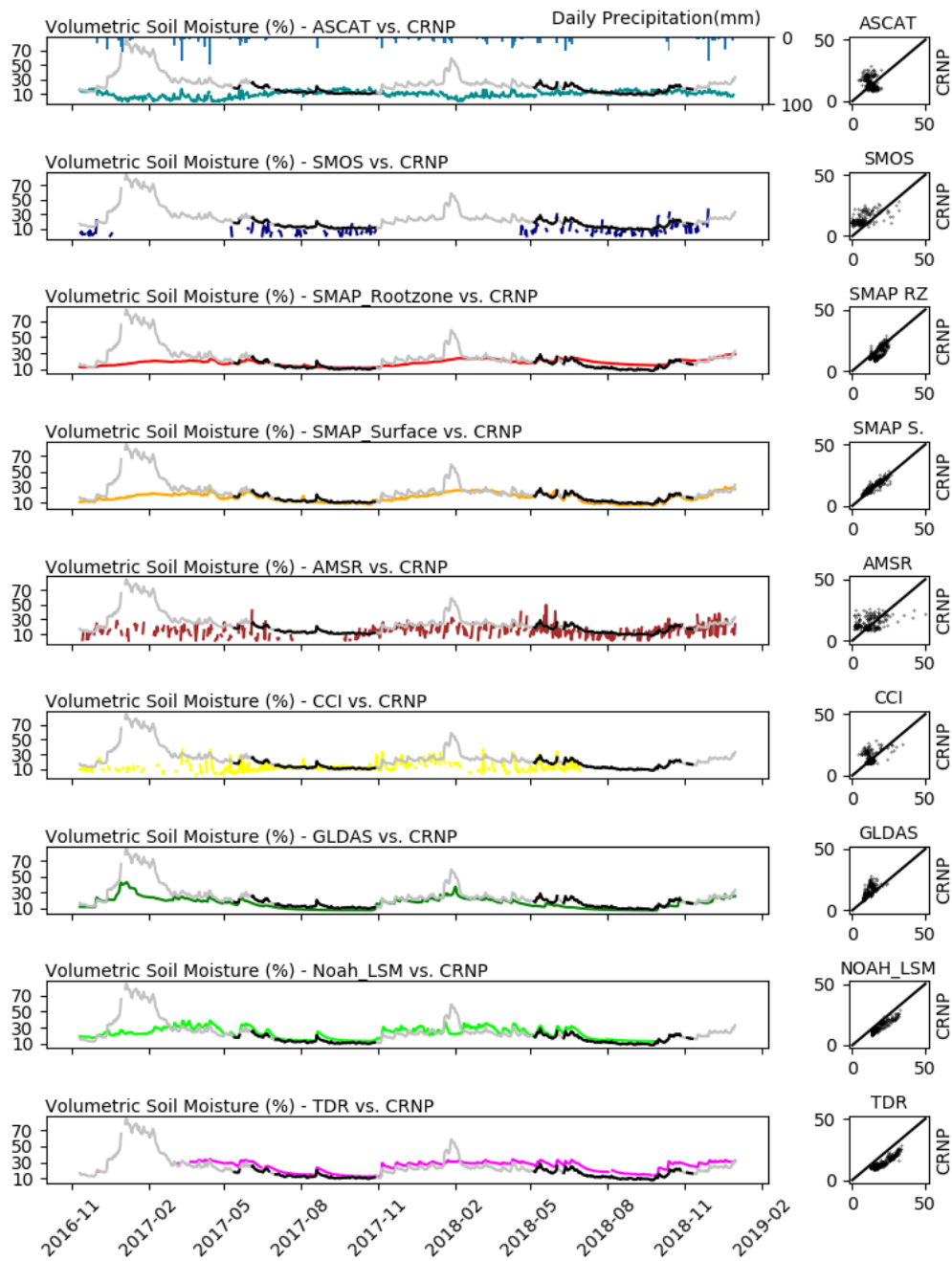


Figure 4.1: Comparisons of time series for different soil moisture products with CRNP. CRNP soil moisture values are shown in black, excluded days due to snow are shown in grey, other soil moisture products are shown in different colors.

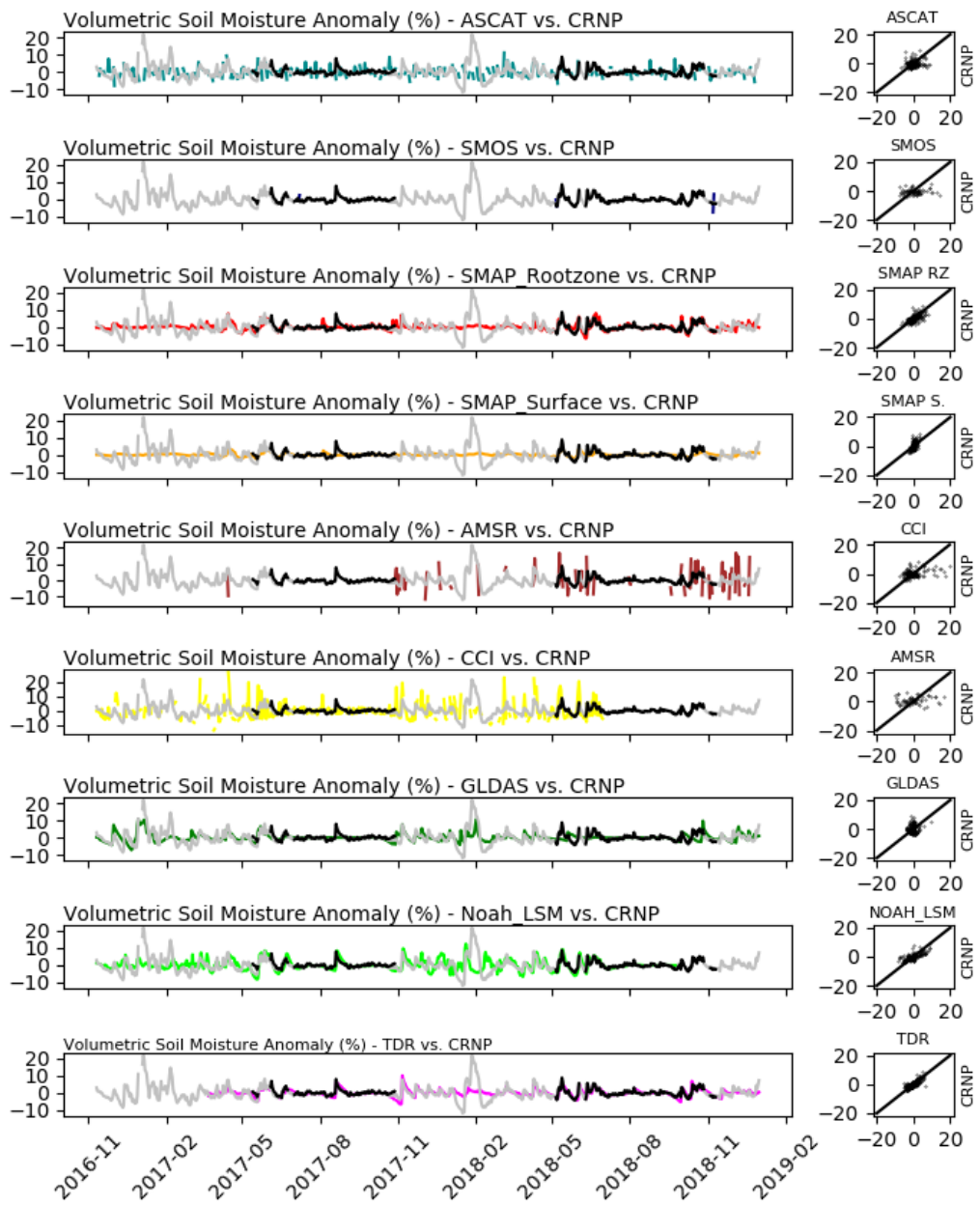


Figure 4.2: Comparisons of the anomalies (with respect to fifteen days averages) for different soil moisture products with the anomalies of CRNP. CRNP soil moisture values are shown in black, excluded days due to snow are shown in grey, other soil moisture products are shown in different colors.

4.4.2 Comparison of Soil Moisture Products for COSMOS Database

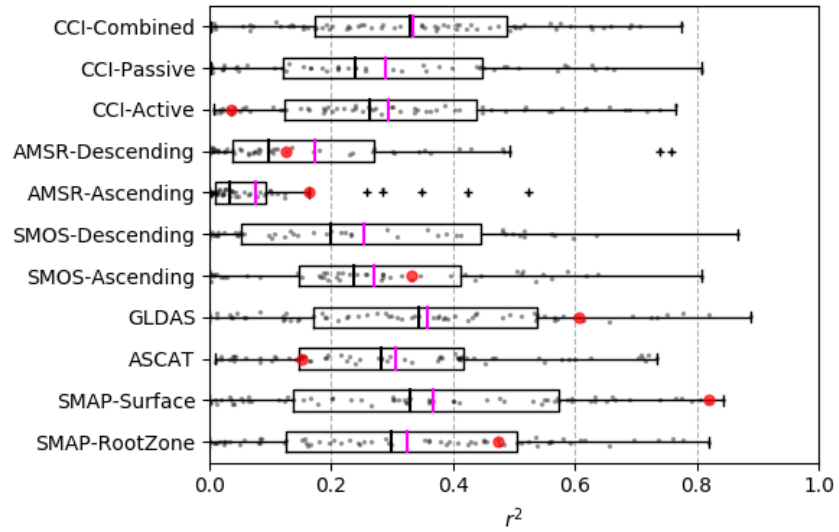
For all of the stations of COSMOS database, r^2 values with the corresponding CRNPs are shown in Appendix B (Figures B.1 for SMAP surface product, B.2 for SMAP root-zone product, B.3 for ASCAT, B.4 for SMOS (descending), B.5 for SMOS (ascending), B.6 for AMSR (descending), B.7 for AMSR (ascending), and B.8 for GLDAS).

RMSE values with the corresponding CRNPs are shown in Appendix B (Figures B.9 for SMAP surface product, B.10 for SMAP root-zone product, B.11 for ASCAT, B.12 for SMOS (descending), B.13 for SMOS (ascending), B.14 for AMSR (descending), B.15 for AMSR (ascending), and B.16 for GLDAS).

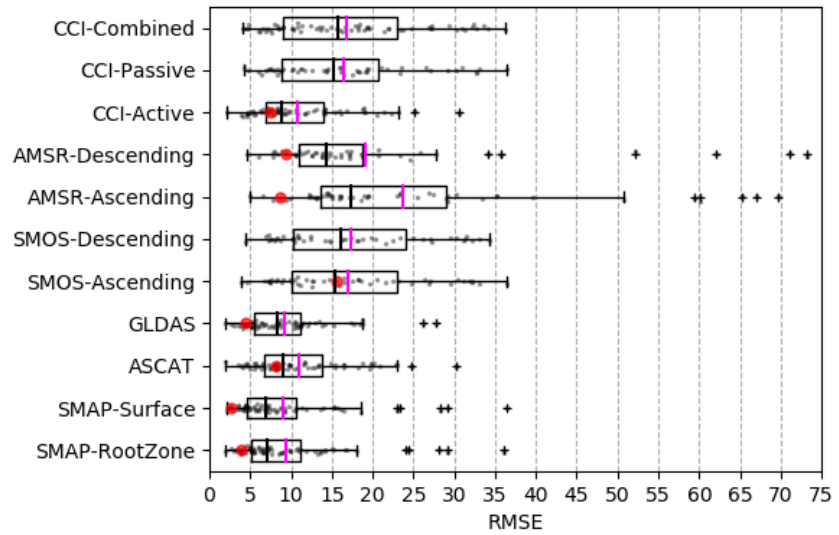
ubRMSE values with the corresponding CRNPs are shown in Appendix B (Figures B.17 for SMAP surface product, B.18 for SMAP root-zone product, B.19 for ASCAT, B.20 for SMOS (descending), B.21 for SMOS (ascending), B.22 for AMSR (descending), B.23 for AMSR (ascending), and B.24 for GLDAS).

Statistical measures defined in Chapter 3.4 have been utilized to all soil moisture products and all stations of the COSMOS database including the Çakıt Basin CRNP. All of the stations' r^2 values with the satellite products have been summarized in Figure 4.3a, ubRMSE and RMSE values are shown in Figure 4.3a - Figure 4.3b and Figure 4.4a - Figure 4.4b.

Mean and median values of statistical measures for all stations and satellite products are summarized in Table 4.2 and Table 4.3.

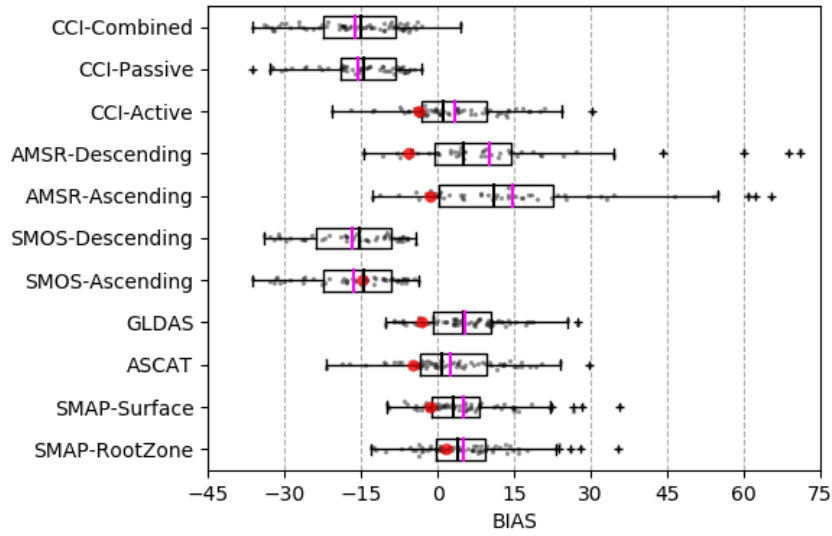


(a)

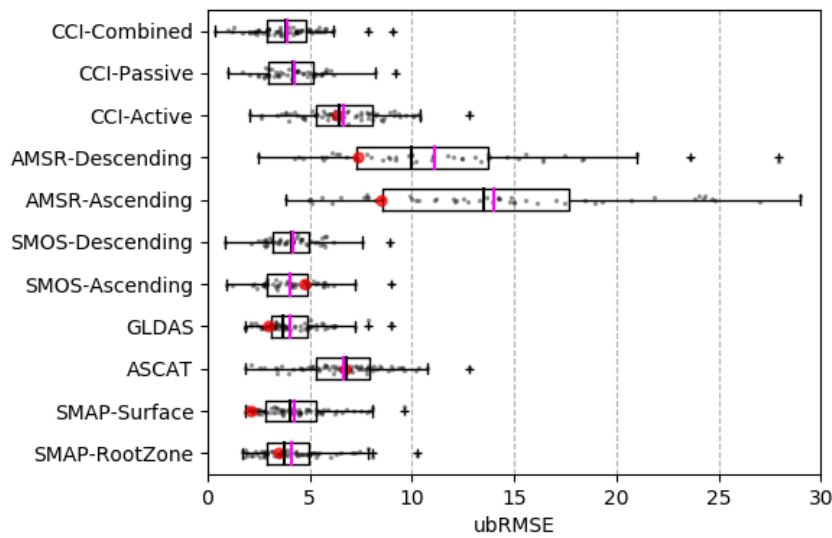


(b)

Figure 4.3: a) r^2 and b) RMSE values between Satellite and CRNP Based Soil Moisture Data. Points in red indicate Çakıt Basin CRNP, gray points indicate the other CRNP stations and pink lines indicate the average values.



(a)



(b)

Figure 4.4: a) Bias and b)ubRMSE values between Satellite and CRNP Based Soil Moisture Data. Points in red indicate Çakıt Basin CRNP, gray points indicate the other CRNP stations and pink lines indicate the average values.

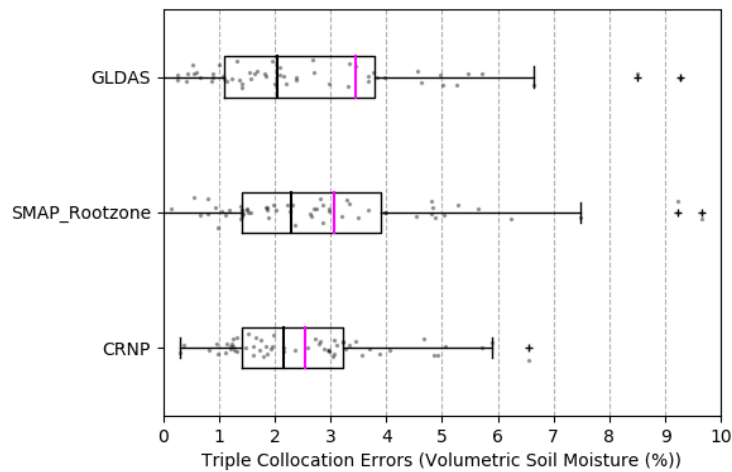
Table 4.2: Mean Values of r^2 , RMSE, ubRMSE and bias values of soil moisture products with CRNPs

	r^2	RMSE	ubRMSE	Bias
SMAP-Rootzone	0.32	9.37	4.13	5.09
SMAP-Surface	0.37	9.06	4.24	5.10
ASCAT	0.31	10.94	6.64	2.61
GLDAS	0.36	9.23	4.04	5.27
SMOS-Ascending	0.27	16.98	4.06	-16.34
SMOS-Descending	0.25	17.31	4.19	-16.64
AMSR-Ascending	0.07	23.64	14.00	14.64
AMSR-Descending	0.17	19.18	11.12	10.12
CCI-Active	0.29	10.83	6.64	3.27
CCI-Passive	0.29	16.38	4.23	-15.67
CCI-Combined	0.33	16.83	3.85	-16.10

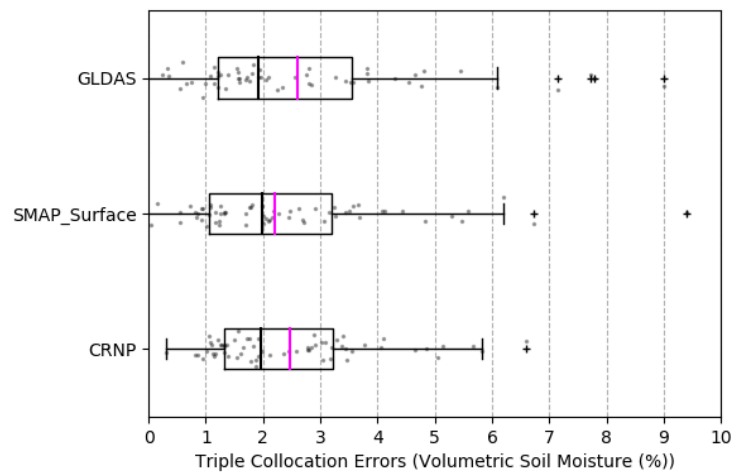
Table 4.3: Median Values of r^2 , RMSE, ubRMSE and bias values of soil moisture products with CRNPs

	r^2	RMSE	ubRMSE	Bias
SMAP-RootZone	0.30	7.08	3.75	4.09
SMAP-Surface	0.33	6.95	4.02	3.17
ASCAT	0.28	9.05	6.81	0.76
GLDAS	0.34	8.40	3.69	5.00
SMOS-Ascending	0.24	15.34	4.01	-14.40
SMOS-Descending	0.20	16.10	4.10	-15.24
AMSR2-Ascending	0.03	17.33	13.47	10.96
AMSR2-Descending	0.10	14.33	9.99	5.19
CCI-Active	0.26	8.87	6.41	1.10
CCI-Passive	0.24	15.23	4.20	-14.47
CCI-Combined	0.33	15.80	3.82	-14.87

It is assumed that the main assumptions of triple collocation analyses [57] are satisfied for the soil moisture products used in this study and all products have reasonably high r^2 values with low ubRMSE. Triple collocation studies have been performed for the CRNP stations of COSMOS database and Çakıt Basin CRNP and the results are presented with Figure 4.5 for satellite based (SMAP surface and rootzone), observed (CRNP) and modelled (GLDAS) products.



(a)



(b)

Figure 4.5: Triple collocation errors of soil moisture products of data triplets including SMAP (a) rootzone and (b) surface products, average values are indicated with pink lines.

4.5 Summary and Discussion of the Results

In this study, the soil moisture data obtained from the Çakıt Basin CRNP and all of the available CRNPs in the COSMOS database have been used to validate the most commonly used five spaceborne soil moisture products (ASCAT, SMAP, SMOS, AMSR, CCI) and a global land surface model (GLDAS). The validations have been made through direct comparisons and triple correlation tests.

Validation of different soil moisture products with CRNP's shows that SMAP-surface product has a remarkable coupling with the CRNP measurements having $r^2=0.82$ m^3/m^3 and ubRMSE=2.1%. The coefficient of determination value between CRNP and SMAP is the highest among all of the stations in the COSMOS database. Besides the SMAP rootzone soil moisture product, all of the soil moisture products underestimate the CRNP measurements.

For the accuracy of ASCAT products, this study produces similar results with a previous study [99] where ASCAT soil moisture products have been validated by FLUXNET [102] data. This study also supports the findings of the previous studies which suggest that the ascending node products of passive sensors are slightly more accurate than the descending ones [98]. CCI-combined is a product which has been developed by combining several active and passive sensor soil moisture products including the ones that have been investigated in this study. CCI combined and CRNP has a good coupling by means of coefficient of determination, yet SMAP surface soil moisture product is still more accurate than CCI which indicates that even combining all the products can not produce better results than SMAP surface product. Both rootzone and surface products of SMAP has been found to be more accurate for drier regions where vegetation is sparse. Adversely, ASCAT soil moisture products produce better results for areas with denser vegetation. In general, the comparisons of CRNPs of COSMOS database with ASCAT and SMAP surface products yield equally good statistics supporting the findings of [95, 103]. It is also stated in a recent study [18] that SMAP surface is the most accurate satellite base soil moisture product when compared to ground observations of CRNPs. By means of ubRMSE metrics, all of the satellite soil moisture products except AMSR have similar values with CRNP observations. Evaluation of bias values indicates that SMOS products

and CCI passive products have a tendency to underestimate CRNP while the other products estimations depends on the study sites. In general, satellite products with passive microwave sensors such as SMOS and AMSR are much less successful in estimating in-situ soil moisture observations and they show much higher errors and lower correlations. In addition to that, the temporal resolutions of these products are highly limited thus making use of them in hydrological applications is not practical.

According to triple collocation statistics (Figure 4.5), SMAP surface product has relatively lower errors with observed and modelled soil moisture products. Signal to noise ratios of SMAP products are greater than 1dB for most of the stations which indicates the meaningful soil moisture signal is greater than the noise. CRNP has relatively less errors for the triplets, which include the SMAP surface soil moisture data compared to the triplets, which include the SMAP rootzone data. For Çakıt Basin, signal to noise ratios of SMAP rootzone and surface products are 1.69 and 6.42 respectively, in other words the estimations of SMAP rootzone includes much more noise when compared to SMAP surface product. SMAP surface product also has lower triple collocation errors than GLDAS product supporting the findings of [18].

Although the horizontal footprint of CRNPs are much larger than many of its in-situ counterparts, it still has a scale mismatch with the much larger grid cells of the satellite products. Therefore the difference between horizontal and vertical measurement scales of CRNPs and satellite products are considered to be one of the main source of errors. The different algorithms and methods used for inferring soil moisture values from satellite images also affects the difference between correlation statistics for soil moisture products since the soil moisture retrieval methods of satellite products depend on site conditions such as vegetation, topography, soil type, snow cover, temperature and volume scattering properties [13]. The reason of the inaccuracy of ASCAT product for Çakıt Basin is for example due to sub-surface scattering phenomena of dry soil which is a problem mainly occurring in the Mediterranean region.

When the results of the soil moisture products other than the spaceborne ones are investigated, it can be seen in Figure 4.1 that CRNP and TDR sensors have similar trends with a slight underestimation on the CRNP side, which may be due to the vertical footprint of CRNP (12-25cm) which is slightly deeper than that of TDR (5cm).

Land surface models also produce highly reliable results when compared to Çakıt Basin CRNP. Noah LSM outputs of both GLDAS and the local model produce consistent results where the local model is slightly better as it is expected since the local model is forced with in-situ data and the grid size of GLDAS (625km²) is much larger than the horizontal footprint of CRNP.

As a result, it can be stated that most of the spaceborne soil moisture products, especially the ones with active sensors, has a good potential to be used in conjunction with CRNP observations especially for larger areas where in-situ validation is required. The main disadvantage of CRNP is its inability to measure soil moisture, where there exist snow cover. Although there are several attempts to overcome the disadvantages of CRNP for unfavorable conditions, using satellite soil moisture data as a secondary source of information can be beneficial for hydrological studies. Similarly, CRNP data can be used to enhance the temporal and spatial resolutions of satellite products and can be used in calibration of the soil moisture retrieval algorithms. Results of validation highly depend on the site conditions and the areas where the CRNPs are located, thus these types of studies should be conducted for areas having different attributes. Although, CCI products, which are the combinations of different satellite products, constitute a successful effort for many locations as they produce improved statistics, for some locations including the Çakıt Basin these products may produce fairly poor results which is mainly due to selection of inaccurate soil moisture products for the combination process.

CHAPTER 5

ASSESSMENT OF THE RELATION BETWEEN EVAPORATION AND SOIL MOISTURE

5.1 General

Soil moisture and evapotranspiration are the two key elements of hydrological studies having their own dynamics in relation with the water and energy exchanges between different stages of the hydrological cycle. Understanding the behavior of terrestrial evaporation and soil water is crucial in all fields of soil water studies including agriculture. However, being the most difficult variable to measure in the field makes our knowledge on evaporation highly limited when compared to the knowledge on other elements of the cycle. In addition to that, acquiring reliable information about soil moisture content on large areas may require intensive effort due to the heterogeneous nature of the soil. Soil evaporation has been studied for a long time by different researches based on the concept of soil mechanics. Previous studies [104, 105] were mostly focused on a very small scale and consist of theoretical conclusions, which were very difficult to apply at the field, where recent studies were able to identify the relation between soil moisture and evaporation at the field for certain soil types by using several different methods such as measuring the changes in gas concentrations above the soil [106, 107], by using thermal properties of soil and transforming heat fluxes to soil evaporation [108, 109] and making use of conceptual models of dry soil layers [110, 111]. Many current techniques make use of eddy covariance sensors or lysimeters to obtain evapotranspiration. However, spatial footprint of the volumetric soil content is highly limited when compared to the spatial footprint of EC sensors or other means of evaporation data. Comparing direct field measurements is very challenging due to the scale mismatch between evaporation and soil moisture mea-

surements. For this reason, the current studies investigating the relation between soil moisture and evaporation are based mainly on proxy methods. The most common approach is using satellite based observations for both soil moisture and evaporation [112, 113]. In these types of analyses, drying rates of the upper soil layer are investigated to model soil evaporation. On the other hand, soil moisture values obtained from Cosmic Ray Neutron Sensing methodology was also used previously in similar researches [114, 115] as it has been previously used in many other studies involving satellite validation [18, 19]. According to a study conducted in Australia [115], a direct relation between soil moisture and evaporation does not exist, on the other hand, the probability distributions of these two variables are similar to each other which means they cannot be considered separately. A previous study suggest that the relation between these two variables are highly affected by soil heterogeneity hence regional studies may yield different results than the local ones [116]. A similar study managed to achieve a formulation of evapotranspiration using soil moisture and runoff information by utilizing a water balance approach [114]. There are various studies in the literature trying to enhance land surface models by utilizing soil moisture data [117, 118, 119, 120, 121, 122, 123, 124, 125, 126, 127, 128]. A study in 2013 [129] modified Penman Monteith (PM) [130] by introducing soil moisture data and MODIS-NDVI satellite information to the PM model. It has been shown that the daily evaporation estimates are significantly improved. Another study in Australia also suggests evaporation estimates of models can be slightly improved with soil moisture data especially in drier locations [131]. In a more recent study [113], the researchers tried to improve the evapotranspiration calculations of PT-JPL ET model by introducing SMAP satellite soil moisture information. They found out that the errors of the model are significantly reduced if the soil moisture is integrated into soil evaporation or transpiration especially in drier areas with large amounts of soil evaporation.

5.2 Evaporation Data of the Study Area

For this study, soil moisture data are obtained from the Cosmic Ray Neutron Probes of COSMOS database and the Cosmic Ray Sensor located in the Çakıt Basin. The

details on obtaining CRNP based soil moisture dataset are provided in Section 3.2.1. For Çakıt Basin evaporation data have been obtained by three different sources. Evapotranspiration data have been obtained from Eddy covariance sensor based observations which serve as the only measurement based evapotranspiration estimates of the site, whereas Actual Evapotranspiration (ET_a) values retrieved from local Noah LSM and GLDAS based Noah LSM evapotranspiration outputs provide model based evapotranspiration data. The time interval of the analyses is between October 1, 2016 and September 30, 2018. Time series of evapotranspiration products are provided in Figure 5.1.

5.3 Methodology of Comparing Soil Moisture and Evaporation

Since soil moisture and evaporation data are defined in different units, all data which are used in the studies were standardized by using the methodology given in [115] (Equation 5.1)

$$x_{std} = \frac{x - \bar{x}}{\sigma} \quad (5.1)$$

where; \bar{x} is the mean value of the dataset and σ is the standard deviation.

Snow filtering for soil moisture data was made as it is mentioned in Chapter 4. 69 stations from the COSMOS database have data between October 1, 2016 and September 30, 2018. 53 stations with more than 100 days of data from those stations were used in the analysis. For Çakıt Basin, relation between soil moisture and ET_a values are further investigated by both comparing them directly and analyzing the similarities between the cumulative distribution functions (cdf). Two different sources of evapotranspiration information are taken into account for the analyses. First one is based on Eddy covariance system data and the second one is the Noah LSM output. Eddy covariance system data are obtained from a study conducted for the Çakıt Basin [132] where the data had been converted to evapotranspiration by utilizing energy balance methods at daily basis. Soil moisture data are obtained from the CRNP. The scaled soil moisture and evapotranspiration products are provided in Figure 5.2

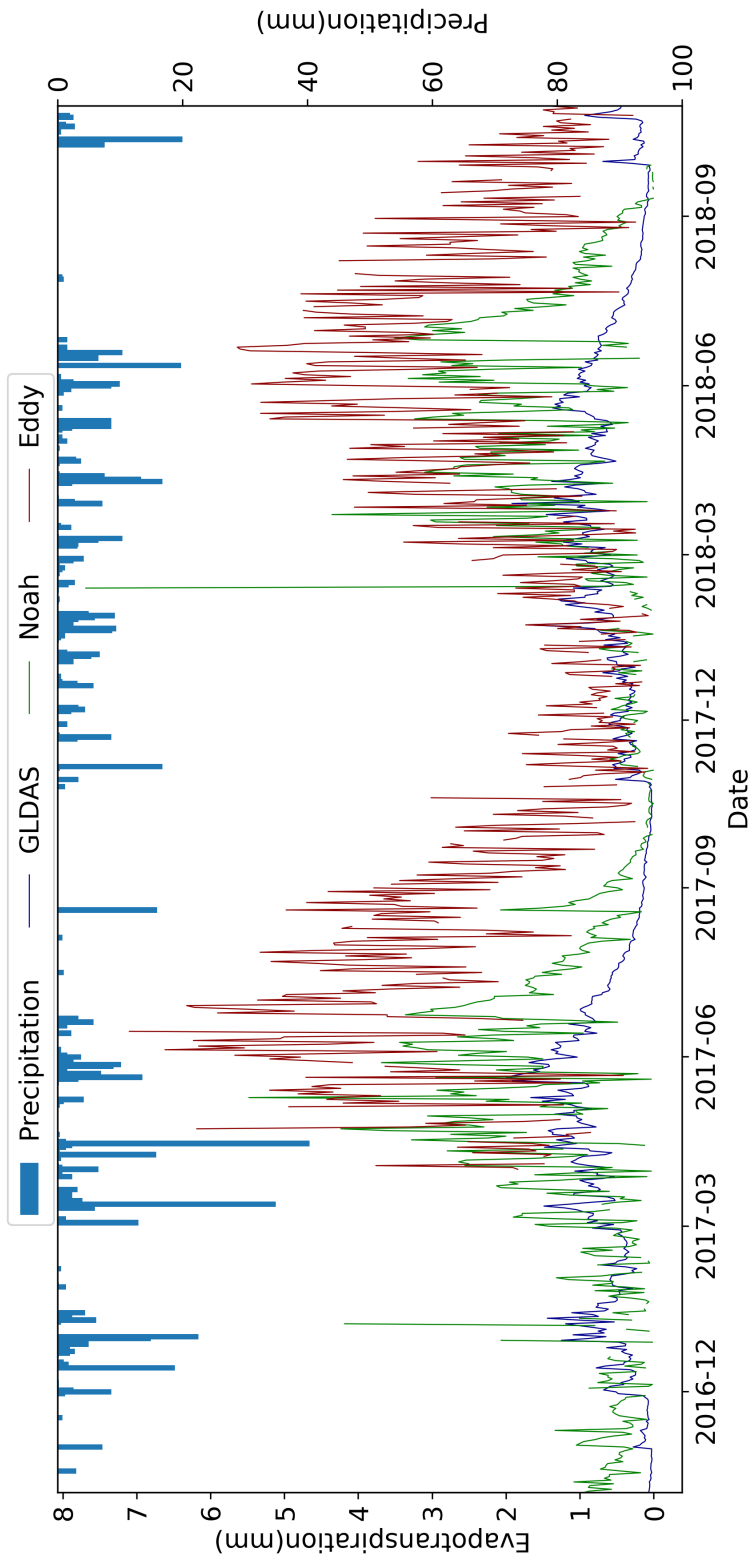


Figure 5.1: Time series of actual daily evapotranspiration values of GLDAS, Noah LSM and Eddy covariance sensor for Çakıt Basin.

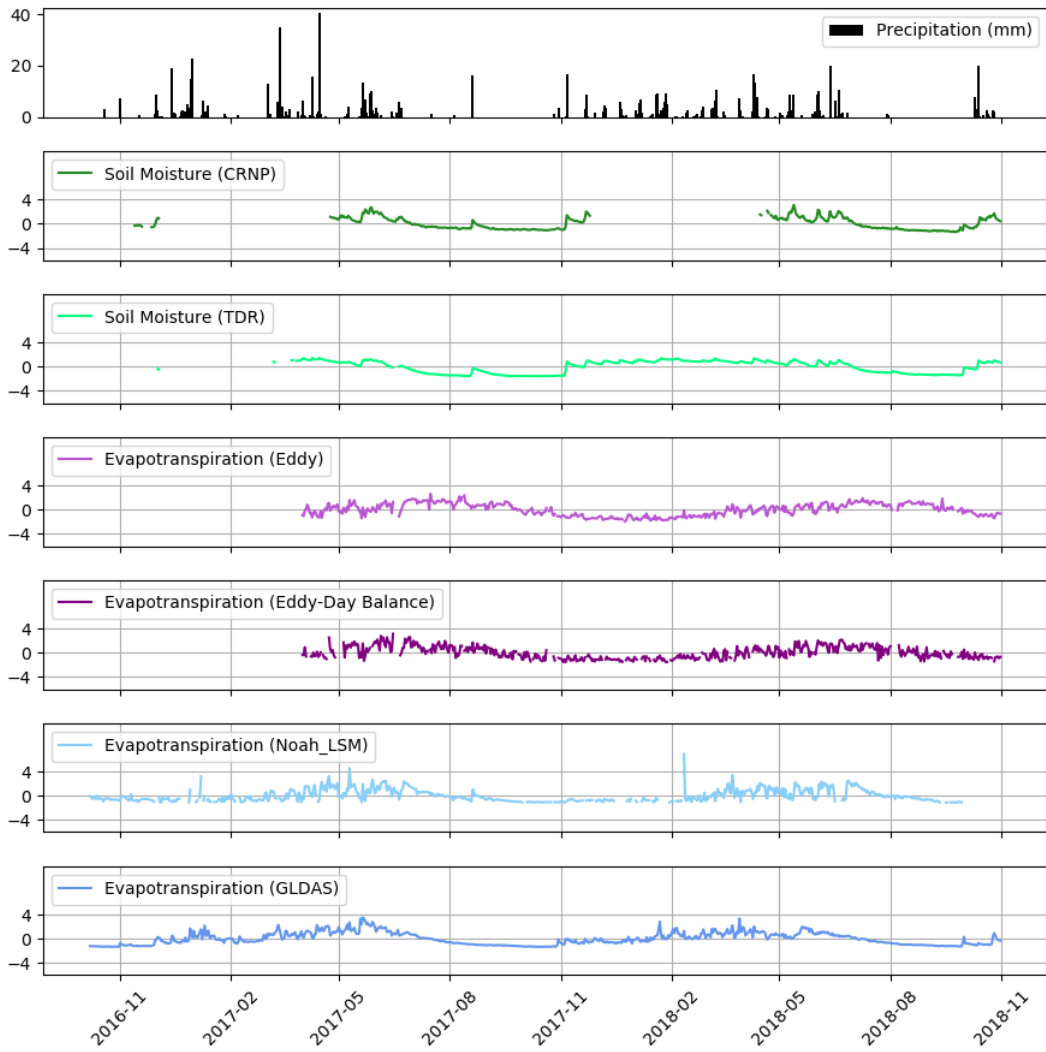


Figure 5.2: Time series of scaled soil moisture and evapotranspiration products.

5.4 Results

5.4.1 The Relation Between Evapotranspiration and Soil Moisture Products of GLDAS

Within the scope of this study, the relation between soil moisture and evaporation is further investigated through comparing GLDAS Noah LSM soil moisture and evaporation outputs for the entire planet. For the comparisons, 3 hourly actual evaporation and 10cm depth soil moisture outputs of GLDAS Noah LSM have been utilized. Since the evapotranspiration values are highly variable within a day, daily summation of evapotranspiration values and daily averages of soil moisture values have been used in the analyses. Time scale of the analyses is between March 2015 and December 2018. Figure 5.3 shows the r^2 values obtained for each GLDAS pixel, which has 25km width. r^2 values obtained from monthly and weekly averages are provided in Appendix C (Figure C.1 and Figure C.2). For each month r^2 values of soil moisture and evaporation are provided in Appendix C (Figures C.3 - C.14).

5.4.2 The Relation Between Evapotranspiration and CRNP Based Soil Moisture

Direct relation between CRNP based soil moisture and evaporation estimates for Çakıt Basin are shown in Figures 5.4a - 5.4c. For all of the stations of the COSMOS database, r^2 and RMSE values (Section 3.4) of CRNP based standardized soil moisture and GLDAS based standardized actual evapotranspiration data have been calculated and summarized in Figure 5.5a and Figure 5.5b, where the red dot shows the Çakıt Station and the blue dot shows the local Noah model value for the same station. Gray dots indicate stations in the COSMOS database. The r^2 values obtained from the quantile-quantile values of the soil moisture data of each COSMOS station with the corresponding GLDAS Noah LSM based evapotranspiration data are provided in Figure 5.5c. Distribution of r^2 and RMSE values on the world map is shown in Figure 5.6 and Figure 5.7.

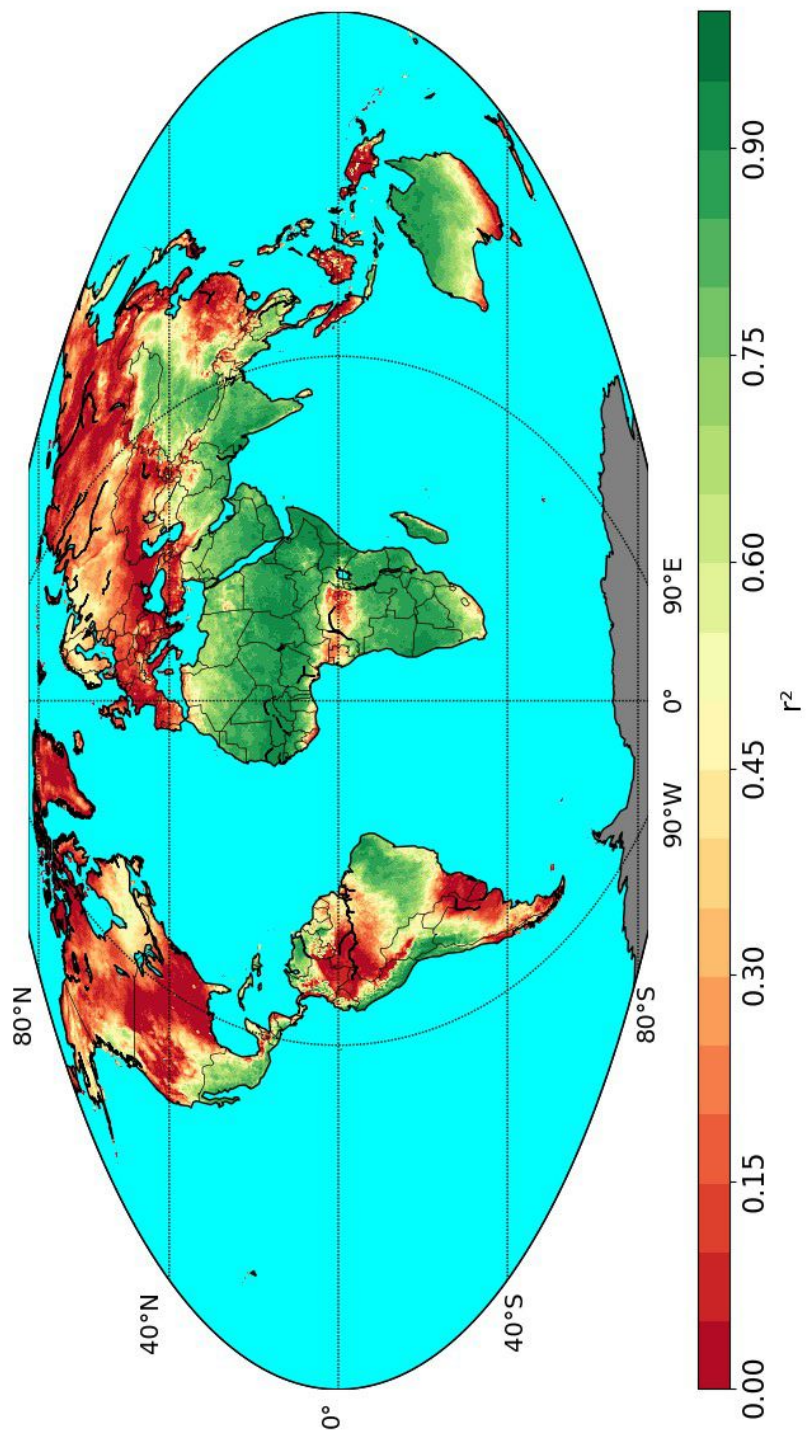
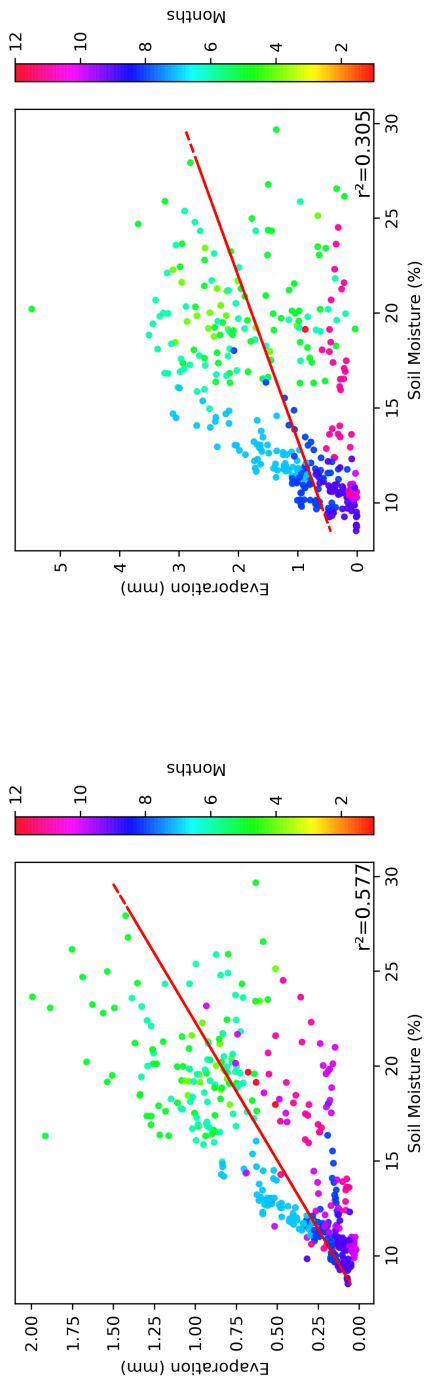
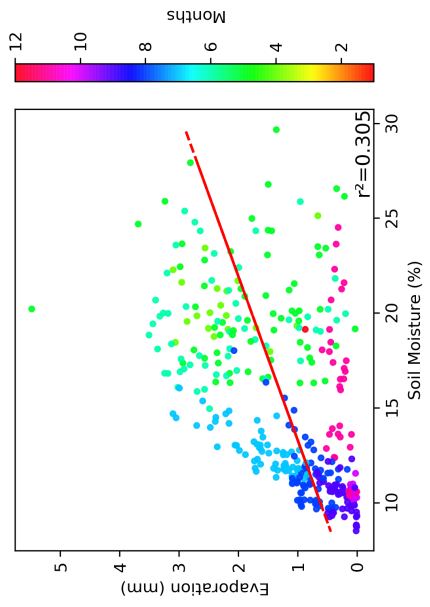


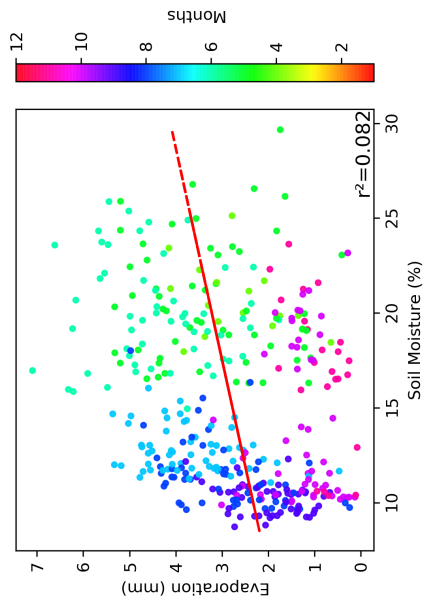
Figure 5.3: r^2 values of the comparison between GLDAS Noah LSM soil moisture and evapotranspiration outputs



(a)

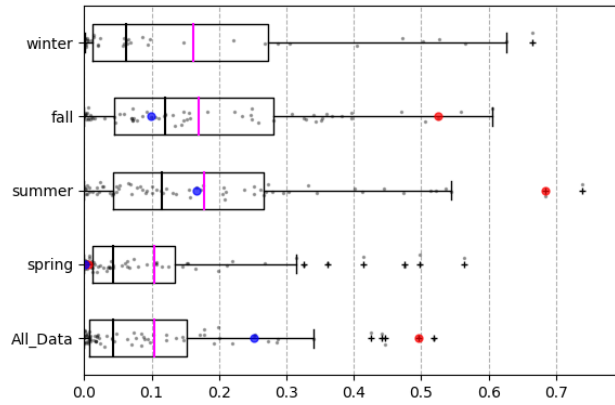


(b)

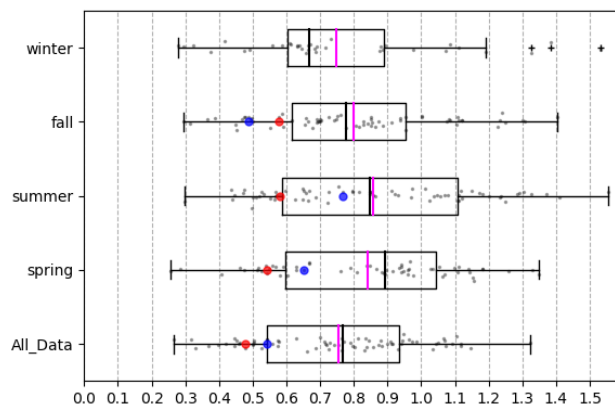


(c)

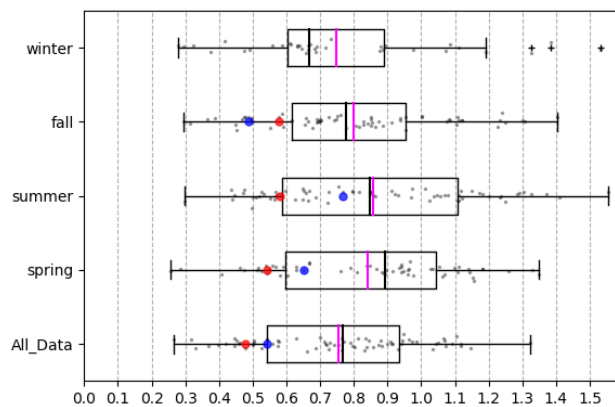
Figure 5.4: The relation between CRNP based daily volumetric soil moisture and evaporation values based on a) GLDAS b) Local Noah LSM c) Eddy Covariance Sensor.



(a)

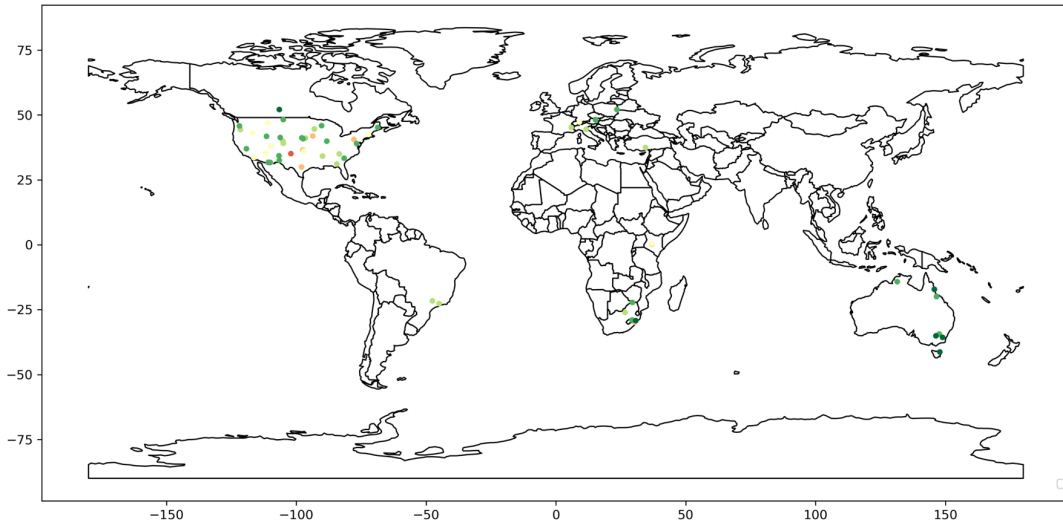


(b)

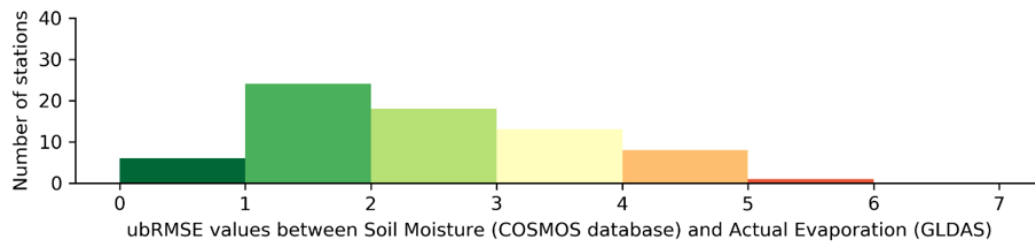


(c)

Figure 5.5: a) r^2 and b) RMSE c) r^2 of the quantiles of CRNP based standardized soil moisture and GLDAS based standardized actual evapotranspiration data.

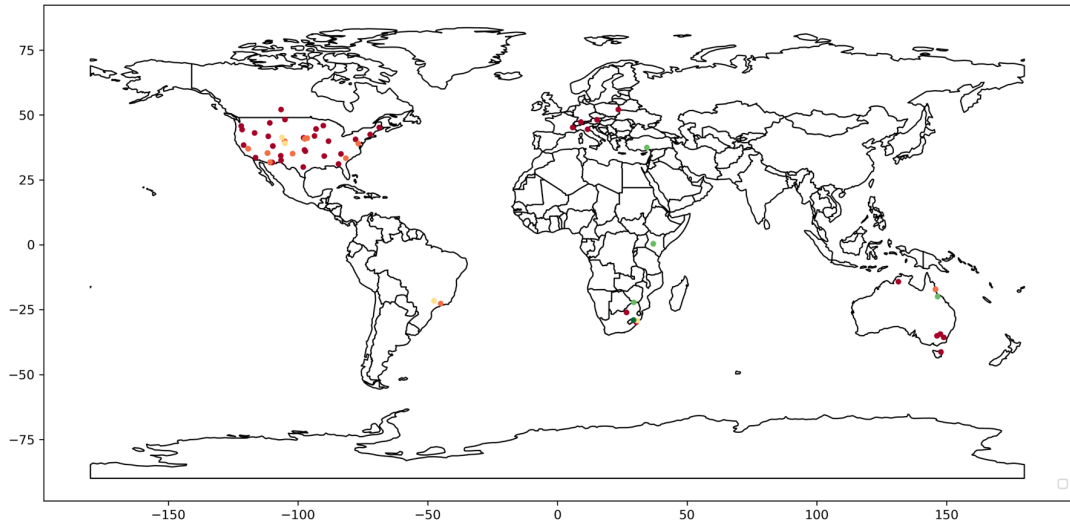


(a)

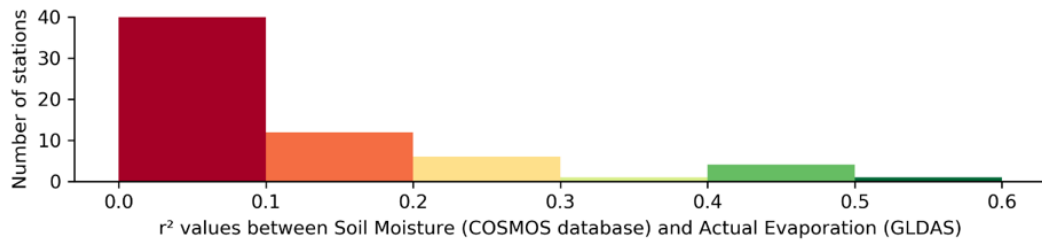


(b)

Figure 5.6: a) RMSE values between standardized GLDAS evapotranspiration outputs and soil moisture data of COSMOS stations shown on the world map b) Histogram of RMSE values.



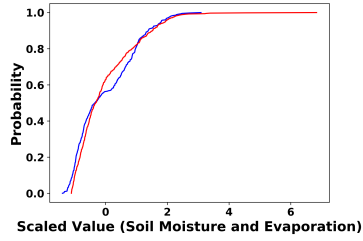
(a)



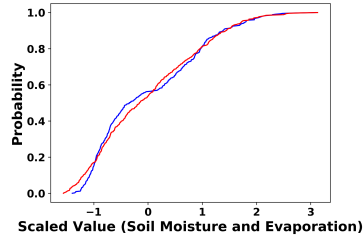
(b)

Figure 5.7: a) r^2 values between standardized GLDAS evapotranspiration outputs and soil moisture data of COSMOS stations shown on the world map b) Histogram of r^2 values.

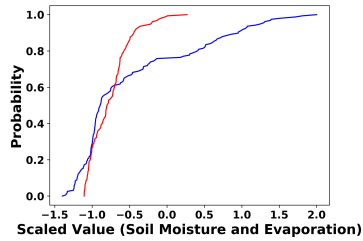
Cumulative distribution functions for soil moisture and ET are compared for each season and shown in Figure 5.8. Daily changing values are the differences in values between consecutive days, a similar analysis conducted by using the daily changing values of ET and soil moisture are shown in Figure 5.9. The relation between soil moisture and ET_a was further investigated by non parametric quantile-quantile plots (Q-Q plots), which are presented in Figure 5.10. The similarity between the Q-Q graph and the red line shows that the two data are sampled from the same distribution.



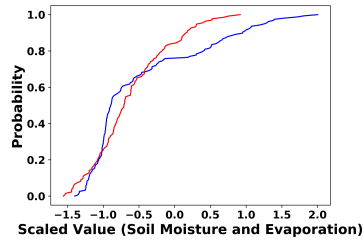
(a) Noah LSM - all data



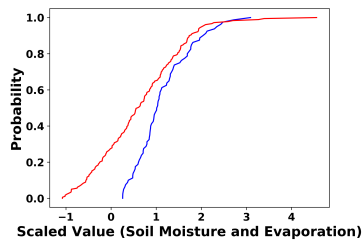
(b) Eddy - all data



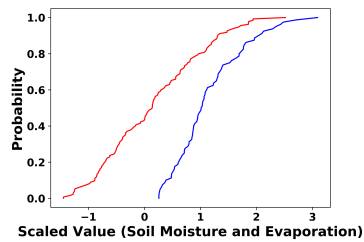
(c) Noah LSM - Fall



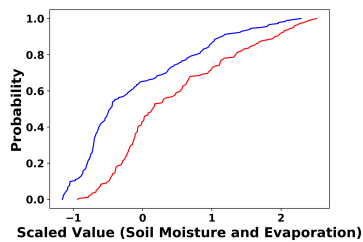
(d) Eddy - Fall



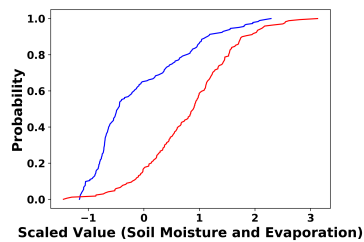
(e) Noah LSM - Spring



(f) Eddy - Spring

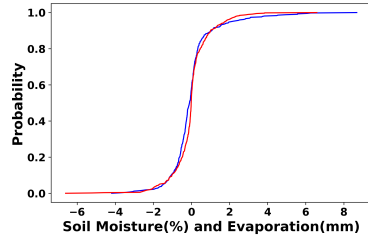


(g) Noah LSM - Summer

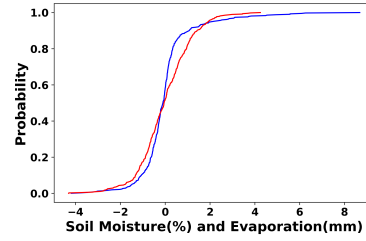


(h) Eddy - Summer

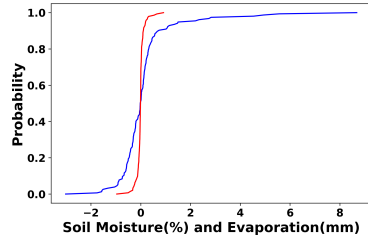
Figure 5.8: Cumulative Distribution Functions of Soil Moisture (CRNP) and Evapotranspiration (Noah LSM or Eddy). (Blue:Soil Moisture, Red:Evapotranspiration)



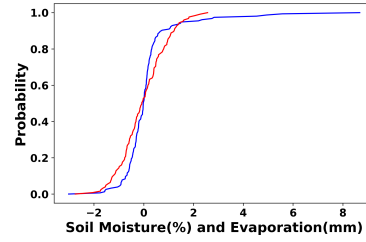
(a) Noah LSM - all data



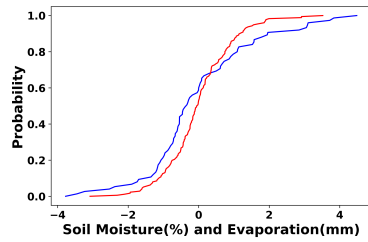
(b) Eddy - all data



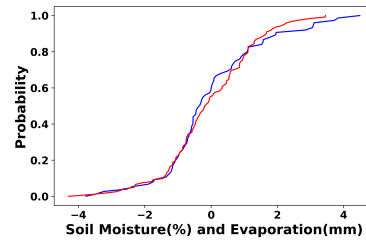
(c) Noah LSM - Fall



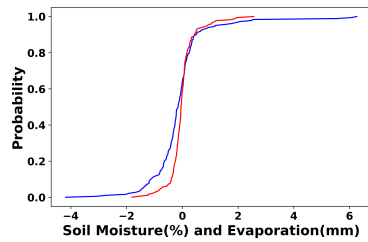
(d) Eddy - Fall



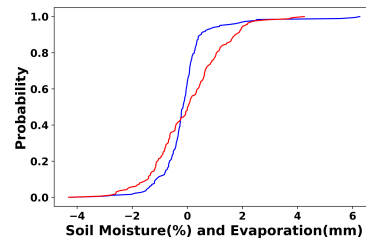
(e) Noah LSM - Spring



(f) Eddy - Spring

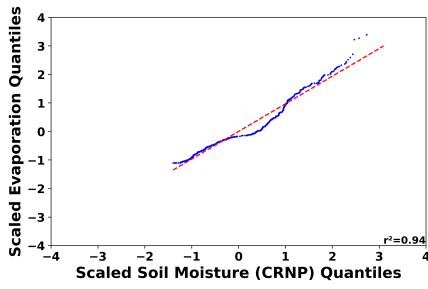


(g) Noah LSM - Summer

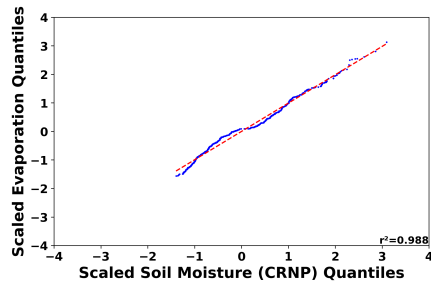


(h) Eddy - Summer

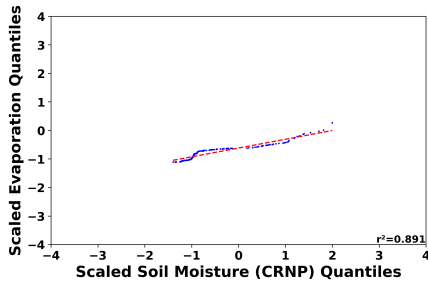
Figure 5.9: Cumulative Distribution Functions of daily changing values for Soil Moisture (CRNP) and Evapotranspiration (Noah LSM or Eddy). (Blue:Soil Moisture, Red:Evapotranspiration)



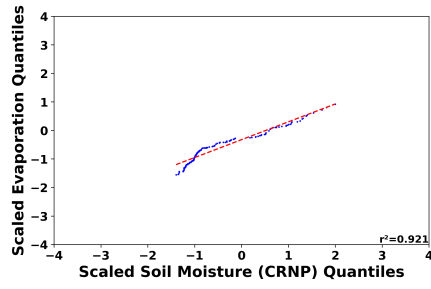
(a) Noah LSM - all data



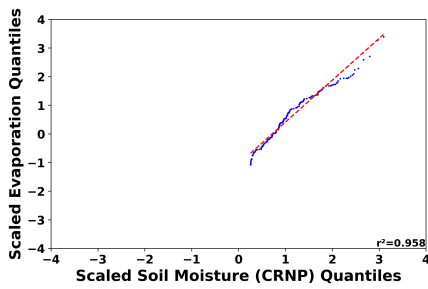
(b) Eddy - all data



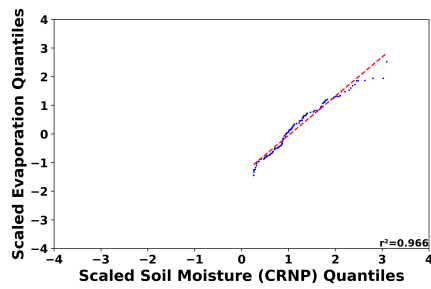
(c) Noah LSM - Fall



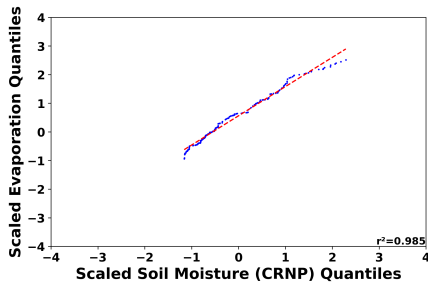
(d) Eddy - Fall



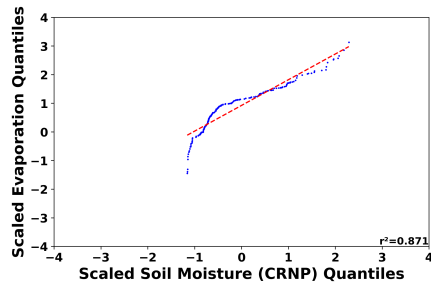
(e) Noah LSM - Spring



(f) Eddy - Spring



(g) Noah LSM - Summer



(h) Eddy - Summer

Figure 5.10: Q-Q Plots of Soil Moisture (CRNP) and Evapotranspiration (Noah LSM or Eddy). (Blue:Soil Moisture, Red:Evapotranspiration)

5.5 Summary and Discussion of the Results

In this study, the relation between evapotranspiration and soil moisture is investigated through comparing CRNP based soil moisture values with Eddy covariance and land surface model based evapotranspiration values. For comparison purposes, soil moisture and evapotranspiration data have been normalized to have the same unit of measures. Cumulative distribution functions and quantile-quantile plots of soil moisture and evapotranspiration values have also been compared. GLDAS Noah LSM actual evapotranspiration outputs have been used to calculate modelled evapotranspiration with the soil moisture values obtained from CRNPs of the COSMOS database. In addition to the CRNPs of the COSMOS database, the evapotranspiration outputs have also been compared with the soil moisture outputs of GLDAS.

It has been found that evapotranspiration and soil moisture have a relatively predefinable relation thus further studies may focus on improvement of soil moisture outputs of hydrological models via introducing evapotranspiration measurements into hydrological models.

In the drier months, it can be seen that the relationship between soil moisture and evaporation is stronger (Figures C.7-C.11). ET_a calculated by Eddy covariance system is higher than the other ET_a products for the entire data series.

Both soil moisture and evapotranspiration data have similar cdf's especially for the daily changing values and summer season. It is reasonable for drier days to better relate daily changing ET_a and soil moisture since the lack of rain and runoff creates a more direct relation between these two parameters by means of the water cycle.

The results of Noah LSM for Figures 5.8-5.10 show that ET_a obtained from Noah LSM has more similar distribution with the soil moisture data obtained from the CRNP compared to the Eddy based ET_a .

For Çakıt station it can be seen that the GLDAS based Noah LSM ET products have much higher correlation than local Noah model products with soil moisture. There are two main reasons for the difference of the results of two ET_a products of Çakıt Basin. Firstly, GLDAS utilizes spatially coarser forcing data obtained from global

datasets, and Noah LSM uses point data obtained directly from the site. Secondly, the semi-arid condition of the basin has been emphasized more strongly in the local Noah LSM, which makes the top soil layer dry much faster thus producing much sharper changes in the daily ET_a outputs.

The results of comparing GLDAS soil moisture and evapotranspiration data suggest that in warmer climates the correlations are more prominent and for the Mediterranean region the correlations are higher in summer and fall months.

CHAPTER 6

INTEGRATION OF SOIL MOISTURE DATA INTO HYDROLOGICAL MODELLING

6.1 General

An hydrological process for a basin can be simplified as water entering the basin (precipitation), stored in the basin (snow, soil moisture, groundwater) and leaving the basin (evaporation and discharge). All of the elements of the hydrological cycle are interrelated with each other in this process. Hydrological models try to mimic the natural phenomena having their main focus on estimating the discharge accurately. In practical hydrology, conceptual hydrological models have been widely used in many studies such as flood estimation and drought monitoring. Conceptual models such as NAM model [133] mostly rely on calibration of various parameters, which affect the relation between rainfall and runoff, in order to estimate discharge accurately. On the other hand, discharge is not the only product that can be estimated with a hydrological model. It is possible to repeat the same process by using observed and simulated soil moisture data instead of the discharge. However, soil moisture and discharge are interrelated parameters, thus, considering both of them in the calibration process should improve the estimates of the hydrological models. There are several studies in literature that suggest improvement of hydrological models through soil moisture data assimilation [134, 135]. Introducing soil moisture data into physically based models such as Noah LSM is also possible. In this case, the model relies on the input meteorological and atmospheric forcing affecting the provided initial conditions in accordance with the laws of physics instead of calibration of the model with observed variables. In other words, introducing soil moisture data to physically based models are not made by calibration, but it is made via data assimilation to improve the soil

moisture outputs. The most common approach is to use Ensemble Kalman Filter (EnKF) approach [136]. There are several studies in the literature, which manage to improve soil moisture estimates of physical models by assimilating satellite based soil moisture [137, 138, 121]. Most of the recent publications on this area utilizes NASA's Land Information System (LIS) [139], which provides several land surface models and forcing fields as well as the one dimensional EnKF suite available for researchers.

6.2 Hydrological Models

Hydrological models have been created in order to simulate the relationships between parameters in the hydrological cycle. There are several types of hydrological models, which can be classified under three main headings namely metric, conceptual and physical models [140]. Metric models try to identify the rainfall-runoff relation of a basin through empirical formulations such as unit hydrograph theory [141], the rational method [142] and Soil Conservation Services (SCS) Curve Number method [143], which mostly rely on observations. Conceptual models utilize a system approach to understand the inputs and outputs of a basin and simulate the rainfall-runoff relation through the mathematical conceptualization of the relation between different water storages in the system. Properties of each water storage are determined through calibration of the conceptual models to make simulated outputs similar to the observed ones. Conceptual models are generally lumped models, in other words they represent the study area with single values for site characteristics or meteorological variables. HEC-HMS (Hydrologic Modeling System) [144], HBV (Hydrologiska Byråns Vattenbalansavdelning) [145] and NAM (NedborAfstromnings Model) [133] are just a few of many examples of conceptual models. Physical models simulate the laws of physics and calculate energy and water balance for the basin. Physical models utilize the equations of conservation of mass and energy directly, and unlike conceptual models, there is no parameter calibration for this type of models. On the other hand, great amount of input data is required for physical models to represent water and energy transfers between the elements of the hydrological cycle. MIKE-SHE (Système Hydrologique Européen) [146], SWAT (Soil and Water Assessment

Tool) [147], VIC (Variable Infiltration Capacity) [148] and Noah LSM (Land Surface Model) [149, 150] are just few of many examples of physical models.

6.2.1 NAM Model

In this thesis, NAM model [133] has been used as the conceptual model in order to establish the relation between rainfall and runoff. NAM model has been used in vast amount of hydrological studies [151, 152, 153, 154, 155, 156, 157]. NAM model considers the basin as a system consisting of four water storage units and formulates the interrelations between different water storages. According to the NAM model, water can be stored in the snow cover, on the surface of the basin, inside the vegetation root zone or as groundwater. The assumed interrelations and the model structure of the NAM model has been shown by [155] as in Figure 6.1.

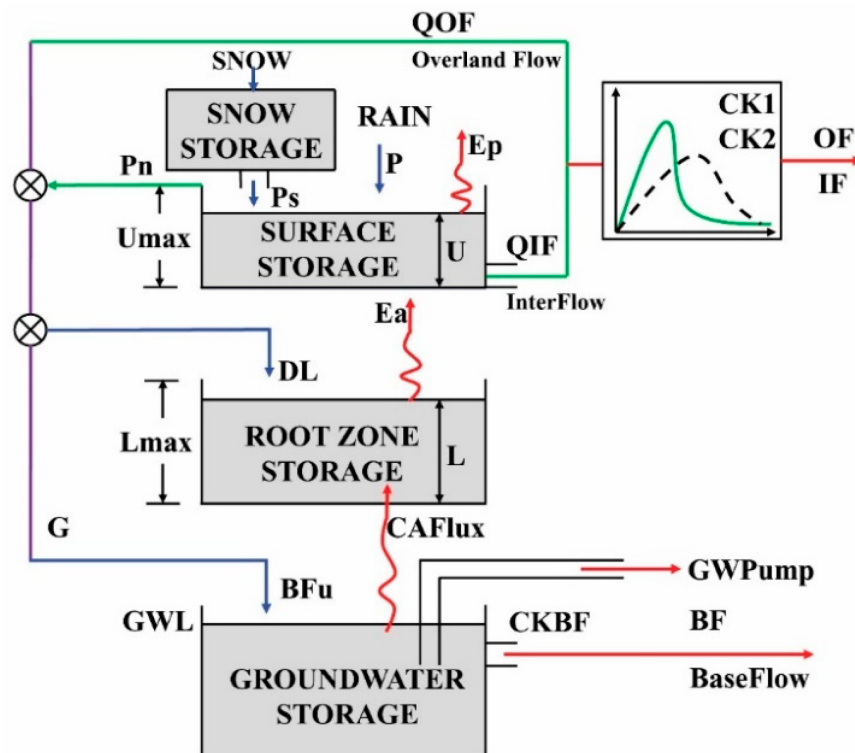


Figure 6.1: Schematic Representation of Modeling with NAM [155]

Snow storage represents the amount of water which is stored in the snow form. The model assumes precipitation as snow if the air temperature is lower than the base

temperature parameter (T_0) and if the air temperature is above than T_0 , NAM model assumes the melting of the snow to surface storage (6.1), where C_{snow} is the degree-day coefficient.

$$QS = \begin{cases} C_{snow} (T - T_0) & \text{for } T > T_0 \\ 0 & \text{for } T \leq T_0 \end{cases} \quad (6.1)$$

The second type of storage of water is the surface storage. Evapotranspiration occurs from surface storage at the potential evapotranspiration rate (E_p) if the amount of water stored in the surface storage (U) is greater than or equal to the requirements of E_p . If this criterion is not met, actual evaporation rate (E_a) is calculated by using Eq.6.2, where L denotes the water stored in the root zone and L^* is the maximum amount of water that can be stored in the root zone. The third type of water storage is the root zone water storage, which represents the amount of water stored at the lower zone where the roots of plants can use and transform some of the available water to transpiration. Excess amount of water is infiltrated to the last storage type, which is the groundwater storage.

$$E_a = (E_p - U) \frac{L}{L^*} \quad (6.2)$$

U_{max} denotes the maximum possible water available at the surface storage before the excess precipitation (P_N) is transformed to the overland flow (QOF). QOF is calculated by using (Eq.6.3) where, the parameter $CQOF$ is the coefficient of runoff and the parameter TOF is the threshold value for overland flow.

$$QOF = \begin{cases} CQOF \frac{L/L^* - TOF}{1 - TOF} P_N & \text{for } L/L^* > TOF \\ 0 & \text{for } L/L^* \leq TOF \end{cases} \quad (6.3)$$

The remaining portion of U is transformed into E_a , interflow (QIF) and infiltration water to the groundwater storage (G). QIF is calculated by using Eq. 6.4, where the parameter $CKIF$ is the time constant, and the parameter TIF is the threshold value for interflow. Baseflow is also calculated with the same approach by using the parameter $CKBF$ which is the time constant for baseflow. Overlandflow is calculated by

using the same routing approach where the parameter CK_{12} is the time constant of overland flow and it is calculated by using Eq.6.5. OF_{min} denotes the minimum over-flow for linear routing and it is taken as 0.4mm/h. β is the constant of the Manning formula for flow routing and it is taken as 0.4.

$$QIF = \begin{cases} (CKIF)^{-1} \frac{L/L^* - TIF}{1 - TIF} U & \text{for } L/L^* > TIF \\ 0 & \text{for } L/L^* \leq TIF \end{cases} \quad (6.4)$$

$$CK = \begin{cases} CK_{12} & \text{for } OF < OF_{min} \\ CK_{12} \left(\frac{OF}{OF_{min}} \right)^{-\beta} & \text{for } OF \geq OF_{min} \end{cases} \quad (6.5)$$

G is calculated by using Eq. 6.6. where the parameter TG is the threshold value for groundwater infiltration.

$$G = \begin{cases} (P_N - QOF) \frac{L/L_{max} - TG}{1 - TG} & \text{for } L/L_{max} > TG \\ 0 & \text{for } L/L_{max} \leq TG \end{cases} \quad (6.6)$$

Summation of interflow, outflow and baseflow gives the simulated discharge at each time step ($Q_{sim}(t)$)

Soil moisture accumulated at the root zone for each time step t is calculated by using Eq.6.7, where (ΔL) is the change in the soil moisture content which is calculated by using Eq.6.8.

$$L(t) = L(t - 1) + \Delta L \quad (6.7)$$

$$\Delta L = P_N - QOF - G \quad (6.8)$$

Since NAM is a lumped conceptual model, the basin characteristics are represented through several parameters as presented above (U_{max} , L_{max} , $CQOF$, $CKIF$, CK_{12} , TOF , TIF , TG , $CKBF$, C_{snow}) and calibration of these parameters is essential to reduce the difference between observed and model-simulated outputs.

Codes for NAM conceptual model are provided in [63].

6.2.2 Noah Land Surface Model

In this thesis, NOAH Land Surface Model (NOAH LSM) [149] is investigated as the physical model, which utilizes energy balance and water balance equations to simulate the soil moisture by using the forcing variables namely, precipitation, wind speed, air temperature, relative humidity, surface pressure, incoming shortwave radiation and incoming longwave radiation. Noah LSM can simulate soil moisture via multiple (preferably four) layers of soil moisture and considers the movement of water through these layers [150]. Besides the 1-D column version of NOAH LSM, there exist a global dataset named GLDAS [85], which provides outputs of four different land surface models including NOAH LSM. Land surface models available at GLDAS utilize a global dataset to produce their outputs at the global scale [158].

6.3 The Use of Soil Moisture Data in NAM Conceptual Hydrological Model

Elements of the hydrological cycle such as precipitation, runoff, soil moisture, evaporation have direct relation with each other, which indicates that having information on more variables may help estimating the other ones. A single element of an hydrological cycle can be estimated by using the other elements of the cycle and the same result can be reached, which is also known as the equafinality [159]. Considering the rainfall flow relationship in particular, there is a non-linearity in the relation [160], which is most probably due to the relation of runoff with the other elements of the cycle such as soil moisture. In other ways, estimation of runoff through precipitation can be enhanced via introducing the soil moisture data in the runoff estimation system (hydrological model). This issue has been investigated in many other studies. For example [20] investigated the usage of satellite based scatterometer data in a conceptual model to enhance the discharge estimates, [21] used a similar approach with a physical model. Improvement of discharge estimates through introduction of multiple variables (soil moisture and evaporation) has also been discussed [22, 23]. A recent study [24] investigated the introduction of CRNS based soil moisture in a conceptual

hydrological model established for a vegetated study site and slight improvements of discharge estimates are suggested. Conceptual hydrological models, such as NAM model, continuously accounts the water stored in each water storage unit including the root zone, thus introducing observed soil moisture data is expected to improve the model results.

Water accounting scheme of the NAM model has been presented in Section 6.2.1. The parameters that affect the mechanism of the hydrological cycle (U_{max} , L_{max} , $CQOF$, $CKIF$, CK_{12} , TOF , TIF , TG , $CKBF$, C_{snow}) are calibrated by considering the model performance. The model performance can be assessed through several statistical measures, which are presented in Section 3.4.

6.3.1 Obtaining Soil Moisture Time Series for NAM

In this study, NAM model has been set up for Çakıt Basin and Darboğaz sub-basin. Unlike the common approach of calibrating parameters through discharge estimation [133], estimation of soil moisture values are also taken into account in the calibration process. However, utilizing the soil moisture values obtained from the CRNP and SMAP directly to the NAM model is not possible because of three main reasons. Firstly, there are periods of missing data that should be filled for CRNP dataset, secondly, the measurement depth of both products does not match the definition of soil rootzone of NAM model, and lastly, the soil water accounting of NAM model is made by calculating the stored water in the soil root zone as surface water index (SWI), whereas CRNP and SMAP provides volumetric soil moisture. The latter problem is the simplest one since SWI can be obtained by dividing volumetric soil moisture data by the porosity value of the study area, which has been measured as 0.51 during the initial calibration campaign of CRNP.

6.3.1.1 SMAP Based Soil Moisture Data for the Root Zone

Recent studies on satellite validation suggest that SMAP product is the most accurate and reliable satellite based soil moisture product [19, 18] and for Çakıt Basin this product shows very high correlation with Çakıt Basin CRNP and proves to be an

accurate soil moisture data alternative for this region [19]. SMAP L4 9 km EASE-Grid Surface product [82] is able to provide continuous soil moisture inference of the entire planet at 3 hour temporal resolution. These unique attributes make SMAP soil moisture data a promising product to be used in hydrological modelling. In this study, SMAP soil moisture product has been obtained from the six SMAP grids whose center points are shown with red signs and one SMAP grid whose center point is shown with purple sign in Figure 3.1.

6.3.1.2 CRNP Based Continuous Soil Moisture Data for the Root Zone

There are gaps in the CRNP time series due to inability of CRNP to measure soil moisture in snowy days since it can not distinguish snow and soil water [1]. Nonetheless, having continuous time series of soil moisture data is essential for water accounting and for determination of the performance of model estimation. In order to obtain continuous time series of soil moisture, the gaps have been filled with data of TDR and Noah LSM soil moisture outputs. For the study area, root zone depth is theoretically between 80cm and 120cm [161]. Therefore, in this study, root zone is assumed as the area between surface and one meter depth of soil. On the other hand, vertical measurement depth of CRNP between 12 and 25cm for the study period at Çakıt basin is below the root zone depth. In order to obtain the root zone soil moisture, vertical soil moisture profile has been obtained by using the well known Richard's Equation [162] for touchet silt loam type of soil.

6.3.2 Calculation of Root Zone Soil Moisture

For each time step soil moisture data measured by using CRNS at the effective depth of CRNP has been converted into root zone soil moisture and the final time series has been exponentially filtered in time domain [20] to account for the time needed for the movement of water inside the soil. For exponential filtering, characteristic time length (T) is used as 20 days as it has been proposed by [163] for soil depth of 0-100 cm. Root zone depth is assumed to be one meter in order to represent possible various vegetation rooting depth which may range from 80cm to 120cm for the study

area [161].

The effective depth of CRNP depends on the amount of soil water [164, 165] as it is also presented in Section 3.2.1, Figure 3.4b. Effective measurement depth of CRNP can be calculated with Eq.6.9 [164].

$$z^* = \frac{5.8}{\rho_{bd}\tau + \theta + 0.0829} \quad (6.9)$$

where: z^* : Effective measurement depth of CRNP (cm), ρ_{bd} : Dry bulk density of soil (g/cm^2), τ : Weight fraction of lattice and bound water, θ : Soil moisture content (m^3/m^3).

Root zone soil moisture values are estimated for each time step by using the soil moisture profile given in Figure 6.2. Similarly, SMAP based surface soil moisture data have also been converted into root zone soil moisture and estimated root zone soil moisture data have been provided in Figure 6.3.

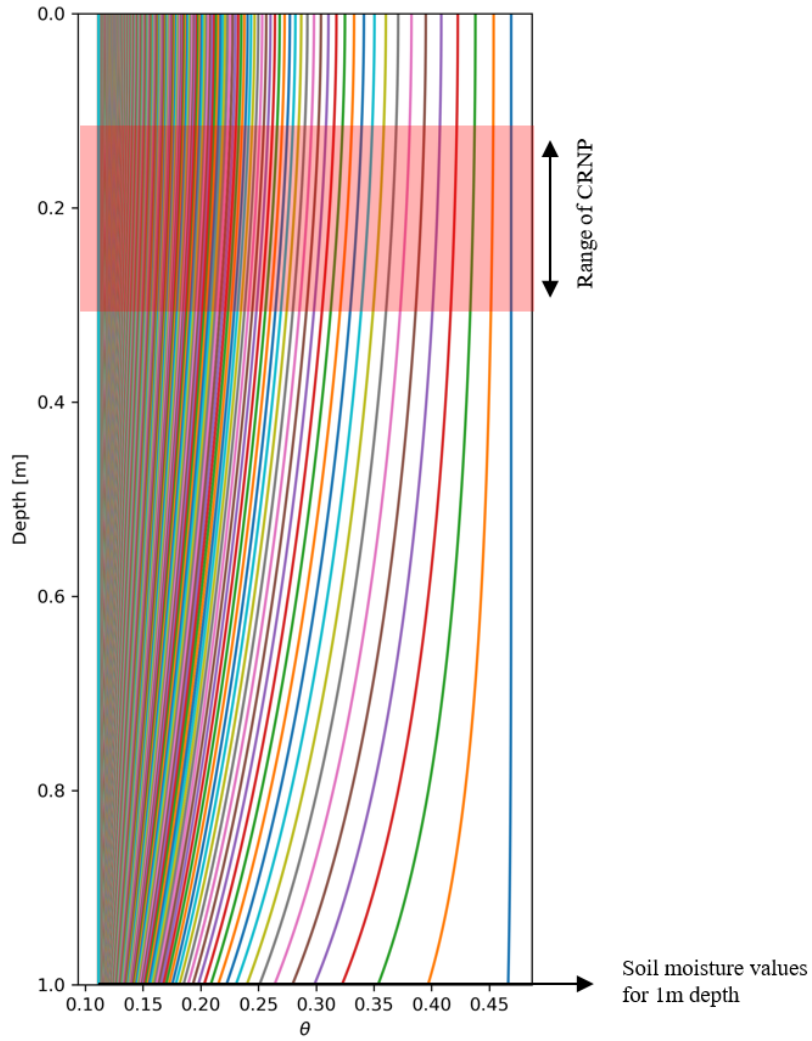


Figure 6.2: Estimated Soil Moisture Profiles of Çakıt Basin by Richards Equation

6.3.3 Calibration of the Parameters in NAM model

The calibration and validation of the model have been done by using rainfall, runoff, potential evaporation and soil moisture data. The calibration period is between 2016-10-01 and 2018-09-30 whereas the validation period is between 2018-10-01 and 2019-07-01. In this study, calibration of the NAM model has been done by using three different approaches:

1. Calibration of NAM by using the observed discharge.

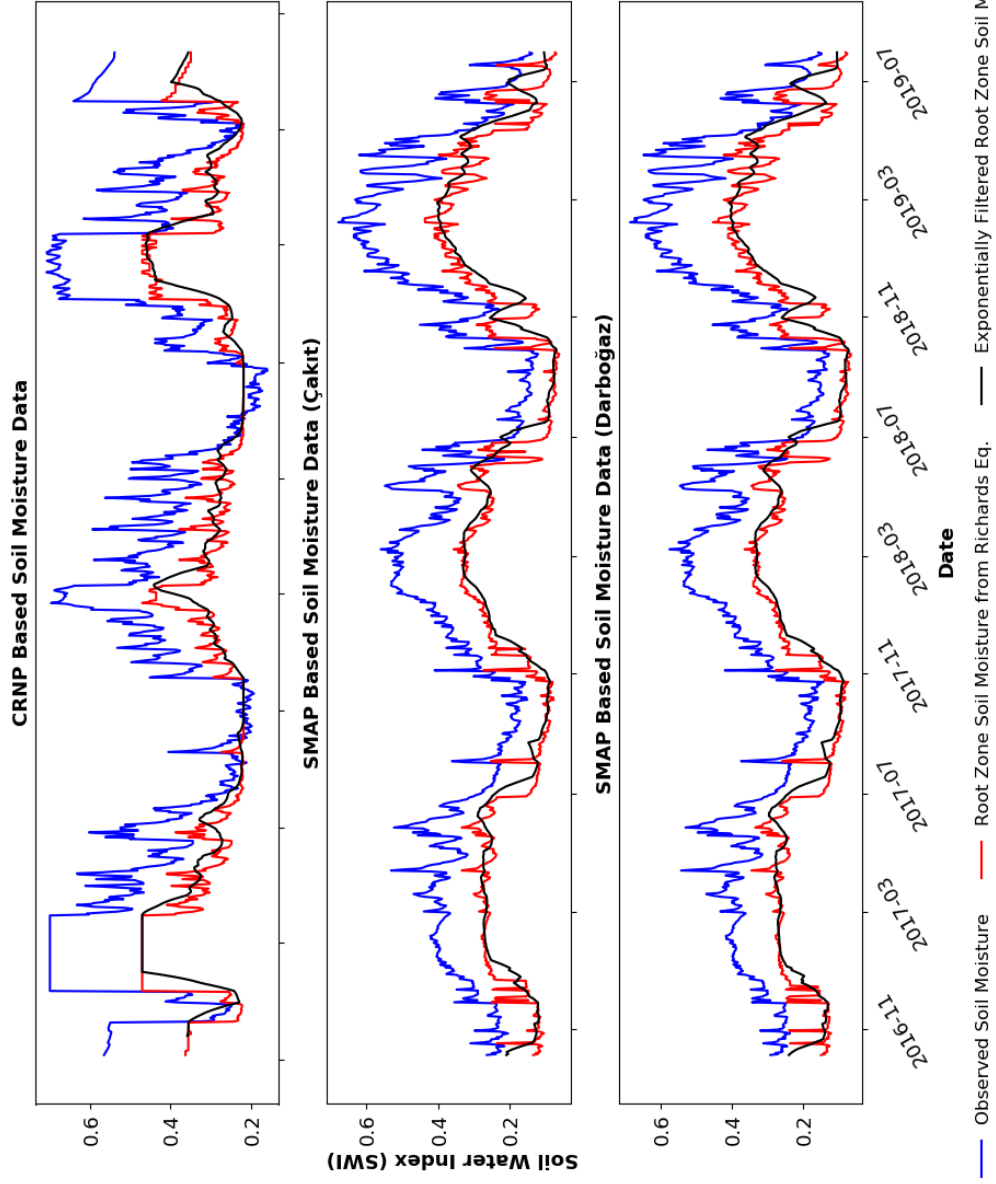


Figure 6.3: Estimated root zone soil moisture values of CRNP and SMAP based soil moisture

2. Calibration of NAM by using the observed soil moisture.
3. Calibration of NAM by using the combination of observed discharge and soil moisture.

For the first method, model simulated discharge data is made as similar as possible to the observed discharge values by changing the model parameters defined in section 6.2.1. For this purpose, parameters that will create the Nash Sutcliffe Efficiency of discharge values (NSE_Q , Eq. 3.7) have been selected. For the second approach, a similar methodology is applied using soil moisture data instead of discharge and parameters that will create the Nash Sutcliffe Efficiency of soil moisture values (NSE_{SM} , Eq. 3.7) have been selected. The third one is a hybrid calibration approach that has been used in various hydrological studies involving calibration with secondary datasets [166]. In this approach, calibration of the model parameters has been made by selecting the parameters which minimize the joint objective function (Eq.6.10). F_Q is the objective function representing the discharge and F_{SM} is the objective function representing the soil moisture data. The parameter a denotes the weighting coefficient for discharge. In literature, the a value is taken as 5/7 in different studies [167]. A sensitivity study that is conducted for Çakıt and Darboğaz basins also suggests that taking this value as 5/7 is reasonable (results of this study are provided in Appendices D). γ (The transformation parameter) was taken as 0.3 and for future studies, a sensitivity analyses for this parameter can also be conducted. For F_{SM} , Nash Sutcliffe Efficiency of soil moisture values (NSE_{SM} , Eq. 3.7) is used for the objective function. For F_Q , combination of various statistical measures have been used as it is suggested by [166] (Eq. 6.11). Although the magnitudes of each objective function affecting F_Q may be different and a set of weighting factors could be applied to $F_{\log NS} + F_{BoxNS} + F_{KGE} + F_{bias}$, in order to stay in line with the previous studies, additional weighing for sub-objective functions has not been utilized.

$$F_{Joint} = a \cdot F_Q + (1 - a) \cdot F_{SM} \quad (6.10)$$

$$F_Q = F_{\log NS} + F_{BoxNS} + F_{KGE} + F_{bias} \quad (6.11)$$

where: $F_{\log NS}$: Logarithmic Nash Sutcliffe Efficiency (logNSE) based objective function (Eq. 6.12), F_{BoxNS} : Nash Sutcliffe Efficiency of Box-Cox transformed flows based objective function (Eq. 6.13), F_{KGE} : Kling-Gupta efficiency based objective function (Eq. 6.15), F_{bias} : Mean bias score based objective function (Eq. 6.16)

$$F_{\log NS} = \frac{\sum_{t=1}^{T_c} [\ln(Q_{sim}(t) + v) - \ln(Q_{obs}(t) + v)]^2}{\sum_{t=1}^{T_c} [\ln(Q_{sim}(t) + v) - \ln(\bar{Q}_{obs}(t) + v)]^2} \quad (6.12)$$

$$F_{BoxNS} = \frac{\sum_{t=1}^{T_c} (Q_{sim}(t)' - Q'_{obs,t})^2}{\sum_{t=1}^{T_c} (Q'_{sim,t} - \bar{Q}'_{obs})^2} \quad (6.13)$$

$$Q_t' = \frac{(Q + 1)^\gamma - 1}{\gamma} \quad (6.14)$$

$$F_{KGE} = \sqrt{(1 - r)^2 + \left(1 - \frac{\sigma_{sim}}{\sigma_{obs}}\right)^2 + \left(1 - \frac{\bar{Q}_{sim}}{\bar{Q}_{obs}}\right)^2} \quad (6.15)$$

$$F_{bias} = \left[\max\left(\frac{\bar{Q}_{sim}}{\bar{Q}_{obs}}, \frac{\bar{Q}_{obs}}{\bar{Q}_{sim}}\right) - 1 \right]^2 \quad (6.16)$$

where, v : Smallest non-zero observed discharge value, Q_t' : Box-Cox transformed discharge (Eq. 6.14), γ : The transformation parameter = 0.3 [168], r : Pearson correlation coefficient value of observed and simulated discharges.

6.3.4 Setup of the NAM Model

For Çakıt Basin and Darboğaz sub-basin, NAM model has been established by using precipitation and temperature data of Darboğaz Meteorological Observation Station, potential evaporation data of Noah LSM outputs, discharge data of Çakıt and Darboğaz streamflow gauging stations as well as the soil moisture data, which are obtained by using various methods as it is mentioned in Section 6.3.1. The model has been run for two basins in order to assess the representativeness of the CRNP for basins with different sizes. All of the required input data for NAM model are provided in Figure 6.4.

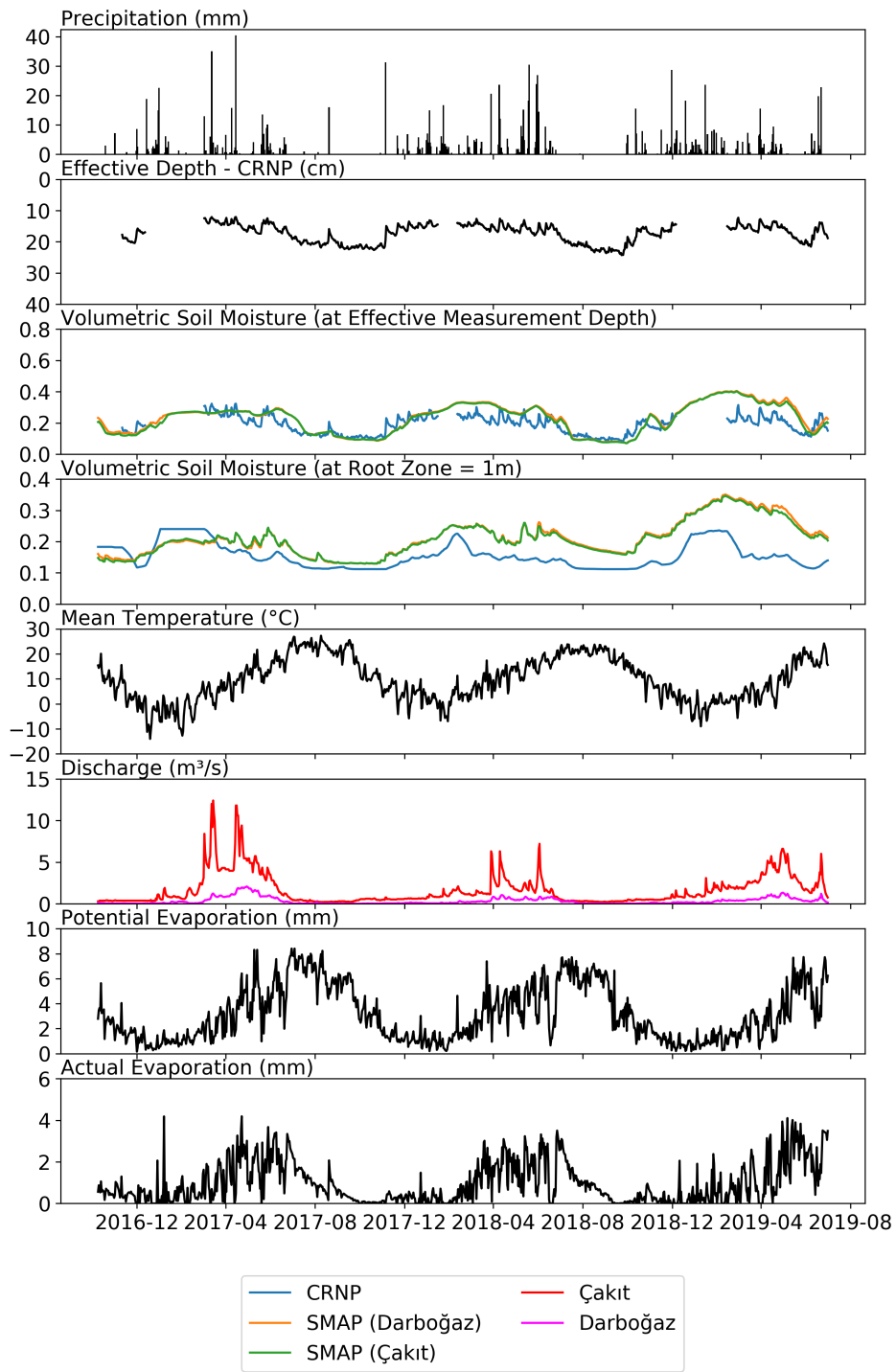


Figure 6.4: Effective depth of CRNP soil moisture observations, water balance, root zone soil moisture along with the meteorological data for Çakıt and Darboğaz Basins

6.4 Results of the Hydrological Modelling

The results of NAM model have been obtained for three different calibration methods applied to both basins. Calibration methods including soil moisture data are applied for both CRNP and SMAP data separately, therefore there are five different parameter sets that are obtained for five model runs as shown in Figure 6.5 for Çakıt Basin and in Figure 6.6 for Darboğaz sub-basin.

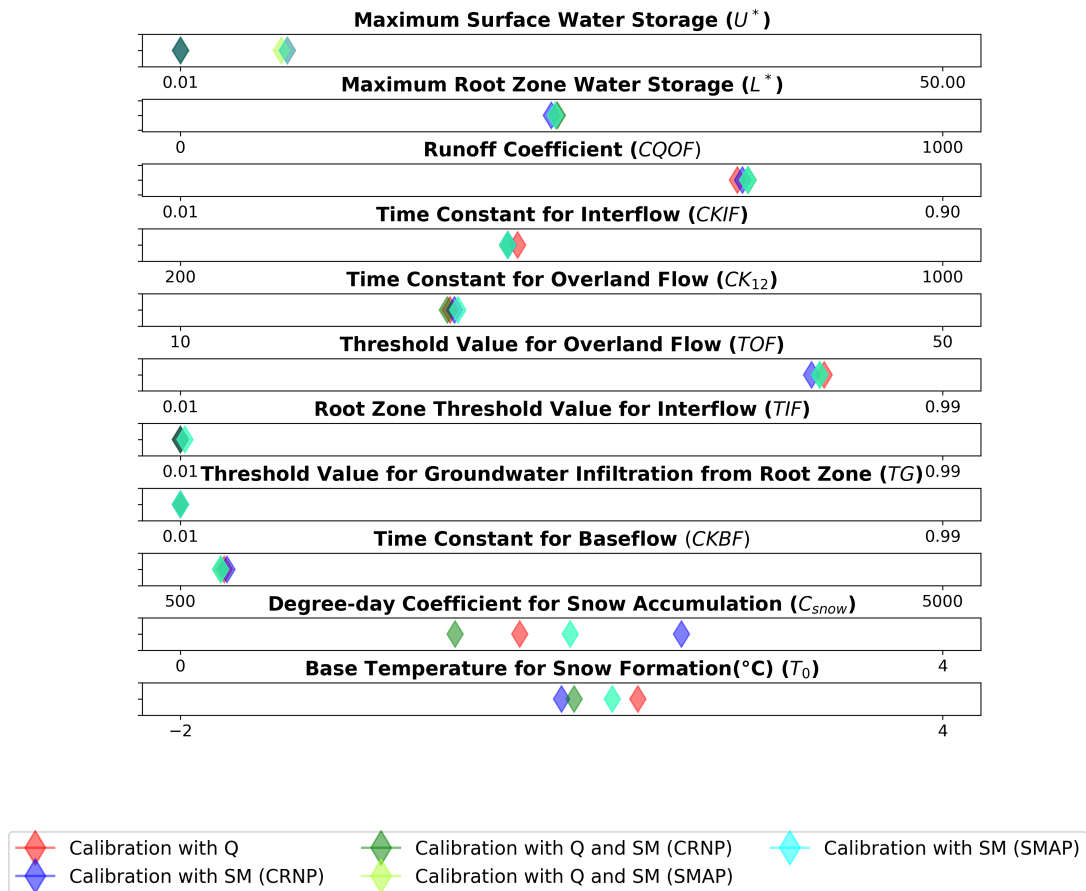


Figure 6.5: Hydrological model parameters obtained from different calibration methods for Çakıt Basin

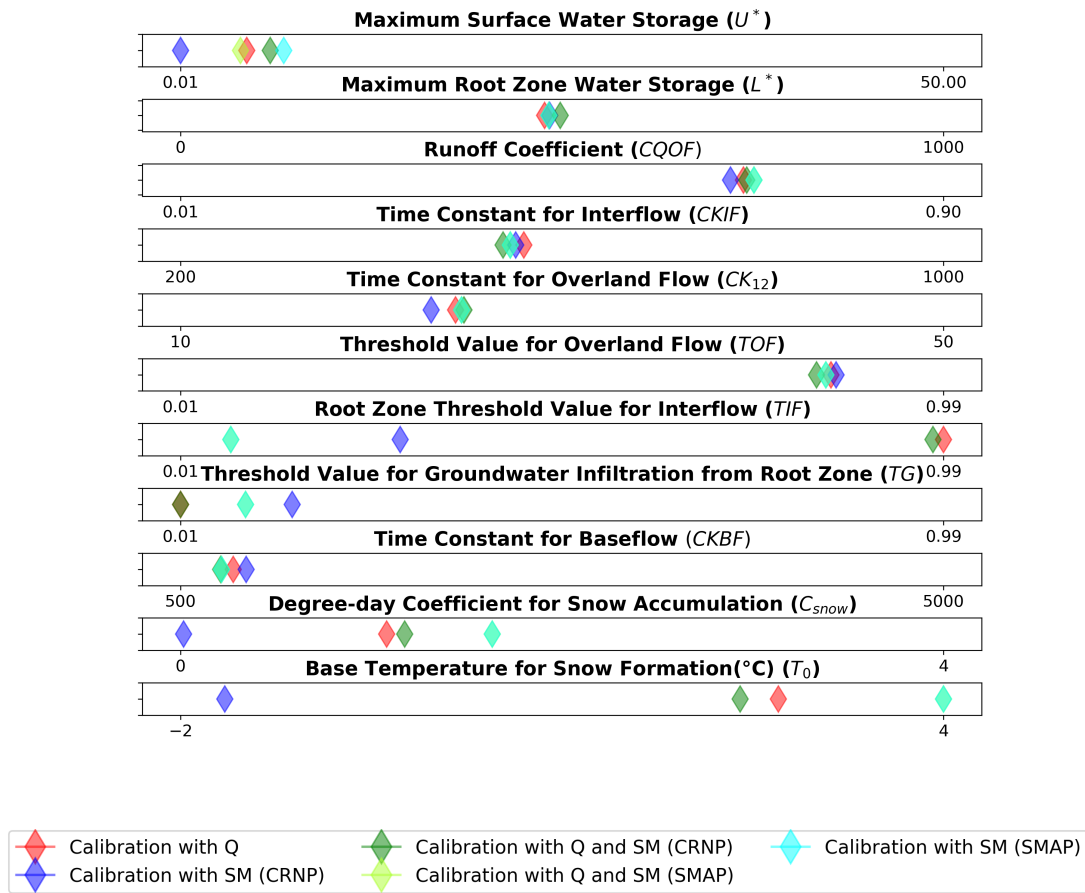


Figure 6.6: Hydrological model parameters obtained from different calibration methods for Darboğaz sub-basin

Maximum Surface Water Storage (U^*), Degree-day Coefficient for Snow Accumulation (C_{snow}) and Base Temperature for Snow Formation (T_0) are the parameters, which are significantly different for Çakıt Basin. In other words, calculations of snow and surface water storage yields different results for different calibration types for this basin. The parameters for Darboğaz sub-basin, on the other hand, much greatly varies for each calibration type, which would affect water accounting of all water storage types.

Finally, the model has been run by using the parameters obtained by calibration for both basins for the entire duration including the validation period. Discharge time series for two basins in calibration and validation periods are provided in Figure 6.7

and Figure 6.9. The same figures are also provided in log-scale with Figure 6.8 and Figure 6.10.

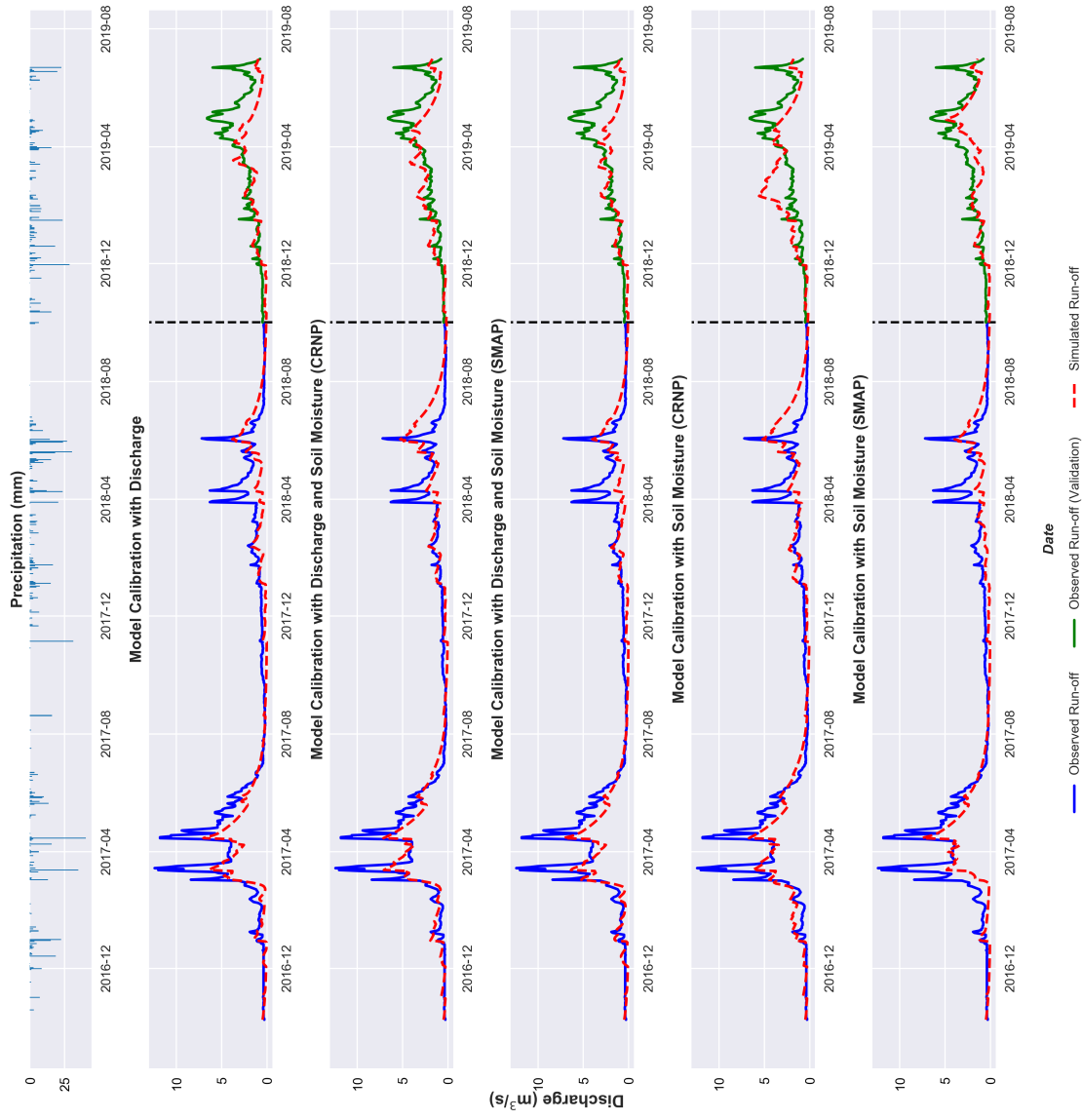


Figure 6.7: Simulated and Observed Discharge Values for Çakıt basin, vertical dashed line indicates the calibration and validation periods

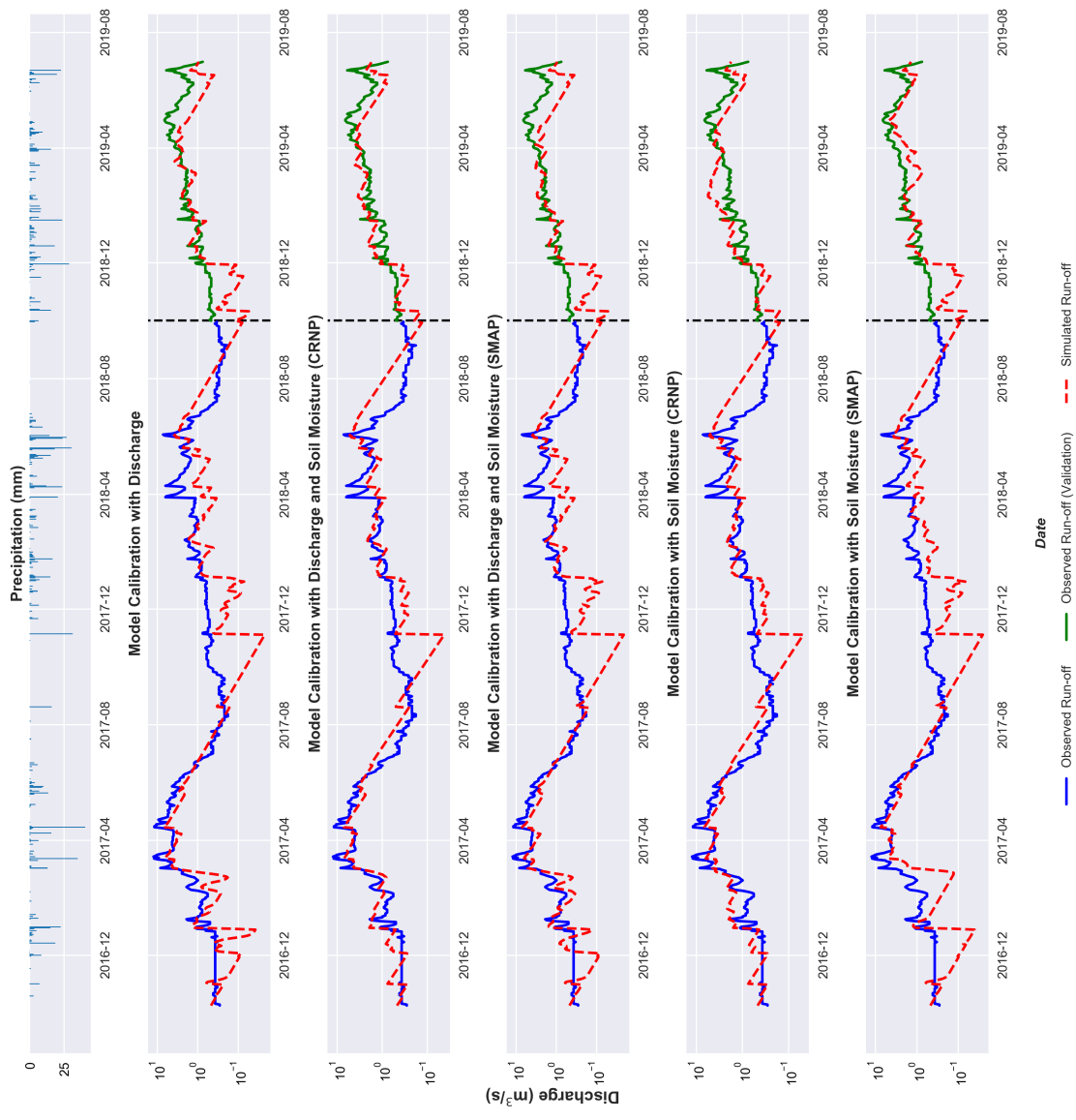


Figure 6.8: Simulated and Observed Discharge Values for Çakıt basin (Logarithmic Scale), vertical dashed line indicates the calibration and validation periods

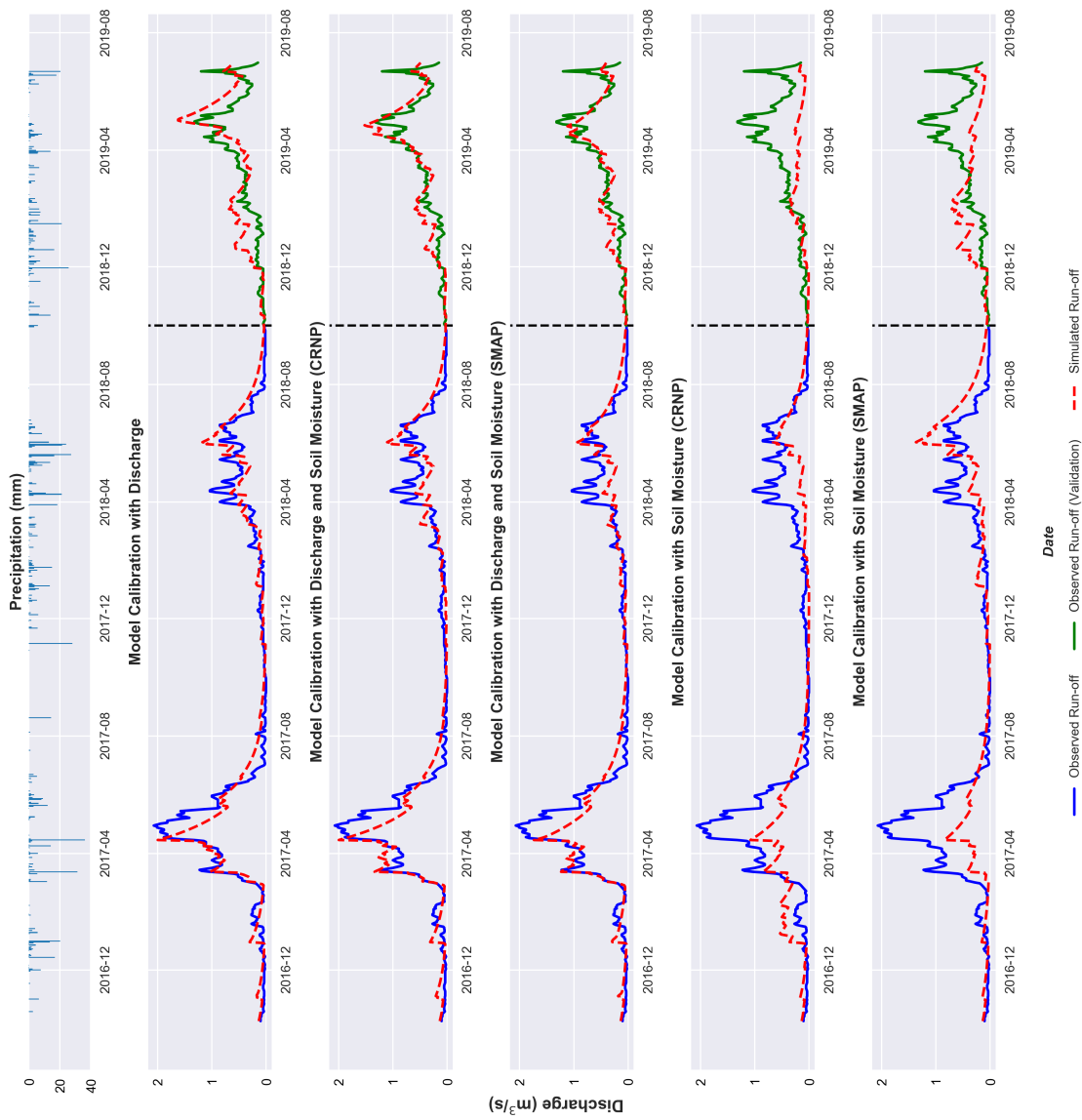


Figure 6.9: Simulated and Observed Discharge Values for Darboğaz sub-basin, vertical dashed line indicates the calibration and validation periods

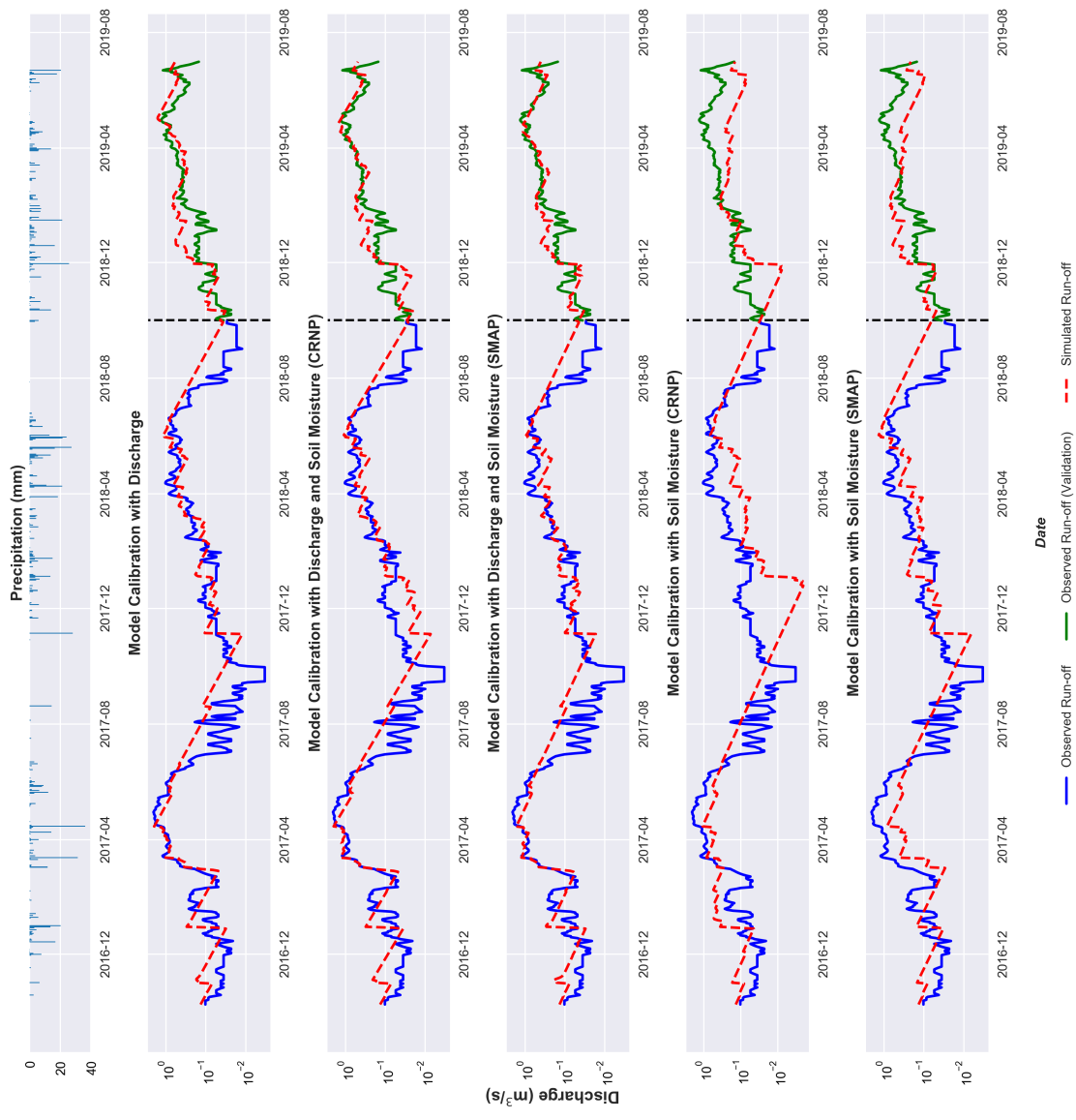


Figure 6.10: Simulated and Observed Discharge Values for Darboğaz sub-basin (Logarithmic Scale), vertical dashed line indicates the calibration and validation periods

The relations between observed and simulated discharge values are investigated by using the statistical measures which are defined in Section 3.4. The statistical measures are provided for calibration period (Figure 6.11 and Figure 6.13) and for validation period (Figures 6.12 and 6.14) for both Çakıt basin and Darboğaz sub-basin. In these figures, indicators which are closer to the right end of the graphs indicate better performance of the model by means of estimating discharges. The statistical measures are also provided with Table 6.1 for Çakıt Basin and Table 6.2 for Darboğaz sub-basin. In Figures 6.11 - 6.14 the values of VE and PBIAS are provided as absolute values, whereas in Table 6.1 and Table 6.2 they are provided as percentages.

Table 6.1: Statistical Measures of NAM simulations with Respect to the Calibration Methods - Çakıt Basin

Calibration Period					
	Discharge	Discharge and Soil Moisture (CRNP)	Soil Moisture (CRNP)	Discharge and Soil Moisture (SMAP)	Soil Moisture (SMAP)
NSE	0.680	0.724	0.685	0.697	0.629
log NSE	0.274	0.604	0.600	0.338	0.155
RMSE	1.098	1.020	1.090	1.068	1.182
PBIAS	32.678	2.290	-0.996	28.822	33.828
r²	0.895	0.856	0.835	0.893	0.859
VE (%)	-32.7	-2.3	1.0	-28.8	-33.8
KGE	0.559	0.812	0.762	0.593	0.548
Validation Period					
NSE	0.172	0.458	0.049	0.097	0.552
log NSE	-0.219	0.600	0.495	-0.285	0.060
RMSE	1.338	1.082	1.434	1.397	0.984
PBIAS	37.874	8.466	-7.869	35.394	30.862
r²	0.661	0.691	0.527	0.575	0.873
VE (%)	-37.9	-8.5	7.9	-35.4	-30.9
KGE	0.423	0.643	0.533	0.405	0.561

Table 6.2: Statistical Measures of NAM simulations with Respect to the Calibration Methods - Darboğaz sub-basin

	Calibration Period				
	Discharge	Discharge and Soil Moisture (CRNP)	Soil Moisture (CRNP)	Discharge and Soil Moisture (SMAP)	Soil Moisture (SMAP)
NSE	0.836	0.803	0.454	0.831	0.797
log NSE	0.734	0.762	0.371	0.727	0.717
RMSE	0.173	0.190	0.316	0.176	0.193
PBIAS	-1.360	1.951	40.321	4.917	14.555
r²	0.914	0.896	0.802	0.913	0.911
VE (%)	1.4	-2.0	-40.3	-4.9	-14.6
KGE	0.899	0.899	0.323	0.885	0.727
	Validation Period				
NSE	0.659	0.723	-0.369	-0.011	0.543
log NSE	0.729	0.669	-0.163	0.473	0.671
RMSE	0.182	0.164	0.364	0.313	0.210
PBIAS	-12.944	-2.630	64.035	-40.595	18.237
r²	0.847	0.857	0.551	0.815	0.776
VE (%)	12.9	2.6	-64.0	40.6	-18.2
KGE	0.736	0.855	-0.066	0.316	0.569

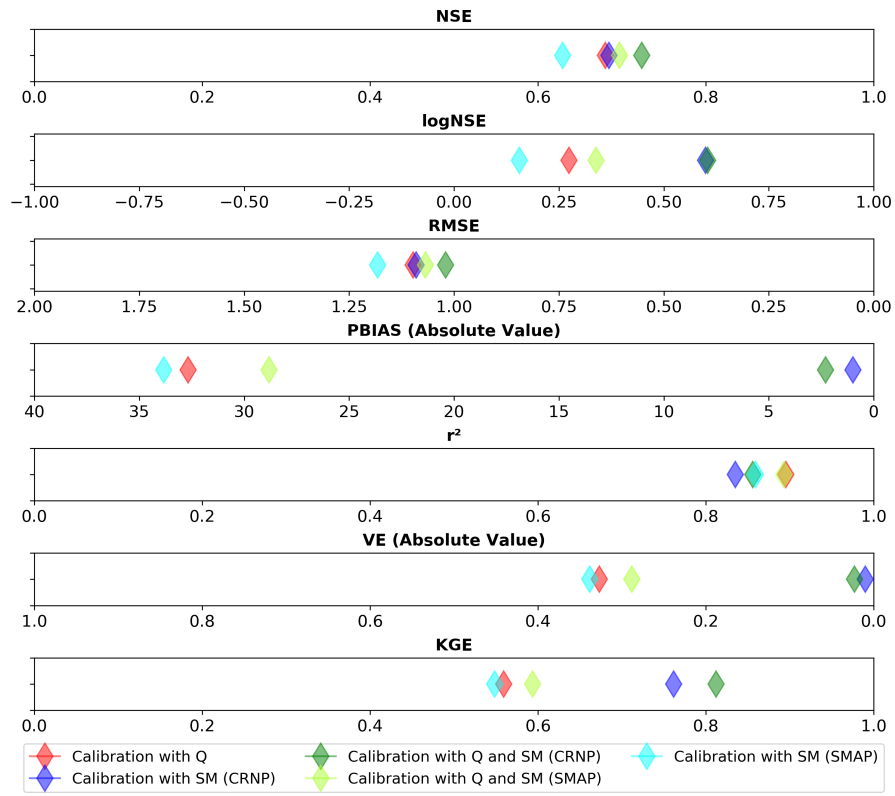


Figure 6.11: Statistical measures for Calibration period - Çakıt Basin.

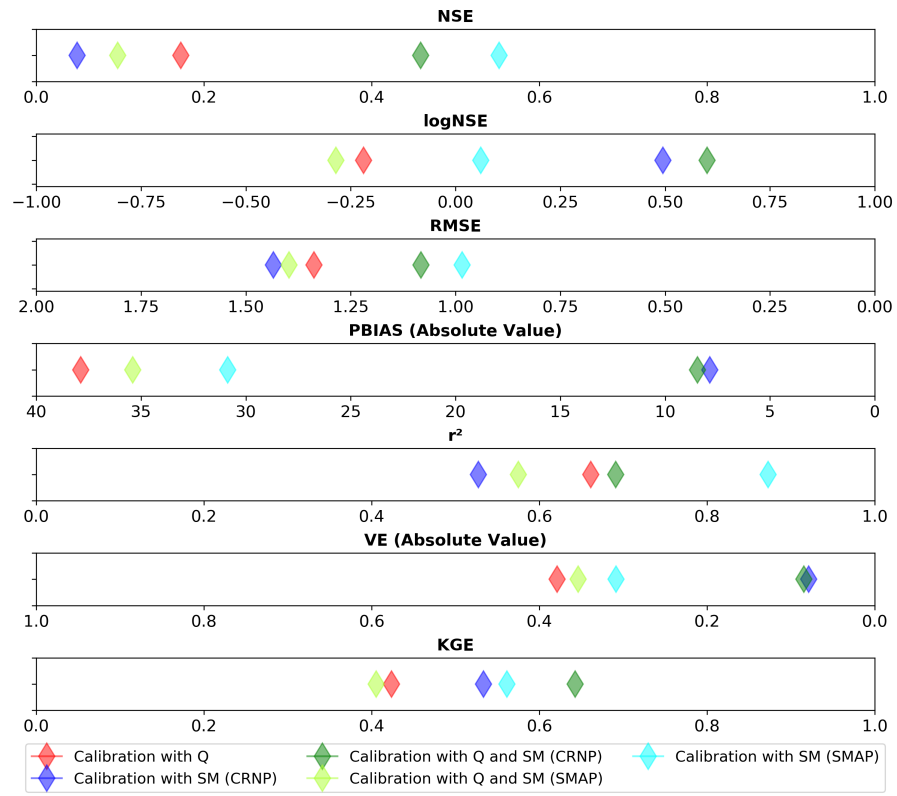


Figure 6.12: Statistical measures for Validation period - Çakıt Basin.

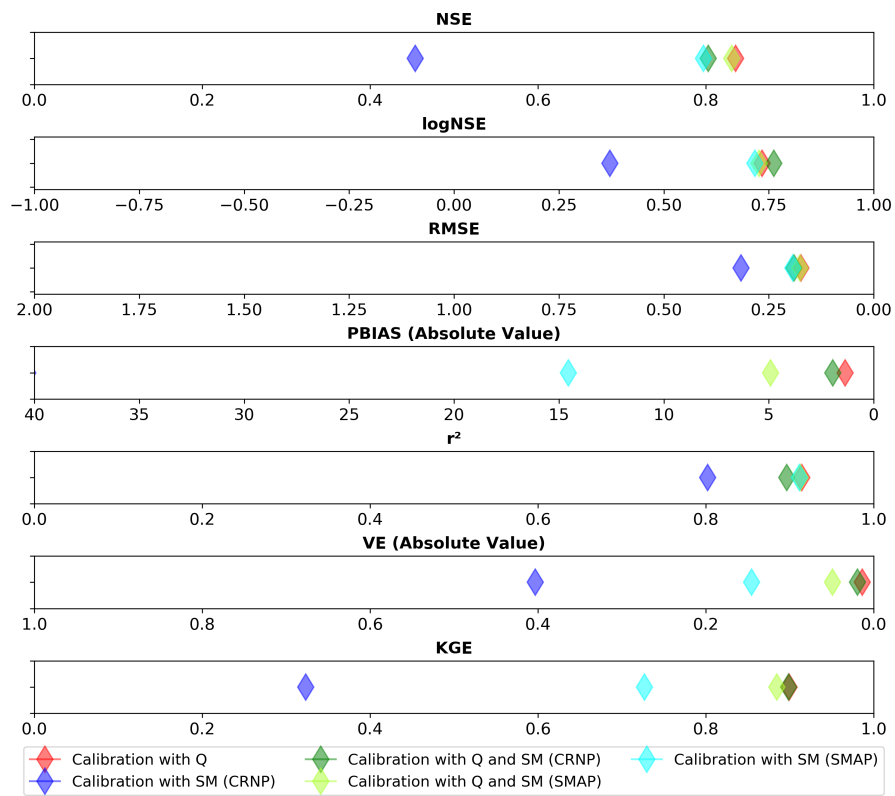


Figure 6.13: Statistical measures for Calibration period - Darboğaz sub-basin.

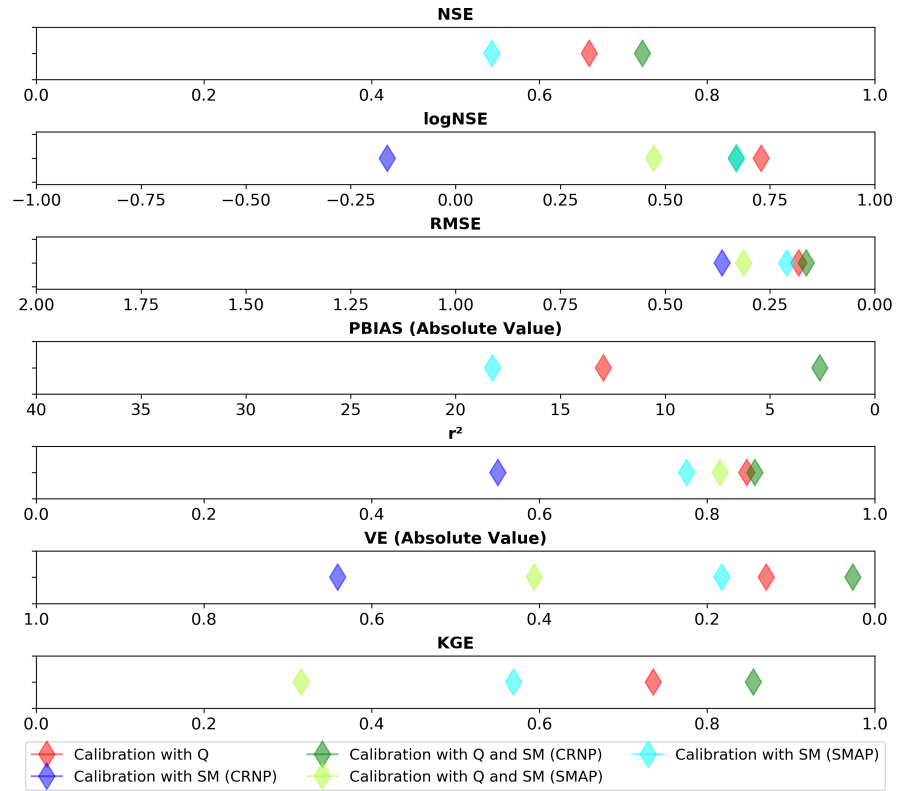


Figure 6.14: Statistical measures for Validation period - Darboğaz sub-basin.

6.5 Comparison of Basin Water Balance with Observed and Simulated Soil Moisture Data

In addition to the water storage calculations through hydrologic modelling with NAM, water balance of Çakıt basin and Darboğaz sub-basin have been simply calculated by using Equation 6.17.

$$S_{WB}(t) = S_{WB}(t - 1) + P(t) - Q_{obs}(t) - ET_a(t) \quad (6.17)$$

where; $S_{WB}(t)$: Water storage at time t, P : Precipitation, Q_{obs} : Observed discharge, ET_a : Actual evaporation output of local Noah LSM.

Variables used in the water balance calculations for Çakıt Basin and Darboğaz sub-

basin are shown in Figure 6.15.

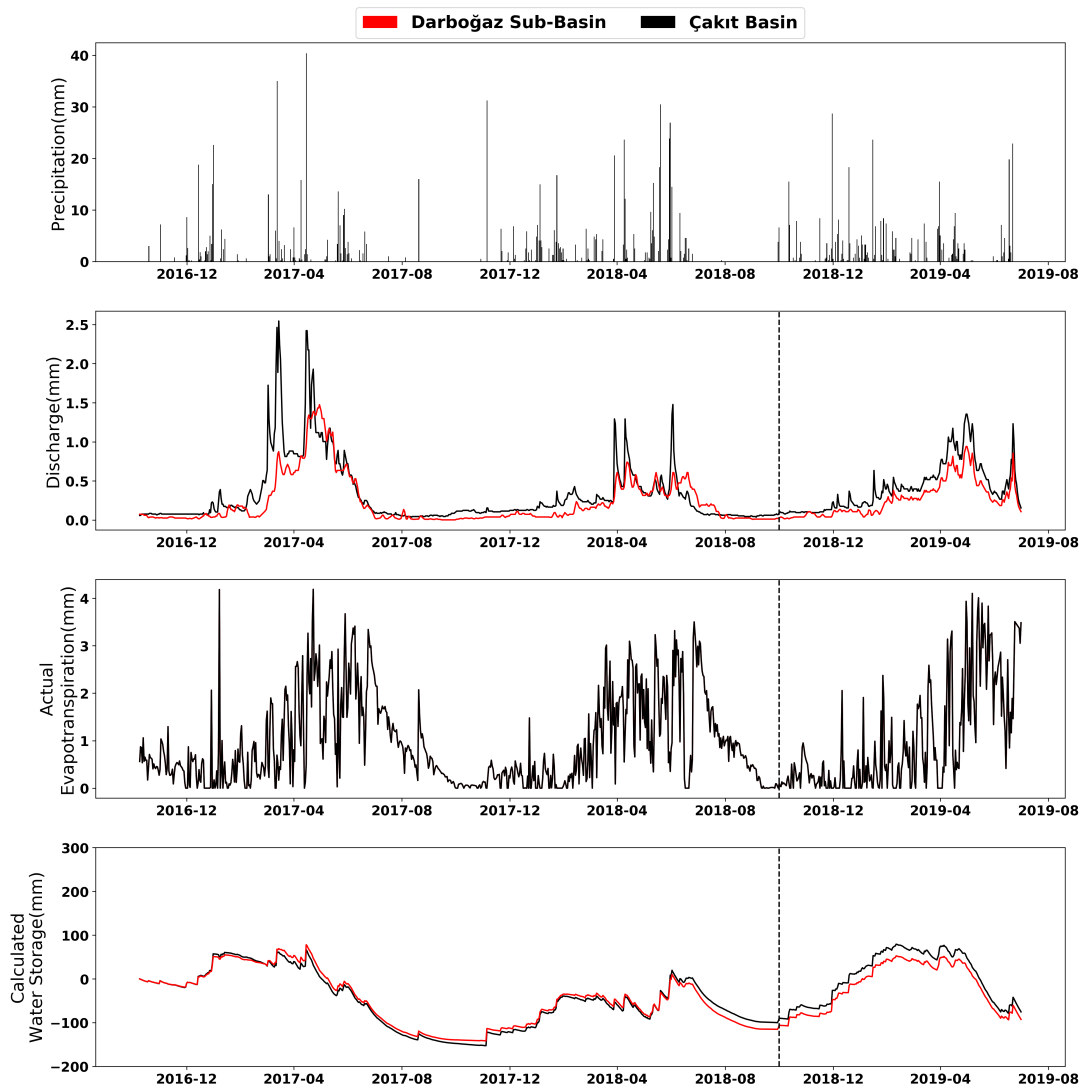


Figure 6.15: Variables of Water Balance Calculations for Çakıt Basin and Darboğaz sub-basin, vertical dashed line indicates the calibration and validation periods

Soil moisture outputs of NAM model for different calibration methods which are given in Section 6.4 are compared with the water storage of the basin, which is calculated by using Equation 6.17. The comparisons of time series are provided in Figure 6.16.

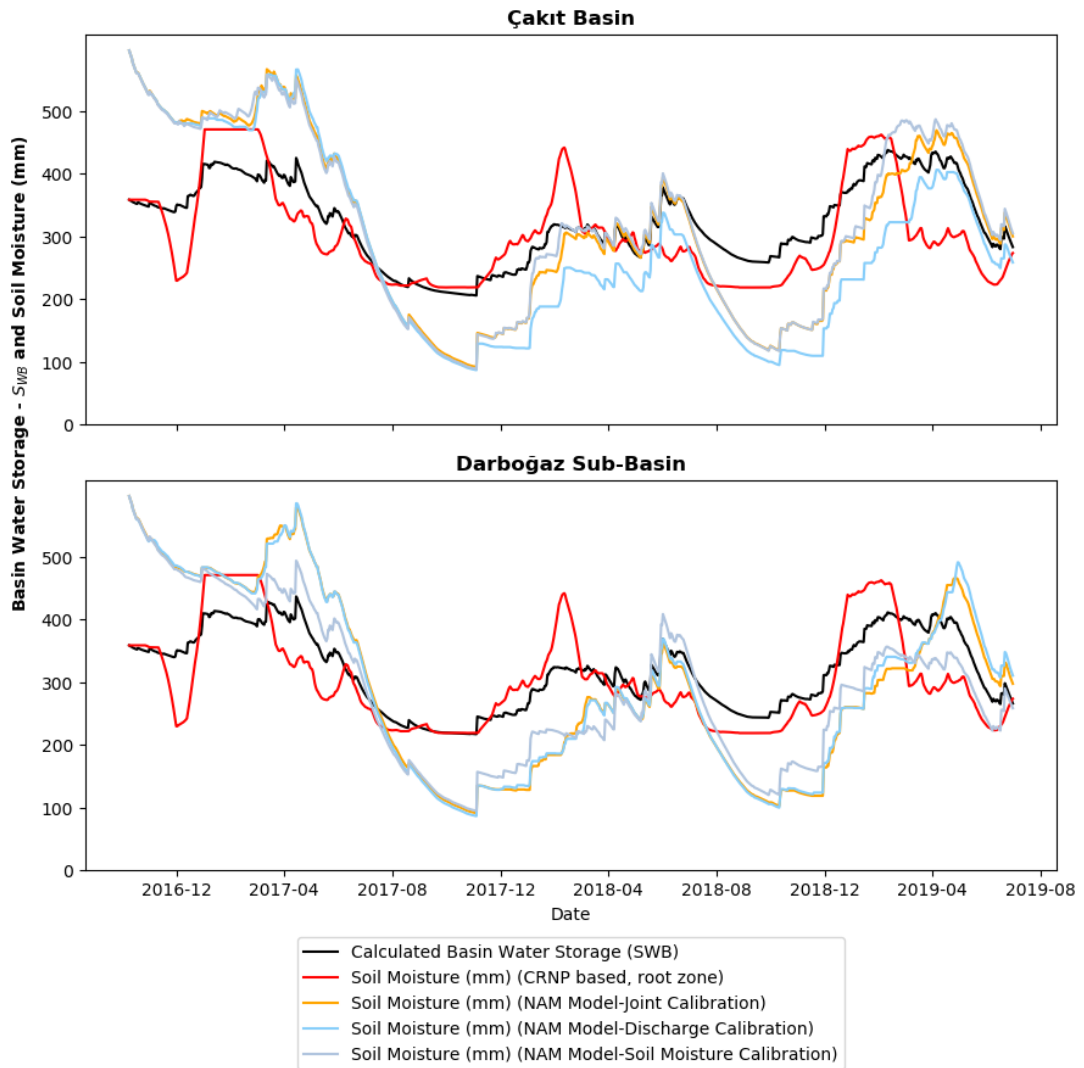


Figure 6.16: Comparison of Water Balance and Model Soil Moisture Outputs of Çakıt Basin and Darboğaz sub-basin

6.6 Summary and Discussion of the Results

In this study, soil moisture values obtained from CRNP located in the Çakıt Basin and SMAP soil moisture data have been used to improve the NAM conceptual hydrological model. For this purpose, three different calibration schemes have been defined where the first one is based on discharge, the second one is based on soil moisture and the third one is based on the combination of discharge and soil moisture. The NAM model has been run for both Çakıt Basin and Darboğaz sub-basin for the pre-

defined calibration options. The first two years of the time period have been used as the calibration period and the remaining part is used for the validation. Root zone soil moisture values of both soil moisture datasets are estimated by using a closed form solution of Richard's equation for the soil moisture profile.

The results show that the resulting statistics are better if soil moisture data are introduced in the model together with the discharge data. NSE and KGE values are significantly improved and using CRNP as the soil moisture data source rather than SMAP makes the improvements slightly more prominent. When the two basins are compared, it can be seen that the statistics became better for the Darboğaz sub-basin when the soil moisture data is introduced in the calibration. Introducing SMAP soil moisture data produced greater effect than CRNP for Çakıt basin. For some statistical measures, even using soil moisture data alone for the calibration improved the model estimates, however, the best results are obtained when soil moisture and discharge values are used in combination.

It should also be noted that the calibration period of the model spans two water years which is a very limited time range for such studies. Despite lacking sufficient amount of time for calibration, the model estimated discharge values quite accurately for the validation period. If there was more time for calibration, the first few months of calibration data could be excluded from the analyses to account for the warm up period for the model and the resulting statistics could be much better. Additionally, for this study, missing data of CRNP have been filled with the other source of soil moisture data (TDR and Noah LSM), a full-scale usage of CRNP data may be more efficient due to certain limitations of these two additional data sources. In addition, the peak discharges occurring in the second year of calibration can not be properly estimated by the modelling approach used in this study. NAM model is not capable of modelling rain-on-snow phenomena [169], which is assumed to accelerate snow melting and change of state of water storage from snow storage to surface storage. In spite of the above-mentioned flaws in the modelling study, NAM model performed very well for both basins and the effect of joint calibration in improving the model statistics is clear.

The findings of this study are in line with a recent study, which has been conducted

by a similar manner with CRNP soil moisture data obtained from a study site located in United Kingdom [24], which also found that introducing soil moisture data into a conceptual hydrological models improves model statistics. The difference of the two studies is mainly the site characteristics, where [24] makes use of a vegetated site, in this study, a semi-arid study site has been selected. Therefore, when the results of these two studies are combined, it can be said that the CRNP based soil moisture values are able to improve the model statistics of conceptual hydrological models for dry or wet sites.

Besides the hydrological model, water stored in the basin has also been calculated with water budget calculations. For Çakıt Basin, calculated water storage values are highly correlated with the model soil moisture outputs and the observed soil moisture values for the entire time range of the analyses. In summary, it can be said that the calculated water storages are in close coupling with the observed and simulated soil moisture values for both basins and for both soil moisture data sources. When the model outputs and the calculated water storages are compared, a certain time lag can be seen between these two data, which is mostly due to the snow melting which could not be adequately determined by the model. The time lag and the temperatures in the melting season have an inverse relation, which shows the importance of snow storage for the specific study area.

CHAPTER 7

CONCLUSIONS AND RECOMMENDATIONS

7.1 Conclusions

In this thesis, CRNP neutron counts obtained from the CRNP station in Çakıt Basin, which is a semi-arid study site with sparse vegetation located in the south of Turkey, constitute the starting point of all of the hydrological studies. After retrieving the soil moisture data by using the neutron counts with necessary correction and conversion processes, the data have been compared with TDR sensor data and Noah LSM soil moisture outputs. For Çakıt basin, CRNP soil moisture measurements are in line with both soil moisture datasets. Although the correlation with CRNP and TDR is very high ($r^2=0.855$), TDR soil moisture values are mostly larger (around 10%) than CRNP soil moisture values. One of the reasons of this difference is probably due to the difference of vertical footprints of TDR and CRNP where TDR is located at 5cm depth and the vertical measurement scale of CRNP is between 12 and 25cm depending on the soil moisture content and in semi arid locations, the evaporation of upper soil is more dominant than infiltration.

In the second part of this study, CRNP based soil moisture values are used in validation of satellite soil moisture products. Satellite soil moisture products have become an important tool for hydrological studies due to the recent advancements in satellite technology and retrieval algorithms. In this study, the effectiveness of CRNP soil moisture measurements have also been investigated for validation of different types of spaceborne soil moisture products. ASCAT, SMOS, SMAP, AMSR, CCI and GLDAS soil moisture datasets have been validated by using CRNP soil moisture data of several CRNP stations of COSMOS database and the Çakıt Basin CRNP. This

study revealed that the SMAP soil moisture products have higher correlations with CRNPs at drier locations including Çakıt basin and ASCAT soil moisture product have higher correlations with CRNPs at vegetated areas. This differences are highly due to entirely different retrieval algorithms and techniques used for these two satellite products. When all of the stations of the COSMOS database is considered, Çakıt Basin CRNP produced better statistics for the validation of most of the products except ASCAT product which is known to operate poorly in dry locations. In this study, soil moisture values were also obtained from a local Noah Land Surface Model. The outputs of this model are also in line with the CRNP and TDR measurements. Although local Noah Model produced slightly better results than global Noah LSM of GLDAS for Çakıt Basin, GLDAS Noah LSM was able to produce statistics as good as the local model. In summary, it has been found that SMAP surface soil moisture product and GLDAS Noah LSM product have very well correlation with most of the CRNPs. Since having continuous soil moisture data is highly important for hydrological studies, these two products have very good potentials to be used in these kind of applications. Using these products in conjunction with in-situ soil moisture products such as CRNPs will make them more effective.

As the third part of this study, the relation between evaporation and soil moisture have been investigated through CRNP soil moisture measurements. Eddy covariance based evapotranspiration estimates and Noah LSM actual evapotranspiration outputs have been used for the evaporation data. Although the correlations are not very strong, both datasets have similar cumulative distribution functions. In drier months the correlations between soil moisture and evaporation are stronger. Daily changing values of soil moisture and evaporation has also been investigated and for drier days, it makes sense to better correlate soil moisture with the daily varying ET_a because the absence of rain and runoff create a more direct relationship between these two parameters through the hydrological cycle. For global investigations on soil moisture and evaporation, GLDAS Noah LSM actual evapotranspiration values have been compared with the CRNP soil moisture measurements of COSMOS database. In order to account for the locations without CRNP observations, GLDAS based soil moisture and evapotranspiration values have also been compared with each other for each GLDAS pixel on Earth. The results indicate that in drier locations and periods, the correlations are

more pronounced. In Mediterranean region where the Çakıt CRNP is located, correlations with soil moisture and evaporation depend on the study months and periods.

In the final part of this study, CRNP based soil moisture values have been used to improve hydrological modeling. Improvement of conceptual rainfall-runoff models by introducing soil moisture data obtained from CRNPs is a very recent research topic. It is found in this study that, introducing CRNP and SMAP based soil moisture values improve the resulting statistics of NAM conceptual model when used in combination with the discharge data in calibration. Using CRNP instead of SMAP based soil moisture data creates slightly better results. The resulting statistics for Darboğaz sub-basin is more improved than Çakıt basin when the soil moisture is introduced in calibration. One of the reasons of this difference is thought to be the areal coverage of the CRNP being more representative for Darboğaz sub-basin than Çakıt basin. One must note that the model has been managed to be improved by using only two years of calibration data. With available long term data, it is also possible to calibrate the model covering wet and dry periods of the basin which will likely to produce more effective results. One additional possible source of error for this study is the need for filling the missing data of CRNP with TDR measurements and Noah LSM outputs. Without this need, introducing CRNP to the conceptual hydrological model may be more effective. In this study, it has been shown that introducing CRNP based soil moisture data in a semi-arid study area of Turkey positively affected the performance of NAM conceptual model. Comparisons of the soil moisture outputs of NAM model with the water balance calculations yield very high correlations for both Çakıt and Darboğaz basins. When basin water balance calculations are compared with the soil moisture data and model outputs, calculated water balances are also in-line with CRNP based soil moisture values indicating the potential of CRNPs to be used in basin scale hydrological studies. For both basins, the soil moisture observations and the model outputs have certain time lags where the lagging duration is inversely correlated with the temperature at the snow melting season indicating the prominence of the snow storage and melting and the snow melting physics are most probably depend on more complex relations such as the rain on snow phenomena which can not be modeled through NAM conceptual model.

7.2 Recommendations

The first application of CRNP in Turkey has been presented in this study through validation of satellite soil moisture products and introducing soil moisture values into hydrological model calibration. The number of CRNPs in the Mediterranean region is very limited and in this region satellite soil moisture products may show different characteristics from the other locations of the world. It is also found that the relation between evaporation and soil moisture is not constant and depends on the study period for this area. Also for agricultural studies and applications, knowing soil moisture in large areas is essential for reaching the optimum yield and water management. For this type of studies, CRNP has an important potential to be used in improving the accuracies of satellite soil moisture products. For hydrological studies covering large basins, using several CRNPs together with reliable satellite soil moisture products would produce the required soil moisture data at the required temporal and spatial scale. For further studies, the CRNP network should be expanded in such areas and performance of satellite products should be further investigated. In this respect, CRNP observation networks should be established to provide reliable and consistent data for hydrological and agricultural studies.

In this study, in order to convert CRNP neutron counts to soil moisture measurements, N_0 soil moisture method has been used and Richard's equation have been used for calculation of soil moisture at the root zone. For further studies, neutron transport models can be studied together with data assimilation techniques to obtain soil moisture values for different layers and rootzone soil moisture products and hydrological model outputs can also be validated in this way.

The effect of vegetation on CRNP measurements are not discussed in this thesis due to lack of vegetation in the study site. Future studies should also focus on correcting neutron counts with respect to vegetation.

Studies regarding the introduction of soil moisture data into hydrological modelling, including this thesis, use a joint calibration function for soil moisture and discharge while calculation of the objective function of discharge depends on four distinct statistical measures which may have different weights on the calculations. For future

studies, a multi-criteria decision making system may be developed to better represent each one of the statistical measures defined for discharge calibration.

It has also been shown in this study that evapotranspiration and soil moisture has a relation which can be used in further studies to improve the estimates of hydrological models with introducing measured evaporation data in model calibration together with discharge and soil moisture data.

REFERENCES

- [1] M. Zreda, D. Desilets, T. Ferré, and R. L. Scott, “Measuring soil moisture content non-invasively at intermediate spatial scale using cosmic-ray neutrons,” *Geophysical research letters*, vol. 35, no. 21, 2008.
- [2] S. Evett, “Exploits and endeavors in soil water management and conservation using nuclear techniques,” 2000.
- [3] W. Gardner and D. Kirkham, “Determination of soil moisture by neutron scattering,” *Soil Science*, vol. 73, no. 5, pp. 391–402, 1952.
- [4] V. F. Hess, “Observations of the penetrating radiation on seven balloon flights,” *Physik. Zeitschr*, vol. 13, pp. 1084–1091, 1912.
- [5] S. Glasstone and M. C. Edlund, “The elements of nuclear reactor theory,” 1952.
- [6] H. A. Bethe, S. A. Korff, and G. Placzek, “On the interpretation of neutron measurements in cosmic radiation,” *Physical Review*, vol. 57, no. 7, p. 573, 1940.
- [7] L. Hendrick and R. Edge, “Cosmic-ray neutrons near the earth,” *Physical Review*, vol. 145, no. 4, p. 1023, 1966.
- [8] M. Kodama, S. Kudo, and T. Kosuge, “Application of atmospheric neutrons to soil moisture measurement,” *Soil science*, vol. 140, no. 4, pp. 237–242, 1985.
- [9] G. F. Knoll, *Radiation detection and measurement*. John Wiley & Sons, 2010.
- [10] D. Desilets and M. Zreda, “Footprint diameter for a cosmic-ray soil moisture probe: Theory and monte carlo simulations,” *Water Resources Research*, vol. 49, no. 6, pp. 3566–3575, 2013.
- [11] M. Zreda, “Land-surface hydrology with cosmic-ray neutrons: Principles and applications,” *J Jpn Soc Soil Phys*, vol. 132, pp. 25–30, 2016.

- [12] E. Tebbs, F. Gerard, A. Petrie, and E. De Witte, “Emerging and potential future applications of satellite-based soil moisture products,” in *Satellite Soil Moisture Retrieval*, pp. 379–400, Elsevier, 2016.
- [13] L. Brocca, W. T. Crow, L. Ciabatta, C. Massari, P. De Rosnay, M. Enenkel, S. Hahn, G. Amarnath, S. Camici, A. Tarpanelli, *et al.*, “A review of the applications of ascat soil moisture products,” *IEEE Journal of Selected Topics in Applied Earth Observations and Remote Sensing*, vol. 10, no. 5, pp. 2285–2306, 2017.
- [14] W. T. Crow and M. T. Yilmaz, “The auto-tuned land data assimilation system (atlas),” *Water resources research*, vol. 50, no. 1, pp. 371–385, 2014.
- [15] A. Al-Yaari, J.-P. Wigneron, A. Ducharne, Y. Kerr, W. Wagner, G. De Lannoy, R. Reichle, A. Al Bitar, W. Dorigo, P. Richaume, *et al.*, “Global-scale comparison of passive (smos) and active (ascat) satellite based microwave soil moisture retrievals with soil moisture simulations (merra-land),” *Remote Sensing of Environment*, vol. 152, pp. 614–626, 2014.
- [16] L. Brocca, S. Hasenauer, T. Lacava, F. Melone, T. Moramarco, W. Wagner, W. Dorigo, P. Matgen, J. Martínez-Fernández, P. Llorens, *et al.*, “Soil moisture estimation through ascat and amsr-e sensors: An intercomparison and validation study across europe,” *Remote Sensing of Environment*, vol. 115, no. 12, pp. 3390–3408, 2011.
- [17] W. Dorigo, A. Gruber, R. De Jeu, W. Wagner, T. Stacke, A. Loew, C. Albergel, L. Brocca, D. Chung, R. Parinussa, *et al.*, “Evaluation of the esa cci soil moisture product using ground-based observations,” *Remote Sensing of Environment*, vol. 162, pp. 380–395, 2015.
- [18] C. Montzka, H. R. Bogaen, M. Zreda, A. Monerris, R. Morrison, S. Muddu, and H. Vereecken, “Validation of spaceborne and modelled surface soil moisture products with cosmic-ray neutron probes,” *Remote sensing*, vol. 9, no. 2, p. 103, 2017.
- [19] M. B. Duygu and Z. Akyürek, “Using cosmic-ray neutron probes in validating

satellite soil moisture products and land surface models,” *Water*, vol. 11, no. 7, p. 1362, 2019.

- [20] J. Parajka, V. Naeimi, G. Blöschl, W. Wagner, R. Merz, and K. Scipal, “Assimilating scatterometer soil moisture data into conceptual hydrologic models at the regional scale,” *Hydrology and Earth System Sciences*, vol. 10, no. 3, pp. 353–368, 2006.
- [21] D. Kundu, R. W. Vervoort, and F. F. van Ogtrop, “The value of remotely sensed surface soil moisture for model calibration using swat,” *Hydrological Processes*, vol. 31, no. 15, pp. 2764–2780, 2017.
- [22] F. Avanzi, T. Maurer, S. D. Glaser, R. C. Bales, and M. H. Conklin, “Information content of spatially distributed ground-based measurements for hydrologic-parameter calibration in mixed rain-snow mountain headwaters,” *Journal of Hydrology*, vol. 582, p. 124478, 2020.
- [23] B. Széles, J. Parajka, P. Hogan, R. Silasari, L. Pavlin, P. Strauss, and G. Blöschl, “The added value of different data types for calibrating and testing a hydrologic model in a small catchment,” *Water resources research*, vol. 56, no. 10, p. e2019WR026153, 2020.
- [24] K. Dimitrova-Petrova, J. Geris, E. M. Wilkinson, R. Rosolem, L. Verrot, A. Lilly, and C. Soulsby, “Opportunities and challenges in using catchment-scale storage estimates from cosmic ray neutron sensors for rainfall-runoff modelling,” *Journal of Hydrology*, p. 124878, 2020.
- [25] L. J. Briggs *et al.*, “Mechanics of soil moisture,” 1897.
- [26] L. Richards and W. Gardner, “Tensiometers for measuring the capillary tension of soil water,” *Agronomy Journal*, vol. 28, no. 5, pp. 352–358, 1936.
- [27] A. Ridley and J. Burland, “A new instrument for the measurement of soil moisture suction,” *Géotechnique*, vol. 43, no. 2, pp. 321–324, 1993.
- [28] D. Singh and S. J. Kuriyan, “Estimation of unsaturated hydraulic conductivity using soil suction measurements obtained by an insertion tensiometer,” *Canadian Geotechnical Journal*, vol. 40, no. 2, pp. 476–483, 2003.

- [29] E. T. Selig and S. Mansukhani, "Relationship of soil moisture to the dielectric property," *Journal of the Geotechnical Engineering Division*, vol. 101, no. 8, pp. 755–770, 1975.
- [30] G. Topp, J. Davis, and A. Annan, "Electromagnetic determination of soil water content using tdr: I. applications to wetting fronts and steep gradients," *Soil Science Society of America Journal*, vol. 46, no. 4, pp. 672–678, 1982.
- [31] K. Noborio, "Measurement of soil water content and electrical conductivity by time domain reflectometry: a review," *Computers and electronics in agriculture*, vol. 31, no. 3, pp. 213–237, 2001.
- [32] W. Whalley, T. Dean, and P. Izzard, "Evaluation of the capacitance technique as a method for dynamically measuring soil water content," *Journal of agricultural engineering research*, vol. 52, pp. 147–155, 1992.
- [33] J. Minet, S. Lambot, G. Delaide, J. A. Huisman, H. Vereecken, and M. Vanclooster, "A generalized frequency domain reflectometry modeling technique for soil electrical properties determination," *Vadose Zone Journal*, vol. 9, no. 4, pp. 1063–1072, 2010.
- [34] C. Gardner, T. Dean, and J. Cooper, "Soil water content measurement with a high-frequency capacitance sensor," *Journal of Agricultural Engineering Research*, vol. 71, no. 4, pp. 395–403, 1998.
- [35] A. Chanzy, A. Tarussov, F. Bonn, and A. Judge, "Soil water content determination using a digital ground-penetrating radar," *Soil science society of America journal*, vol. 60, no. 5, pp. 1318–1326, 1996.
- [36] S. L. SU, D. Singh, and M. S. Baghini, "A critical review of soil moisture measurement," *Measurement*, vol. 54, pp. 92–105, 2014.
- [37] D. A. De Vries, "Thermal properties of soils," *Physics of plant environment*, 1963.
- [38] K. Noborio, K. McInnes, and J. Heilman, "Measurements of soil water content, heat capacity, and thermal conductivity with a single tdr probe 1," *Soil Science*, vol. 161, no. 1, pp. 22–28, 1996.

- [39] J. M. Tarara and J. M. Ham, “Measuring soil water content in the laboratory and field with dual-probe heat-capacity sensors,” *Agronomy Journal*, vol. 89, no. 4, pp. 535–542, 1997.
- [40] T. Jackson, K. Mansfield, M. Saafi, T. Colman, and P. Romine, “Measuring soil temperature and moisture using wireless mems sensors,” *Measurement*, vol. 41, no. 4, pp. 381–390, 2008.
- [41] V. S. Palaparthi, H. Kalita, S. G. Surya, M. S. Baghini, and M. Aslam, “Graphene oxide based soil moisture microsensor for in situ agriculture applications,” *Sensors and Actuators B: Chemical*, vol. 273, pp. 1660–1669, 2018.
- [42] M. F. L’Annunziata, “Nuclear radiation, its interaction with matter and radioisotope decay,” *Handbook of Radioactivity Analysis*, pp. 1–122, 2003.
- [43] FAO and IAEA, “Comparison of soil water measurement using the neutron scattering, time domain reflectometry and capacitance methods. results of a consultants meeting,” tech. rep., Joint FAO/IAEA Division of Nuclear Techniques in Food and Agriculture, 2000.
- [44] L. Stevanato, G. Baroni, Y. Cohen, F. Cristiano Lino, S. Gatto, M. Lunardon, F. Marinello, S. Moretto, and L. Morselli, “A novel cosmic-ray neutron sensor for soil moisture estimation over large areas,” *Agriculture*, vol. 9, no. 9, p. 202, 2019.
- [45] J. Dong, T. E. Ochsner, M. Zreda, M. H. Cosh, and C. B. Zou, “Calibration and validation of the cosmos rover for surface soil moisture measurement,” *Vadose Zone Journal*, vol. 13, no. 4, 2014.
- [46] H. R. Bogen, F. Herrmann, J. Jakobi, C. Brogi, A. Ilias, J. A. Huisman, A. Panagopoulos, and V. Pisinaras, “Monitoring of snowpack dynamics with cosmic-ray neutron probes: A comparison of four conversion methods,” *Frontiers in water*, vol. 2, p. 19, 2020.
- [47] J. R. Mchenry and A. C. Gill, “Measurement of soil moisture with a portable gamma ray scintillation spectrometer,” *Water Resources Research*, vol. 6, no. 3, pp. 989–992, 1970.

- [48] V. Strati, M. Albéri, S. Anconelli, M. Baldoncini, M. Bittelli, C. Bottardi, E. Chiarelli, B. Fabbri, V. Guidi, K. Raptis, *et al.*, “Modelling soil water content in a tomato field: proximal gamma ray spectroscopy and soil–crop system models,” *Agriculture*, vol. 8, no. 4, p. 60, 2018.
- [49] G. Rouze, C. Morgan, and A. McBratney, “Understanding the utility of aerial gamma radiometrics for mapping soil properties through proximal gamma surveys,” *Geoderma*, vol. 289, pp. 185–195, 2017.
- [50] A. L. Kaleita, L. F. Tian, and M. C. Hirschi, “Relationship between soil moisture content and soil surface reflectance,” *Transactions of the ASAE*, vol. 48, no. 5, pp. 1979–1986, 2005.
- [51] D. Robinson, C. Campbell, J. Hopmans, B. K. Hornbuckle, S. B. Jones, R. Knight, F. Ogden, J. Selker, and O. Wendroth, “Soil moisture measurement for ecological and hydrological watershed-scale observatories: A review,” *Vadose Zone Journal*, vol. 7, no. 1, pp. 358–389, 2008.
- [52] L. Isaksen and A. Stoffelen, “Ers scatterometer wind data impact on ecmwf’s tropical cyclone forecasts,” *IEEE transactions on geoscience and remote sensing*, vol. 38, no. 4, pp. 1885–1892, 2000.
- [53] D. Entekhabi, S. Yueh, P. E. O’Neill, K. H. Kellogg, A. Allen, R. Bindlish, M. Brown, S. Chan, A. Colliander, W. T. Crow, *et al.*, “Smop handbook—soil moisture active passive: Mapping soil moisture and freeze/thaw from space,” 2014.
- [54] J. Font, A. Camps, A. Borges, M. Martín-Neira, J. Boutin, N. Reul, Y. H. Kerr, A. Hahne, and S. Mecklenburg, “Smos: The challenging sea surface salinity measurement from space,” *Proceedings of the IEEE*, vol. 98, no. 5, pp. 649–665, 2010.
- [55] R. M. Parinussa, T. R. H. Holmes, N. Wanders, W. A. Dorigo, and R. A. M. de Jeu, “A preliminary study toward consistent soil moisture from amsr2,” *Journal of Hydrometeorology*, vol. 16, no. 2, pp. 932–947, 2015.
- [56] W. Dorigo, W. Wagner, C. Albergel, F. Albrecht, G. Balsamo, L. Brocca, D. Chung, M. Ertl, M. Forkel, A. Gruber, *et al.*, “Esa cci soil moisture for

improved earth system understanding: State-of-the art and future directions,” *Remote Sensing of Environment*, vol. 203, pp. 185–215, 2017.

- [57] A. Gruber, W. A. Dorigo, W. Crow, and W. Wagner, “Triple collocation-based merging of satellite soil moisture retrievals,” *IEEE Transactions on Geoscience and Remote Sensing*, vol. 55, no. 12, pp. 6780–6792, 2017.
- [58] Y. Y. Liu, W. A. Dorigo, R. Parinussa, R. A. de Jeu, W. Wagner, M. F. McCabe, J. Evans, and A. Van Dijk, “Trend-preserving blending of passive and active microwave soil moisture retrievals,” *Remote Sensing of Environment*, vol. 123, pp. 280–297, 2012.
- [59] D. Desilets, M. Zreda, and T. Ferré, “Nature’s neutron probe: Land surface hydrology at an elusive scale with cosmic rays,” *Water Resources Research*, vol. 46, no. 11, 2010.
- [60] A. Hawdon, D. McJannet, and J. Wallace, “Calibration and correction procedures for cosmic-ray neutron soil moisture probes located across australia,” *Water Resources Research*, vol. 50, no. 6, pp. 5029–5043, 2014.
- [61] G. Demir, “Soil water content estimation from point scale to plot scale,” *Middle East Technical University, Master Thesis*, 2018.
- [62] M. Zreda, W. Shuttleworth, X. Zeng, C. Zweck, D. Desilets, T. Franz, and R. Rosolem, “Cosmos: the cosmic-ray soil moisture observing system,” *Hydrology and Earth System Sciences*, vol. 16, no. 11, pp. 4079–4099, 2012.
- [63] M. Duygu, “Codes and data of the phd. thesis.” https://github.com/dubemu/MustafaBerkDuygu_PhD_files, 2021.
- [64] R. Baatz, H. Boga, H.-J. Hendricks Franssen, J. Huisman, C. Montzka, and H. Vereecken, “An empirical vegetation correction for soil water content quantification using cosmic ray probes,” *Water Resources Research*, vol. 51, no. 4, pp. 2030–2046, 2015.
- [65] D. Desilets, M. Zreda, and T. Prabu, “Extended scaling factors for in situ cosmogenic nuclides: new measurements at low latitude,” *Earth and Planetary Science Letters*, vol. 246, no. 3-4, pp. 265–276, 2006.

- [66] R. Rosolem, W. Shuttleworth, M. Zreda, T. Franz, X. Zeng, and S. Kurc, “The effect of atmospheric water vapor on neutron count in the cosmic-ray soil moisture observing system,” *Journal of Hydrometeorology*, vol. 14, no. 5, pp. 1659–1671, 2013.
- [67] “Nmdb, real-time database for high-resolution neutron monitor measurements.” <http://www.nmdb.eu/>. Accessed: February 28, 2021.
- [68] “The cosmic-ray soil moisture observing system (cosmos).” <http://cosmos.hwr.arizona.edu>. Accessed: February 28, 2021.
- [69] D. Smart and M. Shea, “World grid of calculated cosmic ray vertical cutoff rigidities for epoch 2000.0,” in *Proceedings of the 30th International Cosmic Ray Conference*, vol. 1, pp. 737–740, 2008.
- [70] J. Evans, H. Ward, J. Blake, E. Hewitt, R. Morrison, M. Fry, L. Ball, L. Doughty, J. Libre, O. Hitt, *et al.*, “Soil water content in southern england derived from a cosmic-ray soil moisture observing system–cosmos-uk,” *Hydrological Processes*, vol. 30, no. 26, pp. 4987–4999, 2016.
- [71] “Cosmic-ray soil moisture monitoring network-uk (cosmos-uk).” <https://cosmos.ceh.ac.uk>. Accessed: February 28, 2021.
- [72] H. R. Boga, “Tereno: German network of terrestrial environmental observatories,” *Journal of large-scale research facilities JLSRF*, vol. 2, p. 52, 2016.
- [73] “Terrestrial environmental observatories (tereno).” <https://www.tereno.net>. Accessed: February 28, 2021.
- [74] “Australian cosmic-ray neutron soil moisture monitoring network (cosmoz).” <https://cosmoz.csiro.au>. Accessed: February 28, 2021.
- [75] H. R. Boga, P. Ney, J. Jakobi, R. Baatz, F. Herrmann, H. Vereecken, M. Schrön, S. Zacharias, M. Zreda, D. B. Boorman, J. G. Evans, M. Szczykulska, Y. Kerr, A. Mialon, P. Nasta, N. Romano, R. Rosolem, D. Power, J. Iwema, M. Andreasen, M. C. Looms, K. H. Jensen, D. Rasche, A. Güntner, T. Blume, S. Oswald, P. Schattan, S. Achleitner, B. Fersch, A. Patil, H. Kunstmann, J. Geris, K. Dimitrova-Petrova, Z. Mengistu, J. Nitychoruk, F. Frances, M. A.

Eguibar-Galán, E. Albentosa-Hernández, M. G. Sanchis, A. Lidón, A. del Campo, V. Pisinaras, A. Panagopoulos, H. Said, G. Weltin, S. I. Seneviratne, M. B. Duygu, and Z. Akyürek, “Cosmos-europe: A european network of cosmic-ray neutron soil moisture sensors,” in press.

- [76] “The eumetsat satellite application facility on support to operational hydrology and water management (h-saf).” <http://hsaf.meteoam.it>. Accessed: February 28, 2021.
- [77] M. Rodell and H. K. Beaudoin, “Gldas noah land surface model 14 monthly 0.25×0.25 degree version 2.0,” *Goddard Earth Sciences Data and Information Services Center: Greenbelt, MD, USA*, 2013.
- [78] F. Nachtergaele, H. van Velthuisen, L. Verelst, N. Batjes, K. Dijkshoorn, V. van Engelen, G. Fischer, A. Jones, and L. Montanarella, “The harmonized world soil database,” in *Proceedings of the 19th World Congress of Soil Science, Soil Solutions for a Changing World, Brisbane, Australia, 1-6 August 2010*, pp. 34–37, 2010.
- [79] K. McMullan, M. A. Brown, M. Martín-Neira, W. Rits, S. Ekholm, J. Marti, and J. Lemanczyk, “Smos: The payload,” *IEEE Transactions on Geoscience and Remote Sensing*, vol. 46, no. 3, pp. 594–605, 2008.
- [80] “Barcelona expert center remote sensing research, data distribution and visualization services. bec is a joint initiative of the spanish research council (csic) and the technical university of catalonia (upc), mainly funded by the spanish national program on space..” <http://bec.icm.csic.es>. Accessed: February 28, 2021.
- [81] R. Reichle, G. De Lannoy, R. Koster, W. Crow, and J. Kimball, “Smop 14 9 km ease-grid surface and root zone soil moisture geophysical data, version 2,” *National Snow and Ice Data Center Distributed Active Archive Center, accessed*, vol. 10, 2016.
- [82] “Earth science data systems (esds) of nasa.” earthdata.nasa.gov. Accessed: February 28, 2021.

- [83] D. Entekhabi, E. G. Njoku, P. E. O'Neill, K. H. Kellogg, W. T. Crow, W. N. Edelstein, J. K. Entin, S. D. Goodman, T. J. Jackson, J. Johnson, *et al.*, "The soil moisture active passive (smap) mission," *Proceedings of the IEEE*, vol. 98, no. 5, pp. 704–716, 2010.
- [84] "European space agency climate change initiative." `climate.esa.int`. Accessed: February 28, 2021.
- [85] M. Rodell, P. Houser, U. Jambor, J. Gottschalck, K. Mitchell, C.-J. Meng, K. Arsenault, B. Cosgrove, J. Radakovich, M. Bosilovich, *et al.*, "The global land data assimilation system," *Bulletin of the American Meteorological Society*, vol. 85, no. 3, pp. 381–394, 2004.
- [86] S. B. Idso and R. D. Jackson, "Thermal radiation from the atmosphere," *Journal of geophysical Research*, vol. 74, no. 23, pp. 5397–5403, 1969.
- [87] J. E. Nash and J. V. Sutcliffe, "River flow forecasting through conceptual models part i—a discussion of principles," *Journal of hydrology*, vol. 10, no. 3, pp. 282–290, 1970.
- [88] J. S. Armstrong and F. Collopy, "Error measures for generalizing about forecasting methods: Empirical comparisons," *International journal of forecasting*, vol. 8, no. 1, pp. 69–80, 1992.
- [89] S. Sorooshian, Q. Duan, and V. K. Gupta, "Calibration of rainfall-runoff models: Application of global optimization to the sacramento soil moisture accounting model," *Water resources research*, vol. 29, no. 4, pp. 1185–1194, 1993.
- [90] J. Devore, *Probability and Statistics for Engineering and the Sciences*. Nelson Education, 2011.
- [91] R. E. Criss and W. E. Winston, "Do nash values have value? discussion and alternate proposals," *Hydrological Processes: An International Journal*, vol. 22, no. 14, pp. 2723–2725, 2008.
- [92] H. V. Gupta and H. Kling, "On typical range, sensitivity, and normalization of mean squared error and nash-sutcliffe efficiency type metrics," *Water Resources Research*, vol. 47, no. 10, 2011.

- [93] X. Zhu, R. Cao, M. Shao, and Y. Liang, “Footprint radius of a cosmic-ray neutron probe for measuring soil-water content and its spatiotemporal variability in an alpine meadow ecosystem,” *Journal of Hydrology*, vol. 558, pp. 1–8, 2018.
- [94] S. Kim, Y. Y. Liu, F. M. Johnson, R. M. Parinussa, and A. Sharma, “A global comparison of alternate amsr2 soil moisture products: Why do they differ?,” *Remote Sensing of Environment*, vol. 161, pp. 43–62, 2015.
- [95] H. Kim, R. Parinussa, A. G. Konings, W. Wagner, M. H. Cosh, V. Lakshmi, M. Zohaib, and M. Choi, “Global-scale assessment and combination of smap with ascat (active) and amsr2 (passive) soil moisture products,” *Remote Sensing of Environment*, vol. 204, pp. 260–275, 2018.
- [96] M. Kędzior and J. Zawadzki, “Comparative study of soil moisture estimations from smos satellite mission, gldas database, and cosmic-ray neutrons measurements at cosmos station in eastern poland,” *Geoderma*, vol. 283, pp. 21–31, 2016.
- [97] T. E. Ochsner, M. H. Cosh, R. H. Cuenca, W. A. Dorigo, C. S. Draper, Y. Hagimoto, Y. H. Kerr, E. G. Njoku, E. E. Small, M. Zreda, *et al.*, “State of the art in large-scale soil moisture monitoring,” *Soil Science Society of America Journal*, vol. 77, no. 6, pp. 1888–1919, 2013.
- [98] F. Lei, W. T. Crow, H. Shen, R. M. Parinussa, and T. R. Holmes, “The impact of local acquisition time on the accuracy of microwave surface soil moisture retrievals over the contiguous united states,” *Remote Sensing*, vol. 7, no. 10, pp. 13448–13465, 2015.
- [99] K. A. K. Deng, S. Lamine, A. Pavlides, G. P. Petropoulos, P. K. Srivastava, Y. Bao, D. Hristopoulos, and V. Anagnostopoulos, “Operational soil moisture from ascat in support of water resources management,” *Remote Sensing*, vol. 11, no. 5, p. 579, 2019.
- [100] A. Stoffelen, “Toward the true near-surface wind speed: Error modeling and calibration using triple collocation,” *Journal of Geophysical Research: Oceans*, vol. 103, no. C4, pp. 7755–7766, 1998.

- [101] D. J. Leroux, Y. H. Kerr, P. Richaume, and R. Fieuzal, "Spatial distribution and possible sources of smos errors at the global scale," *Remote Sensing of Environment*, vol. 133, pp. 240–250, 2013.
- [102] D. Baldocchi, E. Falge, L. Gu, R. Olson, D. Hollinger, S. Running, P. Anthoni, C. Bernhofer, K. Davis, R. Evans, *et al.*, "Fluxnet: A new tool to study the temporal and spatial variability of ecosystem-scale carbon dioxide, water vapor, and energy flux densities," *Bulletin of the American Meteorological Society*, vol. 82, no. 11, pp. 2415–2434, 2001.
- [103] T. Vather, C. Everson, M. Mengistu, and T. Franz, "Cosmic ray neutrons provide an innovative technique for estimating intermediate scale soil moisture," *South African Journal of Science*, vol. 114, no. 7-8, pp. 79–87, 2018.
- [104] H. Penman, "Laboratory experiments on evaporation from fallow soil," *The Journal of Agricultural Science*, vol. 31, no. 4, pp. 454–465, 1941.
- [105] J. R. Philip, "Evaporation, and moisture and heat fields in the soil," *Journal of meteorology*, vol. 14, no. 4, pp. 354–366, 1957.
- [106] H. Ashktorab, W. Pruitt, and K. Paw U, "Partitioning of evapotranspiration using lysimeter and micro-bowen-ratio system," *Journal of irrigation and drainage engineering*, vol. 120, no. 2, pp. 450–464, 1994.
- [107] D. I. Stannard and M. A. Weltz, "Partitioning evapotranspiration in sparsely vegetated rangeland using a portable chamber," *Water Resources Research*, vol. 42, no. 2, 2006.
- [108] J. Heitman, X. Xiao, R. Horton, and T. Sauer, "Sensible heat measurements indicating depth and magnitude of subsurface soil water evaporation," *Water Resources Research*, vol. 44, no. 4, 2008.
- [109] Z. Xiao, S. Lu, J. Heitman, R. Horton, *et al.*, "Measuring subsurface soil-water evaporation with an improved heat-pulse probe," *Soil Science Society of America Journal*, vol. 76, no. 3, pp. 876–879, 2012.
- [110] P. K. Deol, J. L. Heitman, A. Amoozegar, T. Ren, and R. Horton, "Inception and magnitude of subsurface evaporation for a bare soil with natural surface

- boundary conditions,” *Soil Science Society of America Journal*, vol. 78, no. 5, pp. 1544–1551, 2014.
- [111] E. Balugani, M. Lubczynski, C. Van Der Tol, and K. Metselaar, “Testing three approaches to estimate soil evaporation through a dry soil layer in a semi-arid area,” *Journal of hydrology*, vol. 567, pp. 405–419, 2018.
- [112] E. E. Small, A. M. Badger, R. Abolafia-Rosenzweig, and B. Livneh, “Estimating soil evaporation using drying rates determined from satellite-based soil moisture records,” *Remote Sensing*, vol. 10, no. 12, p. 1945, 2018.
- [113] A. J. Purdy, J. B. Fisher, M. L. Goulden, A. Colliander, G. Halverson, K. Tu, and J. S. Famiglietti, “Smop soil moisture improves global evapotranspiration,” *Remote Sensing of Environment*, vol. 219, pp. 1–14, 2018.
- [114] A. P. Schreiner-McGraw, E. R. Vivoni, G. Mascaro, and T. E. Franz, “Closing the water balance with cosmic-ray soil moisture measurements and assessing their relation to evapotranspiration in two semiarid watersheds,” 2016.
- [115] R. B. Jana, A. Ershadi, and M. McCabe, “Examining the relationship between intermediate-scale soil moisture and terrestrial evaporation within a semi-arid grassland,” 2016.
- [116] P. J. Wetzel and J.-T. Chang, “Concerning the relationship between evapotranspiration and soil moisture,” *Journal of climate and applied meteorology*, vol. 26, no. 1, pp. 18–27, 1987.
- [117] C. D. Peters-Lidard, S. V. Kumar, D. M. Mocko, and Y. Tian, “Estimating evapotranspiration with land data assimilation systems,” *Hydrological Processes*, vol. 25, no. 26, pp. 3979–3992, 2011.
- [118] L.-F. Lin, A. M. Ebtehaj, J. Wang, and R. L. Bras, “Soil moisture background error covariance and data assimilation in a coupled land-atmosphere model,” *Water Resources Research*, vol. 53, no. 2, pp. 1309–1335, 2017.
- [119] J. Yin, X. Zhan, Y. Zheng, J. Liu, C. R. Hain, and L. Fang, “Impact of quality control of satellite soil moisture data on their assimilation into land surface model,” *Geophysical Research Letters*, vol. 41, no. 20, pp. 7159–7166, 2014.

- [120] A. K. Sahoo, G. J. De Lannoy, R. H. Reichle, and P. R. Houser, "Assimilation and downscaling of satellite observed soil moisture over the little river experimental watershed in georgia, usa," *Advances in water resources*, vol. 52, pp. 19–33, 2013.
- [121] B. Li, D. Toll, X. Zhan, and B. Cosgrove, "Improving estimated soil moisture fields through assimilation of amsr-e soil moisture retrievals with an ensemble kalman filter and a mass conservation constraint," *Hydrology and Earth System Sciences*, vol. 16, no. 1, pp. 105–119, 2012.
- [122] A. N. Flores, R. L. Bras, and D. Entekhabi, "Hydrologic data assimilation with a hillslope-scale-resolving model and l band radar observations: Synthetic experiments with the ensemble kalman filter," *Water Resources Research*, vol. 48, no. 8, 2012.
- [123] C. Draper, R. Reichle, G. De Lannoy, and Q. Liu, "Assimilation of passive and active microwave soil moisture retrievals," *Geophysical Research Letters*, vol. 39, no. 4, 2012.
- [124] Q. Liu, R. H. Reichle, R. Bindlish, M. H. Cosh, W. T. Crow, R. de Jeu, G. J. De Lannoy, G. J. Huffman, and T. J. Jackson, "The contributions of precipitation and soil moisture observations to the skill of soil moisture estimates in a land data assimilation system," *Journal of Hydrometeorology*, vol. 19, no. 11, 2018.
- [125] S. V. Kumar, R. H. Reichle, R. D. Koster, W. T. Crow, and C. D. Peters-Lidard, "Role of subsurface physics in the assimilation of surface soil moisture observations," *Journal of hydrometeorology*, vol. 10, no. 6, pp. 1534–1547, 2009.
- [126] R. H. Reichle, W. T. Crow, and C. L. Keppenne, "An adaptive ensemble kalman filter for soil moisture data assimilation," *Water resources research*, vol. 44, no. 3, 2008.
- [127] R. H. Reichle, R. D. Koster, P. Liu, S. P. Mahanama, E. G. Njoku, and M. Owe, "Comparison and assimilation of global soil moisture retrievals from the advanced microwave scanning radiometer for the earth observing system (amsr-

- e) and the scanning multichannel microwave radiometer (smmr),” *Journal of Geophysical Research: Atmospheres*, vol. 112, no. D9, 2007.
- [128] R. H. Reichle and R. D. Koster, “Global assimilation of satellite surface soil moisture retrievals into the nasa catchment land surface model,” *Geophysical Research Letters*, vol. 32, no. 2, 2005.
- [129] L. Sun, S. Liang, W. Yuan, and Z. Chen, “Improving a penman–monteith evapotranspiration model by incorporating soil moisture control on soil evaporation in semiarid areas,” *International Journal of Digital Earth*, vol. 6, no. sup1, pp. 134–156, 2013.
- [130] J. Monteith, “Evaporation and surface temperature,” *Quarterly Journal of the Royal Meteorological Society*, vol. 107, no. 451, pp. 1–27, 1981.
- [131] B. Martens, D. Miralles, H. Lievens, D. Fernández-Prieto, and N. E. Verhoest, “Improving terrestrial evaporation estimates over continental australia through assimilation of smos soil moisture,” *International Journal of Applied Earth Observation and Geoinformation*, vol. 48, pp. 146–162, 2016.
- [132] D. D. Yanmaz, “Estimating evapotranspiration by metric model over çakit basin,” *Middle East Technical University, Master Thesis*, 2019.
- [133] S. A. Nielsen and E. Hansen, “Numerical simulation of the rainfall-runoff process on a daily basis,” *Hydrology Research*, vol. 4, no. 3, pp. 171–190, 1973.
- [134] E. Han, V. Merwade, and G. C. Heathman, “Implementation of surface soil moisture data assimilation with watershed scale distributed hydrological model,” *Journal of hydrology*, vol. 416, pp. 98–117, 2012.
- [135] C. Otlé and D. Vidal-Madjar, “Assimilation of soil moisture inferred from infrared remote sensing in a hydrological model over the hapex-mobilhy region,” *Journal of Hydrology*, vol. 158, no. 3-4, pp. 241–264, 1994.
- [136] G. Welch, G. Bishop, *et al.*, “An introduction to the kalman filter,” 1995.
- [137] C. Draper, J.-F. Mahfouf, J.-C. Calvet, E. Martin, and W. Wagner, “Assimilation of ascats near-surface soil moisture into the sim hydrological model over

- france,” *Hydrology and Earth System Sciences*, vol. 15, no. 12, pp. 3829–3841, 2011.
- [138] P. R. Houser, W. J. Shuttleworth, J. S. Famiglietti, H. V. Gupta, K. H. Syed, and D. C. Goodrich, “Integration of soil moisture remote sensing and hydrologic modeling using data assimilation,” *Water Resources Research*, vol. 34, no. 12, pp. 3405–3420, 1998.
- [139] S. V. Kumar, C. D. Peters-Lidard, Y. Tian, P. R. Houser, J. Geiger, S. Olden, L. Lighty, J. L. Eastman, B. Doty, P. Dirmeyer, *et al.*, “Land information system: An interoperable framework for high resolution land surface modeling,” *Environmental modelling & software*, vol. 21, no. 10, pp. 1402–1415, 2006.
- [140] R. Jaiswal, S. Ali, and B. Bharti, “Comparative evaluation of conceptual and physical rainfall–runoff models,” *Applied Water Science*, vol. 10, no. 1, pp. 1–14, 2020.
- [141] F. F. Snyder, “A conception of runoff-phenomena,” *Eos, Transactions American Geophysical Union*, vol. 20, no. 4, pp. 725–738, 1939.
- [142] M. B. McPherson, “Some notes on the rational method of storm drain design,” American Society of Civil Engineers, 1969.
- [143] A. T. Hjelmfelt Jr, “Investigation of curve number procedure,” *Journal of Hydraulic Engineering*, vol. 117, no. 6, pp. 725–737, 1991.
- [144] A. D. Feldman, “Hec models for water resources system simulation: theory and experience,” in *Advances in hydroscience*, vol. 12, pp. 297–423, Elsevier, 1981.
- [145] S. Bergström, *Development and application of a conceptual runoff model for Scandinavian catchments*. 1976.
- [146] J. Refshaard, B. Storm, *et al.*, “Mike she.,” *Computer models of watershed hydrology.*, pp. 809–846, 1995.
- [147] J. G. Arnold, R. Srinivasan, R. S. Muttiah, and J. R. Williams, “Large area hydrologic modeling and assessment part i: model development 1,” *JAWRA*

Journal of the American Water Resources Association, vol. 34, no. 1, pp. 73–89, 1998.

- [148] E. F. Wood, D. P. Lettenmaier, and V. G. Zartarian, “A land-surface hydrology parameterization with subgrid variability for general circulation models,” *Journal of Geophysical Research: Atmospheres*, vol. 97, no. D3, pp. 2717–2728, 1992.
- [149] F. Chen, K. Mitchell, J. Schaake, Y. Xue, H.-L. Pan, V. Koren, Q. Y. Duan, M. Ek, and A. Betts, “Modeling of land surface evaporation by four schemes and comparison with five observations,” *Journal of Geophysical Research: Atmospheres*, vol. 101, no. D3, pp. 7251–7268, 1996.
- [150] M. Ek, K. Mitchell, Y. Lin, E. Rogers, P. Grunmann, V. Koren, G. Gayno, and J. Tarpley, “Implementation of noah land surface model advances in the national centers for environmental prediction operational mesoscale eta model,” *Journal of Geophysical Research: Atmospheres*, vol. 108, no. D22, 2003.
- [151] N. Agrawal and T. Desmukh, “Rainfall runoff modeling using mike 11 nam—a review,” *International Journal of Innovative Science, Engineering & Technology*, vol. 3, no. 6, pp. 659–667, 2016.
- [152] C. Doulgeris, P. Georgiou, D. Papadimos, and D. Papamichail, “Evaluating three different model setups in the mike 11 nam model,” pp. 241–249, 2011.
- [153] C. Doulgeris, P. Georgiou, D. Papadimos, and D. Papamichail, “Ecosystem approach to water resources management using the mike 11 modeling system in the strymonas river and lake kerkini,” *Journal of environmental management*, vol. 94, no. 1, pp. 132–143, 2012.
- [154] E. K. Lafdani, A. M. Nia, A. Pahlavanravi, A. Ahmadi, and M. Jajarmizadeh, “Research article daily rainfall-runoff prediction and simulation using ann, an-fis and conceptual hydrological mike11/nam models,” *Int. J. Eng. Technol*, vol. 1, pp. 32–50, 2013.
- [155] P. Qi, Y. J. Xu, and G. Wang, “Quantifying the individual contributions of climate change, dam construction, and land use/land cover change to hydrological drought in a marshy river,” *Sustainability*, vol. 12, no. 9, p. 3777, 2020.

- [156] M. M. Rahman, D. Arya, N. Goel, and A. P. Dhamy, “Design flow and stage computations in the teesta river, bangladesh, using frequency analysis and mike 11 modeling,” *Journal of Hydrologic Engineering*, vol. 16, no. 2, pp. 176–186, 2011.
- [157] F. T. Teshome, H. K. Bayabil, L. Thakural, F. G. Welidehanna, *et al.*, “Verification of the mike11-nam model for simulating streamflow,” *Journal of Environmental Protection*, vol. 11, no. 02, p. 152, 2020.
- [158] J. Sheffield, G. Goteti, and E. F. Wood, “Development of a 50-year high-resolution global dataset of meteorological forcings for land surface modeling,” *Journal of Climate*, vol. 19, no. 13, pp. 3088–3111, 2006.
- [159] H. H. Savenije, “Equifinality, a blessing in disguise?,” *Hydrological processes*, vol. 15, no. 14, pp. 2835–2838, 2001.
- [160] K. Beven, “How far can we go in distributed hydrological modelling?,” 2001.
- [161] A. Phocaides, “Technical handbook on pressurized irrigation techniques,” *FAO, Rome*, vol. 372, 2000.
- [162] M. T. Van Genuchten, “A closed-form equation for predicting the hydraulic conductivity of unsaturated soils,” *Soil science society of America journal*, vol. 44, no. 5, pp. 892–898, 1980.
- [163] W. Wagner, G. Lemoine, and H. Rott, “A method for estimating soil moisture from ers scatterometer and soil data,” *Remote Sensing of Environment*, vol. 70, no. 2, pp. 191–207, 1999.
- [164] T. E. Franz, M. Zreda, T. Ferre, R. Rosolem, C. Zweck, S. Stillman, X. Zeng, and W. Shuttleworth, “Measurement depth of the cosmic ray soil moisture probe affected by hydrogen from various sources,” *Water Resources Research*, vol. 48, no. 8, 2012.
- [165] M. Köhli, M. Schrön, M. Zreda, U. Schmidt, P. Dietrich, and S. Zacharias, “Footprint characteristics revised for field-scale soil moisture monitoring with cosmic-ray neutrons,” *Water Resources Research*, vol. 51, no. 7, pp. 5772–5790, 2015.

- [166] Y. Li, S. Grimaldi, V. R. Pauwels, and J. P. Walker, “Hydrologic model calibration using remotely sensed soil moisture and discharge measurements: The impact on predictions at gauged and ungauged locations,” *Journal of hydrology*, vol. 557, pp. 897–909, 2018.
- [167] C. Francois, A. Quesney, and C. Ottlé, “Sequential assimilation of ers-1 sar data into a coupled land surface–hydrological model using an extended kalman filter,” *Journal of Hydrometeorology*, vol. 4, no. 2, pp. 473–487, 2003.
- [168] Y. Li, D. Ryu, A. W. Western, and Q. Wang, “Assimilation of stream discharge for flood forecasting: Updating a semidistributed model with an integrated data assimilation scheme,” *Water resources research*, vol. 51, no. 5, pp. 3238–3258, 2015.
- [169] R. D. Harr, “Effects of clearcutting on rain-on-snow runoff in western oregon: A new look at old studies,” *Water Resources Research*, vol. 22, no. 7, pp. 1095–1100, 1986.

APPENDIX A

THE DIRECT RELATIONS BETWEEN SOIL MOISTURE PRODUCTS EXAMINED IN THIS STUDY WITH IN-SITU SOIL MOISTURE OBSERVATIONS

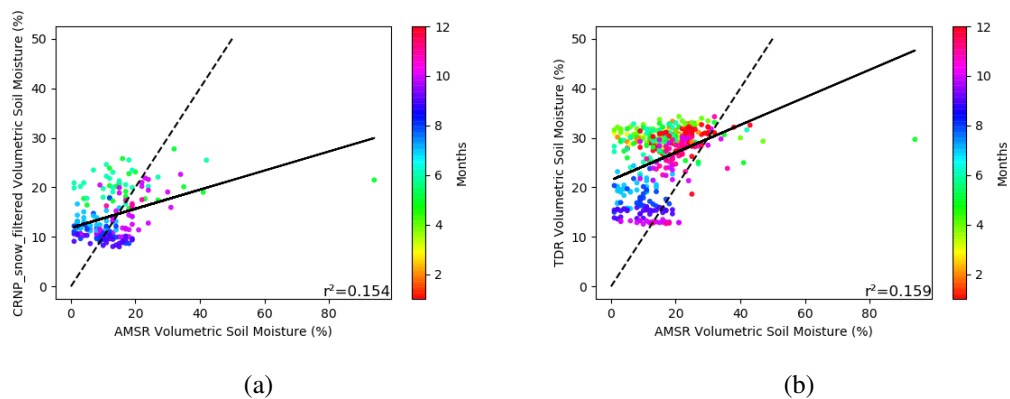


Figure A.1: AMSR (ascending) soil moisture vs. a) CRNP and b) TDR

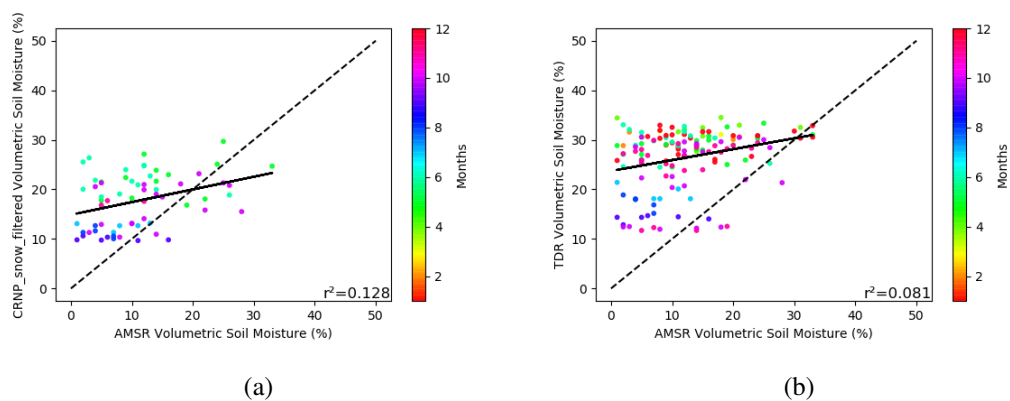
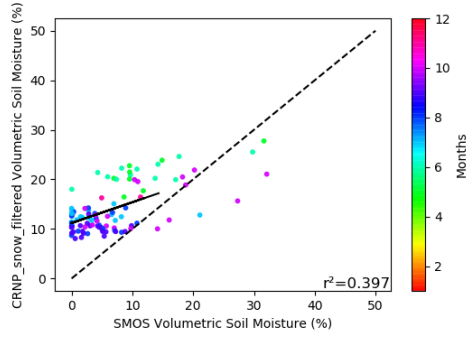
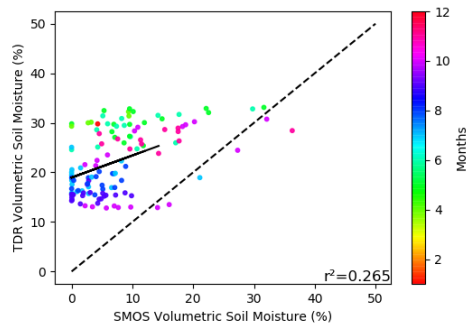


Figure A.2: AMSR (descending) soil moisture vs. a) CRNP and b) TDR

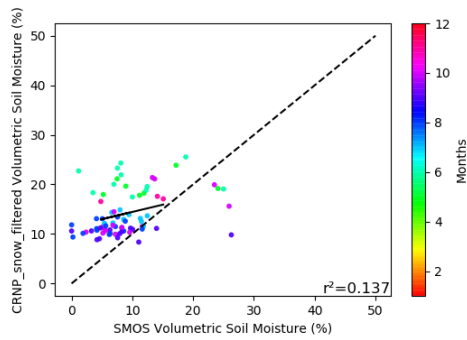


(a)

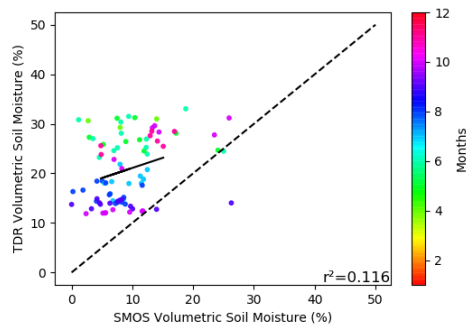


(b)

Figure A.3: SMOS (ascending) soil moisture vs. a) CRNP and b) TDR



(a)



(b)

Figure A.4: SMOS (descending) soil moisture vs. a) CRNP and b) TDR

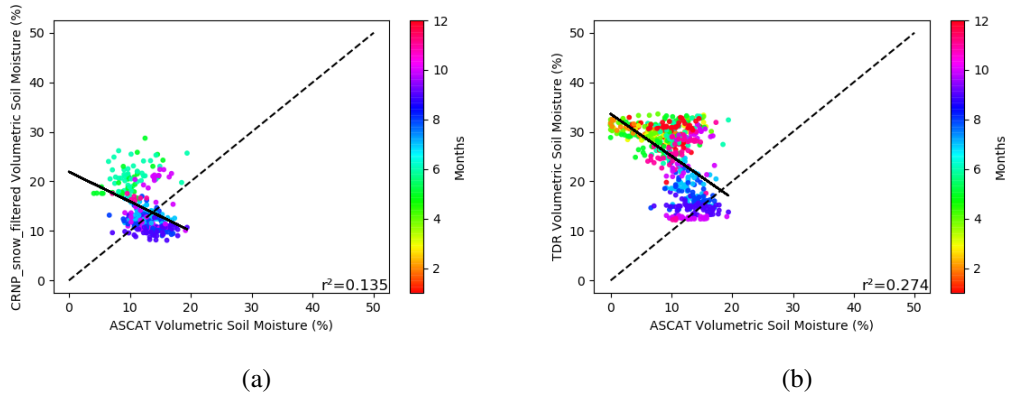


Figure A.5: ASCAT soil moisture vs. a) CRNP and b) TDR

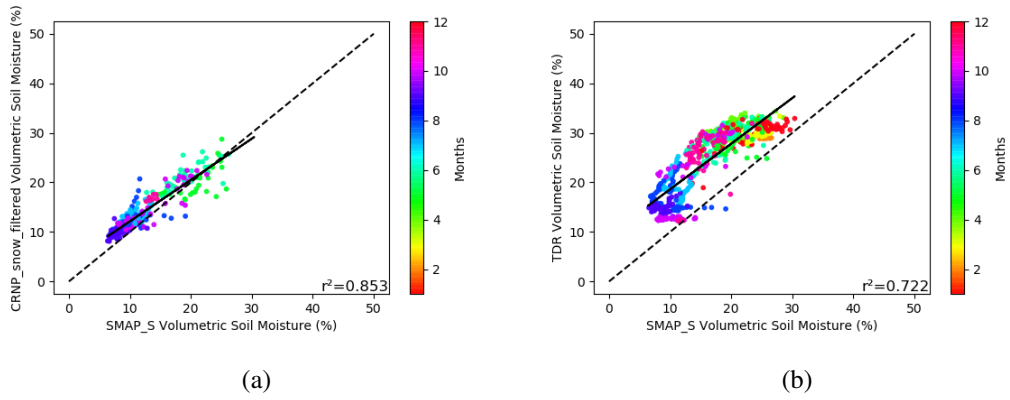
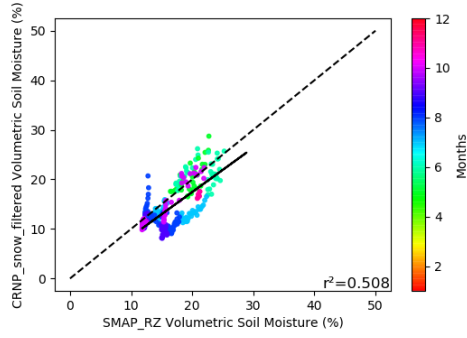
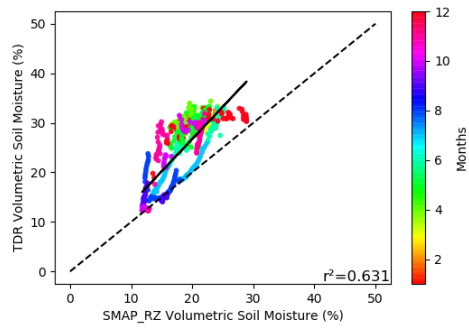


Figure A.6: SMAP surface soil moisture vs. a) CRNP and b) TDR

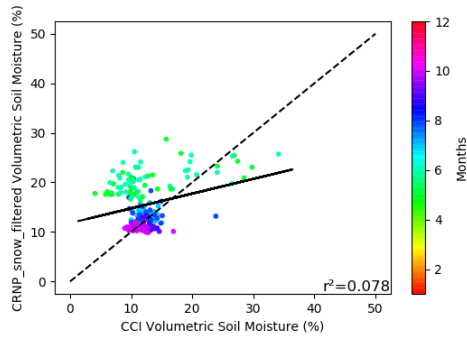


(a)

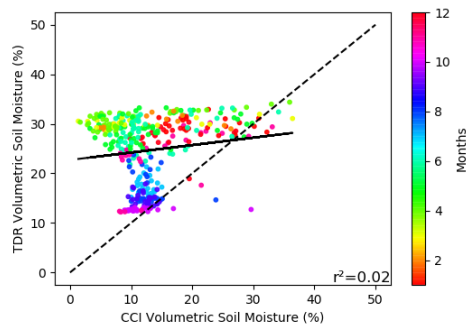


(b)

Figure A.7: SMAP rootzone soil moisture vs. a) CRNP and b) TDR



(a)



(b)

Figure A.8: CCI soil moisture vs. a) CRNP and b) TDR

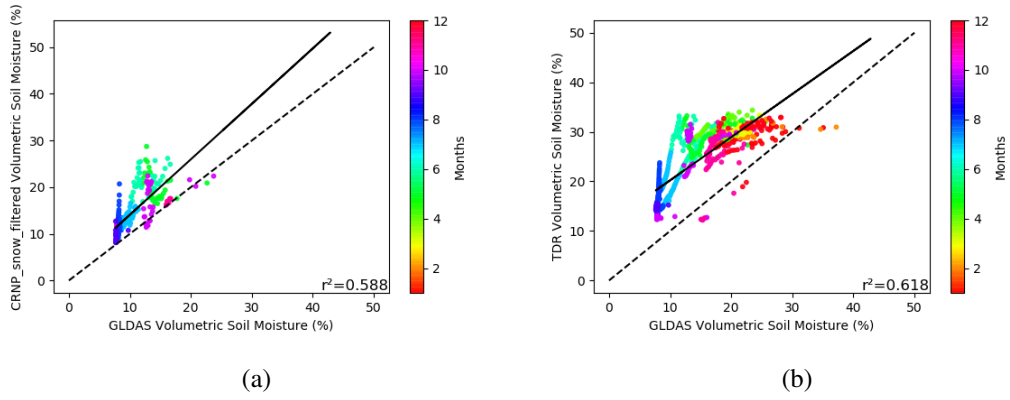


Figure A.9: GLDAS soil moisture vs. a) CRNP and b) TDR

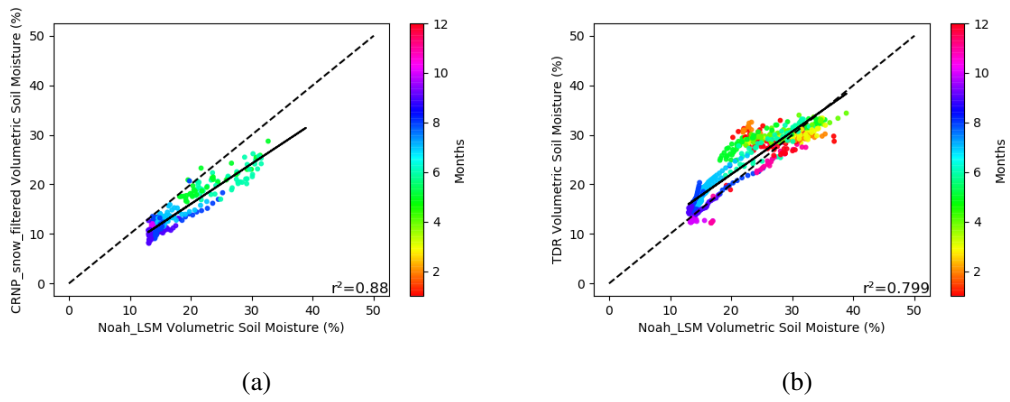
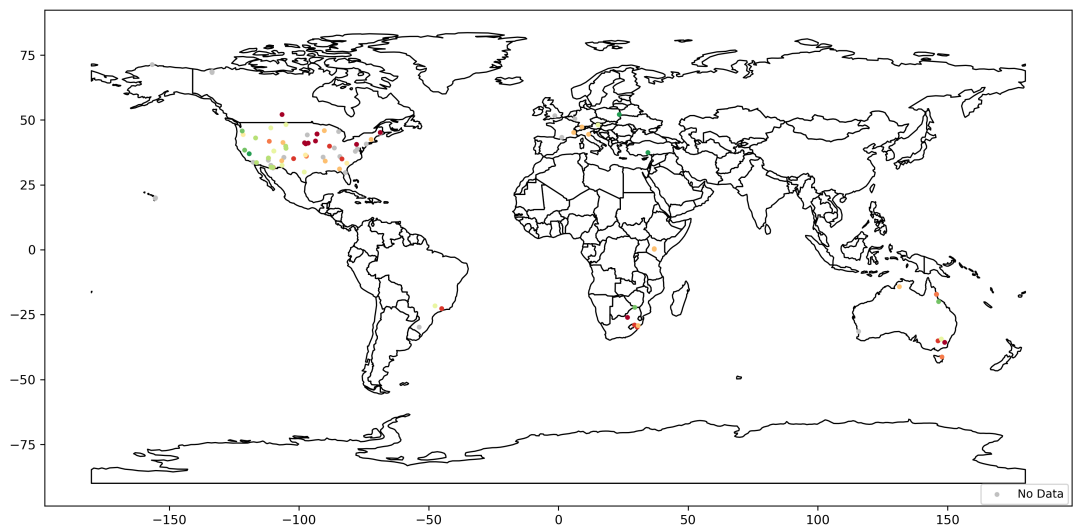


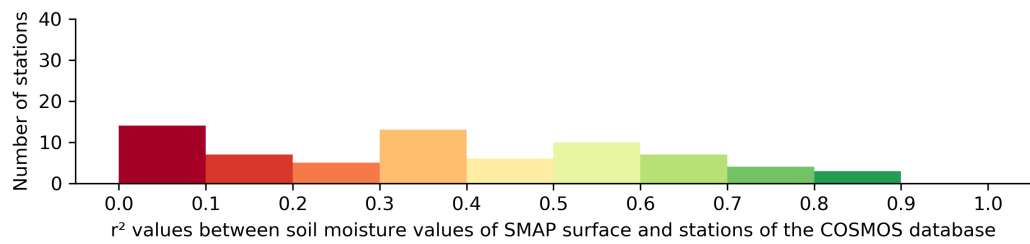
Figure A.10: NOAH LSM soil moisture vs. a) CRNP and b) TDR

APPENDIX B

MAPS OF STATISTICAL MEASURES FOR SATELLITE PRODUCTS VS. COSMOS DATABASE

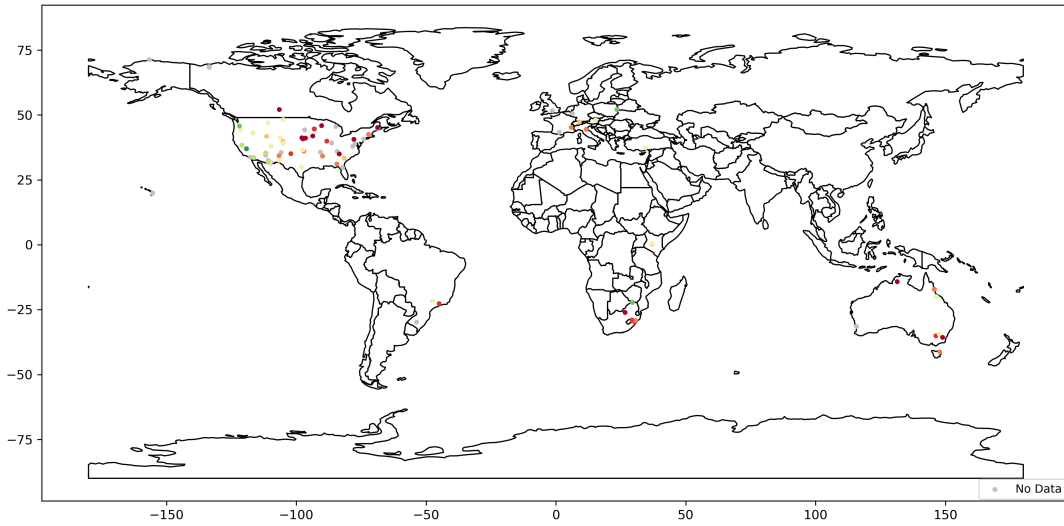


(a)

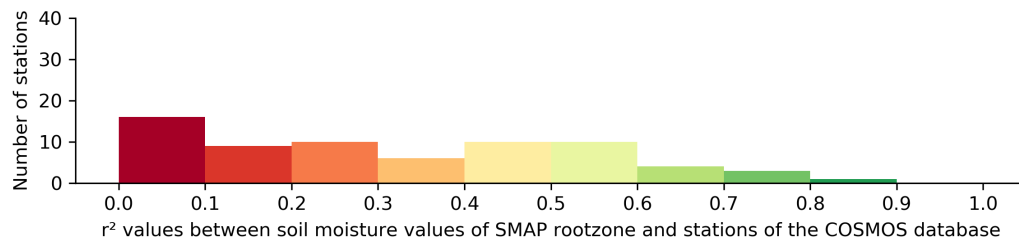


(b)

Figure B.1: a) r^2 values between SMAP surface product and COSMOS stations shown on the world map b) Histogram of r^2 values between SMAP surface product and COSMOS stations

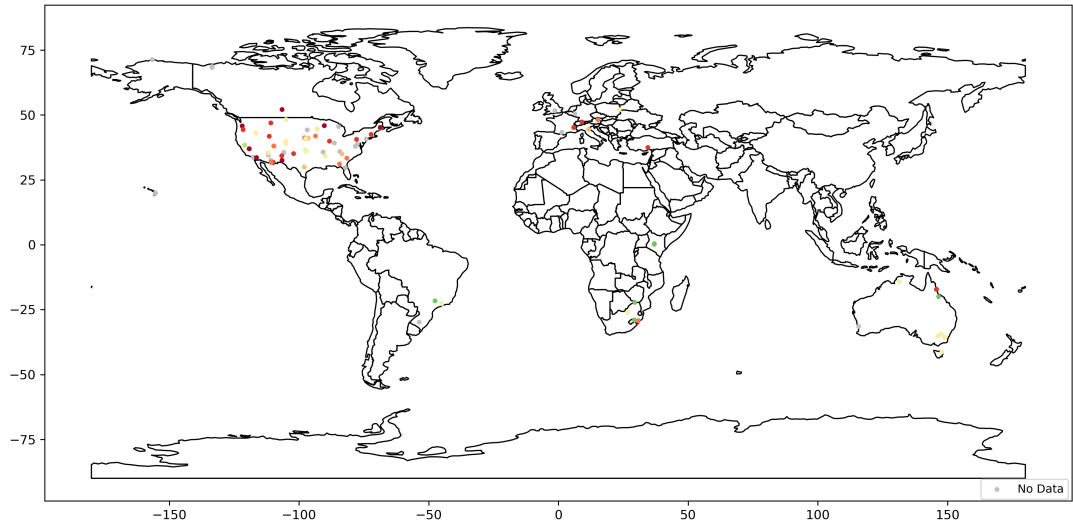


(a)

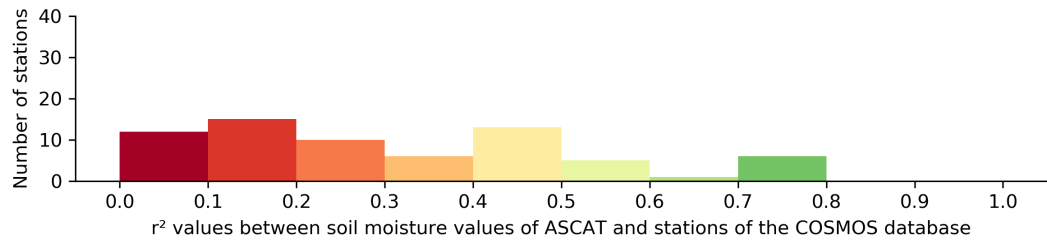


(b)

Figure B.2: a) r^2 values between SMAP rootzone product and COSMOS stations shown on the world map b) Histogram of r^2 values between SMAP rootzone product and COSMOS stations

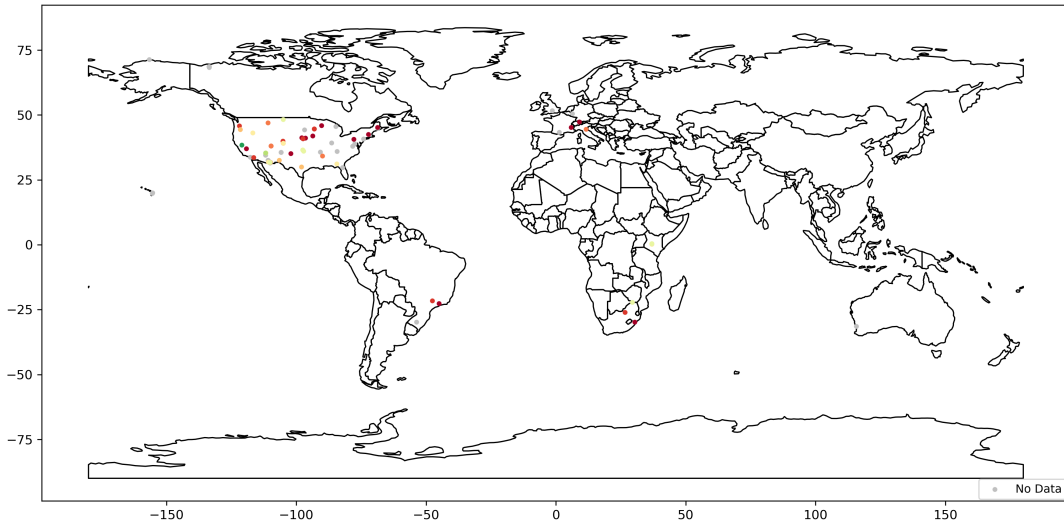


(a)

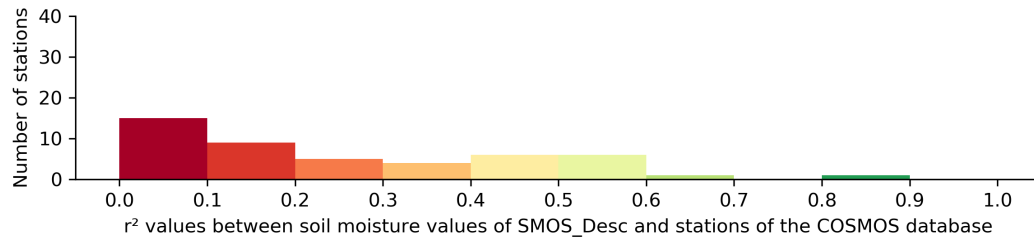


(b)

Figure B.3: a) r^2 values between ASCAT and COSMOS stations shown on the world map b) Histogram of r^2 values between ASCAT and COSMOS stations

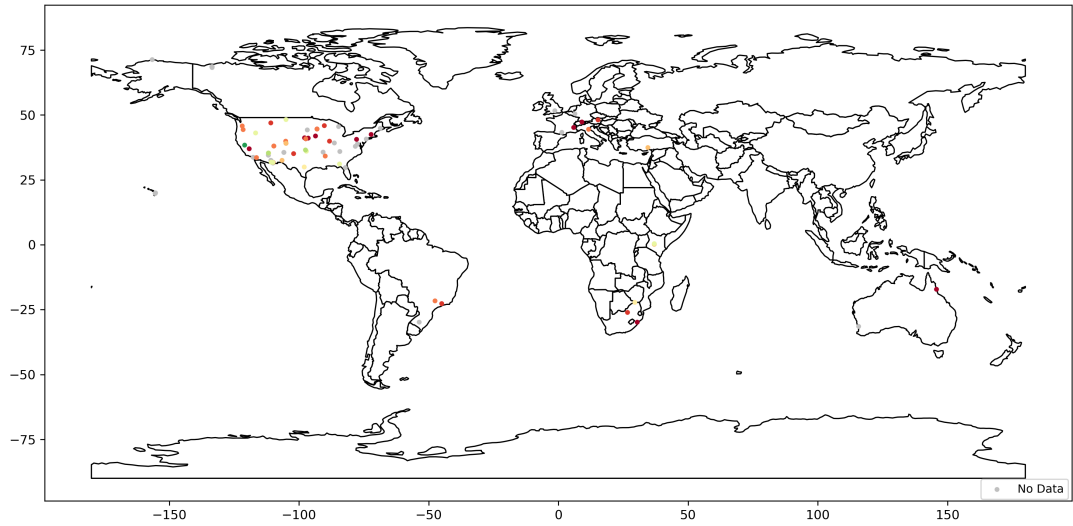


(a)

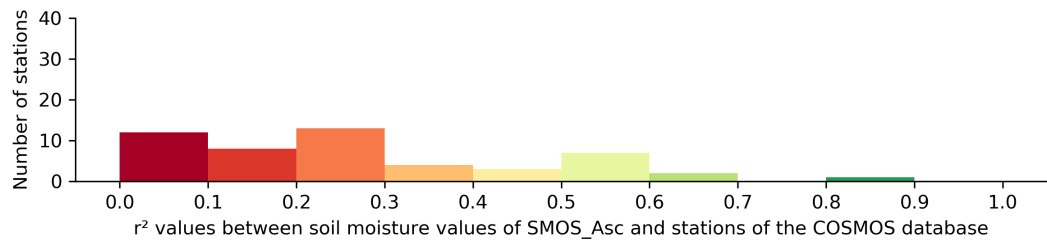


(b)

Figure B.4: a) r^2 values between SMOS descending node product and COSMOS stations shown on the world map b) Histogram of r^2 values between SMOS descending node product and COSMOS stations

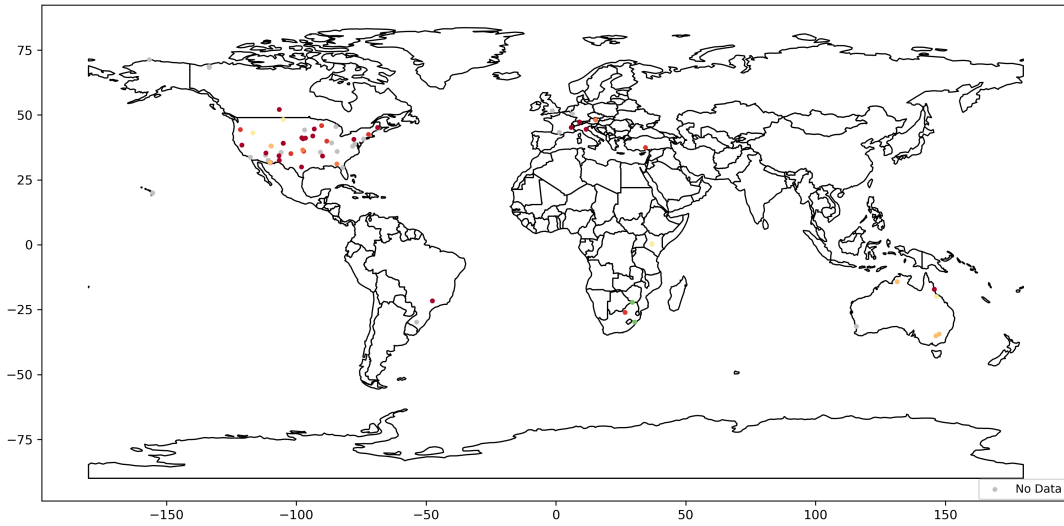


(a)

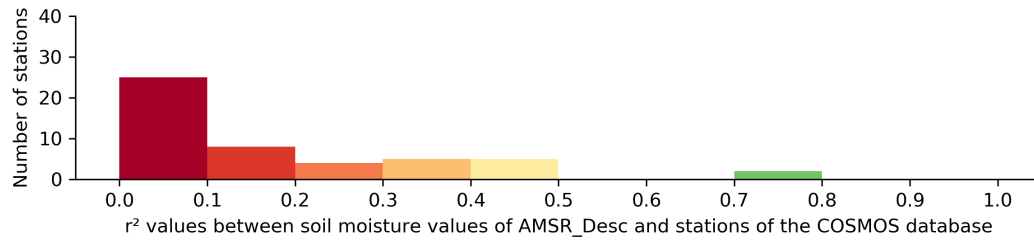


(b)

Figure B.5: a) r^2 values between SMOS ascending node product and COSMOS stations shown on the world map b) Histogram of r^2 values between SMOS ascending node product and COSMOS stations

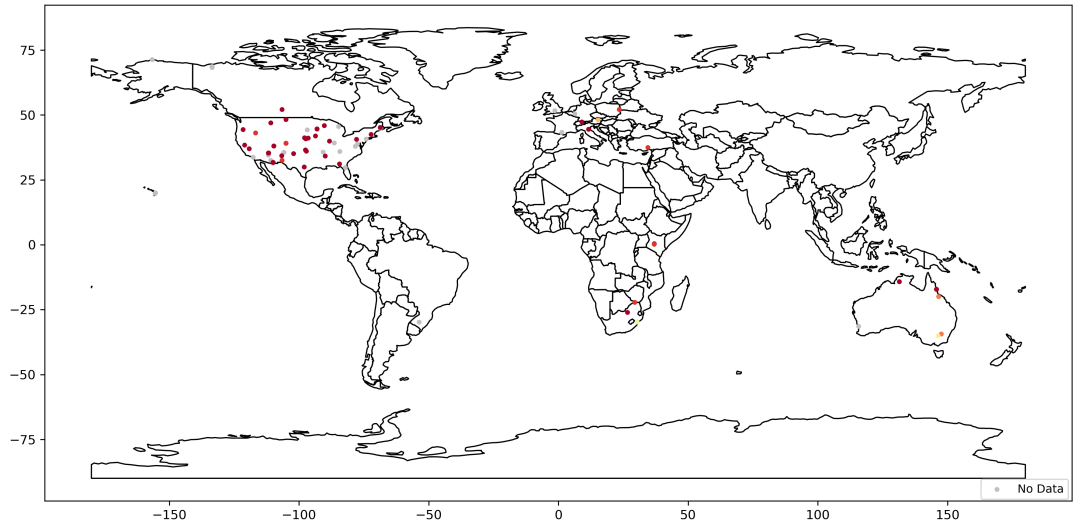


(a)

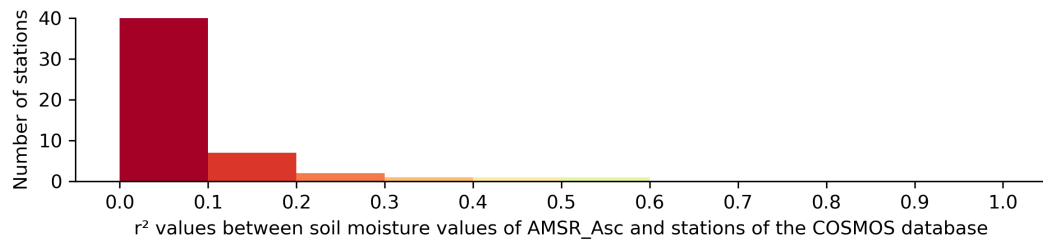


(b)

Figure B.6: a) r^2 values between AMSR descending node product and COSMOS stations shown on the world map b) Histogram of r^2 values between AMSR descending node product and COSMOS stations

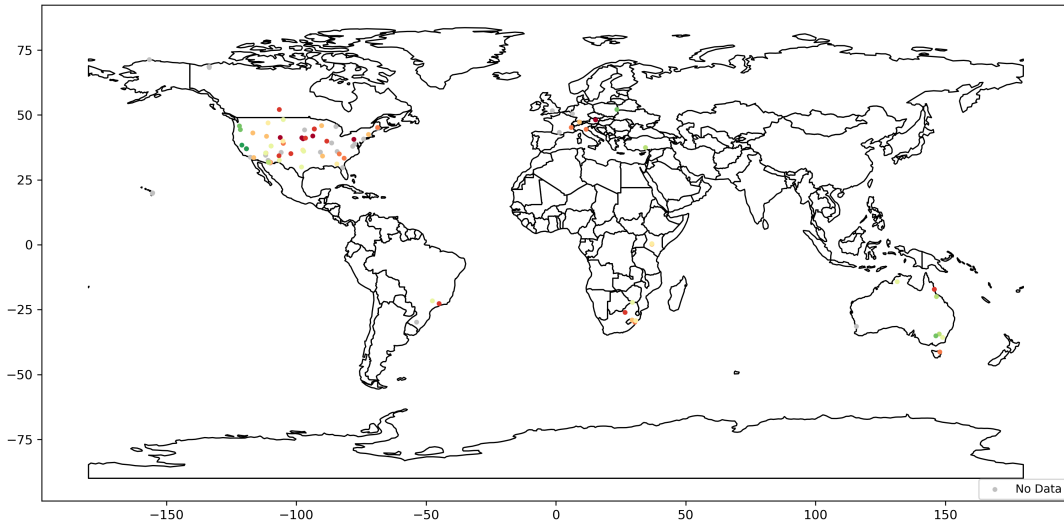


(a)

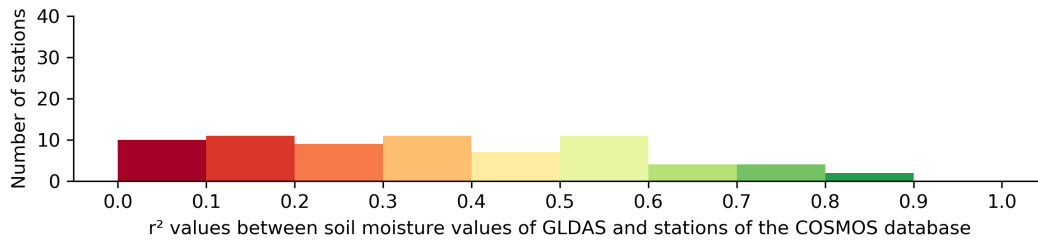


(b)

Figure B.7: a) r^2 values between AMSR ascending node product and COSMOS stations shown on the world map b) Histogram of r^2 values between AMSR ascending node product and COSMOS stations

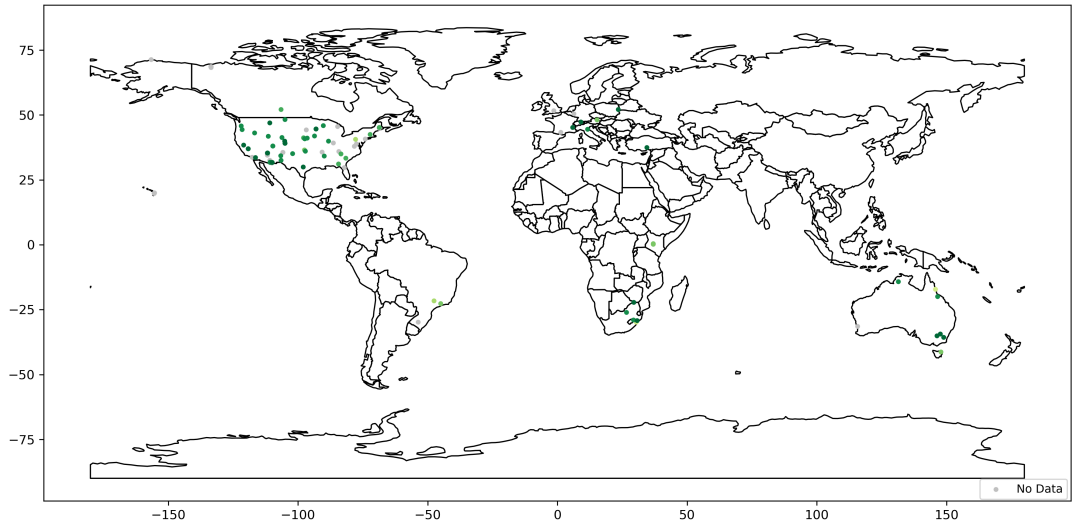


(a)

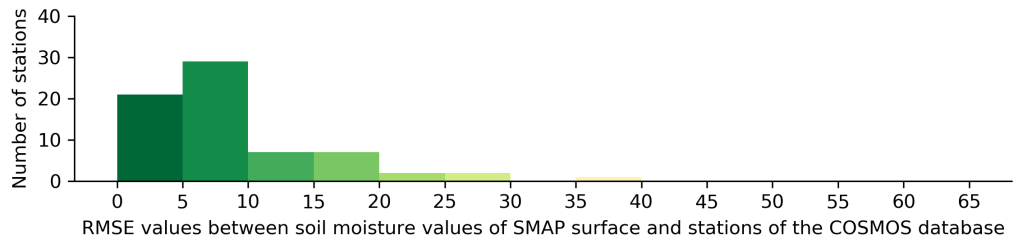


(b)

Figure B.8: a) r^2 values between GLDAS and COSMOS stations shown on the world map b) Histogram of r^2 values between GLDAS and COSMOS stations

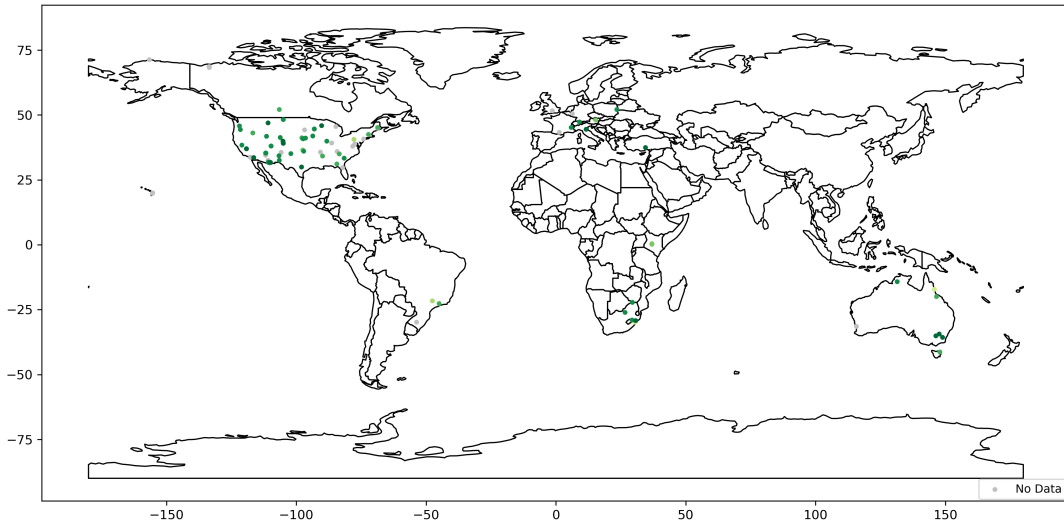


(a)

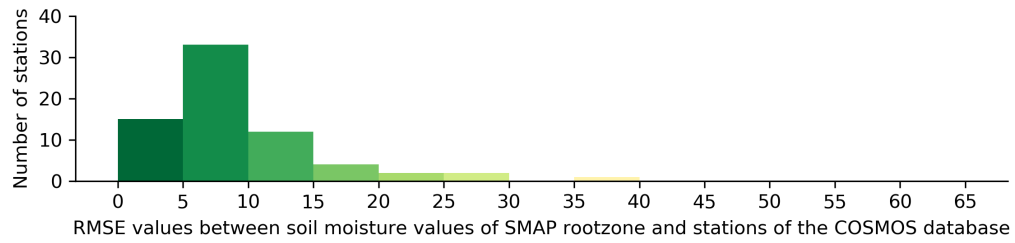


(b)

Figure B.9: a) RMSE values between SMAP surface product and COSMOS stations shown on the world map b) Histogram of RMSE values between SMAP surface product and COSMOS stations

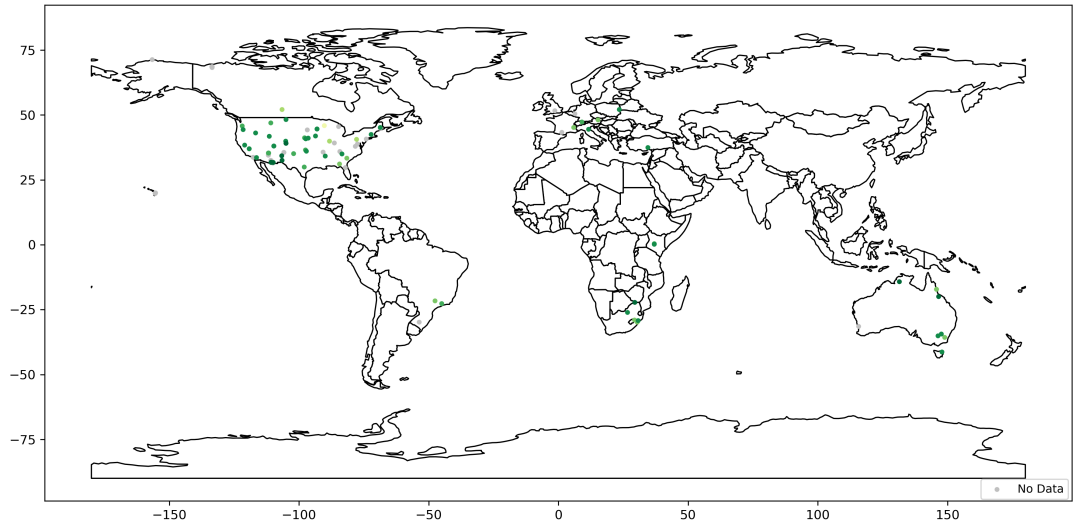


(a)

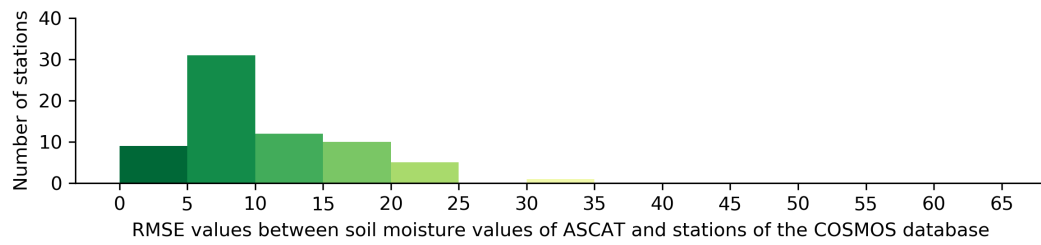


(b)

Figure B.10: a) RMSE values between SMAP rootzone product and COSMOS stations shown on the world map b) Histogram of RMSE values between SMAP rootzone product and COSMOS stations

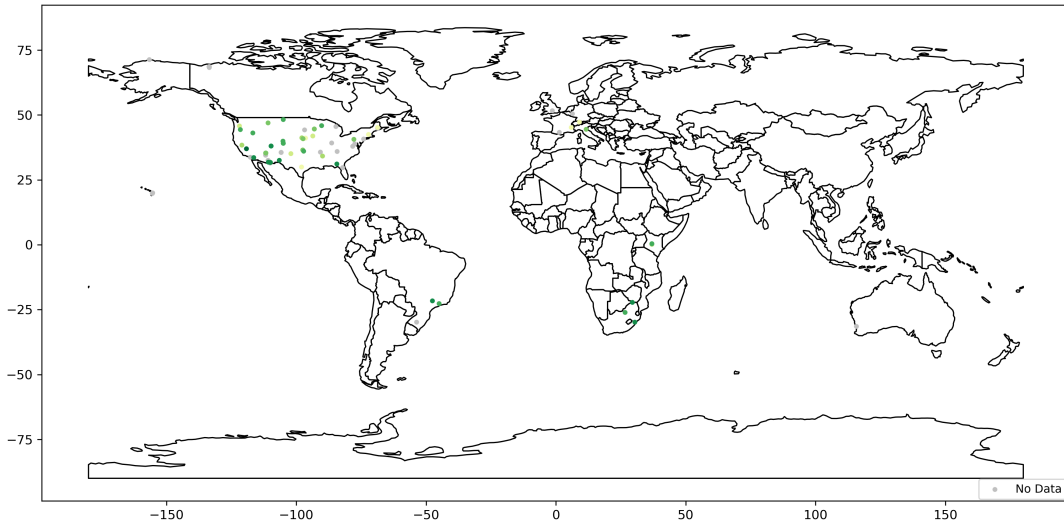


(a)

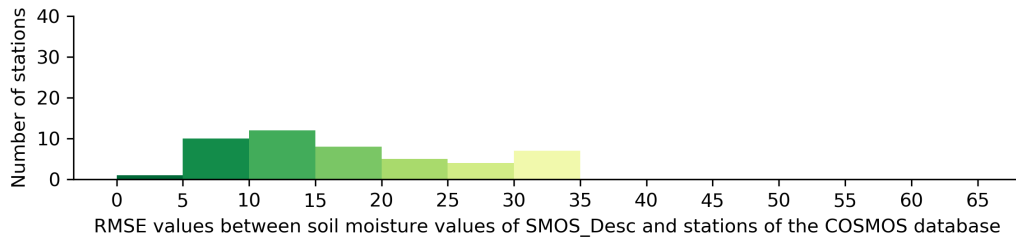


(b)

Figure B.11: a) RMSE values between ASCAT and COSMOS stations shown on the world map b) Histogram of RMSE values between ASCAT and COSMOS stations

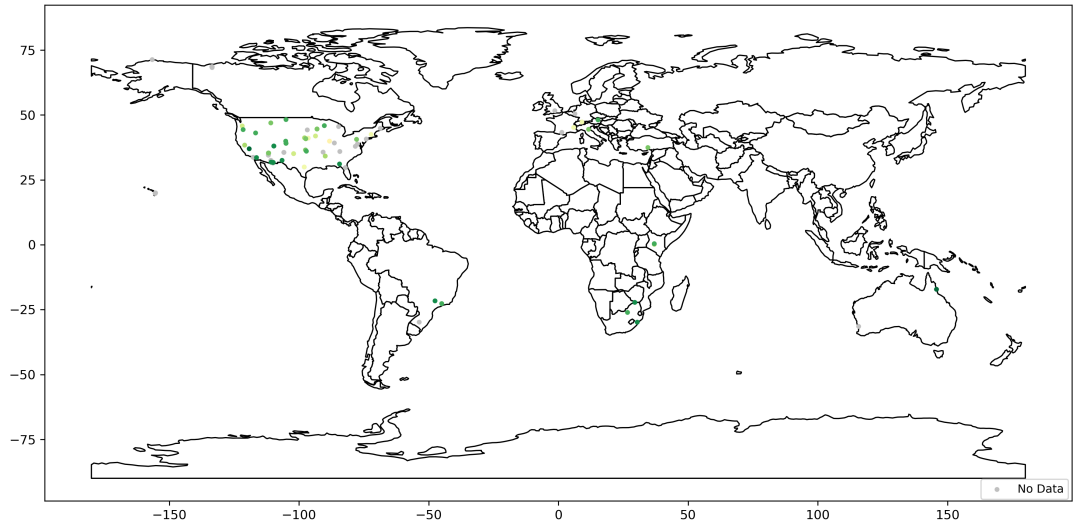


(a)

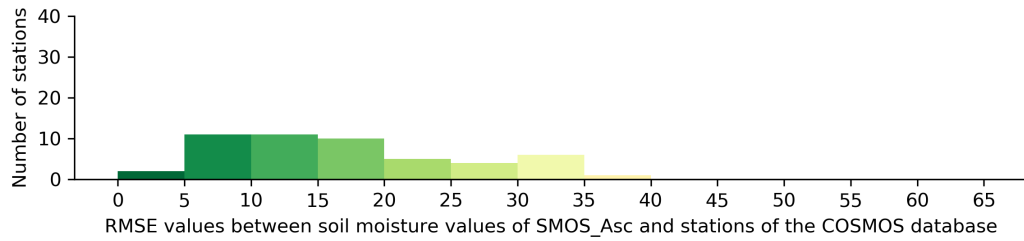


(b)

Figure B.12: a) RMSE values between SMOS descending node product and COSMOS stations shown on the world map b) Histogram of RMSE values between SMOS descending node product and COSMOS stations

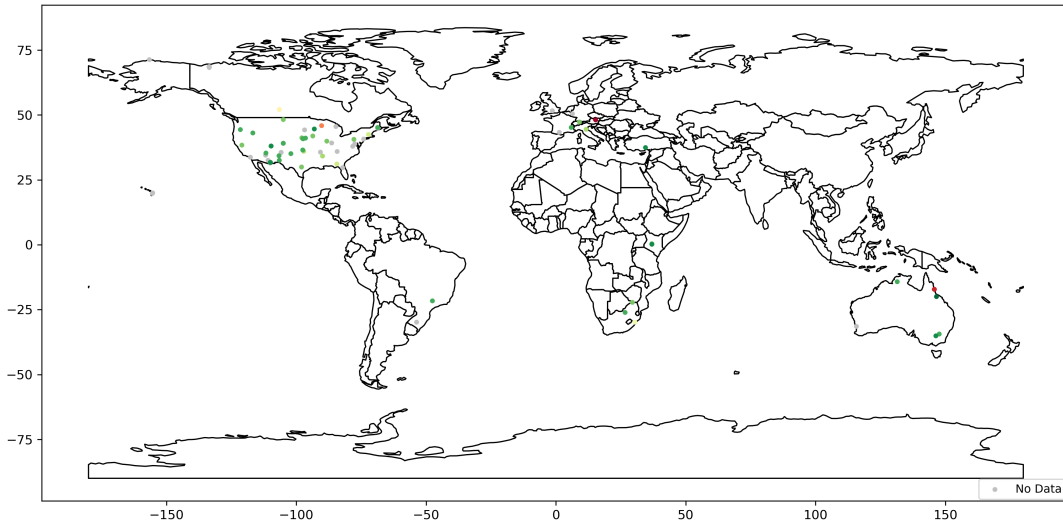


(a)

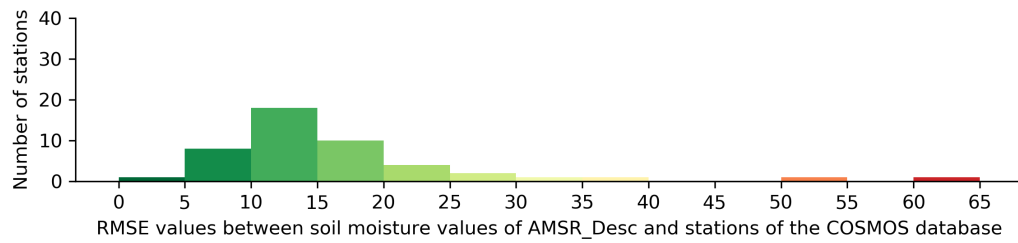


(b)

Figure B.13: a) RMSE values between SMOS ascending node product and COSMOS stations shown on the world map b) Histogram of RMSE values between SMOS ascending node product and COSMOS stations

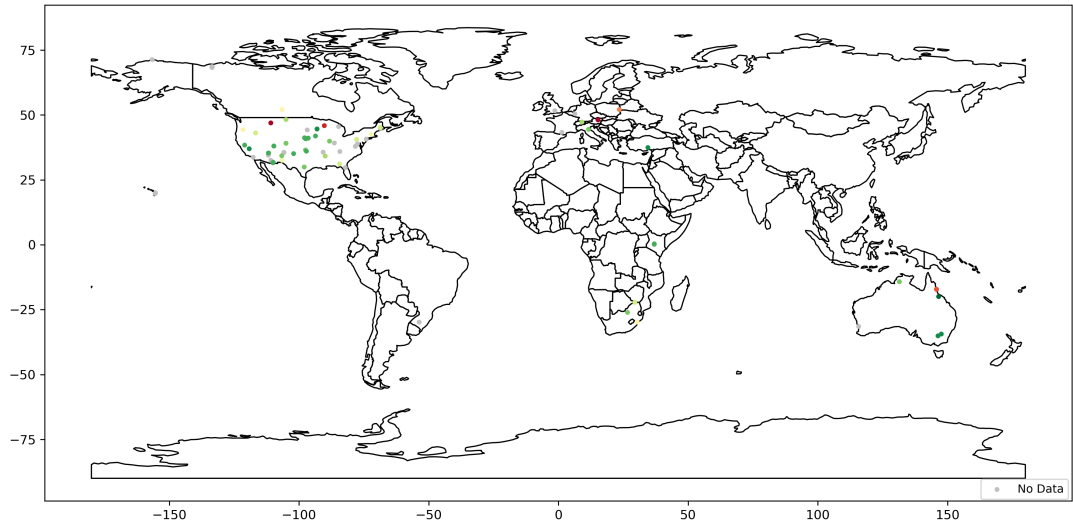


(a)

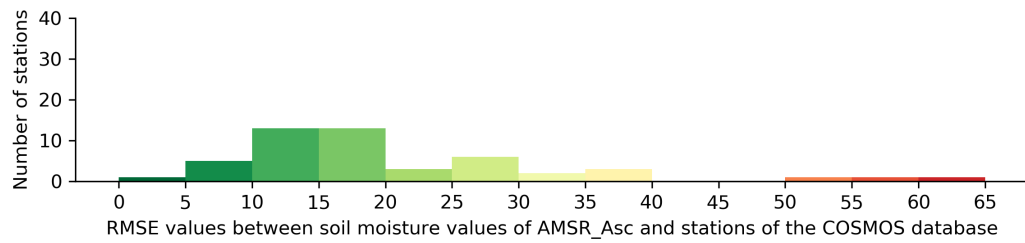


(b)

Figure B.14: a) RMSE values between AMSR descending node product and COSMOS stations shown on the world map b) Histogram of RMSE values between AMSR descending node product and COSMOS stations

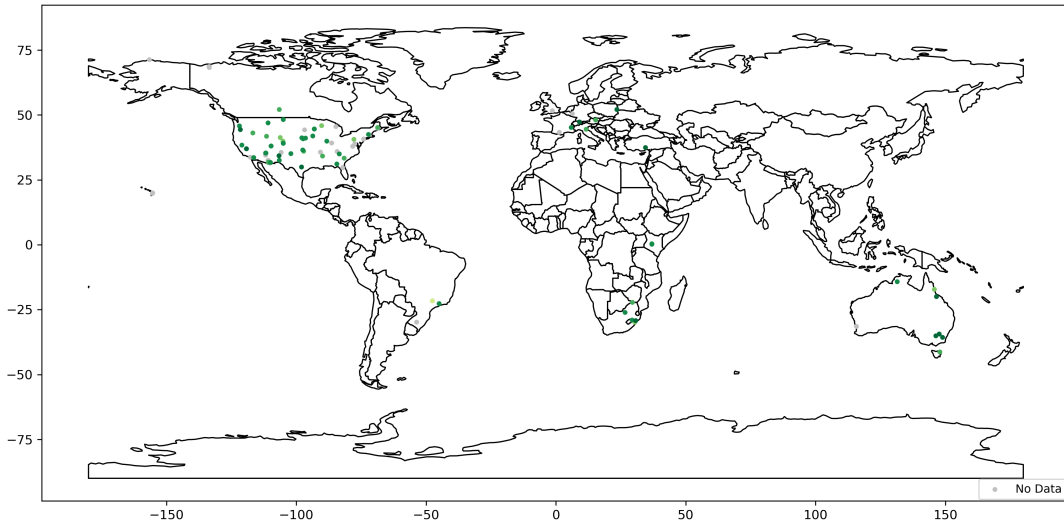


(a)

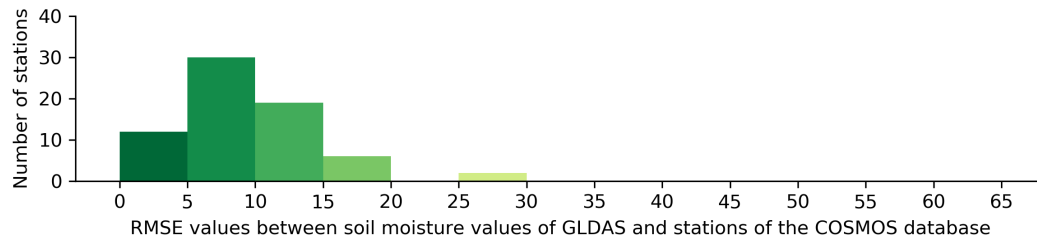


(b)

Figure B.15: a) RMSE values between AMSR ascending node product and COSMOS stations shown on the world map b) Histogram of RMSE values between AMSR ascending node product and COSMOS stations

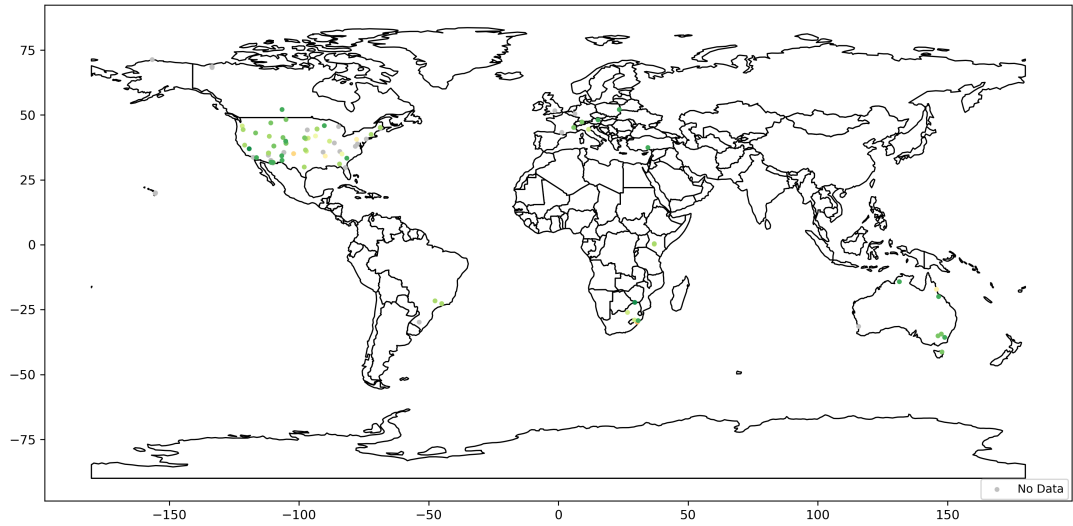


(a)

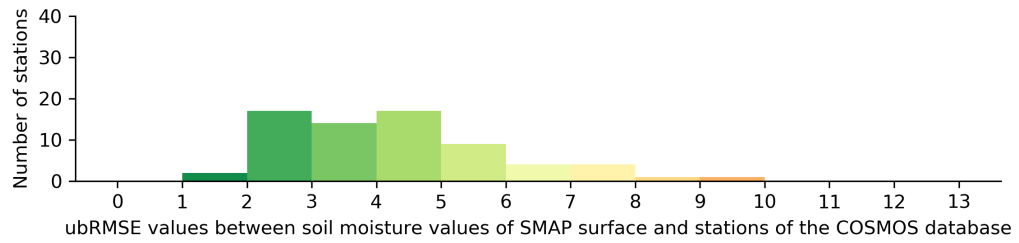


(b)

Figure B.16: a) RMSE values between GLDAS and COSMOS stations shown on the world map b) Histogram of r^2 values between GLDAS and COSMOS stations

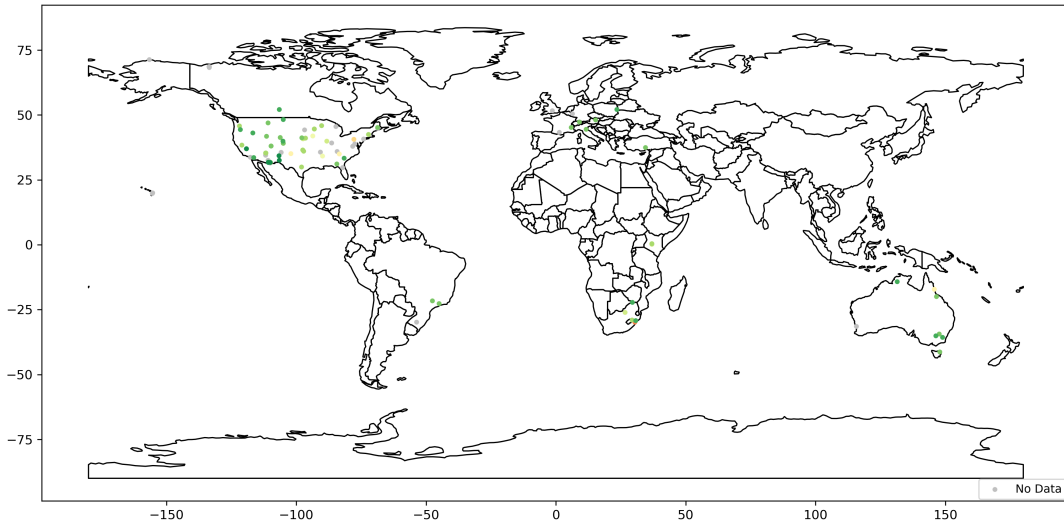


(a)

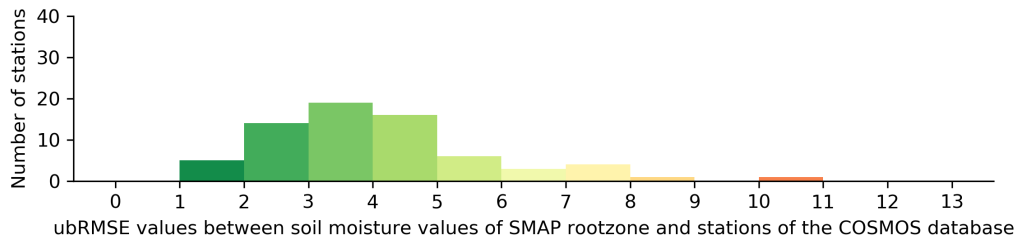


(b)

Figure B.17: a) ubRMSE values between SMAP surface product and COSMOS stations shown on the world map b) Histogram of ubRMSE values between SMAP surface product and COSMOS stations

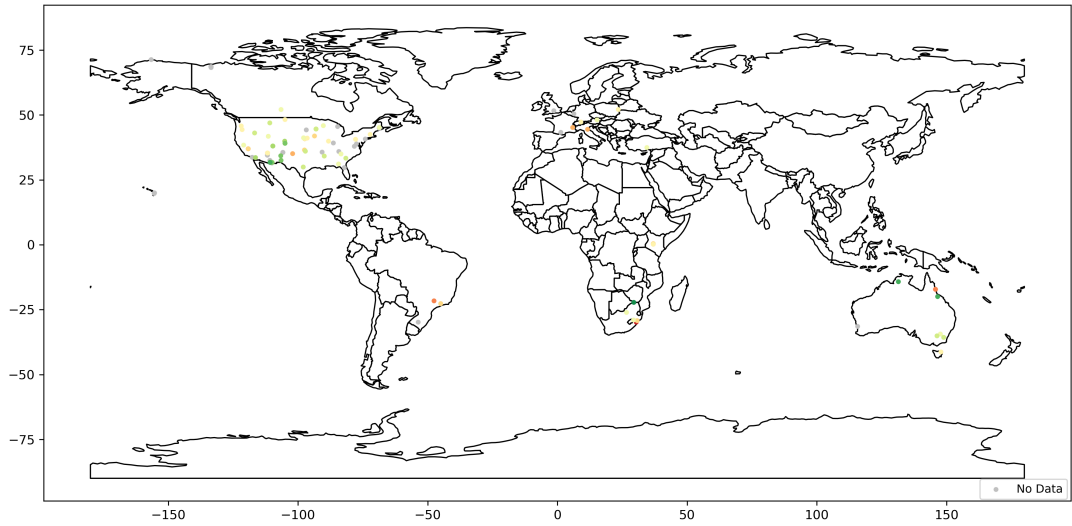


(a)

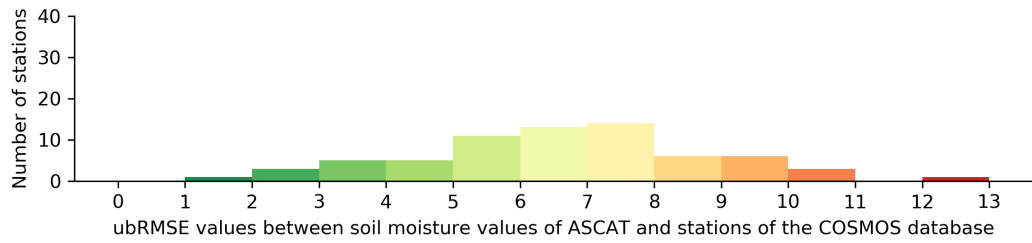


(b)

Figure B.18: a) ubRMSE values between SMAP rootzone product and COSMOS stations shown on the world map b) Histogram of ubRMSE values between SMAP rootzone product and COSMOS stations

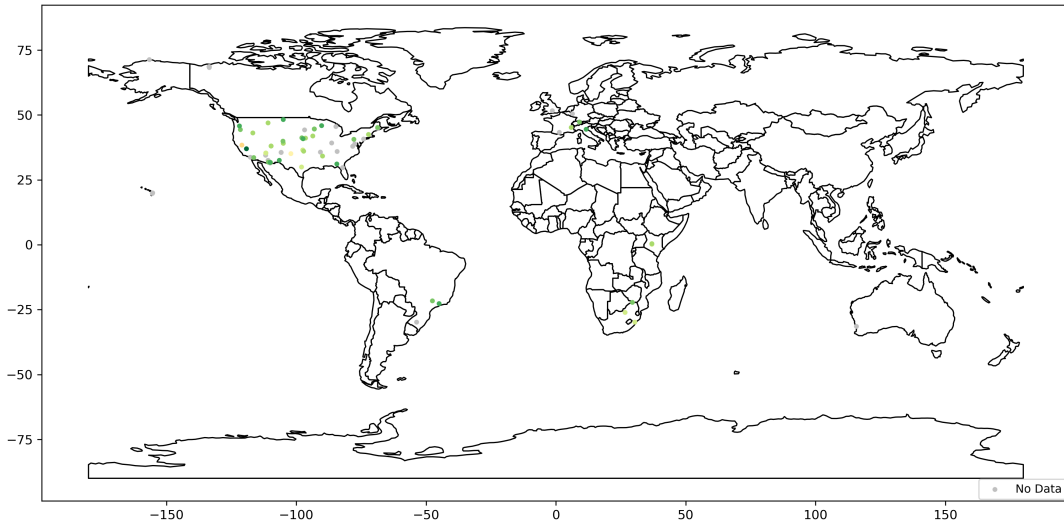


(a)



(b)

Figure B.19: a) ubRMSE values between ASCAT and COSMOS stations shown on the world map b) Histogram of ubRMSE values between ASCAT and COSMOS stations

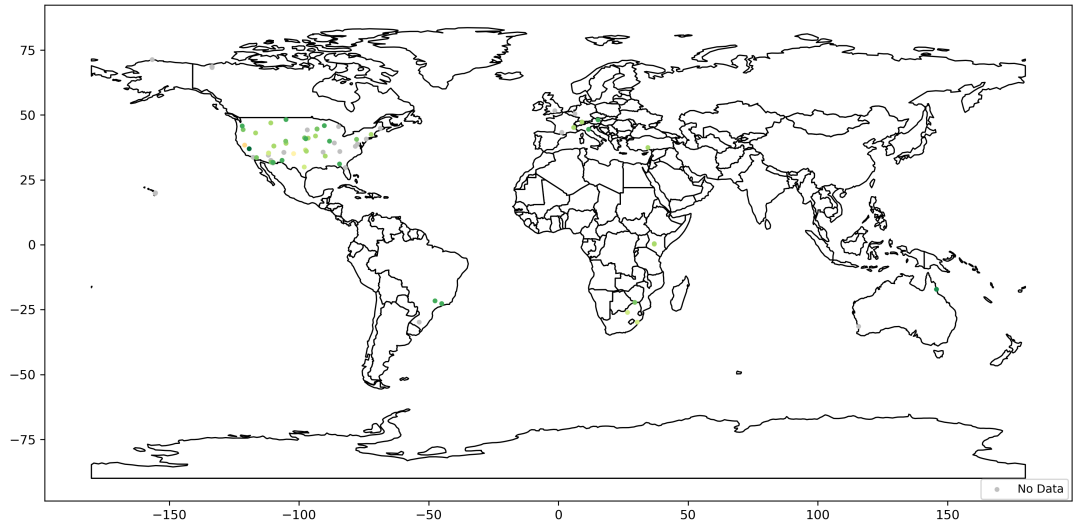


(a)

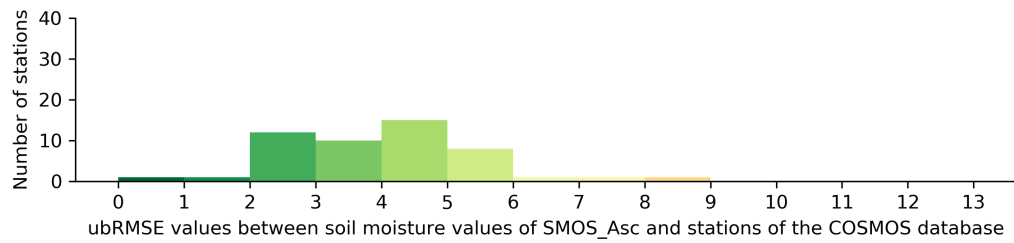


(b)

Figure B.20: a) ubRMSE values between SMOS descending node product and COSMOS stations shown on the world map b) Histogram of ubRMSE values between SMOS descending node product and COSMOS stations

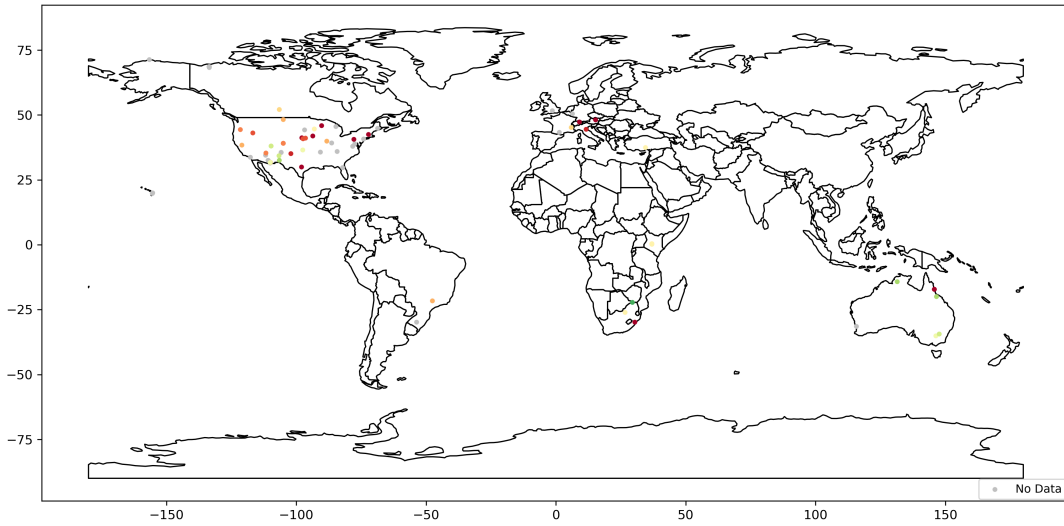


(a)

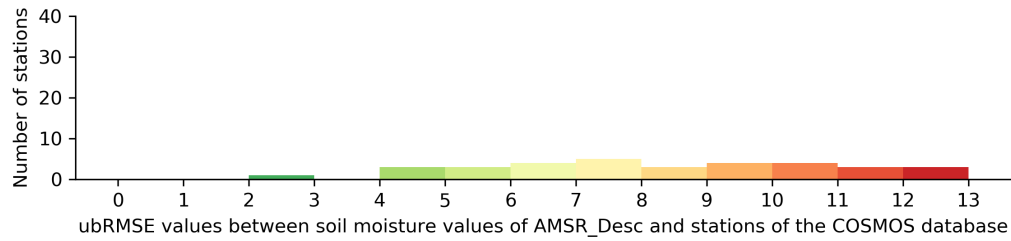


(b)

Figure B.21: a) ubRMSE values between SMOS ascending node product and COSMOS stations shown on the world map b) Histogram of ubRMSE values between SMOS ascending node product and COSMOS stations

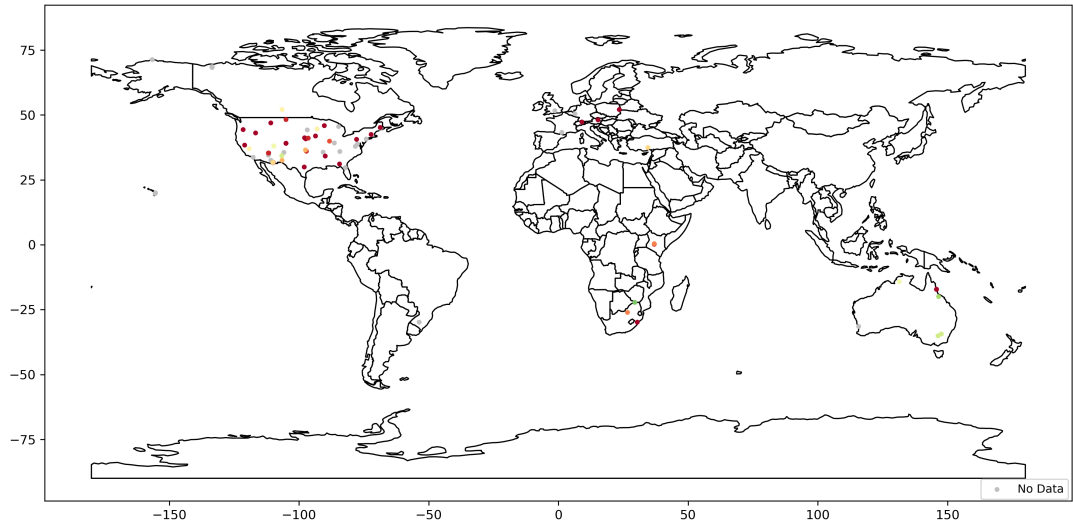


(a)

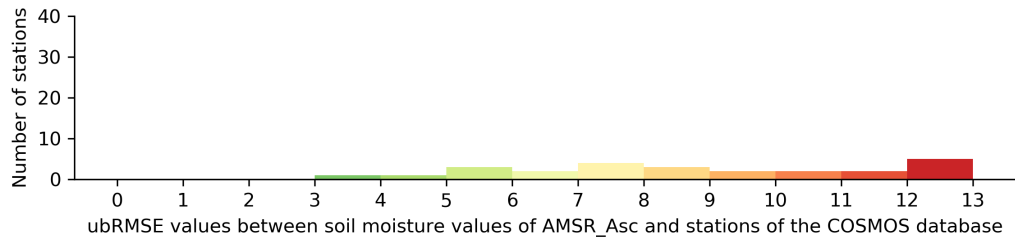


(b)

Figure B.22: a) ubRMSE values between AMSR descending node product and COSMOS stations shown on the world map b) Histogram of ubRMSE values between AMSR descending node product and COSMOS stations

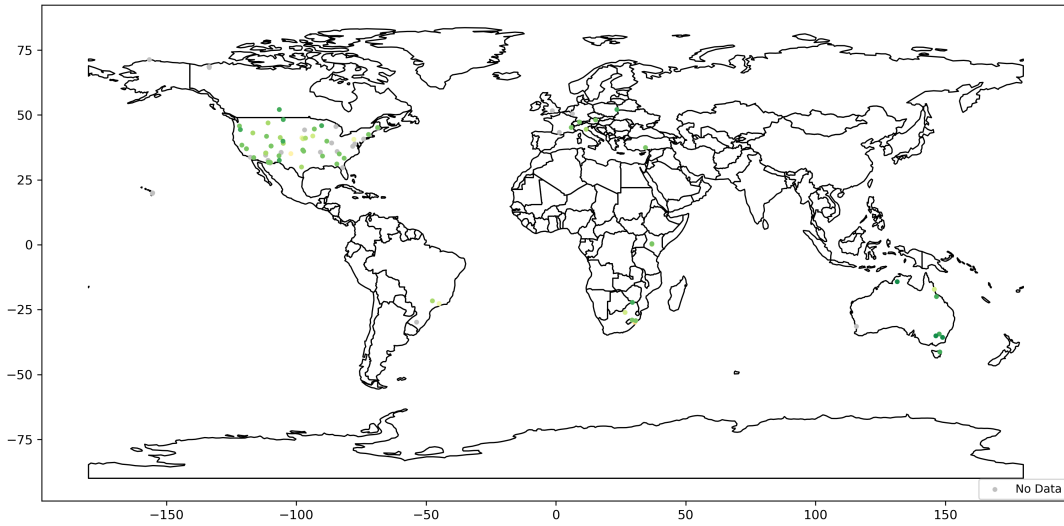


(a)

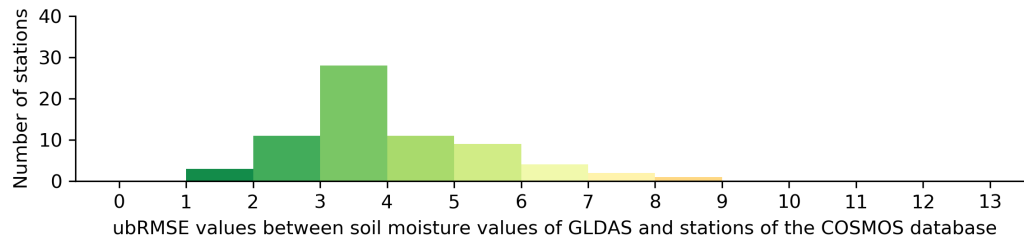


(b)

Figure B.23: a) ubRMSE values between AMSR ascending node product and COSMOS stations shown on the world map b) Histogram of ubRMSE values between AMSR ascending node product and COSMOS stations



(a)



(b)

Figure B.24: a) ubRMSE values between GLDAS and COSMOS stations shown on the world map b) Histogram of ubRMSE values between GLDAS and COSMOS stations

APPENDIX C

EVAPORATION AND SOIL MOISTURE CORRELATION MAPS FOR GLDAS

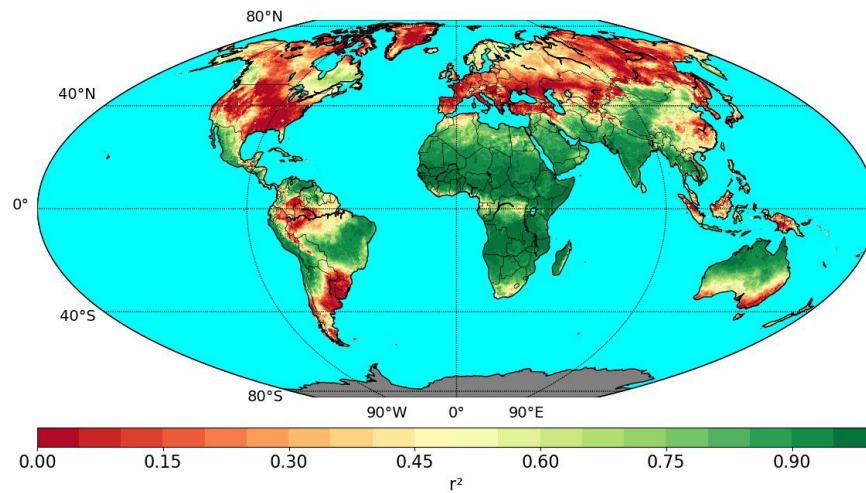


Figure C.1: r^2 values of the comparison between monthly averages of GLDAS Noah LSM soil moisture and evapotranspiration outputs

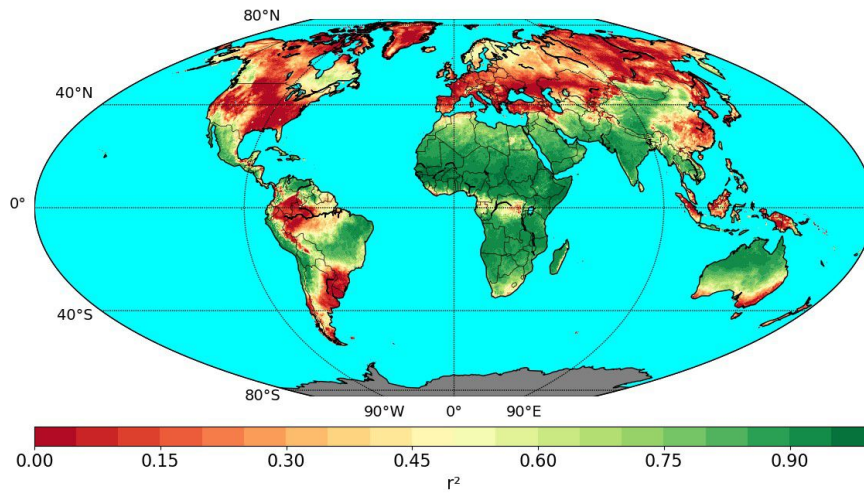


Figure C.2: r^2 values of the comparison between weekly averages of GLDAS Noah LSM soil moisture and evapotranspiration outputs

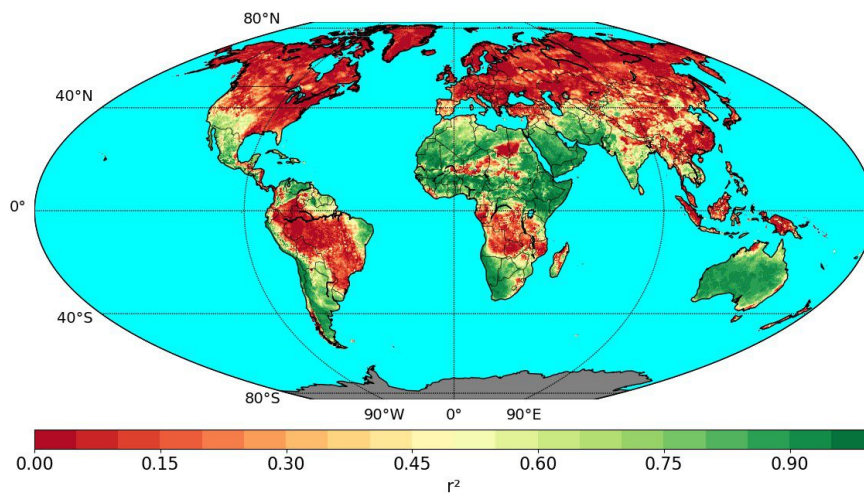


Figure C.3: r^2 values of the comparison between GLDAS Noah LSM soil moisture and evapotranspiration outputs for January

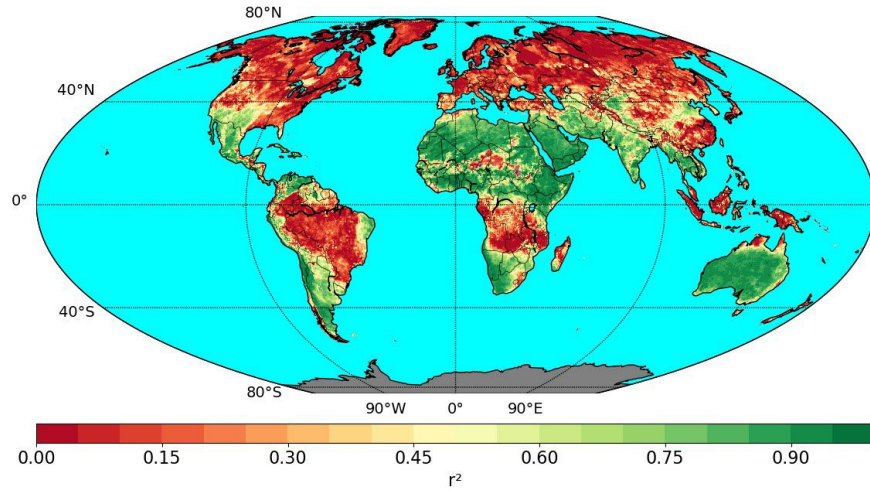


Figure C.4: r^2 values of the comparison between GLDAS Noah LSM soil moisture and evapotranspiration outputs for February

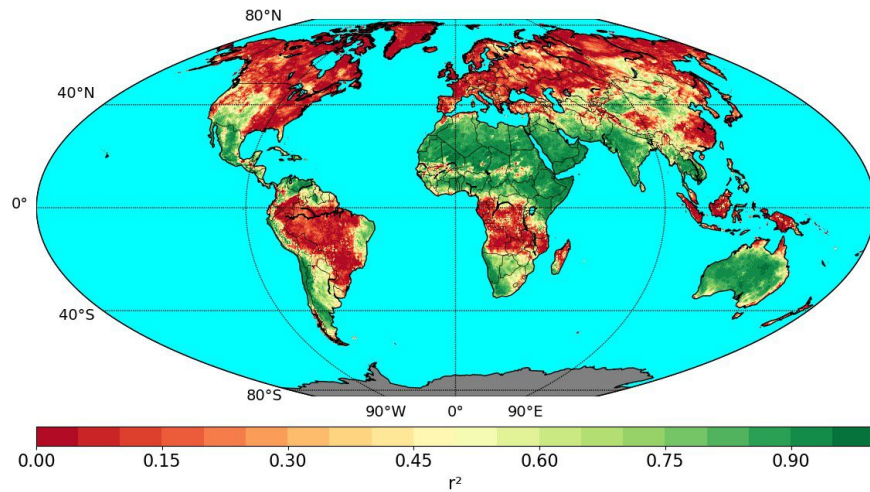


Figure C.5: r^2 values of the comparison between GLDAS Noah LSM soil moisture and evapotranspiration outputs for March

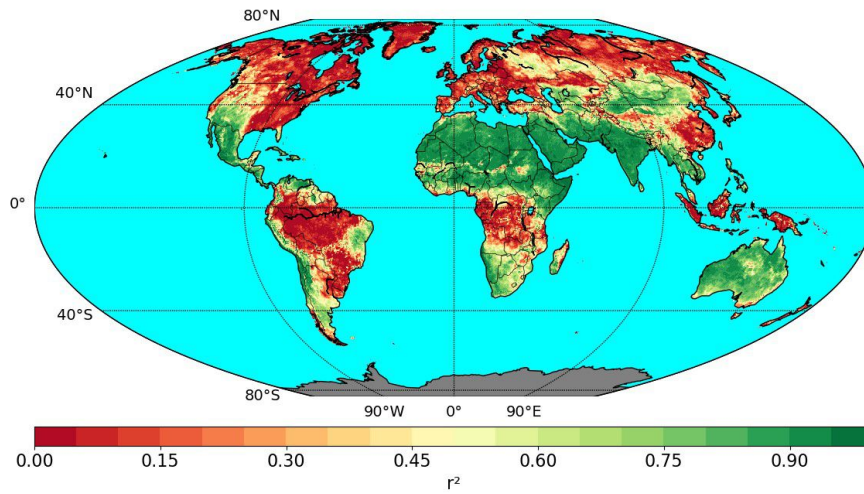


Figure C.6: r^2 values of the comparison between GLDAS Noah LSM soil moisture and evapotranspiration outputs for April

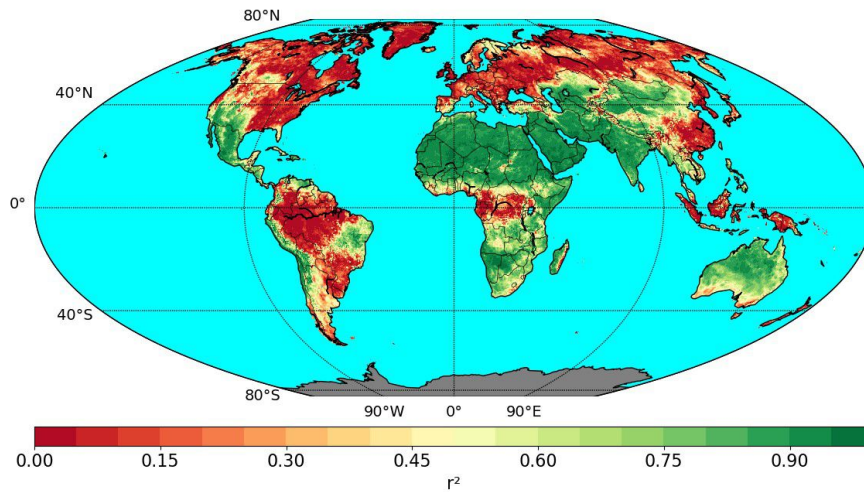


Figure C.7: r^2 values of the comparison between GLDAS Noah LSM soil moisture and evapotranspiration outputs for May

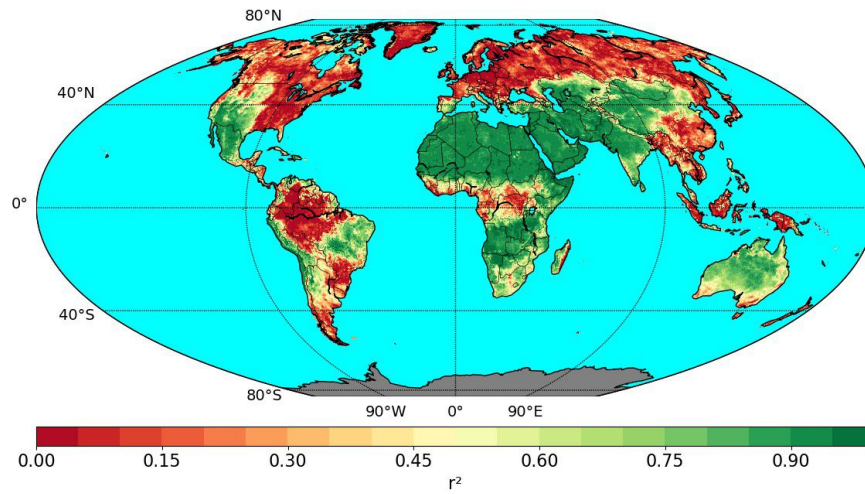


Figure C.8: r^2 values of the comparison between GLDAS Noah LSM soil moisture and evapotranspiration outputs for June

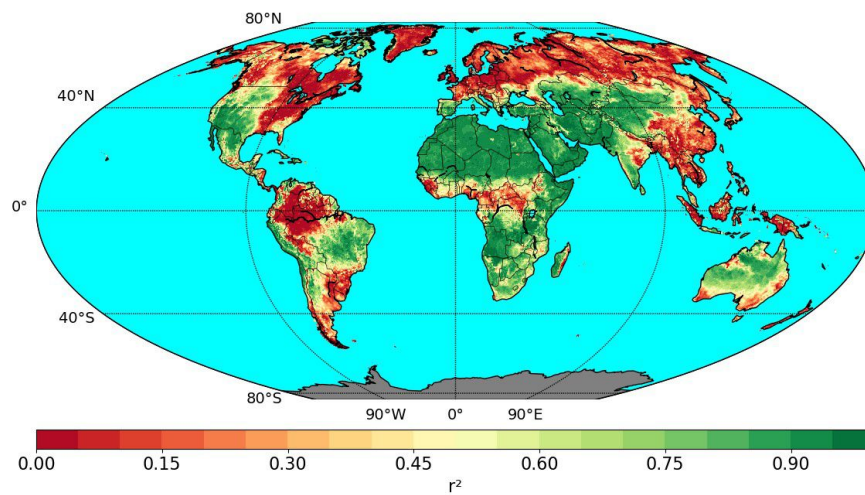


Figure C.9: r^2 values of the comparison between GLDAS Noah LSM soil moisture and evapotranspiration outputs for July

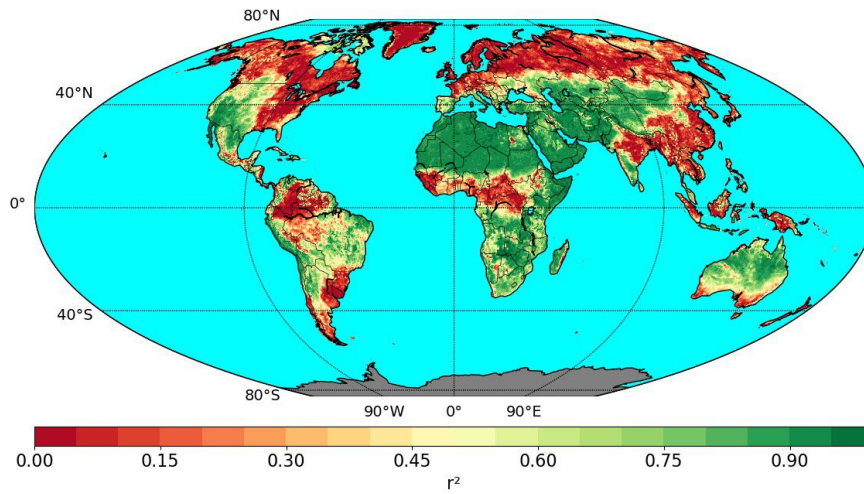


Figure C.10: r^2 values of the comparison between GLDAS Noah LSM soil moisture and evapotranspiration outputs for August

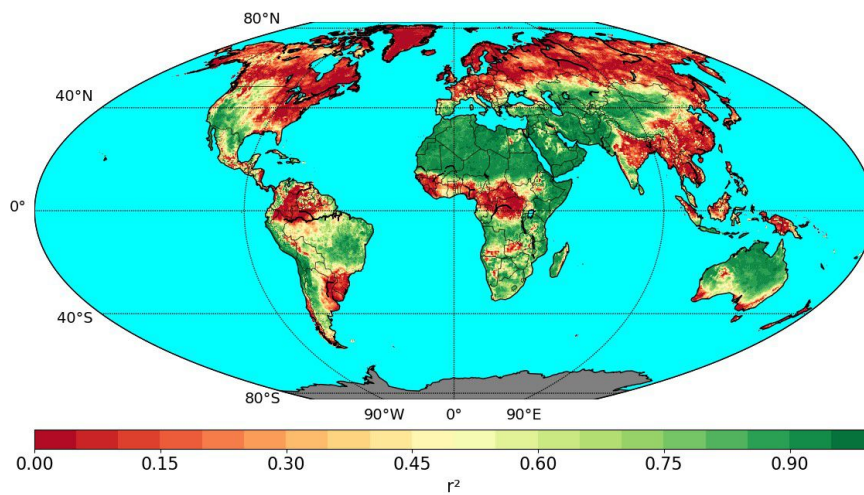


Figure C.11: r^2 values of the comparison between GLDAS Noah LSM soil moisture and evapotranspiration outputs for September

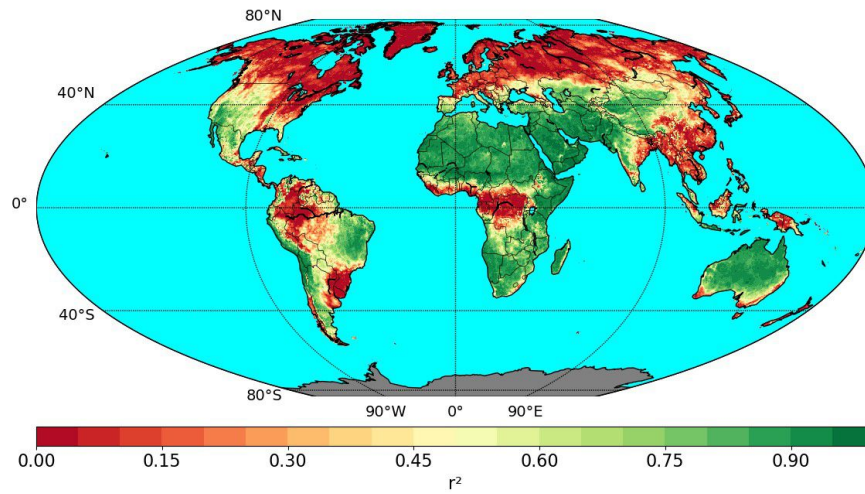


Figure C.12: r^2 values of the comparison between GLDAS Noah LSM soil moisture and evapotranspiration outputs for October

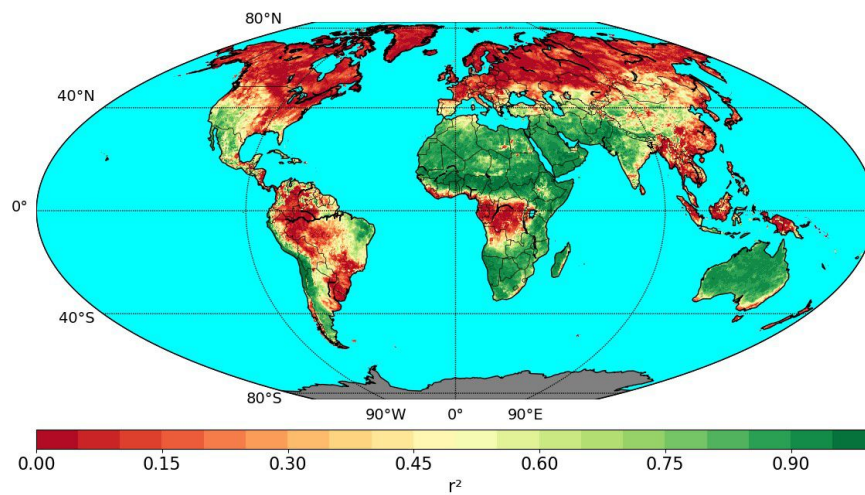


Figure C.13: r^2 values of the comparison between GLDAS Noah LSM soil moisture and evapotranspiration outputs for November

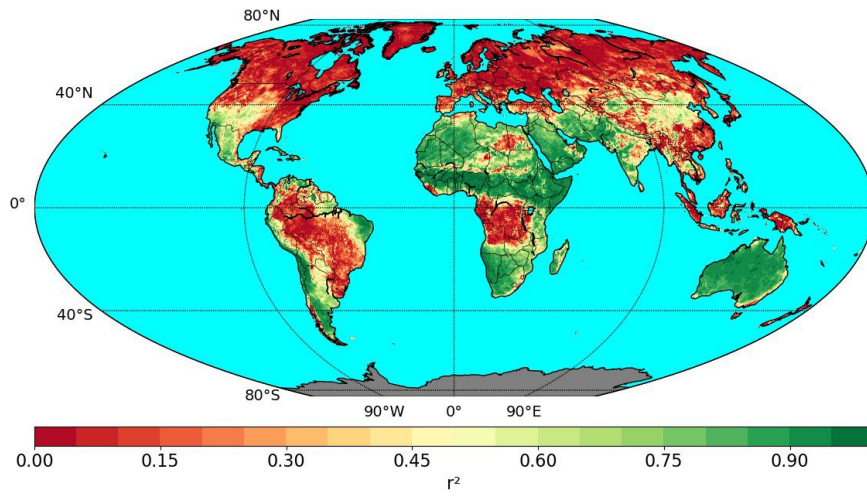
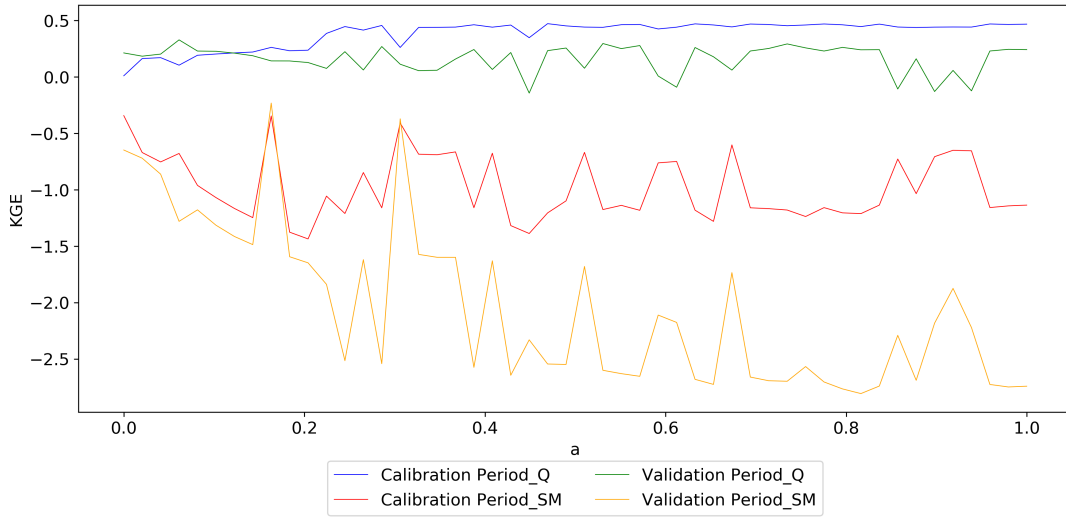


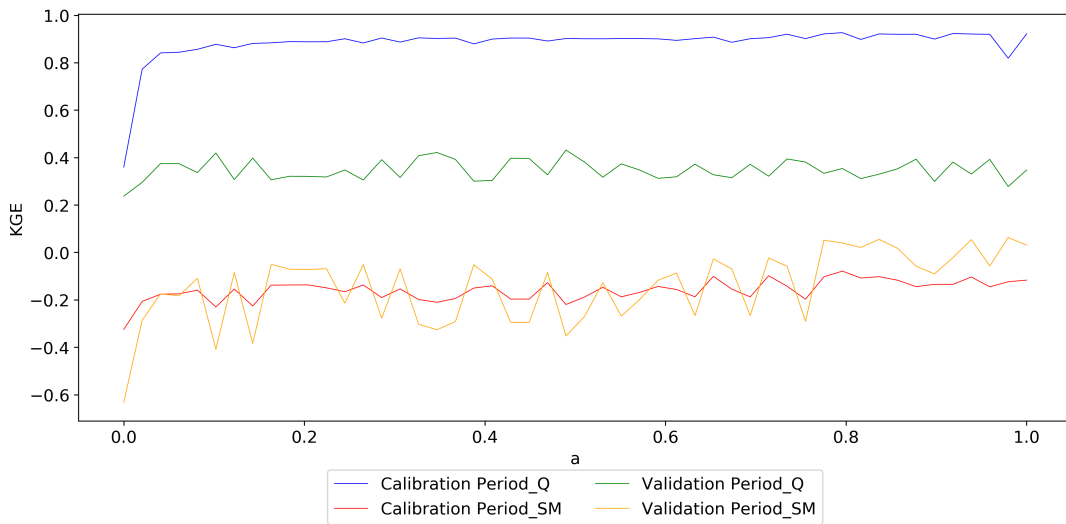
Figure C.14: r^2 values of the comparison between GLDAS Noah LSM soil moisture and evapotranspiration outputs December

APPENDIX D

GRAPHS OF SENSITIVITY ANALYSIS FOR THE WEIGHT FACTOR

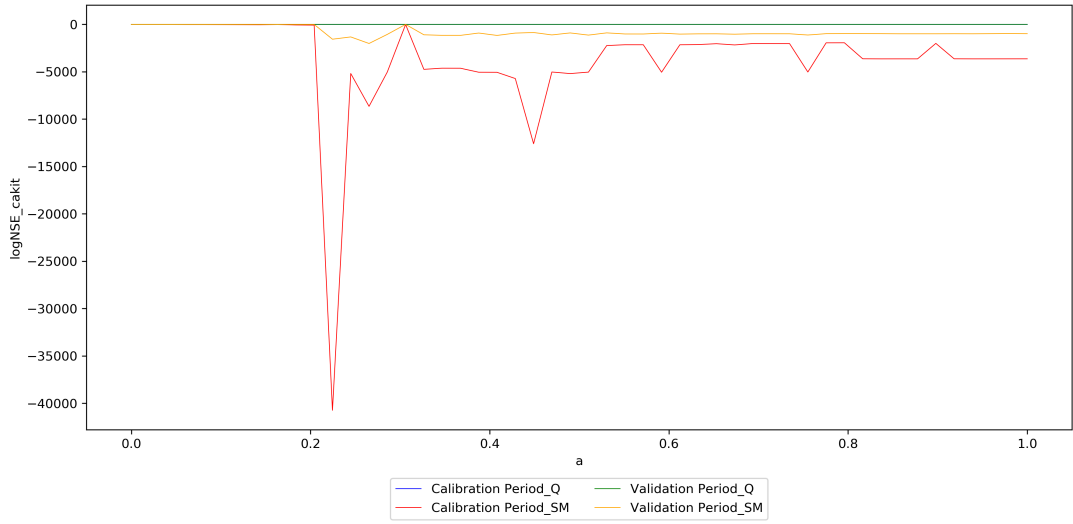


(a)

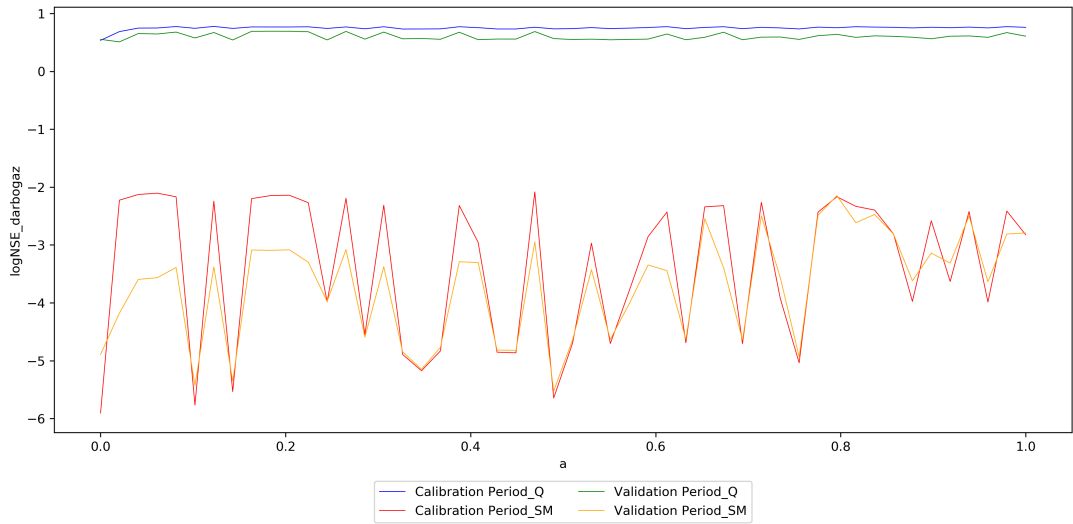


(b)

Figure D.1: KGE Values for different weight factors used for joint calibration of NAM model a) Çakıt Basin b) Darboğaz Sub-Basin

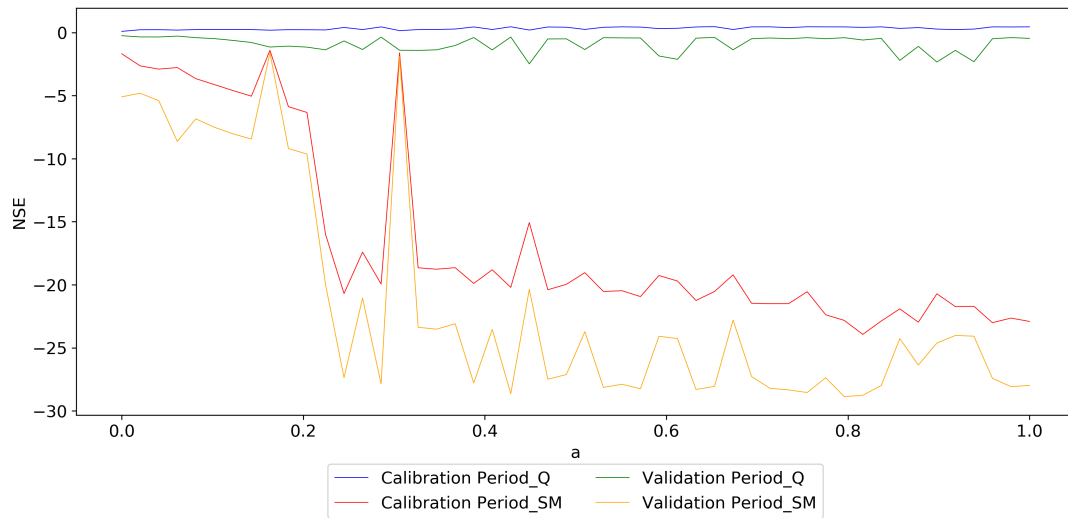


(a)

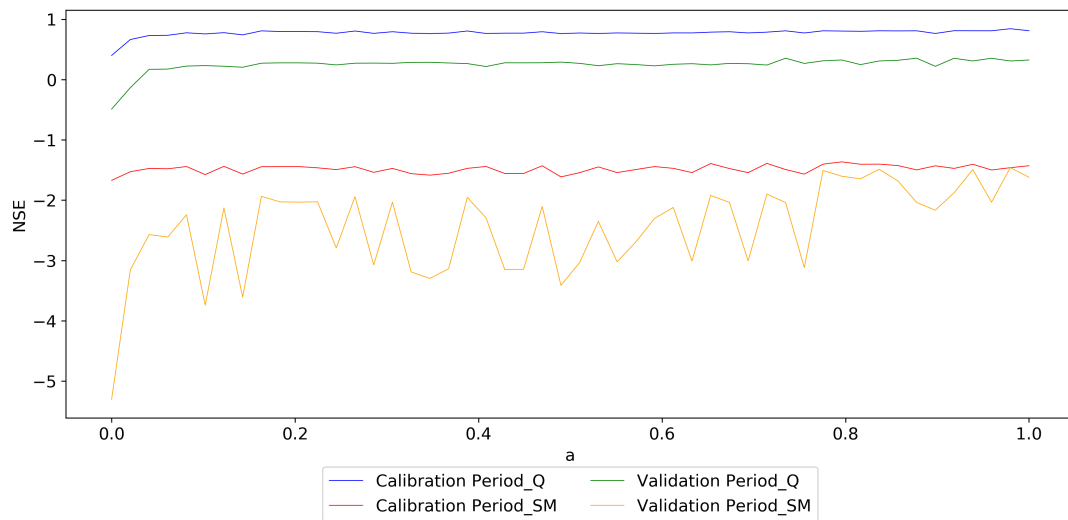


(b)

Figure D.2: logNSE Values for different weight factors used for joint calibration of NAM model a) Çakıt Basin b) Darboğaz Sub-Basin

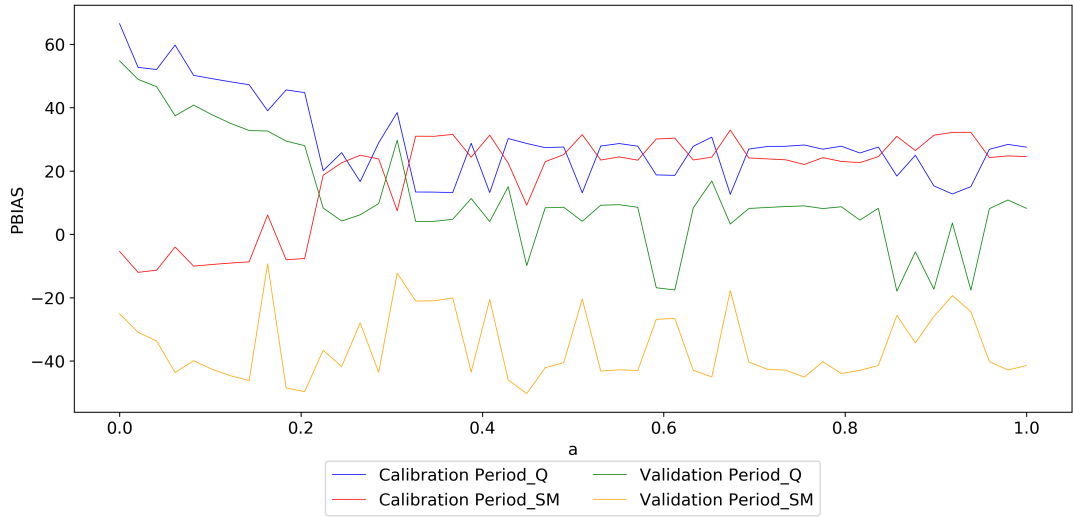


(a)

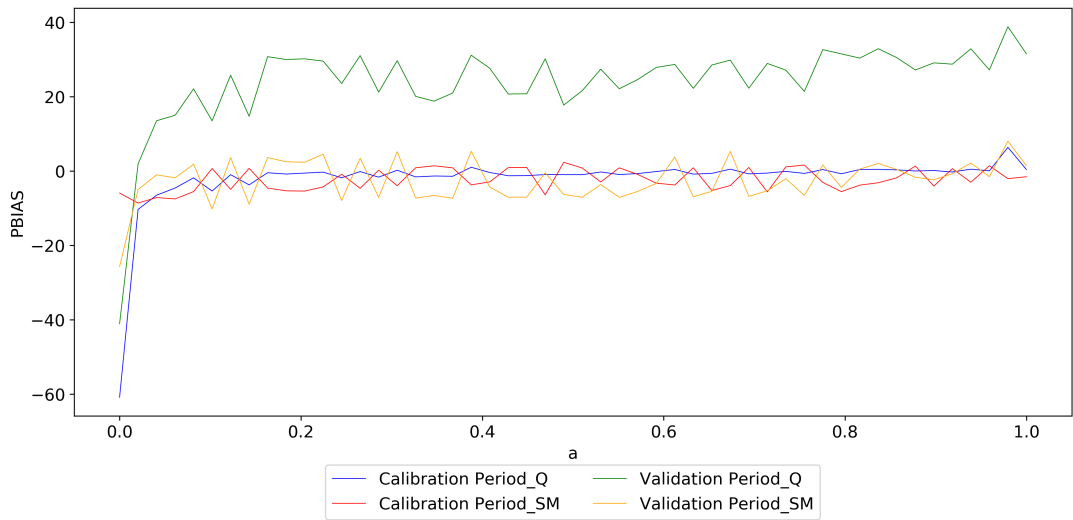


(b)

Figure D.3: NSE Values for different weight factors used for joint calibration of NAM model a) Çakıt Basin b) Darboğaz Sub-Basin

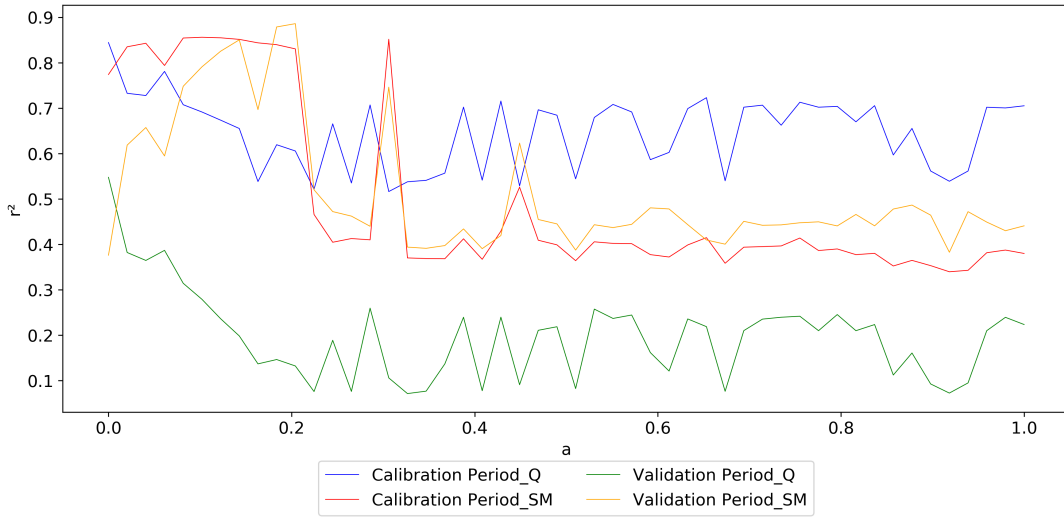


(a)

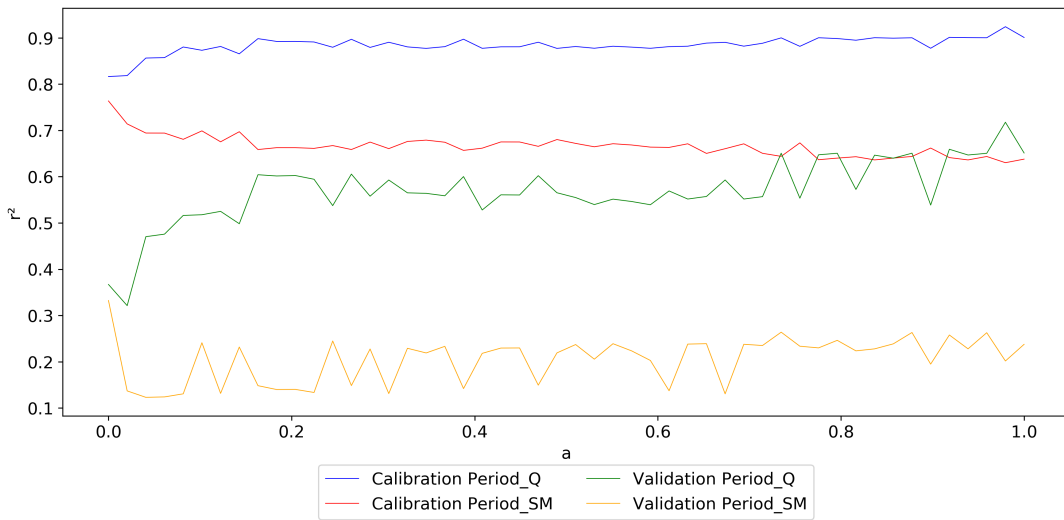


(b)

Figure D.4: PBIAS Values for different weight factors used for joint calibration of NAM model a) Çakıt Basin b) Darboğaz Sub-Basin

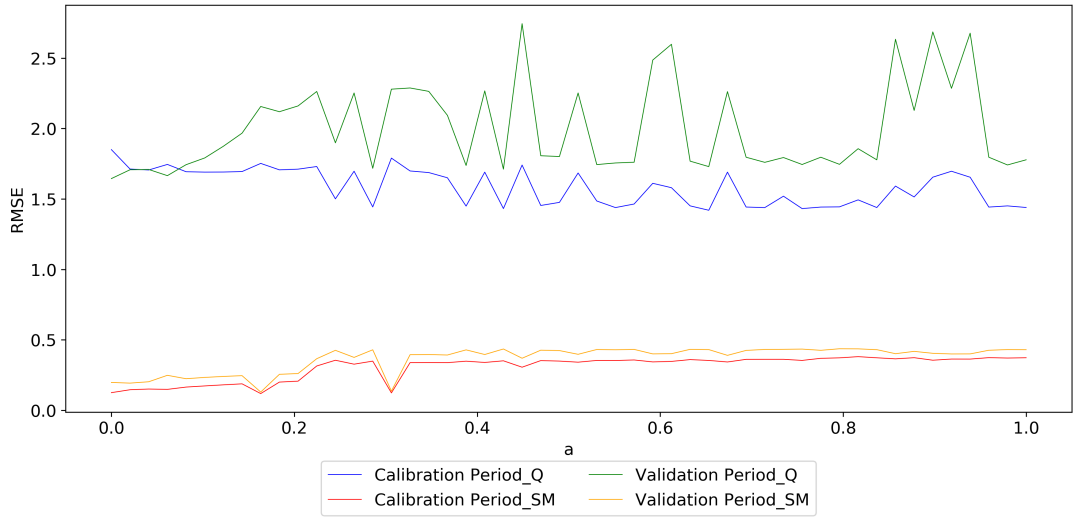


(a)

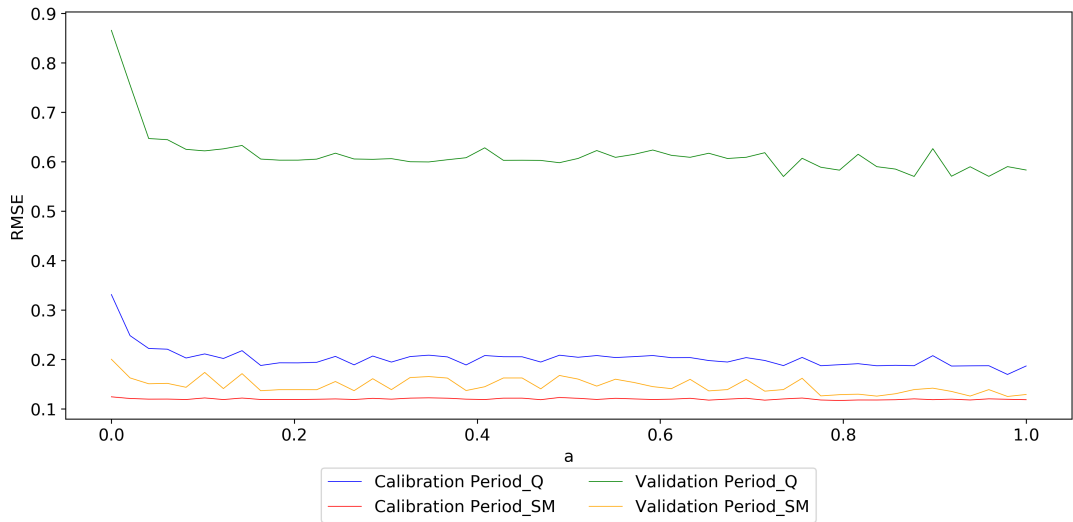


(b)

Figure D.5: r^2 Values for different weight factors used for joint calibration of NAM model a) Çakıt Basin b) Darboğaz Sub-Basin

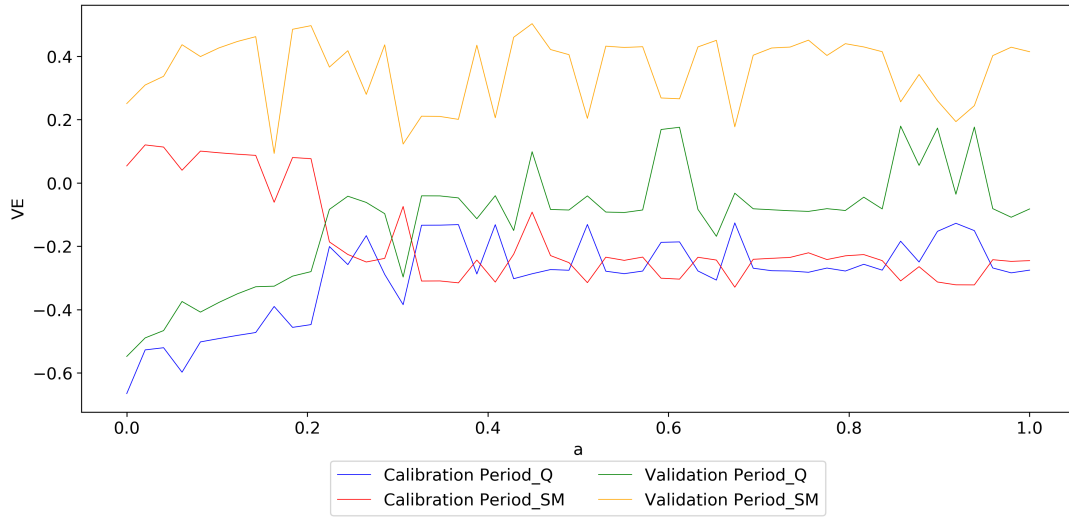


(a)

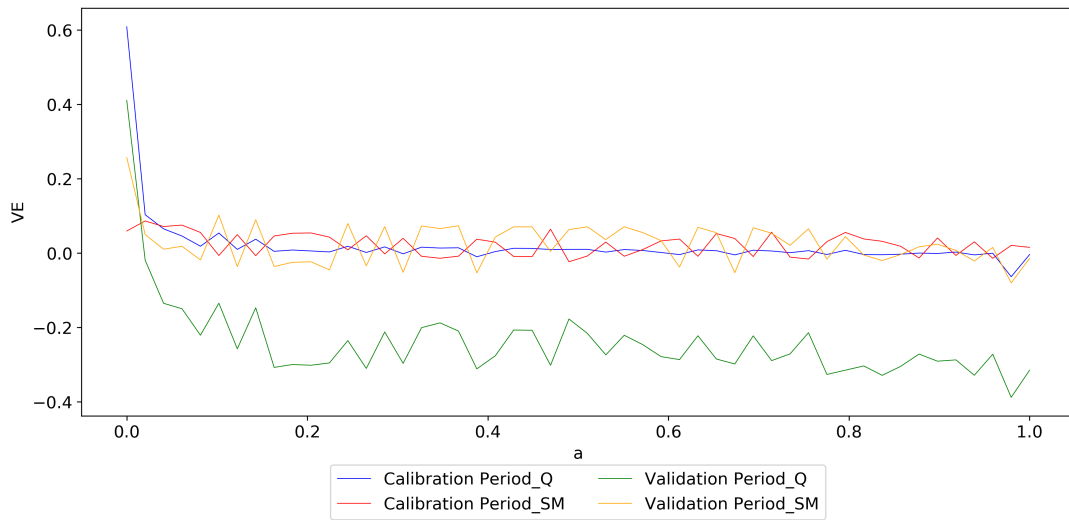


(b)

Figure D.6: RMSE Values for different weight factors used for joint calibration of NAM model a) Çakıt Basin b) Darboğaz Sub-Basin



(a)



(b)

Figure D.7: VE Values for different weight factors used for joint calibration of NAM model a) Çakıt Basin b) Darboğaz Sub-Basin

CURRICULUM VITAE

PERSONAL INFORMATION

Surname, Name : Duygu, Mustafa Berk

Nationality : Turkish

Date and Place of Birth: 1988, Ankara

EDUCATION

Degree	Institution	Year of Graduation
Ph.D	METU Civil Engineering	2021
M.Sc	METU Civil Engineering	2015
B.S	METU Civil Engineering	2011

WORK EXPERIENCE

Year	Place	Enrollment
2015-...	Ministry of Agriculture and Forestry	Senior Expert
2012-2015	Ministry of Forestry and Water Affairs	Junior Expert
2011-2012	Erges Engineering and Consulting	Civil Engineer

FOREIGN LANGUAGES

Advanced English, Basic French

PUBLICATIONS

Duygu, M. B., & Akyürek, Z. (2019). Using Cosmic-Ray Neutron Probes in Validating Satellite Soil Moisture Products and Land Surface Models. *Water*, 11(7), 1362.

Duygu, M. B., Kirmencioğlu, B., & Aras, M. (2017). Essential Tools to Establish a Comprehensive Drought Management Plan-Konya Basin Case Study. *Turkish Journal of Water Science & Management*, 1(1), 54-70.

CONFERENCE PUBLICATIONS

Duygu, M. B., & Akyürek, Z. (2018). Potential use of Cosmic Ray Neutron Probes in estimating state variables in hydrological models. European Geosciences Union General Assembly.

Duygu, M. B., & Akyürek, Z. (2018). Evaluating the use of Cosmic-ray Probes in Validation of Satellite Soil Moisture Products, TERENO International Conference.

Duygu, M. B., & Akyürek, Z. (2019). Using Cosmic-ray Neutron Probes in validating the Satellite Soil Moisture Products and Land Surface Models. European Geosciences Union General Assembly.

Duygu, M. B., & Akyürek, Z. (2019). Improving The Discharge Simulation of a Conceptual Hydrological Model by Introducing Cosmic Ray Neutron Sensor Based Soil Moisture Data. European Geosciences Union General Assembly.

Duygu, M. B., & Akyürek, Z. (2019). Kozmik Işın Nötron Sensöründen (CRNP) Elde Edilen Toprak Neminin Hidrolojik Modellemede Kullanımının Değerlendirilmesi, 10. Ulusal Hidroloji Kongresi.

Duygu, M. B., & Akyürek, Z. (2021). Examining the relationship between CRNP soil moisture data and GLDAS based Noah LSM Evapotranspiration product, 6th international COSMOS Workshop.